

Development of Adenovirus Vector Based Vaccines &
Exploration of Functional Properties of the Adeno-
Associated Virus Assembly-Activating Protein

By

John M. Powers

A DISSERTATION

Presented to

The Department of Molecular & Medical Genetics and the Oregon Health &
Science University School of Medicine in partial fulfillment of the
requirements for the degree of

Doctor of Philosophy

November 2020

Table of Contents

<u>Acknowledgments</u>	<u>i</u>
<u>List of Abbreviations</u>	<u>iii</u>
<u>List of Figures</u>	<u>v</u>
<u>List of Tables</u>	<u>viii</u>
<u>Abstract</u>	<u>ix</u>
<u>Chapter 1. Introduction</u>	<u>1</u>
1.1 History of Gene Therapy	1
1.1.1 Theorizing the Future of Medicine: Early Beginnings.....	1
1.1.2 Evolving the Approach: Transformation to Viral Vectors.....	3
1.2 Adenovirus	5
1.2.1 Classification.....	5
1.2.2 Genome & Viral Proteins	8
1.2.3 Assembly of Viral Nucleocapsid.....	14
1.2.4 Mechanism of Cellular Entry, Trafficking, & Replication	24
1.2.5 Pathogenesis of Adenoviruses	27
1.2.5.1 Immunological Response	32
1.3 Adeno-Associated Virus	36
1.3.1 Classification.....	36
1.3.2 Genome & Viral Proteins	38
1.3.3 Mechanisms of Cellular Entry, Trafficking, & Replication.....	45
1.3.4 Pathogenesis of Adeno-Associated Viruses	54
1.3.4.1 Immunological response.....	56
1.4 Clinical Applications of Gene therapy	56
1.4.1 Adenovirus Vectors.....	56
1.4.1.1 Production of Adenovirus Vectors	57
1.4.1.2 Therapeutic Applications of Adenovirus Vectors	63
1.4.1.3 Adenovirus Vaccine Applications	67

1.4.2	Adeno-Associated Virus vectors	77
1.4.2.1	Production of Adeno-associated Virus Vectors	78
1.4.2.2	Design of Recombinant AAV Vector Capsids.....	79
1.4.2.3	Genome Modifications for Transgene Expression.....	85
1.4.2.4	Therapeutic Applications of Adeno-Associated Vectors	88
1.5	Alphaviruses.....	89
1.5.1	Classification.....	89
1.5.2	Genome and Viral Proteins.....	92
1.5.3	Mechanisms of Cellular Entry, Trafficking, & Replication.....	98
1.5.4	Epidemiology, Hosts, & Vectors.....	102
1.5.5	Pathogenesis	108
1.5.5.1	Immunological Response	109
1.5.5.2	Old World Alphaviruses	113
1.5.5.3	New World Alphaviruses	118
1.5.6	Mayaro Virus.....	121
1.5.6.1	Animal Models of Mayaro Virus.....	122
1.5.7	Vaccines & Therapeutics in Development	123
1.5.7.1	Vaccines.....	124
1.5.7.2	Therapeutics.....	136
1.6	Concluding Summary	139
<u>Chapter 2. Non-Replicating Adenovirus Based Mayaro Virus Vaccine Elicits Protective Immune Responses and Cross Protects Against Other Alphaviruses</u>		
		141
2.1	Abstract.....	141
2.2	Introduction	142
2.3	Results.....	146
2.4	Discussion	169
2.5	Materials and Methods	175
<u>Chapter 3. Adeno-associated Virus (AAV) Assembly-Activating Protein Is Not an Essential Requirement for Capsid Assembly of AAV Serotypes 4, 5, and 11</u>		
		186

3.1	Abstract.....	186
3.2	Introduction.....	188
3.3	Results.....	191
3.4	Discussion.....	215
3.5	Materials and Methods.....	222
<u>Chapter 4. Discussion and Future Directions.....</u>		<u>237</u>
4.1	Novel Viral Vector Vaccination Strategies Against Alphaviruses.....	237
4.2	Functional Role and Importance of Assembly-Activating Protein.....	242
4.3	Concluding Summary.....	246
<u>References.....</u>		<u>249</u>
<u>Appendix. Supplemental Figures.....</u>		<u>346</u>
<u>Supplemental Chapter 1. A Quantitative Dot Blot Assay for AAV Titration and Its Use for Functional Assessment of the Adeno-associated Virus Assembly-activating Proteins.....</u>		<u>350</u>
S.1	Abstract.....	350
S.2	Introduction.....	351
S.3	Methods/Protocol.....	355
S.4	Results.....	370
S.5	Discussion.....	378
S.6	Materials.....	382

Acknowledgments

First and foremost, I would like to thank my advisor, Dr. Daniel Streblow for his help, guidance, and support on my project. He has been an amazing mentor to train under, always having time to chat about the project, and provide insight and knowledge as I learned new skills and techniques. His unwavering support and encouragement have been empowering. I would like to thank all members of the Streblow lab for the help that they have provided on my project. Nicole Haese and Takeshi provided instrumental support for mouse vaccination and challenge experiments. They, along with Michael Denton, Craig Kreklywich, Daniel Streblow, and Patsy Smith all provided helpful assistance during mouse harvest and tissue processing days. Additionally, Lauriel Earley and Kei Adachi from Dr. Hiroyuki Nakai's lab, and Nancy Meyer and Qing Xie from Dr. Michael Chapman's lab were of great support to my projects on AAV.

Many thanks to my dissertation committee members, Dr. Ashlee Moses, Dr. Victor Defilippis, Dr. Cheryl Maslen, and Dr. William Messer, for their perspectives, feedback, and suggestions during our meetings that have helped shape my project. Their willingness to provide letters of support and serve as character references for my post-graduate research pursuits is greatly appreciated.

I'd like to acknowledge the members of the graduate program and graduate studies, including Jackie Wirz, Amanda McCullough, Mushui Dai, Lola Bichler, Crystal Paredes, and Allison Fryer, who all provided support during my graduate career.

Finally, I would like to thank my friends and family and the other members of the PMCB class of 2013 that have supported me throughout my time in graduate school. They have been of great help in my progress through the program.

List of Abbreviations

AAP	Assembly-activating protein
AAV	Adeno-Associated Virus
Ad	Adenovirus
Ad5	Human Adenovirus serotype 5
ADP	Adenovirus death protein
AVP	Adenovirus protease
Cap	Capsid
CAR	Coxsackie and adenovirus receptor
cGAS/STING	cyclic GMP-AMP synthase/stimulator of interferon genes
CHIKV	Chikungunya
Daxx	Death domain associated protein
dLN	Draining lymph node
dpv	days post vaccination
EEEV	Eastern Equine Encephalitis Virus
GON	Group of nine
GOS	Group of six
HEK293	Human embryonic kidney 293 cells
hpi	hours post infection
HSPG	heparan sulfate proteoglycan
HSV	Herpes simplex virus
IFN α R ^{-/-}	Interferon alpha receptor knockout mice
ISG	Interferon stimulated gene
ITR	Inverted terminal repeat
LAV	Live attenuated virus

MAAP	Membrane-associated accessory protein
MAYV	Mayaro Virus
NES	Nuclear export signal
NLR	Nucleotide-binding oligomerization domain-like receptors
NLS	Nuclear localization signal
NPC	Nuclear pore complex
nup	nucleoporin
ONNV	O'nyong'nyong virus
PAMP	Pathogen associated molecular pattern
pTP/TP	precursor terminal protein/terminal protein
RdRp	RNA dependent RNA polymerase
RLR	retinoic acid-inducible gene-1 like receptors
RRE	Rep binding element
SFV	Semliki Forest Virus
SINV	Sindbis virus
TF	TransFrame
TRS	Terminal resolution site
VA RNA	Viral associated RNA
VEEV	Venezuelan Equine Encephalitis Virus
VLP	Viral like particles
WEEV	Western Equine Encephalitis Virus

List of Figures

Figure 1.1.1 Distribution of Viral Vectors used in Clinical Trials Through 2017	5
Figure 1.2.1 Phylogenetic Organization of Adenovirus Species and Types	7
Figure 1.2.2 Schematic Representation of The Ad5 Genome and the Expressed Viral Transcripts	9
Figure 1.2.3 Facets of the Adenovirus Icosahedron	15
Figure 1.2.4 Substrates of the Ad Maturation Protease, AVP	21
Figure 1.2.5 Activation of Inflammatory Signaling by Adenovirus Infection	33
Figure 1.3.1 Clades of AAV	38
Figure 1.3.2 Organization of the AAV2 Genome	39
Figure 1.3.3 Representation of the AAVR Trafficking Pathway	46
Figure 1.3.4 Spatial Orientation and Alignment of Basic Regions Between AAV Serotypes	48
Figure 1.3.5 Parvovirus Rolling-Hairpin Replication	50
Figure 1.4.1 Distribution of Viral Vectors Used in Clinical Trials	57
Figure 1.4.2 Creation of $\Delta E1$ Adenovirus Vector Through Use of Cre-Recombination	60
Figure 1.4.3 Mechanism of Induction of Transgene Specific Immune Responses Following Viral Vector Vaccine Administration	71
Figure 1.4.4 Four Predominant Methods for the Discovery of New AAV Capsids	80
Figure 1.5.1 Phylogenetic relationship of Alphaviruses and Antigenic Complexes	91
Figure 1.5.2 Organization of Alphavirus Genome	94
Figure 1.5.3 Infection Pathway and Pathogenesis of Arthritic Alphaviruses	115

Figure 1.5.4 Structural Features and Presence of DLPs in Alphavirus Species	118
Figure 2.1 AdV-MAYV Vaccine Vector Expression of MAYV Structural Proteins.....	147
Figure 2.2 AdV-MAYV-Induced Antibody Response Neutralize Virus in a Pre-attachment Dependent Manner.....	150
Figure 2.3 Characterization of Anti-MAYV Antibody Responses	152
Figure 2.4 AdV-MAYV Vaccination Elicits Robust T-cell Response Against MAYV E2 Glycoprotein in Wild Type and IFN α R ^{-/-} Mice	154
Figure 2.5 AdV-MAYV Vaccination Protects WT Mice from MAYV challenge ..	156
Figure 2.6 AdV-MAYV Vaccination Reduces Inflammatory Mediators in the Joint	158
Figure 2.7 Passive Transfer of AdV-MAYV Immune Sera Protects Against Pathological Effects of Infection.....	159
Figure 2.8 AdV-MAYV Vaccination of IFN α R ^{-/-} Mice Induces Strong Neutralizing Antibody Responses	160
Figure 2.9 AdV-MAYV Vaccination Protects IFN α R1 ^{-/-} Mice from Lethal Challenge.....	161
Figure 2.10 Passive Transfer of Immune Serum Protects IFN α R1 ^{-/-} Mice from Lethal MAYV Challenge.....	164
Figure 2.11 AdV-MAYV Elicits Cross Neutralizing Antibodies Against Una and Chikungunya Viruses	165
Figure 2.12 AdV-MAYV Vaccination Cross-Protects IFN α R1 ^{-/-} Mice Against Lethal Challenge with CHIKV and Una Virus	168
Figure 3.1 Expression of AAP1 to -12 in HEK 293 Cells	193
Figure 3.2 Sequence alignment of the C-termini of AAP1 to -12	196
Figure 3.3 Intracellular Localization of AAP1 to -12.....	197
Figure 3.4 Quantitative Dot Blot Assay to Determine Titers of VP3 Capsids Produced in the Presence or Absence of AAP	200

Figure 3.5 Capsid Assembly of AAV2, -4, -5, -8, and -9 in HeLa cells.....	203
Figure 3.6 Transmission Electron Microscopy of AAV VP3-Only Capsids Produced With or Without AAP	205
Figure 3.7 Production and Characterization of AAV5 VP1/VP2/VP3 Particles Produced With and Without AAP5	207
Figure 3.8 AAP-VP3 Cross-Complementation Analysis by a Quantitative Dot Blot Assay	211
Figure 3.9 AAP-VP3 Cross-Complementation Among 12 Different AAV Serotypes.....	213
Figure 3.10 Sequence Alignment of Wild-Type AAPs and the Mutated AAPs Encoded by the AAP ORFs Within the cmVP3 ORFs.....	218
Supplemental Figure 1 Convalescent Plasma Samples from Chikungunya Patients Display Detectable Levels of Cross-Protective Antibodies.....	346
Supplemental Figure 2 AdV-UNAV Induces Long Lasting Neutralizing Antibody Responses	347
Supplemental Figure 3 AdV-CHIKV Vectors Stimulate Strong Immune Responses.....	348
Supplemental Figure 4 AdV-CHIKV Vaccination Protects WT Mice from CHIKV Challenge.....	349
Figure S.1 A Representative Dot Blot Analysis to Determine the Titer of a CsCl-Purified AAV Vector.	372
Figure S.2 AAV VP3-AAP Cross-Complementation Dot Blot Assay.....	374
Figure S.3 A Comparison of Enzymatic Activities of Different Nucleases in Unpurified AAV Vector Preparations.....	377

List of Tables

Table 1.2.1. Classification ^A and Selected Features of Human Adenoviruses	28
Table 1.2.2 Association of Adenoviral Diseases and Principal Serotypes in Immunocompetent and Immunocompromised Individuals	30
Table 1.5.1 Published Alphavirus Vaccine Approaches	132
Table 3.1 Theoretically and Experimentally Determined Molecular Masses of FLAG-Tagged AAPs	194
Table 3.2 Nucleolar Association of AAPs	197
Table 3.3 Biochemical Properties of AAP BR1 to BR5	198
Table 3.4 Biochemical Properties of AAP BR1 to BR6 Toward the C-Terminus.....	198
Table S.1 Solution and Buffer Recipes for Dot Blot	382
Table S.2 Plasmid Combinations for AAV VP3-AAP Cross-Complementation Assay Performed in a 6-well Plate Format.....	384
Table S.3 List of Master Mix Reagents.....	385

Abstract

Over the last few decades, the utility of viral vectors has expanded from their initial use as clinical therapeutics for debilitating genetic diseases to include their use as vaccination platforms. When deciding on the optimal viral vector for use, considerations must be made that include target tissue, dose, immunogenicity, and overall safety. Adenovirus vectors have been a compelling vector in gene therapy due to their ability to package large gene-of-interest transgenes. Conversely, while adeno-associated viruses (AAV) have one of the smallest packaging capacities, the wide tissue tropism between different serotypes has made them a select candidate for tissue specific applications even with systemic delivery.

Adenovirus vectors are an optimal vaccine platform as they stimulate robust innate and adaptive immune response. They have higher efficacy and/or safety than live-attenuated, subunit, or nucleic acid vaccines. Upon expression of the delivered transgene antigen they stimulate both innate and adaptive immune responses. Such approaches have been used in attempts to vaccinate against diseases where development of vaccines by traditional routes has struggled. This has included HIV, influenza, Ebola, and bacterial and protozoan pathogens. The ability to produce adenovirus vectors at high titer and recent advances in stabilizing the shelf-life of vectors outside of cold chain storage make them ideal for use in non-clinical settings, such as field use in global vaccination strategies.

Mayaro virus, initially discovered in the Mayaro Province of Trinidad & Tobago in 1954, a member of the family *Togaviridae*, genus *Alphavirus*. While Mayaro most

predominantly circulates in rainforests, especially the jungle canopy, it has emerged as an infectious disease agent with the potential for global distribution and spread in recent years. Increasing tourism to the region and global travel have led to the identification of virus-infected patients in North America, Western Europe, and the Caribbean in recent decades. Currently, there are no licensed vaccines or therapeutics for Mayaro or any other alphavirus, necessitating the development of such approaches. To this end, we developed an adenovirus serotype 5 (AdV) vector that encodes the full-length structural proteins from Mayaro virus that are expressed following intramuscular vaccination. Vaccination with the engineered Mayaro adenovirus vector vaccine rendered wildtype mice largely resistant to infection and enabled survival of highly susceptible interferon alpha receptor knockout mice. Intriguingly, the vaccine also protected mice from Una and Chikungunya alphavirus challenge; viruses that share overlapping regions of distribution and symptoms. Such findings demonstrate the applicability of adenovirus vector-based vaccines against related alphavirus member species.

Adeno-associated virus vectors have also been of significant interest in the field of gene therapy, and the development of novel pseudotyped and rationally designed viral vectors has been of significant interest. Such techniques benefit from deeper understanding of virus biology and key mechanisms in virion assembly and life cycle. In 2010, a +1 frameshifted assembly-activating protein was discovered and identified as critical in the assembly of AAV serotype 2. We undertook a comprehensive analysis of AAV serotypes 1-12 as well as phylogenetically distant

serotypes to examine its functional requirement. We determined that it is not a shared requirement in virion assembly across serotypes and identified varying levels of capsid assembly when heterotypic AAP and structural proteins were co-transfected into production cell lines. These results indicated distinct differences exist in both the ability of structural proteins to self-assemble and absolute requirement of functional AAP for certain serotypes.

Chapter 1.

Introduction

1.1 History of Gene Therapy

1.1.1 Theorizing the Future of Medicine: Early Beginnings

Gene therapy, the process by which foreign genetic material is introduced for therapeutic benefit, has been a continually evolving field since the early 1960's. The idea of a single, long-lasting, and durable treatment that could provide clinical benefit was an alluring prospect, and many postulated that such a breakthrough could be the future of medicine [1-3]. For conditions that lack long term effective treatments, such as inborn errors of metabolism, this field has been of great interest [4-7]. Initial studies identified the potential to utilize innate viral genes for therapeutic benefits in cultured cells from small animals and human patients. Rodgers & colleagues found that Shope papilloma virus (SPV) could increase the arginase activity in rabbit fibroblasts as well as in fibroblasts from patients suffering from argininemia [8, 9]. Similar evidence of therapeutic viral gene expression was observed from UV irradiated herpes simplex virus, SV40, and polyoma viruses following infection of cultured cells [10, 11]. These studies solidified the concept that viral infection could result in long lasting genetic modification of mammalian tissues.

Based on the early findings with SPV, Rodgers and colleagues controversially elected to test the efficacy in humans by injecting three German girls suffering from hyperargininemia with wild-type SPV. This initial trial found that there was no clinical benefit to sisters (age two and seven), and that a larger dose provided to

their five month old sister resulted in a severe allergic reaction and no observed clinical benefit [12, 13]. With the growing advances in the field, and in response to the human testing undertaken by Rodgers and colleagues, Friedmann and Roblin published what would become a landmark article regarding the evolving field and potential therapeutic uses of genetic engineering in humans [14]. Although they echoed prior researchers in elucidating the potential benefits of gene therapy in the treatment of genetic disorders, they largely discussed the ethical and scientific standards that should be considered moving forward [1-3]. These centered on the principle that until standards of care and an understanding of short and long-term effects were developed, human testing should not be further pursued.

In order to adapt the potential of viral elements for gene therapy, major hurdles still existed. While the knowledge that RNA and DNA oncoviruses could be used to express beneficial genes, the understanding of how to amplify and purify human genes and the subsequent safe utilization of viral integration for stable expression was absent [15, 16]. In 1972, Berg *et al.* reported a technique to insert foreign DNA into the SV40 genome using the RI enzyme from *Escherichia coli* (EcoRI). Using this method the galactose operon of *E. coli* was inserted into SV40, providing initial evidence that viral genomes could be edited to introduce new genetic elements [17, 18]. Shortly after, Maniatis *et al.* reported on the ability to insert foreign rabbit β -globulin DNA into bacterial plasmids, which could then be transformed in *E. coli* and grown to obtain large quantities of full length rabbit β -globulin mRNA *in vitro*

[19]. Together, these efforts overcame the previous limitations on obtaining large quantities of recombinant DNA.

In addition to viral based approaches, researchers had also explored the possibility of transfection to deliver naked DNA to cultured cells. These efforts identified DEAE-dextran and calcium phosphate as optimal transfection reagents, although this approach was challenged by low efficiency that resulted in minimal gene expression [20-22]. Even with such knowledge, Martin Cline attempted to transfect hematopoietic stem cells from bone marrow extracted from two patients suffering from β -thalassemia. While the procedure did not overtly harm them, there was no clinical benefit observed. Such a result was not unexpected as it was estimated that transfection of $\sim 10^9$ cells would be needed in order to modify one hematopoietic stem cell for long-term gene expression [23, 24]. Although Cline admitted that it was understood that the experiment was unlikely to provide clinical benefit to the patients, he argued that it served merely as a proof-of-principle experiment to establish such an approach [23, 24]. This defense was not accepted, resulting in the loss of funding and moved the field to again assess the fundamentals that should be observed and practiced in moving towards clinical trials [24, 25]. The results of the study, which are largely unpublished, were important in pushing the field to explore more effective alternatives.

1.1.2 Evolving the Approach: Transformation to Viral Vectors

As transfection was plagued by issues of low efficiency and restricted to *ex vivo* manipulation of cells, the field began to examine new approaches. Although early

efforts utilized oncogenic live viruses such as SV40, polyoma, and herpes simplex viruses to deliver innate viral genes, safer alternatives that were equally effective were explored. Multiple groups were investigating the potential of designing replication incompetent viruses. By removing genetic elements required for viral replication, these vectors would still be able to infect cells and express genetic elements from their viral genomes, but with significant risk reductions when compared to live viruses. Previous studies had identified that viral genomes could be altered without affecting the formation of competent plant and mammalian viruses. Outstanding questions remained on what viruses would be optimal vectors, as well as what viral proteins were necessary for the formation of competent viruses and could not be removed to insert foreign genes [22, 26-28]. By the early 1980's, multiple groups were examining the potential of replication incompetent retroviruses and lentivirus, adenoviruses, adeno-associated viruses, and herpes simplex viruses for use as gene therapy vectors. While each option offered distinct advantages and disadvantages, they were of great interest as they offered increased efficiency over transfection-based approaches, the potential for long term expression from vectors that could integrate into the host genome, and the ability for *in vivo* treatment of solid organs. Continued research and development resulted in increased safety profiles and potential applications. To date, over 3700 clinical trials with viral vectors have been conducted. Close to 100 or more trials have been registered yearly since 1999 [29, 30]. While these trials have predominantly utilized adenoviral and retroviral vectors, the use of other vectors, such as adeno-associated virus, has been consistently rising (**Figure**

1.1.1). The design, production, and applications of adeno-associated virus and adenovirus vectors will be discussed in section 1.4.

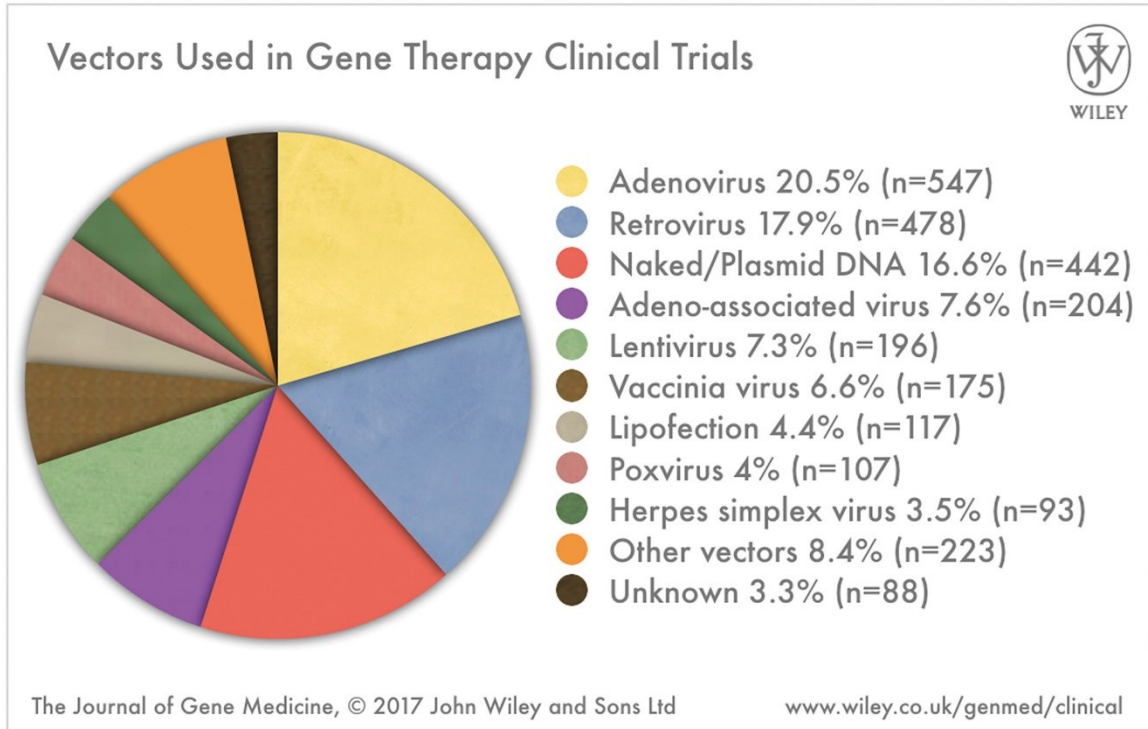


Figure 1.1.1 Distribution of Viral Vectors used in Clinical Trials Through 2017

Adenovirus vectors have been, and continue to be, the predominant vector utilized in gene therapy trials. Reprinted with permission from Ginn *et al.*, 2017 [29].

1.2 Adenovirus

1.2.1 Classification

Adenovirus was first discovered in 1953 during experiments on cultured adenoid tissues obtained from young patients after observing that 63% of cell lines displayed marked cytopathic effect [31]. Transfer of the supernatant from these cultures to fresh adenoids, HeLa cells, or human embryonic tissue resulted in

appearance of the cytopathic effects. These observations were replicated in a number of human, rabbit, hamster, and chicken cell lines. Inoculation of culture supernatant into experimental animals did not replicate any recognizable disease, and as such they designated the pathogen as “adenoid degeneration agent”. Today it is known as adenovirus.

Human adenovirus (Ad) is a member of the family *Adenoviridae*, genus *Mastadenovirus*, and there are 7 phylogenetic species. These species are categorized A – G, and currently over 88 different types have been determined based on novel genomic sequences (**Figure 1.2.1**) [32-35]. Species B is subdivided into two classes, B1 and B2, based on differences in tropism, receptor usage, and sequence homology. Human adenovirus category D (HuAd-D) is the largest species, comprising over half of the identified types. The increasing number of types is the result of genomic recombination events between circulating adenoviruses, the majority of which occur within a designated adenovirus species [36]. Category C (HuAd-C) members serotype 2 (Ad2) and 5 (Ad5) are the predominantly studied serotypes.

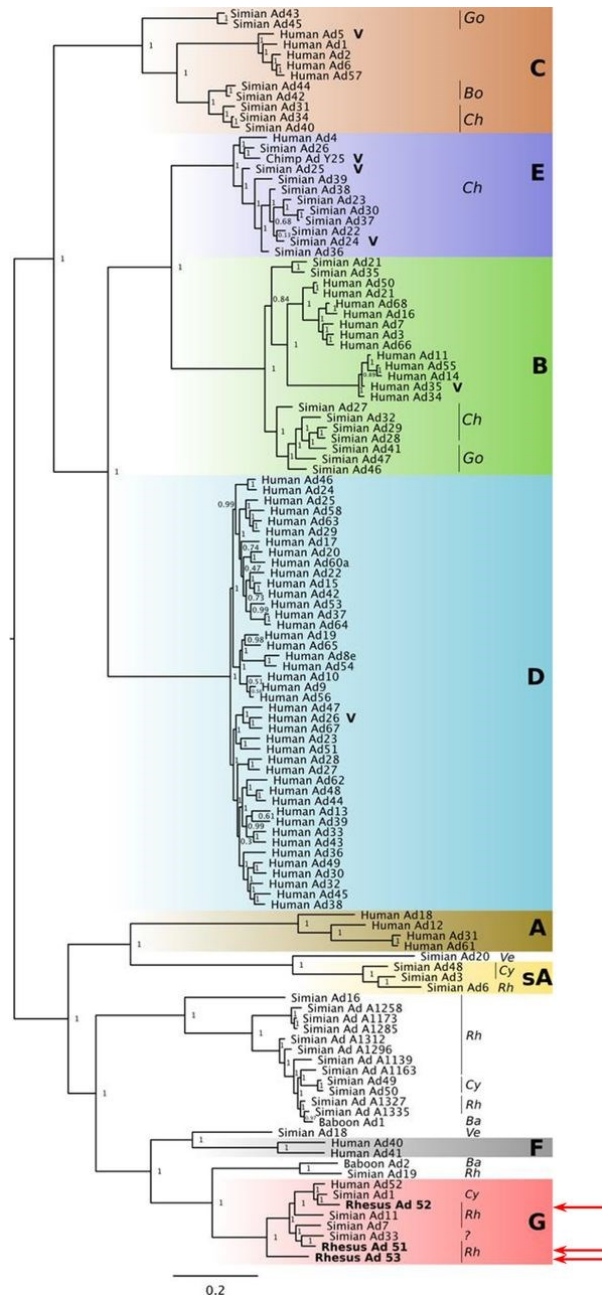


Figure 1.2.1 Phylogenetic Organization of Adenovirus Species and Types

Maximum likelihood phylogenetic tree of adenovirus genomes. Full-length genomes from classified (species A to G) and unclassified human and simian adenoviruses, in addition to the novel vectors, were used to infer an ML phylogenetic tree. The different species are highlighted by colored rectangles (sA, simian species A), and in the case of simian vectors, the host species are noted (Rh, rhesus macaque; Cy, cynomolgus macaque; Go, gorilla; Ve, vervet monkey; Ba, baboon; Bo, bonobo; Ch, chimpanzee). Three novel isolated vectors were closest to species G adenoviruses (red arrows). Other vaccine candidates are highlighted with a V. Reprinted with permission from Abbink *et al.*, 2014 [35].

1.2.2 Genome & Viral Proteins

The adenovirus genome is linear dsDNA roughly 36 kb in length but can vary from 26-45 kb depending on the serotype [37]. The ends of the genome are flanked by inverted terminal repeats (ITR) ranging in size from 36 to over 200 bp [38]. The genome is packaged into a large icosahedral capsid shell with a pseudo- $T = 25$ confirmation that is approximately 150 MDa and 90 nm in diameter [37]. The Ad genome contains three distinct temporally regulated transcription units separated on both strands of the genome, classified as early (E1A, E1B, E2, E3, and E4), delayed-early (IX, IVa2, and E2 late), and late (L1 – L5). They are transcribed by RNA polymerase II (**Fig 1.2.2**) [39]. In contrast, small virus-associated RNAs (VA RNA) are transcribed by RNA polymerase III [40]. The VA RNA products play important roles in transcriptional control, especially the translation of late genes through inhibiting the activities of Dicer and the RNA-induced silencing complex [41, 42]. Transcription of the genes results in ~30 – 40 mRNAs largely by way of alternative splicing, as all but polypeptide IX encode for 2 or more alternative splice products [39].

During infection, the immediate early E1A gene is the first to be expressed and serves to activate genome transcription of the E1B, E2, E3, and E4 genes. Additionally it induces a cellular state favorable for viral replication by driving cells to S-phase and blocking cellular replication [43, 44]. These properties reside in the fact that the E1A protein interacts with a vast array of host cell transcription factors, co-activators, co-repressors, nucleosome remodeling factors, and general

transcription machinery with over 50 different distinct protein targets identified [45, 46]. This dramatic alteration of the steady-state cell environment induces a hospitable environment for viral replication until cell death at the end of the lytic cycle. While the majority of E1A host-cell protein interactions occur in the nucleus, up to ~50% of E1A remains cytoplasmic and induces alterations of proteasomal ATPases and Golgi network assembly/disassembly [46, 47]. Along with this, E1A also functions to reduce the inflammatory response following infection through the transcriptional regulation of type I interferon genes triggered from initial Ad binding and cellular entry as discussed in section 1.2.4 [46, 48].

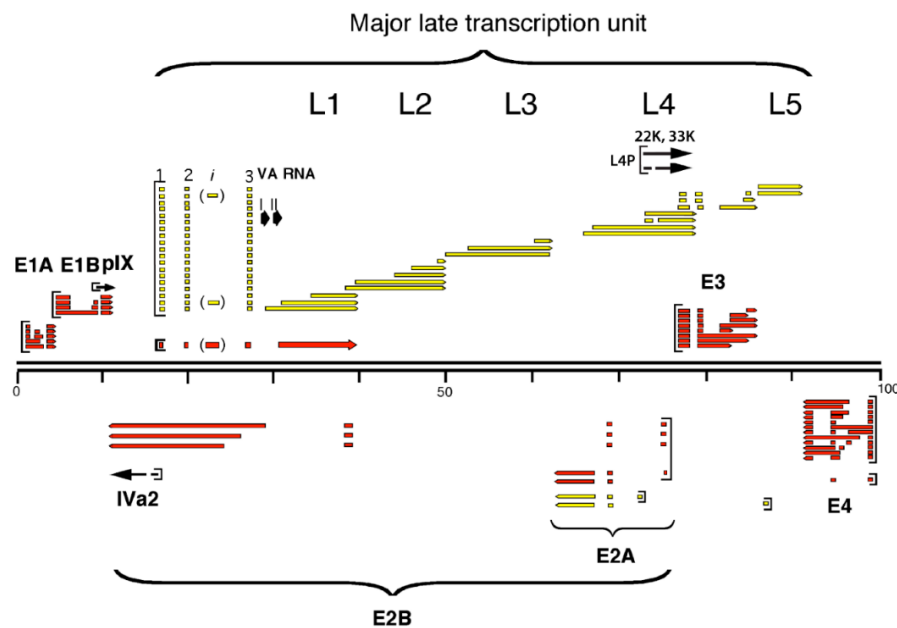


Figure 1.2.2 Schematic Representation of The Ad5 Genome and the Expressed Viral Transcripts

The early transcripts are shown in red and the late are marked in yellow. Intermediate genes are indicated as black arrows. Reprinted from under an open access Creative Common CC BY license Biasiotto *et al.*, 2015 [39].

E1B produces at least five different polypeptides through alternative reading frames and splicing. Two of these, E1B-19K and E1B-55K, have well defined roles in viral replication and cell transformation [49]. Both proteins function to inhibit P53 mediated transcription, working as antagonists to the E1A induced apoptosis [50, 51]. They also work cooperatively with E1A to activate cell cycle progression. E1B-19K, a Bcl-2 homologue, also functions to prevent co-oligomerization of BAK and BAX to block caspase activation, and prevents signaling from Bik/Nbk, and Nip 1, 2, and 3 [52, 53]. E1B-55K has been shown to bind the activator domain of p53, inhibiting its function and transactivation of promoters with a p53 binding site [49]. Transcriptional repression is not p53 specific, as fusion of E1B-55K to Gal4 also results in transcriptional repression from Gal4 binding site promoters, indicating a broad repressive role [54]. Along with the early functions of E1B-55K to establish a permissive environment for viral replication, it also serves to promote viral mRNA export and translation while inhibiting these functions for cellular mRNA. Interaction between E1B-55K and E4orf6 is required for proper function and localization of E1B-55K to the nucleus and viral replication centers. The assembled E1B-55K/E4orf6 complex forms an E3 ubiquitin ligase through E4orf6 host cell interactions. This complex induces proteasomal degradation of host-cell substrates that include p53, DNA damage recognition proteins, and DNA repair proteins [55, 56].

The E2 protein is divided into a promoter proximal (E2A) and distal (E2B) region with unique polyadenylation sites. Together these transcription units encode three

proteins required for viral replication. E2A encodes the ssDNA binding protein (DBP) while E2B encodes the precursor terminal protein (pTP) and DNA polymerase [57]. Due to its role in priming replication, infectious Ad is assembled with pTP covalently bound to the 5' termini of the genome. During replication, DBP protects ssDNA during the elongation phase of replication and enhances the rate of replication [58]. DBP also plays important roles in stabilizing viral mRNA, host-cell transformation, and potentially in capsid assembly/genome packaging [37, 57]. Synthesis of the E2 proteins is regulated by two distinct promoters, one active early in infection, and a second that is active in late stages of infection. Activation and expression from the E2 early promoter is coordinated through E1A following the binding of E2F, activating transcription factor (ATF), transcription initiation factor II D, and E4orf6/7 upstream of the promoter [59]. At this time, activity from the late promoter is repressed by E1A. As the time post infection increases, E1A levels begin to decrease, allowing expression to switch between the promoters. This coordinated switch enables expression from the E2 promoter throughout the course of infection [59].

E3 protein expression is intrinsically important in Ad infection as it regulates the host immune innate and adaptive immune response. It contains two polyadenylation sites that results in the production of two transcription units – E3A and E3B. Proteins from E3 have no effect on viral replication. Instead, they function to reduce the host immune response induced by viral genes upon expression. They have no effect on the initial immune response elicited by viral binding and

cellular uptake [48]. Proteins produced by E3 protect infected cells from cytotoxic T cells by blocking MHC class I restricted antigen presentation, promoting internalization of proapoptotic receptors such as FAS and TRAIL from the cell surface, and downregulating cytokine and chemokine production and signaling [60, 61]. Along with immunomodulatory effects, E3 also produces the adenovirus death protein (ADP) that is largely expressed late in the course of infection and facilitates efficient cell lysis through nuclear membrane breakdown. Typically cultured cells infected with Ad lyse within 2-7 days post infection (dpi), but lysis was impeded and began significantly later in Ad viruses with a non-functional ADP (≥ 6 dpi)[62].

Located at the 3' end of the Ad genome, the E4 region of the genome produces 6 known polypeptides (E4orf1, E4orf2, E4orf3, E4orf4, E4orf6, E4orf6/7) with a seventh, yet unobserved but proposed E4orf3/4 [63, 64]. Together these serve important roles in the viral life cycle that include DNA replication, transition from early to late gene expression, and host cell protein synthesis shutoff [65]. Whole deletions of the E4 region resulted in defective viruses, although the deletion of some regions can be tolerated. For example, E4orf3 and E4orf6 produce polypeptides with similar but non-identical functions that compensate for each other in mutant viruses. These two polypeptides function to increase the production of viral late proteins through stabilization of viral RNA in the nucleus, accumulation of the mRNA in the cytoplasm, and support efficient DNA synthesis and genome replication [64]. As previously mentioned, E4orf6 binds to E1B-55K and this

complex plays important roles in modulating host-cell responses to DNA damage and apoptotic pathways. E4orf4 plays an important role in temporal regulation of viral and cellular gene expression through the hypophosphorylation of E1A and c-Fos, resulting in the reduction of cellular transcription activators and regulators that include AP-1, JunB, and c-Myc [66, 67]. Together, these activities drive replication towards delayed-early and late gene synthesis. E4orf1 and E4orf2 have been indicated as required for the development of tumors in infected tissues for Ad species with observed oncogenic effects in animal models [68]. Following localization to the nucleus, E4orf1 has been shown to promote enhanced glycolysis. This occurs through activation of c-Myc through PI3-kinase and AKT signaling, enabling increased nucleotide biosynthesis for optimal viral replication [69]. E4orf6/7 is responsible for stabilization and activity of the E2 early promoter through the E2F transcription factor, and may also be involved in the regulation of cell cycle genes with E2F promoter sequences [64].

As the infection continues, gene synthesis switches next to the production of the delayed-early structural genes. The role of these delayed-early genes (IX and IVa2) will be discussed in the next section. Finally, late gene synthesis of L1 – L5 occurs. The products of these genes have important roles in temporal regulation of early viral gene expression as well as production of the structural proteins [39]. L1 encodes two structural proteins L1 52K and L1 55K (L1 52/55K), while L2 pre-mRNA is spliced into 4 capsid proteins pIII (penton), pV, pVII, and p μ . Similarly, L3 pre-mRNA also undergoes splicing that results in the production of another 3

structural proteins pVI (hexon), pII, and the adenovirus protease (AVP). L5 encodes the pIV (fiber) structural protein. The L4 pre-mRNA produces 3 regulatory proteins that down regulate early gene expression while enhancing late gene transcription (L4-22K), activate splicing of late gene mRNA (L4-33K), or inhibit cytotoxic lymphocyte induced apoptosis of infected cells (L4-100K). L4 also produces the structural protein pVIII [70, 71]. The roles and interplay between these structural proteins will be discussed below.

1.2.3 Assembly of Viral Nucleocapsid

The capsid structure is composed of three major proteins (penton, hexon, and fiber) along with four minor capsid proteins (IIIa, VI, VIII, and IX). An additional 6 proteins (V, VII, μ , IVa2, terminal protein, and adenovirus protease) are packaged inside of the capsid structure along with the dsDNA genome [37, 72]. Originally, Caspar and Klug predicted Ad to conform to a $T = 25$ triangulation number, requiring that the capsid be formed from 60 icosahedral asymmetric units (AU) consisting of 25 polypeptides [73]. Instead, each AU is in fact formed by 4 trimers of hexon and one penton protein, resulting in a total of 13 polypeptides. In total the capsid is formed from 720 monomers of hexon that form 240 trimers, and 12 penton proteins, resulting in a pseudo- $T = 25$ structure (**Figure 1.2.3**)[74-77].

Hexon is able to adopt a pseudo-hexagonal form that is key to this structural design due to the presence of an 8-stranded β -barrel with a “jellyroll” topology [76, 78]. Each capsid facet is formed through the association of 3 AUs with each other in two tile arrangements. Nine central hexon proteins of each facet belong to the

group of nine (GON) (**Figure 1.2.3 panel A**) while the hexons and penton that are in contact at the 5 fold axis of symmetry (peripentonal hexons) belong to the group of six (GOS) (**Figure 1.2.3 panel B**). These designations and their defining features will be discussed later. The remaining major structural protein, fiber, forms into trimers and extends as projections from penton at the 5 fold axes [79, 80]. Fiber is composed of 3 domains: a N-terminal tail that anchors to penton, a central shaft, and a C-terminal knob. The length of the shaft is dependent on the number of β -strand repeats and is variable between serotypes (5.5 in Ad 35 to 22.5 in Ad 12) [81]. The knob is responsible for receptor binding.

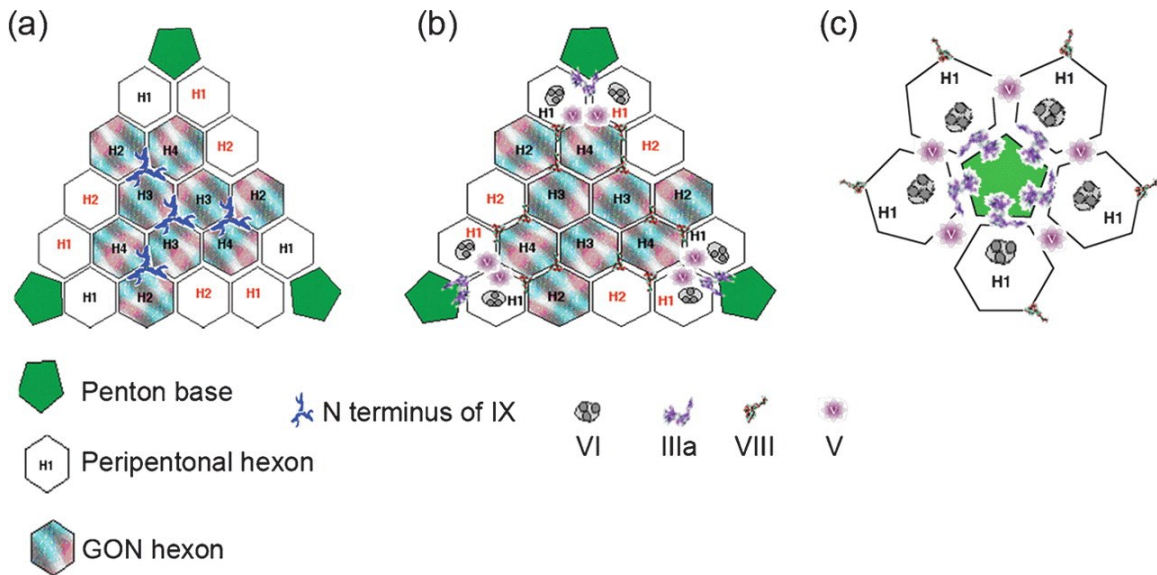


Figure 1.2.3 Facets of the Adenovirus Icosahedron

(A) External view of an adenovirus capsid facet. The GON hexons are multi-colored and the H1 peripentonal hexons are either lettered in black when they are on the same plane as the GONs or lettered in red where they are associated with GONs on a different facet. Similarly, the H2 hexons lettered in orange are associated with GONs on a different facet. The symbol for protein IX is not to scale. (B) Internal view of the adenovirus capsid facet with the same hexon designations as in (A). Note symbols for other structural proteins are not to scale. (C) Internal structure at the GOS

indicating hexon association with penton at the pentameric complex. Reprinted with permission from Russel, 2009 [74].

The minor capsid proteins are commonly referred to as cement proteins. They play integral roles in the formation of the overall capsid structure and GON and GOS designations. Cryo-electron microscopy (cryo-EM) has played an integral role in understanding the structure of the Ad capsid, and specifically the minor proteins. Imaging with 6 Å resolution provided key data on the location of the minor proteins, but it was not until structures were resolved at 3.6 Å that identification of the binding interactions of the minor proteins could be determined [82, 83]. Three of these minor proteins (IIIa, VI, and VIII) are synthesized as precursor proteins and then processed by the Adenovirus protease (AVP) for capsid maturation and will be discussed later.

Protein IX plays one of the most important structural roles in the formation and stability of the capsids. When capsids were dissociated under mild conditions, the GON structures remained intact and led to their aforementioned designation, while the 6 peripentonal hexons and penton in the GOS fully dissociated [84]. This disparity was later resolved when it was identified that 12 copies of the minor capsid protein IX reinforce the association of the hexon trimers at the GON 3-fold axes [85]. While capsids can assemble in the absence of IX, the resulting mutant capsids were substantially more thermolabile than wild-type virus, and following dissociation and sucrose gradient purification did not result in the canonical pattern of GOS and GON structures [86]. In total, 240 copies of IX are present in the Ad

capsid, making it the most abundant minor protein. While IX is present on the outside facets of the capsid the remaining three minor proteins (IIIa, VI, and VIII) reside within the interior of the capsid.

GOS structure and stability is provided by polypeptide IIIa. The important structural role between the GOS members led to the colloquial designation of IIIa as the GOS-glue domain. Five monomers of IIIa are present at each vertex, arranged in a ring around penton, and tether the peripentonal hexons to penton. This binding is facilitated by the N-terminal domain of IIIa. The C-terminus of IIIa possess a polypeptide VIII binding domain that enables tethering of the GOS members to the GON [76, 83]. Along with providing stability at the capsid vertex, IIIa has also been identified to play a role in conjunction with the Ad L1 52/55K protein to promote the packaging of the viral genome into assembled capsids through its positioning at the vertexes [87].

Polypeptide VIII functions as another interior surface protein of the capsid to provide structural support. Each capsid contains a total of ~120 copies of VIII. Stabilization of the AU occurs through a copy of VIII that binds to polypeptide IIIa on peripentonal hexons and the adjacent hexon trimers of the GON, as well as at the 3-fold axis among GON trimers. These binding interactions serve to 'glue' the GOS and GON together, keeping the 12 hexons on each facet bound to each other and providing structural support to the capsids. The monomers of VIII exist in extended conformations with a head, neck, and body domain. Each VIII monomer

binds with four hexon trimers [83]. Two hexons are bound on either side of the body, while the body and head domains each bind to a single hexon themselves.

The remaining minor protein, VI, plays a multi-dynamic role in capsid structure and the infectivity of the virus. Structurally, it binds to a loop in the inner cavity of the hexon trimers, as well as to the dsDNA viral genome [88, 89]. This association does not appear to follow icosahedral symmetry. It is estimated that there are ~360 copies of VI per capsid which is half the amount of hexon monomers (720), but more than the number of hexon trimers (240). It has been observed that VI acts as a cement protein, binding between the peripentonal hexon trimers and penton [72]. It forms a stable complex with polypeptides IIIa and V to stabilize GOS and GON associations, and also binds to polypeptide VIII to stabilize GON hexon trimers [72]. These interactions provide for a total of 6 monomers of polypeptide VI in each AU of the Ad capsid. Reddy *et al.* proposed that another copy of VI could associate with the central hexon trimer in the group of nine (**Figure 1.2.3** – designated H3). These associations would account for a total of 180 copies of VI (120 at the peripentonal interface and 60 at the GON central hexons). It is possible that the remaining copies may also function as non-structural core proteins. Along with its structural role, VI also plays an integral role in endosomal escape and nuclear trafficking as discussed in section 1.2.4.

The six additional Ad structural proteins (V, VII, μ , IVa2, terminal protein, and AVP) reside within the core of the assembled capsid. Like the minor capsid proteins, VII, μ , and terminal protease are cleaved by AVP in order to form mature infectious

particles. Proteins V, VII, and μ are positively charged and associate closely with the viral genome. Each capsid contains approximately 150 copies of V, 500 – 800 copies of VII, and 100 – 300 copies of μ [90]. Dissociation studies of assembled virions identified that disruption with pyridine resulted in cores with a thick fibrous appearance and a morphology similar to cellular chromatin. Following dissociation V, VII, and μ were still bound to the genome resulting in a “beads-on-a-string” morphology [91]. As previously mentioned, polypeptide V binds to both the genome and to polypeptide VI and IIIa. Although it is known that the C-terminus of V binds to VI and the N-terminus binds to the viral genome, the region that binds IIIa is unresolved [72]. These interactions serve to bridge the viral core to the capsid structure. There is limited knowledge on the properties of polypeptide μ , although it is believed to act with bridging functions between either V or VII, and the genome, potentially through protamine-like properties [74]. Polypeptide VII represents ~10% of the total mass of the Ad particle and directly interacts with the viral genome. Upon high ionic strength treatment conditions, only VII remained associated with the viral DNA. Micrococcal nuclease digestion of the resulting product following ionic dissociation resulted in the identification of protected fragments indicating a chromatin-like structure. The resulting products were of heterogeneous size and demonstrated that the associations are significantly less conserved than mammalian histones [91]. Polypeptide μ also plays a supportive role in DNA condensation in the core through charge based interactions between nine arginine residues and the phosphate backbone of the genome [92]. TP is the remaining minor protein that directly interacts with the Ad genome, binding to the

5' termini of the ITR. While it was originally believed that genome packaging was dependent on the presence of TP bound to the ITRs, evidence has since shown that it is not required [93, 94]. Polypeptide IVa2 is intimately involved in the packaging of the viral genome into the capsid. It associates with the late proteins L1 52/55K, L4 22K, and L4 33K to bind to the genome packaging domain, and also binds to polypeptide IIIa [95].

The remaining core protein synthesized from the L3 transcript, AVP, plays an extremely important role in the modification of capsid proteins necessary for capsid maturation. Proteomic studies have identified that each capsid contains ~5 copies of AVP, which process more than 2000 cleavage sites among minor coat proteins (IIIa, VI, and VIII), core proteins (VII, μ , terminal protein), and L1 52/55K following the assembly of the immature capsid (**Figure 1.2.4**) [90, 96]. AVP activation in immature capsids requires the presence of Ad DNA and 11 amino acids from the C-terminus of the precursor protein VI (pVI) [97]. Although not directly involved, recent studies have identified that AVP activity and specificity may be influenced by the presence of protein VII, with the condensation of the DNA and reduction in nucleocapsid pressure postulated as being responsible for efficiency of AVP [98].

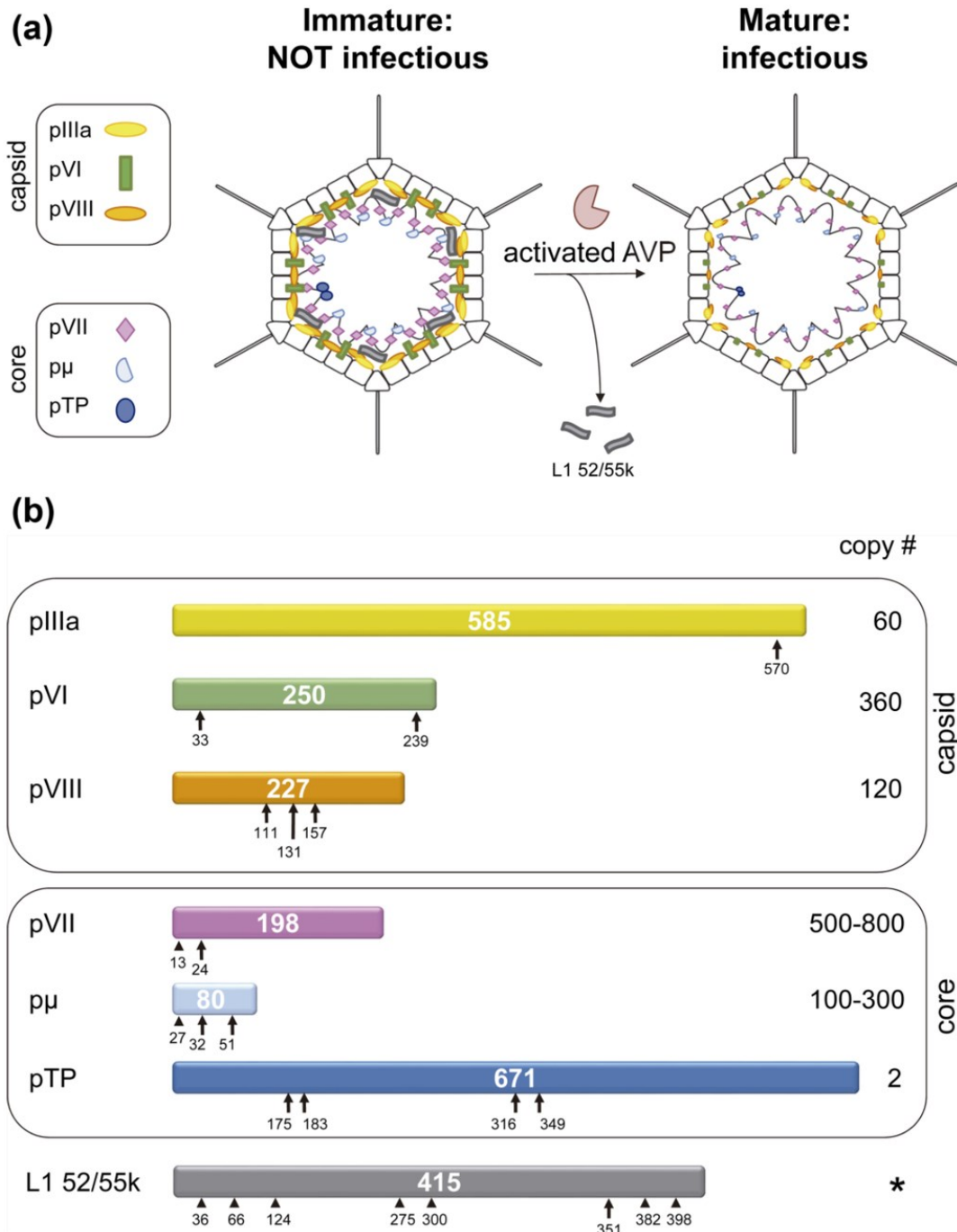


Figure 1.2.4 Substrates of the Ad Maturation Protease, AVP

(a) Schematics showing the location of substrates in the viral particle. **(b)** AVP cleavage sites are denoted by arrows for consensus cleavage sequence sites and arrowheads for non-consensus cleavage sequence sites. Reprinted under open access Creative Common CC BY license. Mangel, 2014 [96].

AVP first binds non-specifically to the viral genome, partially activating it, while pVI binds the viral genomes and diffuses in one-dimension until it intercepts AVP [99]. Once this occurs, AVP autoproteolytically cleaves off the C-terminal 11 amino acids required for activation and formation of the active site [96]. The formed complex remains on the viral genome and slides along to locate and process the precursor proteins [97, 99]. The role of DNA on AVP activity is not sequence specific but rather reliant on the high negative charge of nucleic acids; non-Ad DNA served to support AVP activity, including ssDNA, circular and dsDNA, and transfer RNA. The absence of DNA resulted in a 12-fold reduction in AVP activity [100]. Initial structural studies found that it had no similarity to previously identified proteases. Further studies found that the structure of the active site closely resembled the structure of papain, designating it as a cysteine protease that cleaves at two conserved sequence motifs: (M,I,L)XGX-G and (M,I,L)XGG-X [100]. A number of amino acids are restricted from the variable positions as they have been shown to inhibit AVP cleavage activity, although there is no side-chain specific grouping among them [96, 101]. Due to the density of the nucleocapsid core, the AVP precursor proteins are driven onto the DNA through their non-specific binding properties [91, 99, 102].

Prior to AVP editing, the precursor proteins pIIIa, pVI, pVII, pVIII, and p μ provide ordered structural support to the capsid. While mature capsids shed penton under adverse conditions (*e.g.*, 40 °C, pH 6), immature capsids remained intact, indicating that the precursor proteins likely play a role in stabilizing the vertexes

and preserving capsid curvature during packaging and assembly [103]. Cryo-EM studies between wildtype Ad2 and a temperature sensitive mutant (*ts1*) that does not package AVP found that there was excess density between the peripentonal hexons and the GON. This density is formed from the binding interactions of polypeptide IIIa and polypeptide VIII, forming a “molecular stitch” in the immature capsid [83, 104]. Without AVP cleavage the presence of this stitch is inhibitory to capsid uncoating during infection. Similarly, increased density was observed within the hexon trimers when occupied by pVI. This stronger interaction may inhibit the release of polypeptide VI required for endosomal escape as seen in mature capsids [104]. Protein L1 52/55K also acts in a scaffolding role during capsid assembly, bridging the capsid structure to the genome through its interaction with the Ad packaging signal, IVa2, VII, and IIIa. Following AVP activity these associations are destroyed and L1 52/55K can be released from the virion. It is unclear if further processing by unknown factors is involved in the degradation and release of L1 52/55K [96].

Finally, AVP editing of the viral core proteins is integral for the process of genome replication in infected cells. Processing of pVII and p μ reduces the compaction of the genome, leading to a less organized structure than observed in immature capsids. This reduction in genome compaction increases the accessibility of the genome to cellular replication machinery following infection [104]. The purpose of AVP editing of TP is less clear, although it is believed that processed TP could be responsible for targeting the genomes to the nucleus after endosomal escape in

infected cells, and that mature TP works to enhance genome replication early in infection [96].

Once capsids have assembled and are packaged with viral genomes, the viral progeny must escape from the infected cells. Along with the editing of viral proteins, AVP has also been shown to cleave cytokeratin K18 and actin, which results in the destabilization of the cytoplasm [105]. Similarly, the E3 encoded ADP plays a role in nuclear membrane breakdown in late infections facilitating viral progeny escape from the nucleus and lysis of the cell [62]. At late stages of infection excessive amounts of autophagosomes have been observed, which could lead to further disruption of the cytoplasmic organization, potentially leading to autophagy mediated release of the viral progeny [106].

1.2.4 Mechanism of Cellular Entry, Trafficking, & Replication

The fiber protein is necessary for binding the primary coxsackie and adenovirus receptor (CAR). This receptor is a tight junction protein that interacts with ZO-1 on the cell surface [107, 108]. A number of additional alternative receptors have been identified, including CD46, heparan sulfate glycosaminoglycans, and desmoglein [37]. Following receptor binding, the loop region of penton binds to secondary receptors, such as α_v integrins through an exposed Arg-Gly-Asp (RGD) motif, or α_4 intergrins through a Leu-Asp-Val (LAV) motif [109, 110]. These binding events enable viral internalization either through clathrin-coated vesicles or macropinosomes [111].

Fiber protein is lost from the capsid following receptor binding and internalization and results in destabilization and loss of the proteins at the vertexes (penton, fiber, and VI). This is a crucial step as protein VI is required for endosomal escape through its membrane lytic domain (aa34 – 54). While endosomal acidification was believed to be responsible for the uncoating and morphological alterations in protein VI for endosomal lysis, recent studies have identified that the process can proceed in a pH-independent manner [112]. In the case of wild-type infections acidification results in increased endosomal escape, achieving a maximum rate at pH 5 [112]. Deconstruction of the capsid from acidification results in significant loss of capsid proteins at the vertexes (penton, fiber, and VI), as well as loss or significant reduction in minor proteins (IIIa, VIII, and IX) [112, 113]. During this process of cell entry, adenovirus activates multiple pattern recognition receptors, which induces the production of numerous inflammatory cytokines and chemokines. These perturbations will be discussed later in the section covering pathogenesis (1.2.5).

Following endosomal escape, the remaining hexon proteins of the capsid are able to recruit and bind dynein for microtubule transport to the nuclear membrane. Trafficking is assisted by the association of capsid retained protein VI with the E3 ubiquitin ligase Nedd4 [113, 114]. Once at the nuclear membrane, attachment is facilitated through the binding of hexon protein to the cytoplasmic facing nucleoporin 214 (nup214) at the nuclear pore complex (NPC) [115]. Nup214 exists in a complex with a multitude of nup's at the NPC, including a cytoplasmic facing nup358 and nuclear pore channel nup62. Following hexon attachment to nup214,

the partially disassembled capsid binds to the kinesin-1-light-chain through protein IX while nup358 binds to the kinesin-1-heavy-chain. This association with the kinesin motor complex results in complete disassembly of the capsid and disruption of the NPC through the pulling action of kinesin away from the nucleus, allowing for entry of viral genomes into the nucleus from increased NPC permeability [116].

Once the viral genome has entered the nucleus, viral replication compartments form. Initial expression of the E1A gene is blocked by cellular transcriptional repressors, such as the interferon inducible promyelocytic nuclear body (PML-NB) and protein death domain associated protein (Daxx). These PML-NBs are commonly found in close association with the replication compartments of DNA viruses such as HSV-1, Ad, HCMV, and HPV [117]. The spatial interaction between PML-NBs and the replication compartments has indicated that not only do they serve as repressors for host genes, but that they also play important roles in antiviral defense. To overcome this transcriptional repression the protein VI-Nedd4 complex is able to target the E1A promoter bound Daxx for removal, enabling expression [117]. The mediation of the effects of Daxx is carried forward during replication by E1B-55K, which can also bind Daxx, resulting in proteasomal degradation [118]. Once Daxx has been freed from the E1A promoter, adenovirus transcription can begin through host DNA-dependent RNA polymerase II activity. Transcription of the E2 genes results in the production of the previously described pTP, DBP, and Ad polymerase. Transcription initiation relies on the presence of the core origin region at the extreme 5' terminus which can bind pTP/TP and Ad

polymerase, as well as the auxiliary region for the cellular nuclear transcription factor 1 (NF1) and Oct-1 [119, 120]. DBP stimulates the binding of Ad polymerase to NF1, while Oct-1 tethers pTP/TP to the genome, and the action of the cellular factors induces a bend in the genome. Replication then begins at nucleotide position 4 of the genome [120]. Replication proceeds in a processive fashion from both ends of the genome, with DBP acting to increase rate of replication initiation, increase processivity, facilitate strand displacement, and protect ssDNA intermediates from nuclease attack [119]. Topoisomerase I also participates in stabilizing chain elongation during replication. Replication continues in the replication compartments and eventually protein VII, which has histone like properties, and the packaging ATPase IVa2 become associated with the complexes. Debate exists as to whether genomes are packaged into pre-formed capsids or if capsid structures assemble around the viral replication complexes [37, 121]. Experiments have uncovered that in the case of genome packaging into pre-formed capsids that Ad proteins IVa2, L1 52/55K, and an L4 protein product associate with a packaging domain on the left end of the genome and cooperatively function to drive the insertion of viral genomes [122].

1.2.5 Pathogenesis of Adenoviruses

Adenoviruses are a globally-circulating persistent pathogen and infection is common in young children. They account for ~8% of all childhood respiratory illnesses, ~10% of febrile illnesses, and ~5 – 10% of gastrointestinal infections [123, 124]. Infection with serotypes 2 and 5 are the most common with ~45 – 80%

of adults seropositive, although these rates vary based on geographic regions [124, 125]. Transmission occurs most commonly through aerosol-droplets, fecal-oral routes, and fomites, although rarer transmission has been noted during birth and following organ transplants [126-129]. Between the subgroups, Ad utilizes various primary and secondary receptors resulting in differing tropisms between the species (**Table 1.2.1**) [130].

Table 1.2.1. Classification^A and Selected Features of Human Adenoviruses

Specie	Serotype	Receptor(s) ^B	Adapter molecules ^C	Fiber shaft repeats	RGD motif	Tropism	Seroprev. (%) ^D
A	12, 18, 31	CAR	FIX, FX	23	Yes	Cryptic (enteric, respiratory)	35–70
B1	3, 7, 16, 21, 50	CD46, DSG2, CD80, CD86	FX	6	Yes	Respiratory ocular	2–15 (Ad16, 21, 50) 35–70 (Ad3, 7)
B2	11, 14, 34, 35	CD46, DSG2, CD80, CD86	FX	6	Yes	Renal Respiratory ocular	1–3 (Ad11, 34, 35) 18 (Ad14)
C	1, 2, 5, 6	CAR, VCAM-1, HSPG, MHC1- α 2, SR	FIX, FX, Lf, DPPC	22/18 ^E	Yes	Respiratory ocular lymphoid hepatic	40–80

Specie	Serotype	Receptor(s) ^B	Adapter molecules ^C	Fiber shaft repeats	RGD motif	Tropism	Seroprev. (%) ^D
D	8–10, 13, 15, 17, 19, 20, 22–30, 32, 33, 36–39, 42–49, 51, 53, 54	SA, CD46, CAR	FX	8	Yes	Ocular enteric	3–40
E	4	CAR		12	Yes	Respiratory ocular	45
F	40, 41	CAR		12 (short fiber) 21/22 (long fiber)	No	Enteric	41 (together) ^F
G	52	ND		9 (short fiber) 17 (long fiber)	Yes	Enteric	ND

(A) Acc. to [131]. Ad52 and above have not been serologically characterized and should therefore be referred to as types rather than serotypes. (B) Abbreviations: ND, not determined; CAR, coxsackie and adenovirus receptor; FIX/FX, coagulation factor IX and X, respectively; DSG2, desmoglein-2; Lf, lactoferrin; DPPC, dipalmitoyl phosphatidylcholine; VCAM-1, vascular cell adhesion molecule-1; HSPG, heparan sulfate proteoglycan; MHC1- α 2, major histocompatibility complex- α 2; SR, scavenger receptor; SA, sialic acid. (C) FX and FIX have been shown to bind with different affinities to specific members of species A, B, C, and/or D 63, 65, 71, but have not been shown to promote binding to and/or entry of all these adenoviruses to host cells. The members of species E–G have not been analyzed for FX binding/utilization. (D) Acc. to [132]. (E) Ad6 has only 18 repeats. (F) Acc. to [133]. Reprinted with permission from Arnberg, 2012 [130].

Viral shedding can occur for weeks to years, with lymphoid organs serving as the site for persistent infections [124]. Virions are highly stable at room temperature

and can remain infectious on some surfaces for up to 3 weeks [129]. Common at risk populations include young children; those in crowded quarters such as communities, schools, dormitories, and military facilities; and immunocompromised individuals [126]. While infections in healthy immunocompetent individuals are typically self-limiting and resolve without significant issues, immunocompromised individuals are plagued by high rates of morbidity and mortality [129, 134]. Ad infection typically presents as upper/lower respiratory infections or keratoconjunctivitis, but it can progress to disseminated severe infections that include acute respiratory distress syndrome, pneumonia, gastroenteritis, acute febrile pharyngitis, pharyngoconjunctival fever, acute respiratory disease, pneumonia, pertussis-like syndrome, acute hemorrhagic cystitis, meningoencephalitis, and hepatitis (**Table 1.2.2**) [129, 134, 135].

Table 1.2.2 Association of Adenoviral Diseases and Principal Serotypes in Immunocompetent and Immunocompromised Individuals

Syndrome	Principal serotype(s) in species					
	A	B	C	D	E	F
Upper respiratory illness		All	All			
Lower respiratory illness		3, 7, 21			4	
Pertussis syndrome			5			

Syndrome	Principal serotype(s) in species					
	A	B	C	D	E	F
Acute respiratory disease		7, 14, 21			4	
Acute conjunctivitis		7	1, 2, 3		4	
Acute hemorrhagic conjunctivitis		11				
Pharyngoconjunctival fever		3, 7				
Epidemic keratoconjunctivitis				8, 19, 37		
Gastroenteritis						40, 41
Hemorrhagic cystitis		7, 11, 34, 35				
Hepatitis		3, 7	1, 2, 5			
Myocarditis		7, 21				
Meningoencephalitis		7	2, 5			
Venereal disease			2			
Disseminated disease	31	11, 34, 35	1, 2, 5			40

Reprinted with Permission from Echavarría, 2008 [129].

Currently no vaccine is available for the general public, although all US Department of Defense and Coast Guard basic trainees currently receive oral vaccines against Ad4 and Ad7. The vaccination policy among recruits was instituted due to the significant rates of infection (~80%), disease burden, and likelihood to cause acute respiratory distress [136, 137]. During a 12-year hiatus (1999 – 2011) when vaccine production stopped, the military observed dramatic increases in infections among recruits with significant financial repercussions. There are no specifically approved drugs to treat Ad infections. Cidofovir is used for some pediatric stem cell transplant patients when Ad is detected as it can function as an Ad DNA polymerase chain terminator [138]. Recently, brincidofovir (CMX001), a lipid conjugate of cidofovir, has been tested as it displays better intracellular concentrations, reduced nephrotoxicity, and good oral bioavailability [139].

1.2.5.1 Immunological Response

Infection with WT Ad most commonly occurs via the airway, utilizing either the CAR or CD46 receptors on cell surfaces. Epithelial cells and resident macrophages play important roles in the initial immune response. Studies with Ad5 vectors with deletions in E1 and E3 identified that macrophage internalization occurred within 1 minute of challenge, consistently increasing over time in mice, but that over 65% of the administered vector was eliminated within 24 hours with rapid destruction of the viral genome [140, 141]. Infection of cells stimulates a strong innate immune response due to the pathogen associated molecular patterns (PAMPs) of the capsid and viral genome. These PAMPs are recognized by pattern recognition

receptors (PRRs), inducing the production of type I interferons and pro-inflammatory cytokines and chemokines. The binding of fiber knob to CAR and subsequent penton binding to α v integrins triggers a signaling cascade, inducing nuclear factor kappa-light-chain-enhancer of activated B cells (NF- κ B) through I κ B kinase (IKK) (**Figure 1.2.5**) [142]. After cellular entry, further inflammatory cascade pathways are triggered through the activation of cytosolic DNA sensors by the viral genome. These include toll-like receptor 9 (TLR9), nucleotide-binding oligomerization domain-like receptors (NLRs), retinoic acid-inducible gene-1 like receptors (RLRs), and guanosine monophosphate-AMP synthase/stimulator of interferon genes (cGAS/STING) [142-146].

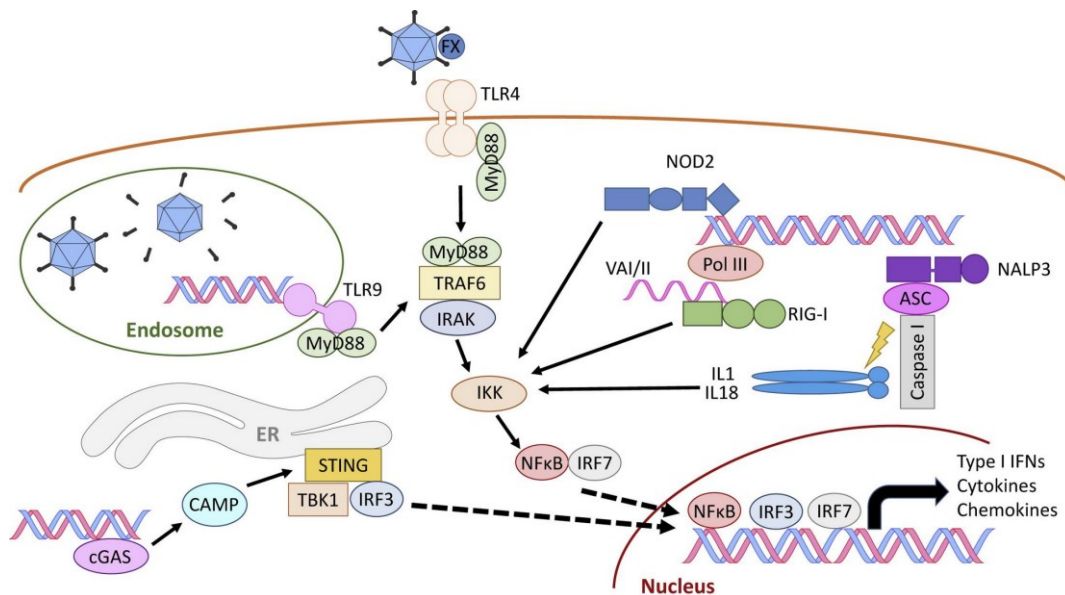


Figure 1.2.5 Activation of Inflammatory Signaling by Adenovirus Infection

The anti-adenoviral immune response is triggered by recognition of pathogen-associated molecular patterns (PAMPs) by PRRs. The membrane surface Toll-like receptor 4 (TLR4) recognizes the

adenoviral capsid prior to viral entry. Following internalization and uncoating, the presence of cytosolic dsDNA results in activation of signaling from TLR9, NOD2, NALP3, and cGAS/STING. These signaling pathways result in the production of type I IFNs and inflammatory cytokines and chemokines. Reprinted under Creative Commons Attribution-Non-Commercial No-Derivatives License, Shaw and Suzuki, 2019 [142]

Expression of the E1A transcription products is able to negatively modulate these responses by repressing the expression of interferon-induced genes and chemokine gene transcription [48, 147, 148]. This activity is likely the reason that the majority of Ad infections are mildly symptomatic and subclinical. In contrast, expression of E1B-55K has been connected to increased TNF- α and IL-6 responses following infection of cotton rat and C57BL/6J mouse lungs [149]. The release of chemotactic molecules recruits immune cells to the site of infection. Antigen presentation through MHC-I and/or MHC-II results in activation of both CD4⁺ and CD8⁺ T cells, as well as natural killer cells [150]. The E3 transcription unit counteracts this activation by downregulating the expression of MHC-I on infected cells, and the secreted E3-49K protein can bind CD45 receptors to suppress natural killer and T cells [151]. Similar activity is obtained through the expression of E3-19K, E3-14.7K, E3-14.5, and E3-10.4K, which function to block the induction of apoptosis by cytotoxic T lymphocytes and macrophages. The elicited Ad-specific immune responses predominantly recognize hexon regions of the capsid. Due to conservation of these regions between Ad serotypes, the elicited CD4⁺ and CD8⁺ T cells are able to cross-react against different serotypes [152-155]. This activity was observed to carry over to non-human serotypes, including chimpanzee adenovirus 6 and 7 [156]. Activation of B cells leads to the

production of serotype-specific antibodies that are directed primarily against the hexon protein of the capsid, although antibodies against fiber and penton do possess neutralizing activity [157, 158]. Studies with Wistar rats that received 3 injections of a replication-defective Ad5 in their parotid gland found that while serum IgM and IgG levels rose after injections on day 0 and day 7, by day 10 serum IgM levels had begun to wane while IgG continued to increase. The third injection on day 14 had no effect on IgM levels and throughout the study no IgA was detectable in the collected serum [159]. Neutralizing antibodies facilitate virus inhibition either through extracellular mechanisms to prevent virus binding to cell receptors, or intracellularly to prevent either endosomal escape or subsequent microtubule trafficking [160-162]. Working in concert, these activities lead to the elimination of Ad following infection.

Initial studies in hamsters and other small rodents led to the designation of Ad species A and B as highly and weakly oncogenic, respectively. Infection of rodent cells has indicated the E1A functions with oncogene properties to immortalize cells and drive the transformation to cancer. While little evidence exists to connect Ad infection to oncogenesis in humans, analysis of pediatric cancers did identify an increased presence of Ad genomes in brain tumors but not in other solid tumors, lymphomas, or leukemias [163-165]. Similarly, a study in 1976 investigated whether DNA from Ad12, a member of the highly oncogenic species A, was present or upregulated between normal and cancerous human gastrointestinal tissues as it is commonly found in fecal excrement. Between 18 normal and 34

gastrointestinal tumors (colon, rectum, small intestine, and stomach) no viral sequences were detected. Assessment of lung tissues between cancerous and healthy human patient tissues again found no genomes in these tissues, indicating that Ad did not play a role in oncogenic transformation [165]. The disparity of these findings between small animals and humans is still unresolved and questions remain on the oncogenic properties of Ad. Interestingly, E1A has been shown to reverse the epithelial-to-mesenchymal cell transition that is a defining feature of carcinoma development, introducing more speculation on the oncogenic properties of adenovirus [47].

1.3 Adeno-Associated Virus

1.3.1 Classification

Adeno-associated virus (AAV) is a linear ssDNA virus with an ~4.7 kb genome. It encodes two genes – *rep* and *cap* – and is flanked by two inverted terminal repeats. The genome is packaged into a small icosahedral capsid (~26 nm) with $T = 1$ symmetry. It belongs to the family *Parvoviridae*, genus *Dependoparvovirus*. AAV was originally discovered as a contaminate in both simian and human adenovirus stocks in 1965 and was determined to act as a non-efficient replicative virus in the absence of adenovirus. Due to the relative simplicity of the viral genome, it serves as an easy to manipulate virus to study the biology of icosahedral capsid assembly. Along with adenovirus, it was later identified that herpes simplex virus 1 (HSV1) was also capable of acting as a helper virus [166-168]. Additional studies have identified that these helper functions are not limited to Ad and HSV1. A number of *herpesviridae* family members are capable of acting as helper viruses including

human cytomegalovirus, varicella-zoster virus, Epstein-Barr virus, and human herpesvirus 6 [169-172]. Additionally, vaccinia virus and papilloma virus are also capable of supporting AAV replication [173, 174].

Isolation of AAV from tissue culture stocks, humans, and non-human primates has led to the identification of thirteen distinct serotypes (AAV1-13)[175], but research continues to unveil new isolates in a wide range of other animals, including bats, chickens, snakes, cows, and pigs [176]. Of these, AAV serotype 2 (AAV2) has been the prototypically studied human serotype. AAVs are classified into clades A – F, although some such as AAV4 and 5 are not members of a designated clade (**Figure 1.3.1**) [177].

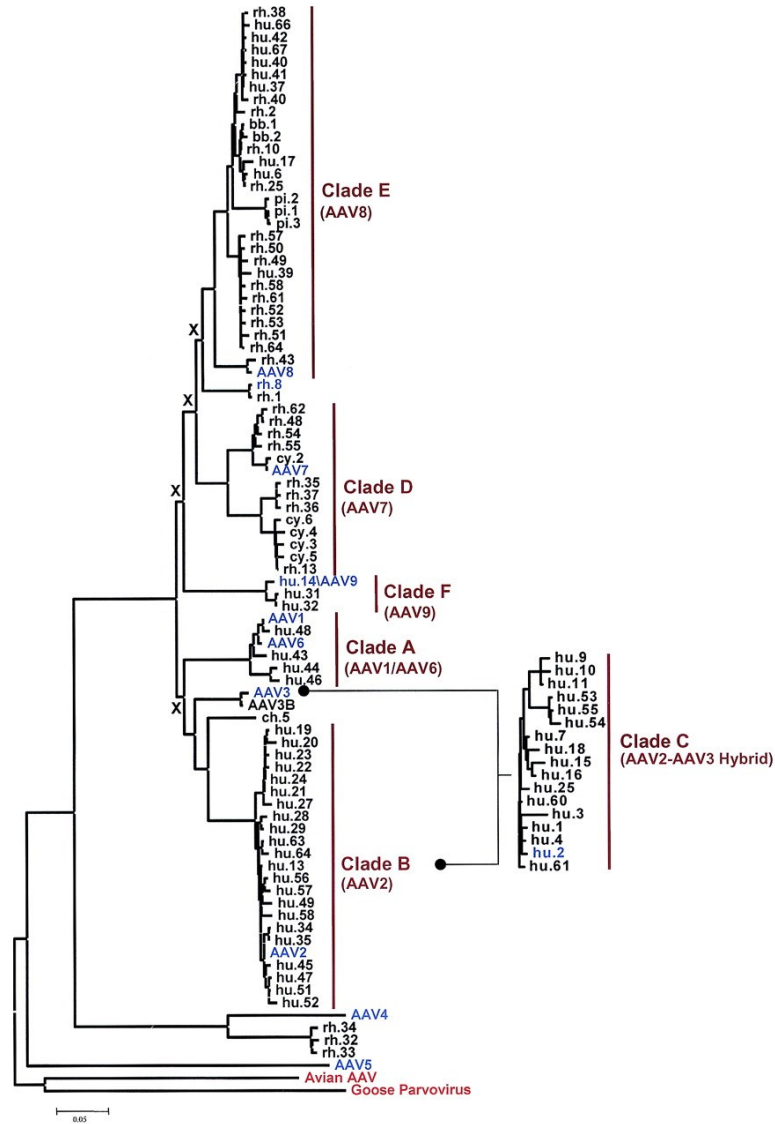


Figure 1.3.1 Clades of AAV

Designated groupings of AAV serotypes into clades. Reprinted with permission from Gao *et al.*, 2004 [177].

1.3.2 Genome & Viral Proteins

AAV2 has provided a significant amount of data on the genome features and lifecycle of AAV. The AAV genome consists of two flanking inverted terminal

repeats (ITR), two open reading frames (*rep* and *cap*), and a polyadenylation signal (Figure 1.3.2). Within the genome there are three promoters – p5, p19, and p40 – designated by their map position in the genome.

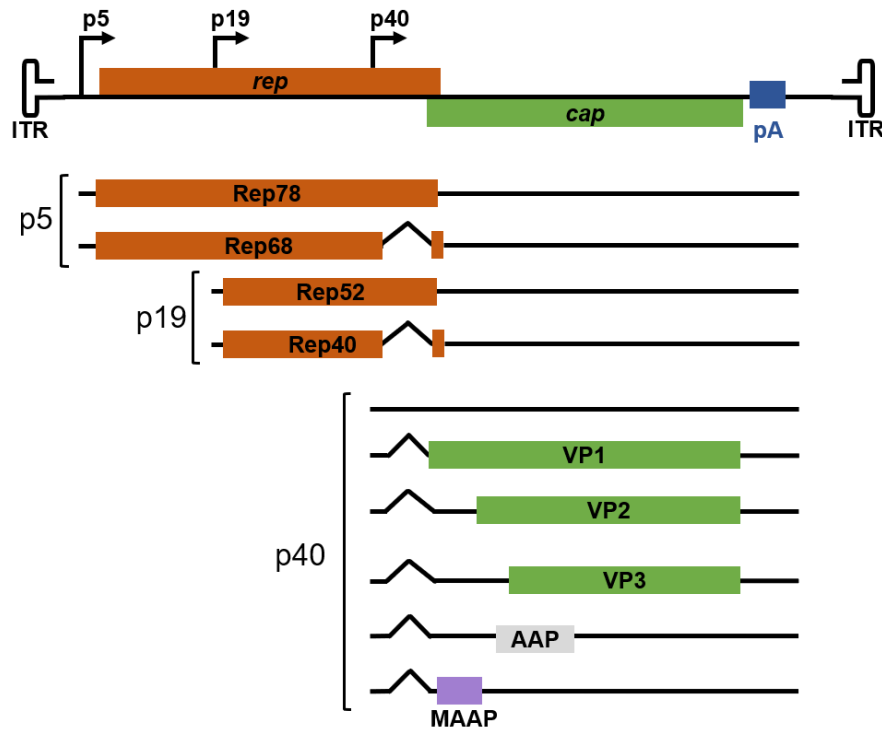


Figure 1.3.2 Organization of the AAV2 Genome

The organization of the AAV2 genome is displayed, representing the positions of the ITRs; p5, p19, and p40 promoters (arrows); and the *rep* and *cap* genes (orange and green rectangles respectively). The *rep* gene is responsible for the production of 4 proteins: Rep 78 and Rep 68 from the p5 promoter, and Rep52 and Rep40 from the p19 promoter. The *cap* gene is responsible for the production of three mRNA products from the p40 promoter: a 2.6 kb sequence with no known function (line), a 2.3 kb mRNA that encodes VP1 and MAAP, and a 2.3 kb mRNA that encodes VP2 and VP3. It is currently unknown which p40 mRNA sequence(s) is responsible for the +1 reading frame products AAP and MAAP. Splice sites are indicated by chevrons. Positions of the genes for AAV2 are: ITR: 1 – 145; 4535 – 4679; p5 TATA box: 265 - 271; p19 TATA box: 843-849; p40 TATA box: 1822 - 1827; Rep: 321 – 2252; Rep78: 321 – 2186; Rep68: 321 – 1906, 2228 – 2252; Rep52: 993 – 2186; Rep40: 993 – 1906, 2228 – 2252; VP: 2203 – 4410; VP1:2203 – 4410; VP2: 2614 – 4410; VP3: 2809 – 4410; Splice site: 1906-2201 and 1906 – 2228 ; AAP: 2729 – 3343; MAAP: ~2282 – 2642; PA: 4420. Genome features from NCBI Reference Sequence: NC_001401.2 [178, 179].

The ITRs consist of 145 nucleotides. The terminal 125 nucleotides consist of 6 palindromic repeats (A, A', B, B', C, and C') that form a T-shaped hairpin structure, as well as an unpaired and thus single stranded D domain of 20 nucleotides. The ITRs exist in alternative configurations, referred to as 'flip' or 'flop'. While these arrangements do not alter the orientation of the A, A', and D domains, it does result in the B and B' domains flipping places with the C and C' domains. The ITRs play an important role in replication, genome packaging, and insertion in the host genome for wildtype virus through a Rep recognition element (RRE) and a terminal recognition sequence (TRS) [180-182].

The *rep* gene produces four proteins through the process of alternative splicing and the use of alternative start codons p5 and p19. The proteins were named by their molecular weight in kilodaltons, resulting in Rep78, Rep68, Rep52, and Rep40. Rep78 and Rep68, the largest, are produced from the p5 promoter, and Rep68 is smaller due to C-terminal splicing [183, 184]. Together these two genes (Rep68/78) are fundamental for virus replication, gene expression, and chromosomal integration. Rep78 has been shown to induce S phase arrest of infected cells, inhibiting DNA replication, and has also been implicated in both caspase dependent and independent apoptosis pathways [185, 186]. Both possess DNA-binding, site and strand specific endonuclease, helicase, and ATPase activity intrinsically required for the AAV lifecycle. Rep68/78 can both bind to the RRE present in the ITRs to recruit the replication complex machinery.

Binding to this site is also important in later stages of replication, as it enables Rep68/78 to nick the ITRs at the TRS, creating a 3' hydroxyl primer for host-cell polymerase to complete synthesis. This replication process will be discussed later.

Rep68/78 also plays an important role in enabling AAV to establish persistent latent infections through insertion into the host genome. Human chromosome 19 (19q13.3-qter) contains an AAV integration site (AAVS1). This site consists of a CpG island with a GCTC motif that allows for Rep68/78 binding as well as a TRS [187-189]. While this site is the preferential integration site in cultured cells, it is not the only site where AAV integration has been observed. Wietzman *et al.* identified that 20-30% of integrations occurred outside of this domain [190]. The existence of the GCTC motif in the genome outside of AAVS1 suggest that other regions, potentially with lower Rep68/78 binding stability, can act as integration sites. As AAV integration is mediated by non-homologous end joining pathway members, integration sites where there is a GCTC motif but no TRS could occur during dsDNA break events [190, 191].

Rep52 and Rep40 are the smaller of the four *rep* proteins and are produced from the p19 promoter. Rep40, like Rep68, is also smaller due to C-terminal splicing. Much like Rep68/78, they are involved in multiple activities required for the AAV lifecycle, including helicase activity and genome packaging into capsids. These *rep* proteins also have a wide array of interactions with cellular proteins, including those in pathways of transcription, translation, splicing, protein degradation, DNA replication or repair, and cell cycle regulation [186, 192].

The *cap* gene encodes 3 structural viral proteins (VP) – VP1, VP2, and VP3 – as well as assembly-activating protein (AAP) and membrane-associated accessory protein (MAAP). The 3 structural proteins share the same C-terminal domain, but differ in their N-terminus, resulting in approximate molecular weights of 87, 72, and 60 kDa. The VPs are synthesized from the p40 promoter and three species are produced that include an unspliced 2.6 kb transcript, and two splice transcripts that are approximately 2.3 kb in size. The 2.6 kb has not been identified to code for any proteins and remains cytoplasmic [193]. In contrast, the alternative splicing used to create the 2.3 kb transcripts utilizes the splice donor site at nucleotide 1906 and acceptor sites at nucleotide 2201 or 2228. In the absence of a helper virus both splice products are observed in equivalent amounts, but upon co-infection the 2228 splice site is favored and significantly more abundant [193]. From the splice products, VP1 is produced from the less abundant 2201 splice site product, while VP2 and VP3 are produced from the 2228 splice site product. Production of VP2 and VP3 from a single mRNA transcript occurs through the use of an ACG and downstream ATG codon respectively [194]. VP3 is the most abundant of the VPs owing to its canonical promoter and abundance as the major splice product. These proteins assemble to form the icosahedral capsid in a ratio of ~1:1:10 for a total of 60 copies of VP1, VP2, and VP3, respectively [193, 195]. The unique N-terminus of VP1 contains a phospholipase A2 domain (PLA2), as well as 3 basic amino acid regions. PLA2 has been found to play a necessary role in endosomal escape, while the basic regions play an important role in intracellular trafficking and resemble nuclear localization signal (NLS) domains [196].

Recently, two proteins have been identified in *cap* from +1 shifted reading frames. AAP is a small protein (23 kDa) that has been shown to be essential for the assembly of functional AAV capsids in a number of AAV serotypes [197, 198]. To date, AAV4, 5, and 11 have been identified as serotypes capable of AAP independent capsid assembly (Chapter 3) [198]. In contrast, serotypes AAV1, 3, and 9 have been found to require expression of only a portion of the AAP N-terminus to direct capsid assembly [199]. Intriguingly, it does not appear that the AAP independent and AAP truncation phenotype is phylogenetically conserved. Although AAV5 resides in a unique phylogenetic clade by itself, that is not the case for the others. AAV4 and 11 are members of a clade with the AAP-dependent AAV12, just as AAV1, 3 and 9 are in clades with full-length AAP-dependent serotypes (**Figure 1.3.1**)[200, 201].

The C- and N-terminus of AAP serve two distinct and critically important roles in capsid assembly. The N-terminal domain contains two hydrophobic domains that are necessary to bind VP proteins [200, 202]. The C-terminal domain is enriched with basic amino acid rich sequences that function as nucleus and nucleolar localizing signals [200, 202]. The function of these signals, in combination with the nuclear localization signals on the VP proteins, enables nuclear localization and subsequent assembly of the capsid [203]. Some AAV serotypes, such as AAV2 and AAV4 have shown distinct localization of assembled capsids and AAP in the nucleoli and subnuclear bodies by colocalization with the nucleolus concentrated protein nucleostemin [198, 204]. These findings indicated an importance of capsid

assembly and/or trafficking of assembled capsids for AAV2 and AAV4 through these compartments, while others such as AAV5, AAV8, and AAV9 did not show such an enrichment (**Chapter 3 – Figure 3.5**). Recently Maurer *et al.* identified that AAP plays a structural support role in VP trimer oligomerization at the 3- and 5-fold capsid axes. Binding of AAP to these regions results in stabilization of VP monomers and helps facilitate oligomerization [205]. Structural analysis of this region has identified factors which could influence the dependence on AAP for capsid assembly. AAP independent serotypes were observed to contain a number of residues in this domain that resulted in reduced hydrophobicity as well as an increase in the formation of hydrogen bonds and salt-bridges [199]. While these features are likely sufficient to enable oligomerization, AAP does still act as a catalyst for capsid assembly in AAP-independent serotypes. These functions of AAP may have played an important evolutionary role for AAV; increasing the mutational freedom for the VP sequences while still enabling faithful capsid assembly [199]. Potential host-cell AAP interactions may exist but have not been clearly identified to date. Previous data has indicated that AAP may have DNA binding properties. 4',6-diamidino-2-phenylindole (DAPI) staining on HeLa cells overexpressing AAP had observable chromatin condensation [206].

MAAP is the most recently identified frame shifted protein from the *cap* cassette. It is also a small protein (~16 kDa) that resides in a +1 frameshifted ORF in VP1 [207]. The exact mechanism and function of MAAP is still unresolved but it appears to be involved in replication and production of AAV.

1.3.3 Mechanisms of Cellular Entry, Trafficking, & Replication

In order to bind to cells, it has been long thought that AAV2 utilizes the promiscuous heparan sulfate proteoglycan (HSPG). A variety of glycans including N-terminal galactose, and N- and O-linked sialic moieties can also be used by various serotypes [208]. Additional secondary receptors, such as human fibroblast growth factor receptor and hepatocyte growth factor receptor have been identified, but their importance for viral binding and entry *in vivo* has not proven them to be essential receptors [209]. Recently though, AAV receptor (AAVR) has been identified as playing a crucial role in the infection cycle for many serotypes (**Figure 1.3.3**) [210]. AAVR is a highly conserved glycosylated membrane protein that recycles from the *trans*-Golgi to the plasma membrane using endosomal vesicles. As such, its role in AAV infection is believed to reside in trafficking endocytosed virus to or out of the Golgi network [209, 211]. AAV2 is known to traffic through perinuclear regions and has been visualized in the Golgi so such an approach is quite plausible [212]. Currently it is unknown at what specific step of infection productive AAV and AAVR interaction occurs, but it has been theorized that it could occur either at the cell surface to facilitate endosomal uptake, within the endosome to deliver AAV to the *trans*-Golgi, or once in the Golgi network it could be involved in *trans*-Golgi escape [210]. AAVR has been identified as non-dispensable for AAV1, AAV2, AAV3B, AAV5, AAV6, AAV8, and AAV9 infection. CRISPR/Cas9 mediated knockouts of AAVR in *in vitro* and *in vivo* experiments have identified that the absence of the receptor substantially decreases the infectivity of these serotypes. Recently, an additional highly conserved receptor, GPR-108, was also

found to play a key role in the entry process for many serotypes [213]. Knockouts of GPR-108 and AAVR did not affect the amount of virus bound to the cell, suggesting that their role is downstream of virus binding. As both of these receptors are present in the Golgi network, it could suggest that AAV undergoes endosomal trafficking to the endomembrane system prior to endosomal escape. This approach would remove the need to escape into the cytoplasm for subsequent cytoplasmic trafficking to the endomembrane system.

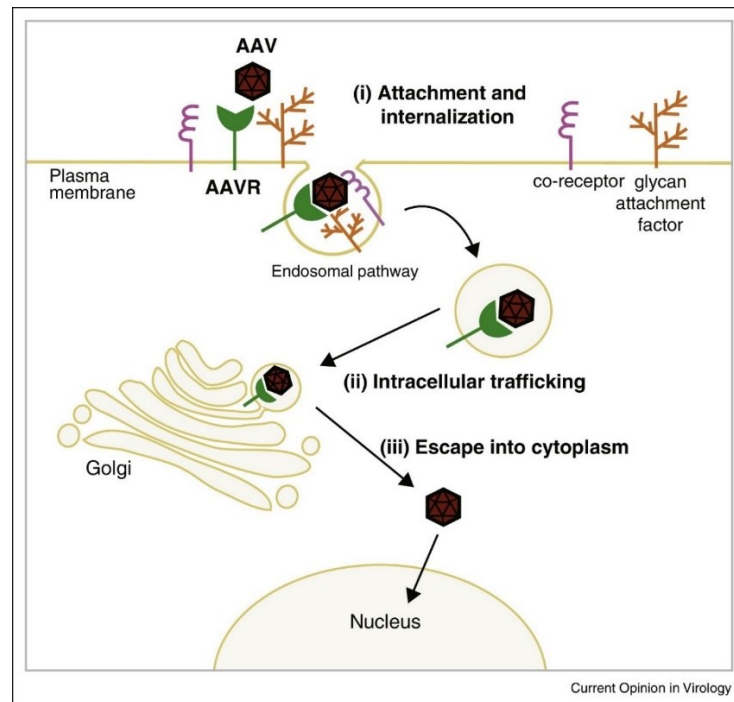


Figure 1.3.3 Representation of the AAVR Trafficking Pathway

(i) AAV binds to glycan attachment factors and co-receptors at the cell surface, facilitating subsequent binding to AAVR either at the cell surface, inside the endosome, or at the trans-Golgi network. (ii) After entering the endosomal pathway AAV is trafficked to the trans-Golgi network, likely facilitated through the native recycling pathway of AAVR. (iii) AAV escapes the trans-Golgi network and is able to traffic to the nucleus through the cytoplasm. Reprinted with permission from Pillay and Carette, 2017 [210].

The predominant mechanism of cell entry following binding remains unclear. Groups have shown that AAV2 utilizes clathrin-dependent, clathrin-independent, and $\alpha V\beta 5$ integrin/Rac-1-dependent mechanisms. [214-216]. The breadth of potential routes and contradictory data suggests that promiscuity may exist, and that entry is not beholden to a single mechanism. Trafficking of AAV containing endosomes has been shown to be facilitated predominantly by microtubule and/or microfilament transport. Disruption of the microtubule network with nocodazole inhibited AAV2 transduction at least 2-fold compared to wildtype cells [217]. The ability of AAVR to bind to VP3 capsid proteins may function as an alternative or supportive trafficking factor during infection [218, 219]. Escape from the endosomes occurs through the mechanism of the unique PLA2 domain of VP1. As endosomes acidify this domain is exposed. The use of endosomal pH buffering drugs, such as chloroquine and ammonium chloride efficiently blocked AAV2 transduction [220]. Similarly, studies where AAV2 and canine parvovirus were injected directly into the cytoplasm, thereby avoiding endosomal trafficking entry pathways, prevented viral accumulation and replication in the nucleus [221, 222]. Alternatively, it is possible that GPR-108 binding to the VP1 unique region could result in PLA2 exposure in a pH independent manner [213].

AAV trafficking to the nucleus is believed to be facilitated by the function of ATP dependent motors on the tubular networks. Some groups have reported on the observation of Brownian diffusion in perinuclear delivery of particles [221]. Once

accumulated at the nucleus, AAV particles are able to enter through nuclear pore complexes, aided by importin- β 1 and possibly importin- α [215, 223]. AAV nuclear import is facilitated by the presence of 5 basic regions (BR1 – 5) that function as nuclear localization signals (NLS) for both intact particles and VP monomers (Figure 1.3.4)[203].

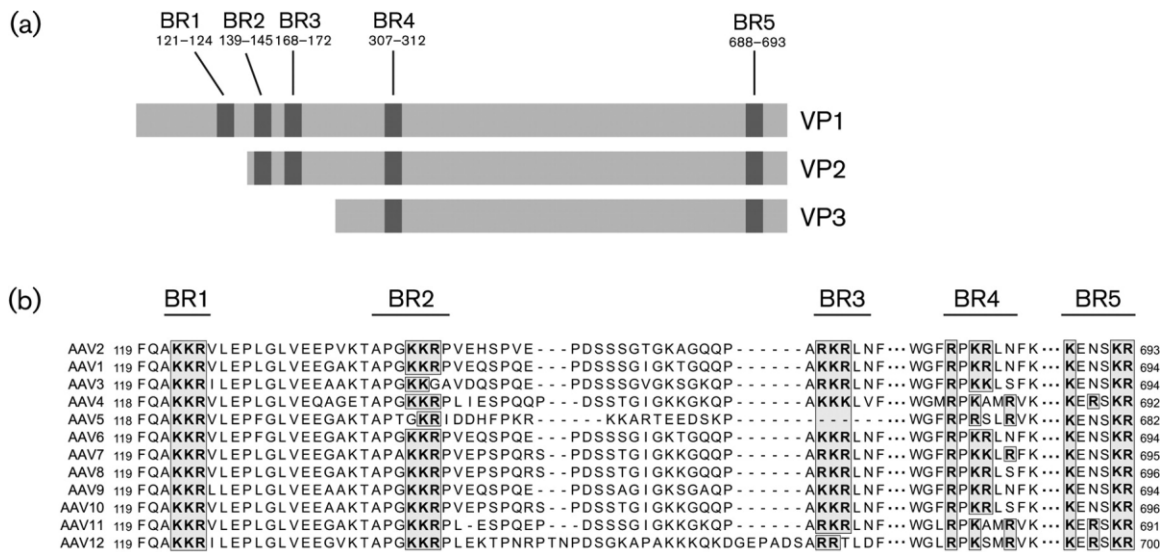


Figure 1.3.4 Spatial Orientation and Alignment of Basic Regions Between AAV Serotypes

(A) Location of basic regions in VP1, VP2, and VP3 are indicated by black bars. (B) Alignment of structural protein amino acid sequences of AAV serotypes 1 – 12 corresponding to the basic regions. Reprinted with permission from Popa-Wagner *et al.*, 2012 [203].

BR1 is unique to VP1 and resides in the N-terminus, BR2 and BR3 are shared between VP1 and VP2, while BR4 and BR5 are common to all three VPs. These regions are largely conserved between serotypes AAV1 – 12 [203]. BR1 and BR2

have shown key roles in virus infectivity. Their deletion resulted in 4-fold and 10-fold decreases respectively, and BR3 is essential for entry of virions into the nucleus [224, 225]. Mutation of these three BRs led to reductions in VP1 and VP2 in assembled capsids. BR4 doesn't appear to play a role in localization to the perinuclear region or import into the nucleus, but mutations in the region identified it plays a role in the proper assembly of intact virions [224]. Similarly, mutations of BR5 resulted in alterations of intranuclear localization of the capsid proteins, as well as likely changed the correct folding of the proteins [203]. Once infectious particles have entered the nucleus, they interact with nucleophosmin and nucleolin, localizing the particles into the nucleolus for capsid uncoating and viral genome release [226-228].

The released AAV genome can then begin the multistep replication process. In 1973 it was observed that the genome termini contained self-complementary ends that could bind to each other, later determined to be hairpin ITR structures [229, 230]. Based on AAVs linear ssDNA genome and ITRs it relies on a process referred to as 'rolling hairpin' replication, first proposed by Tattershall and Ward in 1976 (**Figure 1.3.5**)[168, 231].

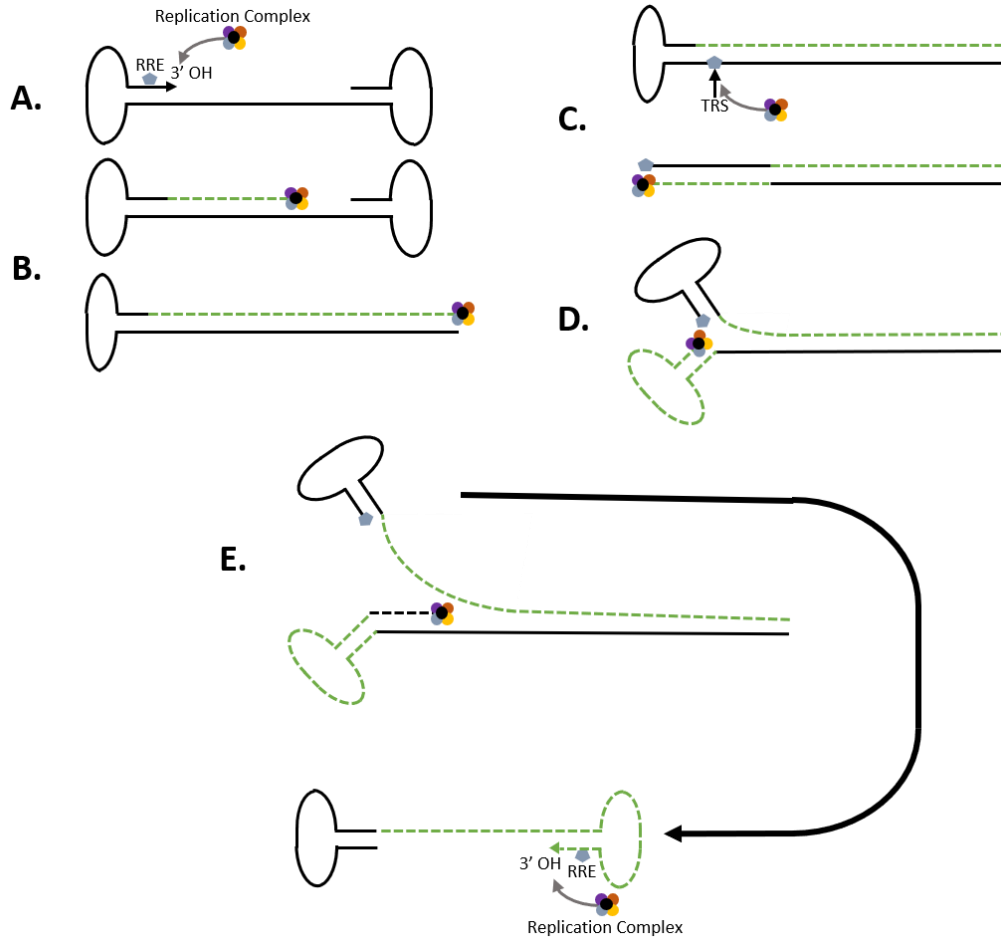


Figure 1.3.5 Parvovirus Rolling-Hairpin Replication

(A) Replication of the viral genome begins using the free 3' hydroxyl group. Rep68/78 (◆) binds at the RRE and recruits the replication complex consisting of host cell polymerase δ and/or η , proliferating cell nuclear antigen (PCNA), replication factor C (RFC), Replication protein A (RPA), and minichromosome maintenance complex (MCM) (●). (B) Replication proceeds and unwinds the 5' ITR, resulting in a duplexed monomer with one covalently closed end. (C) Rep68/78 can then cleave the TRS and remains bound, creating a new 3' hydroxyl group to prime synthesis through the remaining hairpin. (D) The hairpins are then able to refold. (E) As the next round of replication begins strand displacement frees the newly synthesized genome.

In this process, Rep68/78 binds to the RRE proximal to the free 3' hydroxyl group in the ITR. After binding, Rep68/78 serves to recruit the replication complex formed of host-cell proteins. *In vitro* studies on AAV replication have identified that

replication is mediated minimally by the host cell polymerase δ and/or η , proliferating cell nuclear antigen (PCNA), replication factor C (RFC), replication protein A (RPA), and minichromosome maintenance complex (MCM) [232-235]. Interactions between PCNA, RFC, and RPA result in the loading of polymerase onto the genome to enable replication. Once recruited, the 3' hydroxyl group serves as a self-priming locus for the initiation of replication through the second hairpin, using strand-displacement to open the second hairpin. This process is likely facilitated through the specific functions of polymerase δ and η . The high fidelity of polymerase δ , function in lagging strand synthesis, and 3' \rightarrow 5' exonuclease activity are likely important factors in the ability to replicate through the hairpins of AAV [236]. Upon reaching the hairpin structure polymerase η may be recruited based on its translesion synthesis functions to allow polymerase δ to proceed. It is unlikely that polymerase η plays a major role in replication due to its high error rate and low processivity [237]. Synthesis through the ITR results in intermediate dsDNA structure with a covalently closed end formed by the initiating ITR. Rep68/78 nicks the TRS at the closed end resulting in a second 3' hydroxyl group to allow synthesis through the newly opened ITR in a process termed terminal resolution. Two complete duplexed genomes now exist, and through the helicase activity of Rep68/78 the ITRs can be unwound, enabling formation of the ITR hairpin. This results again in a new 3' hydroxyl group that can be used for genome replication. As the polymerase proceeds for a second round of replication it separates the duplexed genomes by single strand displacement [238, 239]. Exponential replication of the genome can then proceed in the same fashion,

producing both plus and minus strands. Rep68/78 remains bound to the 5' phosphate at the TRS. This enables Rep40/52 to bind for subsequent capsid genome packaging through helicase activity [240]. Plus and minus strands are packaged with equal frequencies into the assembled capsids.

The process of replication is dependent on the presence of helper genes for productive replication. These include the previously described host cell replication factors, as well as those from helper viruses. Canonically these viral proteins are from adenovirus (Ad), and in their absence AAV infection results in latent infections. Some evidence has shown that the induction of cell cycle arrest and/or DNA damage *in vitro* can enable helper virus free AAV replication [241, 242]. The potential for Ad contamination and/or the presence of SV40 large T antigen complicates the interpretation, and variable levels of transcription don't suggest this as a preferential method for replication [243]. In latently infected cells, the genome can persist either as episomal concatamers or through integration into the host cell genome at the AAVS1 site on chromosome 19. Other regions that possess Rep68/78 binding motifs can serve as alternative integration sites [187-189]. Integration is facilitated by the binding of Rep68/78 to both the RBEs in the ITR and host genome, enabling endonuclease activity to cleave at both sites at the TRS. Non-homologous recombination then occurs through interactions of Rep68/78 on each genome [190, 244].

Replication of AAV in Ad infected cells relies on the presence of the E1A, E1B55K, E2A, E4orf6, and VA RNA proteins [245]. E1A enables transcription of the AAV

rep ORF, activating the p5 and p19 promoters that are repressed during latency [246]. In the absence of a replication permissive environment, the interaction of Rep68/78 binding to the RRE at the p5 promoter, YY1 binding to two adjacent YY1 binding sites, and a major late transcription factor (MLTF) binding site silences expression from the p5 promoter [247, 248]. During Ad infection, E1A interactions with MLTF and the formation of an E1A-p300-YY1 complex enables activation of p5 transcription. The E2A encoded DNA-binding protein aids by increasing the transcription rate [58, 248, 249]. Although Rep continues to suppress the p5 promoter, it leads to activation of the downstream p19 and p40 promoters [248].

These binding interactions relieve the repression of p5 and enable transcriptional activity. Additionally, E1A is used to drive the cell to S-phase, but it also stabilizes p53, leading to apoptosis [50, 51]. To counteract this, E1B55K and E4orf6 complex with p53 to induce its ubiquitination and subsequent proteosomal degradation [55, 56]. E1B55K and E4orf6 also play necessary roles in the export of AAV from the nucleus of infected cells while inhibiting the export of cellular mRNA [56]. The 72 kDa DNA binding protein (DBP) encoded by E2A functions to stimulate DNA replication, translation, and mRNA processing [56, 58]. The VA RNA is necessary for maintenance of RNA expression levels and inhibits protein kinase R phosphorylation of cellular eukaryotic initiation factor 2 α (eIF-2) that would otherwise prevent viral translation [41, 250].

HSV1 can also act as a helper virus in AAV infected cells. AAV has been shown to interact with 7 HSV1 genes – UL5, UL8, UL9, UL29, UL30, UL42, and UL52. Of

these, a small subset comprising the helicase–primase complex of UL5, UL8, and UL52, together with UL29 are required for AAV genome replication [251]. While UL30 and UL42 enhance AAV replication, they are not a requirement [252]. UL29 produces the major DNA binding protein ICP8, which colocalizes with Rep68/78 [252, 253]. Interactions of the ssDNA binding proteins of ICP8 and host cell RPA enhance the DNA-binding and enzymatic activities of the AAV Rep68/78 proteins [235].

A number of cellular proteins have been identified as interacting with Rep, including proteins involved in transcription and translation, splicing, protein degradation, and DNA replication and repair [185, 186, 192]. The perturbations of the *rep* proteins on these host cell proteins that results in cell cycle arrest and apoptosis explains the need for AAV to establish latent infections when productive replication is not possible.

1.3.4 Pathogenesis of Adeno-Associated Viruses

To date, natural infection with wild-type AAV has not been associated with any known illness [254]. AAVs can infect both dividing and non-dividing cells, and tropism varies between the different serotypes based on their cellular receptors [175, 255, 256]. Primary routes of infection are still being investigated, but most initial infections likely occur in childhood by nasopharyngeal routes. Sexual and fecal-oral transmission is also possible [257-259]. Theories have postulated that AAV infection may correlate with sex and reproductive issues, including

spontaneous abortions, miscarriages, and infertility in men, although no significant link has been found [260-262].

Intriguingly, while AAV has not been associated with any illness, it has been found to function with anti-oncolytic mechanisms [263-265]. For instance, in patients infected with human papillomavirus (HPV), *rep* protein has been shown to bind upstream of the HPV-16 p97 promoter. This promoter binding activity blocks synthesis of the oncogenic E6 protein and leads to a reduction in the occurrence of cervical cancer [174, 191, 266]. It has also been shown to inhibit the oncogenic effects from human Ad5, Ad12, and HSV-2 transformed cell lines [257]. Similarly, AAV Rep78 has been documented as inhibitory to the pathological effects of bovine papillomaviruses, hepatitis B virus, and human immunodeficiency virus [267-269]. The anti-oncogenic role is not solely instigated by *rep* proteins, as the ITRs have also been found to induce apoptosis in p53 knockout cell lines through their ability to initiate DNA damage responses [270].

In contrast, recent studies have suggested that the use of recombinant AAV vectors in gene therapy studies may increase the risk of hepatocellular carcinoma in both rodents and humans [271, 272]. As this currently has only been observed in recombinant AAV vectors, the disparity suggests that the addition of strong promoters and enhancer regions might be responsible for this phenomenon [273, 274].

1.3.4.1 Immunological response

Infection rates between the serotypes vary, but over 90% of the human population is estimated to have been exposed to AAV2. Approximately 30 – 60% of these patients develop humoral responses capable of neutralizing subsequent infections [275-277]. Production of IgM and antibodies from all four IgG subclasses have been observed, although IgG1 is predominant in seropositive individuals [278]. Although neutralizing antibody (NAb) titers are generally high, evidence has shown that Nab bound capsids are still capable of tissue transduction. Moreover, some patients develop non-neutralizing antibodies that may enhance vector biodistribution and transduction of mouse livers [279]. Natural infection has identified that capsid-specific CD4⁺ and CD8⁺ responses are elicited, and that they largely produced IFN- γ or IL2 alone or in combination with factors such as MIP-1 α or perforin [280].

1.4 Clinical Applications of Gene therapy

1.4.1 Adenovirus Vectors

Adenovirus vectors, specifically those based on serotype 2 and 5, have been a stalwart in the field of viral vectors. They are the most commonly used viral vector and have been used since the early introduction of *in vivo* human clinical trials (**Figure 1.4.1**) [29]. Much like lentiviral vectors they can infect both replicating and quiescent cell populations, but as they remain episomal they avoid issues with insertional mutagenesis observed in retroviral vector gene therapy applications. While this provides distinct health and safety benefits their inability to integrate leads to dilution and loss as cells proliferate.

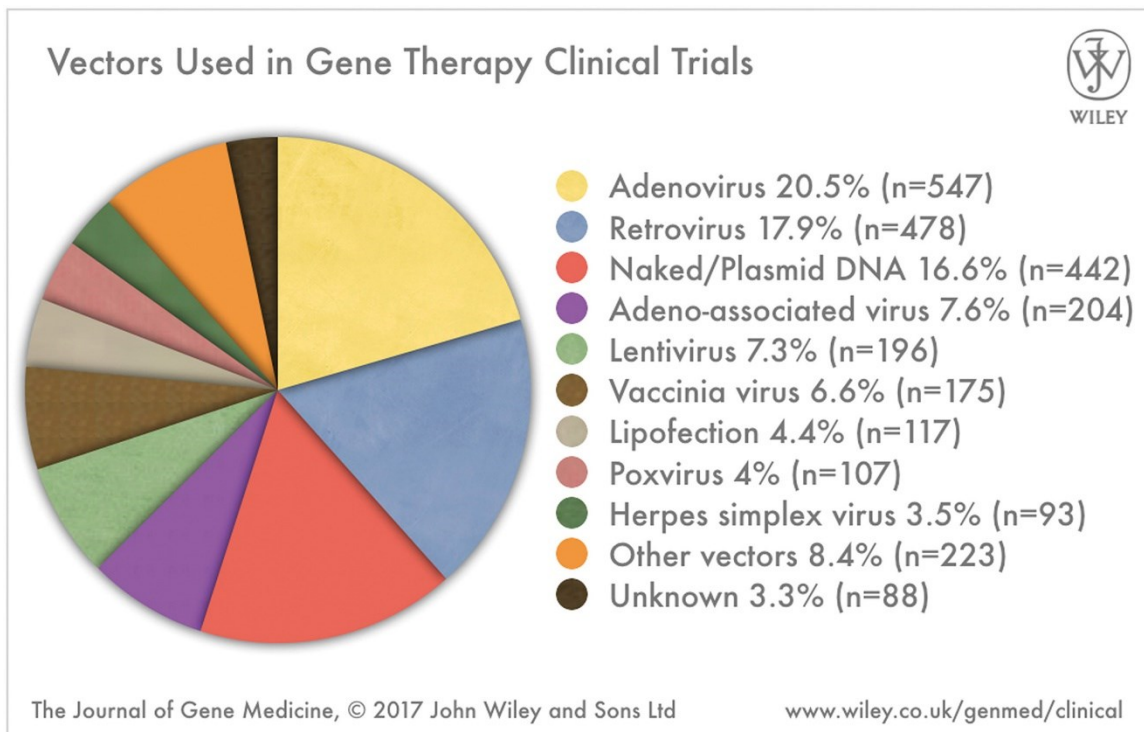


Figure 1.4.1 Distribution of Viral Vectors Used in Clinical Trials

Adenovirus vectors remain the most commonly utilized vectors in clinical gene therapy applications worldwide. Reprinted with permission from Ginn *et al.*, 2017 [29].

1.4.1.1 Production of Adenovirus Vectors

In order to deliver therapeutic genes, the Ad genome must be modified to allow the space required for insertion of the gene of interest (transgene). Three generations of replication incompetent Ad vectors exist. First generation vectors contain deletions of E1 and commonly E3 genes, 2nd generation vectors contain deletions of E1 and E3 along with deletions in E2 and/or E4, while 3rd generation vectors have deletions of all the viral genes and as such are commonly referred to as ‘gutless’ [281]. Modification of the genome through these deletions led to increases in the maximum allowable transgene that can be packaged: ~5.1 – 8.2 kb in 1st

generation, up to ~14 kb in 2nd generation vectors, and ~37 kb in the 3rd generation. Deletion of viral genes also reduces the risk of recombination events that could create replication competent vectors, as well as the immunogenicity of the vectors [282]. Each of these vector generations requires the expression of the deleted genes, with the exception of E3, by trans-complementation for replication and production of the viral vectors. As E3 encodes proteins responsible for immune evasion and protection from host immune responses, it is dispensable for the production of vectors. In 1977 Graham *et al.* reported on the transformation of human embryonic kidney cells (HEK) with sheared adenovirus serotype 5 (Ad5) genomes [283]. The resulting cell line was designated HEK293. It has an insertion of the leftmost 11% of the Ad genome in chromosome 19 at 19q13.2, enabling expression of the E1A and E1B genes [283, 284]. Since then, a number of additional Ad production cell lines have been created through incorporation of the E1A and E1B sequences into the genome. These include PER.C6 and 911 cells from human embryonic retinoblasts. Many of these lines have minimal Ad gene sequences to reduce the risk of crossover events that would lead to replication competent vectors [281]. While the deletions of E1 and E3 in first generation vectors frees space for transgene insertion, low level transcription of the remaining viral genes stimulates immune responses and early clearance of Ad transduced cells. This effect severely limited the applicability of Ad vectors for long-term gene correction approaches [285].

Classically, 1st generation vector production methods utilized recombination to assemble a transgene containing vector. This approach used a plasmid containing the transgene of interest, flanked by a short sequence of Ad genomic DNA, with either a second plasmid containing the remainder of the 3' Ad genome or with restriction digested Ad genomes [282]. Upon co-transfection of cells, these sequences would recombine to create full-length E1 deleted vectors bearing the transgene of interest. This system was not advantageous as the required recombination between sequences was inefficient and incomplete digestion of Ad genomes could easily enable the production of replication competent virus. To circumvent this issue, groups instead utilized recombination approaches in *E. coli* (such as the AdEasy system) or yeast prior to transfection of the vector production cell lines [286, 287]. In 1997 Hardy *et al.* devised a novel system that utilized Cre-*LoxP* recombination to produce either Δ E1 or gutless vectors. The Δ E1 Ad system used a recombinant Δ E1 Ad helper genome plasmid that contained a floxed packaging sequence (ψ), a transgene expression cassette with a single *loxP* site, and a HEK293 cell line that expressed Cre recombinase (CRE8) (**Figure 1.4.2**) [288]. The transgene plasmid was flanked by two Ad ITRs and contained a 5' ψ sequence, a CMV promoter to drive expression of the transgene, a polyadenylation sequence, and a *loxP* site upstream of the 3' ITR. Transfection of the helper virus plasmid resulted in the loss of the E1 and the ψ domain through intramolecular Cre-recombination. Subsequent transfection of the transgene plasmid enabled Cre-recombination with the E1 and ψ deleted helper virus, resulting in a functional vector containing the remaining Ad genes and a small non-functional sequence

with two ITRs. While this system overcame the dramatic limitations imposed by previous recombination approaches, there was still the potential for packaging the helper virus genome from incomplete Cre-recombination. Although vector yields from the initial transfection can consist of up to 30% of infectious virus from the helper plasmid, subsequent production passages decreased the composition of parental virus to 0.2% after 3 passages [282].

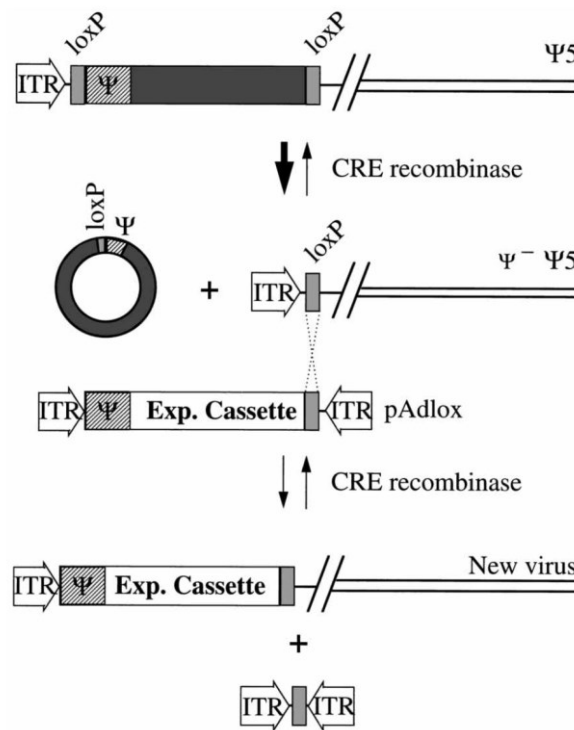


Figure 1.4.2 Creation of $\Delta E1$ Adenovirus Vector Through Use of Cre-Recombination

Cells expressing CRE8 are infected with an adenovirus helper plasmid (Ψ5) that contains a 5' ITR, loxP sites flanking the E1 genes and packing sequence, and the remainder of the 3' Ad genome. Upon infection intramolecular Cre recombination results in the creation of an Ad helper that lacks Ψ and the E1 genes (Ψ-Ψ5), preventing packaging of the helper virus. Next, a transgene plasmid (pAdlox) flanked by Ad ITRs that contains the Ψ signal region and transgene cassette with a 3' loxP site adjacent to the 3' ITR is transfected. Cre activity results in the formation of a functional full-

length Ad Δ E1 vector with a 5' and 3' ITR, an intact Ψ , and the desired transgene, as well as a non-functional product of a 5' and 3' ITR [288].

Second generation production cell lines expanded on the 1st generation lines, expressing E1 while incorporating all or parts of E2 and E4 to reduce the level of viral genes present in the final vector product. The majority of the production lines expressing these transcription units rely on the use of conditionally active promoters, such as tetracycline or glucocorticoid inducible promoters, as the products of these genes are cytotoxic [281]. Although these manipulations increased the size of the transgene that could be packaged, their use was hampered by decreased viral titers and mixed reports as to whether vector immunogenicity was reduced [281, 285, 289, 290]. Due to the minimal improvement over 1st generation vectors in therapeutic applications, their use was soon superseded by 3rd generation gutless vector systems.

While the removal of all viral coding genes from 3rd generation vectors increased transgene stability and reduced the immunogenicity of the vectors, their production required the coinfection with a helper adenovirus carrying the genes not expressed by the helper cell line [291-293]. Further, as Ad capsid packaging is tightly constrained to genome lengths of ~75 – 105% of the native Ad genome (~27 kb – 37.8 kb), this approach required the use of stuffer DNA sequences [294-296]. While lambda phage DNA was initially used, it was identified that it had a negative effect on the longevity of transgene expression and stimulated immune responses against vector transformed cells. Instead, non-coding mammalian or human DNA

have become common stuffer sequences, such as fragments of the hypoxanthine-guanine phosphoribosyltransferase gene [297, 298]. Strategies to avoid incorporation of the helper virus into assembled particles were then required to prevent parental packaging instead of the transgene plasmid. One approach utilized a variation of the aforementioned Cre-*loxP* system. In this approach, the transgene plasmid was designed with a *loxP* site between the 5' ITR and Ψ signal domain. The transgene plasmid was linearized through restriction digests at the ITRs prior to co-transfection with the Ψ 5 helper plasmid. This approach again resulted in the removal of the ψ domain in the Ψ 5 helper plasmid, enabling production of vectors that were largely helper virus free after the initial vector production and purification [288, 295]. Additional methods have included the use of FLP/*frt* recombination or plasmid based expression of the Ad genes [297, 299]. To further increase the purity of vector productions, cesium chloride banding is common. Due to divergent buoyant densities the desired viral vectors can be purified from replication competent particles.

Just as WT Ad stimulates robust innate and adaptive immune responses, so do the vectors. While the 1st – 3rd generation vector systems worked to reduce the number of immunogenic viral genes present in the vector, work has also been pursued to modify the immunogenicity of the capsid protein. Some of these efforts have also involved capsid modifications in order to target cells that do not express CAR or other Ad receptors. This work has been pursued primarily for gene therapy applications as immune activation results in rapid clearance of delivered vector

genomes, significantly limiting the efficacy of treatment [141, 300]. Delivery of vectors closely mirrors the inflammatory response seen in WT Ad infection, and includes elevated levels of IL-6, TNF- α , MIP-2, MIP-1 α , RANTES, and IP-10 shortly after delivery [141, 301]. The release of these cytokines and chemokines, which drive rapid recruitment of inflammatory cells, is largely caused by the vector capsid, specifically the hexon protein [300, 302, 303]. One approach to overcome immune responses in intravenously delivered vectors is the use of liposomes or polymers, such as polyethylene glycol and N[2-hydroxypropyl] methacrylamide. These approaches reduced the activation of neutralizing antibodies and cytotoxic T lymphocytes against the vector, which in turn increased the half-life of circulating virus [304-309]. These approaches are also used in the retargeting of vectors to non-hepatic tissues, likely through an inability of coagulation factor X (FX) to bind to the hexon proteins and facilitate the typical vector tropism [304, 310-313]. Similarly, modifications of the capsid sequence and components itself results in altered tropism of vectors. Modifications of hexon have resulted in decreased hepatic transduction, and use of chimeric or serotype switched fiber knobs that utilize CD46 instead of CAR has altered transduction profiles [313-315].

1.4.1.2 Therapeutic Applications of Adenovirus Vectors

In the early 1990's the first evidence of the capability of Ad vectors for therapeutic applications in small animals emerged. *In vivo* experiments identified the ability to deliver and express alpha 1-antitrypsin in rat lungs and livers, and ornithine transcarbamylase (OTC) in mouse livers [316-318]. Following these successes,

attention turned to the potential for *in vivo* gene correction in humans by Ad vectors. In 1993 Crystal *et al.* utilized an E1/E3 deleted Ad vector to deliver Cystic Fibrosis transmembrane conductance regulator complementary DNA (CFTR cDNA) to 4 adults with the CFTR Δ F508 mutation [319, 320]. Expression of cDNA was limited, with no individuals showing expression longer than 10 days post-administration, but it provided insight into the safety and viability of Ad based gene therapy in the context of CF. The findings were confirmed in additional studies by other groups [321, 322]. By the end of the decade, issues with immunogenicity and transgene expression remained, and groups then began to seek out alternative vectors (e.g., AAV, lentivirus, retrovirus) for cystic fibrosis treatments.

Adenovirus vectors have also been studied extensively in metabolic disease (e.g. OTC, ApoA1, ApoE, arginase deficiency, glycogen storage disease, etc), hemophilia, and diabetic therapeutic applications due to their ability to effectively target the liver [323]. Most of these therapies are still pre-clinical as concerns remain about the immunogenicity of Ad vectors in liver specific gene therapy applications. Much of this fear arose from the death of 18-year-old Jesse Gelsinger in a phase 1 OTC clinical trial that used a 2nd generation Ad5 vector [324]. Jesse was the 18th and final patient in the study and received a dose of 6×10^{11} particles/kg (3.8×10^{13} total particles) into his hepatic artery and 18 hrs post-delivery soon developed a severe immune reaction to the vector with persistent deterioration until he was declared brain dead and life support was removed 98 hours post treatment [324]. His death was the first attributable to the vector itself

in clinical trials. The revelation of his death dramatically altered the landscape of the field. Investigations uncovered that the research team had not informed the FDA and patients of serious side effects experienced by patients at lower doses and that three non-human primates had died from severe side effects with high doses [325]. FDA and NIH investigations also identified an endemic problem of prompt reporting of clinically adverse reactions; of 691 gene therapy patients that had suffered severe illness or death following treatment, only 39 cases had been promptly reported to the recombinant DNA advisory committee [326, 327]. These revelations brought about the creation of the Gene Therapy Clinical Monitoring Plan and Gene Transfer Safety Symposia to increase study oversight and patient protection [325, 328].

In contrast, the use of Ad vectors as oncolytic agents in cancer gene therapy has been an expanding area of research, especially in chemotherapy or radiation resistant cases [142, 329, 330]. As of late 2020, clinicaltrials.gov lists 75 active, recruiting, or enrolling studies utilizing Ad vectors as oncolytic agents against a variety of cancers, including breast, prostate, colorectal, lung, and brain. In contrast to therapeutic Ad vectors, these oncolytic adenoviruses utilize capsid and genome modifications for selective targeting and/or replication in cancerous cells. Mutant of the Ad fiber knob to instead bind upregulated surface receptors on the cancerous cells of interest is a common method in this approach. While Ad5 predominantly utilizes CAR, chimeric vectors using the fiber knob from different serotypes have shown success in increasing vector tropism for cancerous cells.

Ad5 vectors with fiber knobs from Ad3 have shown enhanced transduction of breast and colorectal cancers that overexpress the desmoglein 2 receptor, and Ad35 fiber knob chimeras resulted in increased transduction of epithelial malignancies with elevated expression of CD46 [331, 332]. Modifications of the fiber knob through peptide incorporation has also been utilized to enable CAR independent binding through α V- β 3 and α V- β 5 integrins that are highly expressed on many primary tumor cells [333, 334]. Alternative approaches have utilized hexon specific modifications. These have included the insertion of peptides to target cancerous cells, such as TGF β targeting peptides, as well as hexon modifications to detarget hepatocytes and limit the potential of vector transduction of off-target non-cancerous cells [335, 336].

Vector genome modifications can include mutations/deletions in E1 or E3 genes. These modifications can be used to allow space for the insertion of tumor suppressive, cytotoxic, immune-modulating, or tumor antigen expressing genes. Early genomic modification involved the mutation or deletion of genes to restrict replication of oncolytic adenovirus vectors to cancerous cells. These approaches commonly used deletions of E1B-55K or a portion of E1A [337-340]. Although E1B-55K mediated p53 suppression is required in normal cells for replication, approximately 50% of human cancers possess p53 mutations or deletions, so the activity of E1B-55K is not required [338]. Similarly, although the E1A gene functions to drive healthy cells to S phase through the inactivation of the retinoblastoma (Rb) tumor suppressor gene product, malignant cancers often have

abnormal non-functional expression of Rb. This allows for the deletion of 24 nucleotides from the Rb-binding domain of E1A without otherwise impacting replication in cancerous cells [339, 340]. Additional techniques have involved mutations of E3. These have included mutation of the E3-19K protein to increase membrane permeability and enhanced release of viral progeny, along with E3 deletion mutants to increase MHC-I expression and sensitivity to natural killer and T cells [341-343].

Expression of immunostimulatory transgenes in oncogenic therapies have utilized E3 deletion vectors. Expression of the transgenes is mediated through promoters with selective or upregulated activity in cancerous cells and include human telomerase reverse transcriptase, prostate specific antigen, α -fetoprotein, and cyclo-oxygenase II [344, 345]. Inclusion of transgenes upregulating cytokine production and release, such as GM-CSF, IFN- α , or expression of TLR-9 agonists, IL-12, or IL-18, have all shown success in oncolytic Ad therapy applications [346-351]. Alternatively, incorporation of ligand transgenes such as CD40 results in increased apoptosis, upregulation of T helper cell type 1 cytokines, and the presence of macrophages and CD8⁺ T cells [352, 353].

1.4.1.3 Adenovirus Vaccine Applications

Due to the innate immunogenicity of Ad vectors, they have been extensively tested as carriers of heterologous antigenic transgenes for vaccine applications. The strong innate immune response due to the pathogen associated molecular patterns (PAMPs) of the capsid and viral genome enables signaling through

pattern recognition receptors (PRRs), resulting in the induction of type I interferons and pro-inflammatory cytokines and chemokines as outlined in section 1.2.5.1 (**Figure 1.2.5**). This activity is complimented by the induction of further inflammatory cascade pathways through cytosolic DNA sensors that include toll-like receptor 9 (TLR9), nucleotide-binding oligomerization domain-like receptors (NLRs), retinoic acid-inducible gene-1 like receptors (RLRs), and guanosine monophosphate-AMP synthase/stimulator of interferon genes (cGAS/STING) as described in section 1.2.5.1 [142-146].

Intramuscular delivery of adenovirus vectors results in infection of cells bearing the appropriate receptor (e.g. CAR for Ad5). Following cellular infection, as outlined in section 1.2.4, the incorporation of strong promoters in the transgene, such as the cytomegalovirus immediate-early promoter, enable robust transcription. Long-lasting persistent expression of delivered antigen at the site of vaccination has been noted and may be an important aspect in vaccination as it was shown to enable fully active CD8⁺ T cells and differentiation into central memory cells [354]. A study on multiple human, simian, and chimpanzee Ad vectors identified that it was indeed the durability and longevity of the antigen expression that had the highest correlation with the magnitude of memory CD8⁺ T cell responses, and this association was independent of IFN and STING expression [355]. Intriguingly, serotypes with the highest antigen expression (Ad5 and chAd3) produced lower levels of type I IFN compared to other serotypes, indicating that analysis of optimal vectors to use as vaccine platforms should not be based solely on the ability to

stimulate type I IFN production [355]. Upregulated type I IFN expression correlated with decreased expression of the antigenic transgene and limited the initial expansion of CD8⁺ T cell responses [355]. It is possible that alternative entry and uncoating mechanisms could alter the response of cytoplasmic DNA sensors to trigger the activation of downstream ISG pathways. Following transgene translation these transgene proteins can be post-translationally modified and secreted for future identification and uptake by antigen presenting cells, or presented on MHC class I receptors following proteasomal degradation. Unlike wildtype Ad, vectors with deletions of the E3 gene fail to interfere with the natural expression of MHC class I molecules due to the absence of the E3-19K gene product. Thus, E3 deleted vector transduced cells have an increased sensitivity to natural killer and T cells [341-343]. Similarly, release of antigen through apoptotic/necrotic bodies presents an additional pathway for antigen uptake by antigen presenting cells (**Figure 1.4.3**) [356].

Tissue resident dendritic cells are also targets of Ad vectors, although based on the minimal levels of CAR expression, high multiplicities of infection (MOI) are needed to achieve efficient transduction with Ad5 vectors. Infection of immature dendritic cells with high MOI Ad vectors was shown to enable partial maturation of human monocyte-derived dendritic cells, resulting in upregulation of costimulatory molecules (CD40, CD80, and CD86) and MHC class I and II molecules, and increases in their T cell stimulatory function [357, 358]. Ad5-infected dendritic cells were observed to downregulate their antigen uptake machinery, and the lack of

high levels of CD83 and IL-12 indicated that full maturation and polarization towards a Th1-inducing phenotype was impaired [358]. Infected dendritic cells have also been noted to have elevated levels of chemokines such as MCP-1, MIP-1 α , MIP-1 β , RANTES, MIP-3 β , IL-8, MIG and IP-10. These effects could be a result of the immuno-stimulatory effects of the Ad capsid proteins in transduced cells [358, 359]. Following infection and/or uptake of antigenic peptides, DC migrate to secondary or draining lymphoid tissues which enables presentation of processed antigens to naïve T cells through MHC class I or class II molecules [360].

Similarly, B cells can be activated through direct interaction of their B cell receptor (BCR) to either soluble antigens or membrane bound antigens on dendritic cells or other antigen presenting cells. Following uptake, high affinity antigens can be displayed on the B-cell surface by MHC class II molecules. Interaction with activated CD4⁺ follicular helper cells (Tfh) through MHC class II results in CD40 ligand-based stimulation of the B cell. Activated B cells can then differentiate into plasmablasts producing low-affinity antibodies against the antigen, and these cells subsequently migrate to the B cell germinal center. In the germinal center dark zone B cells can undergo rapid proliferation and somatic hypermutation to modify their affinity for the antigen. Those B cells with high affinity for the antigen are selected by CD4⁺ T follicular helper cells, enabling the production of memory B cells that can be activated upon secondary infections. The developing plasmablasts secrete high affinity antibodies against the specific antigen. A subset of the differentiated plasmablasts migrate to the bone marrow where they establish

as long-lived plasma cells for sustained production of high affinity antibodies. Isotype switching can occur following CD40 ligand stimulation through T cell derived cytokine stimulation [361].

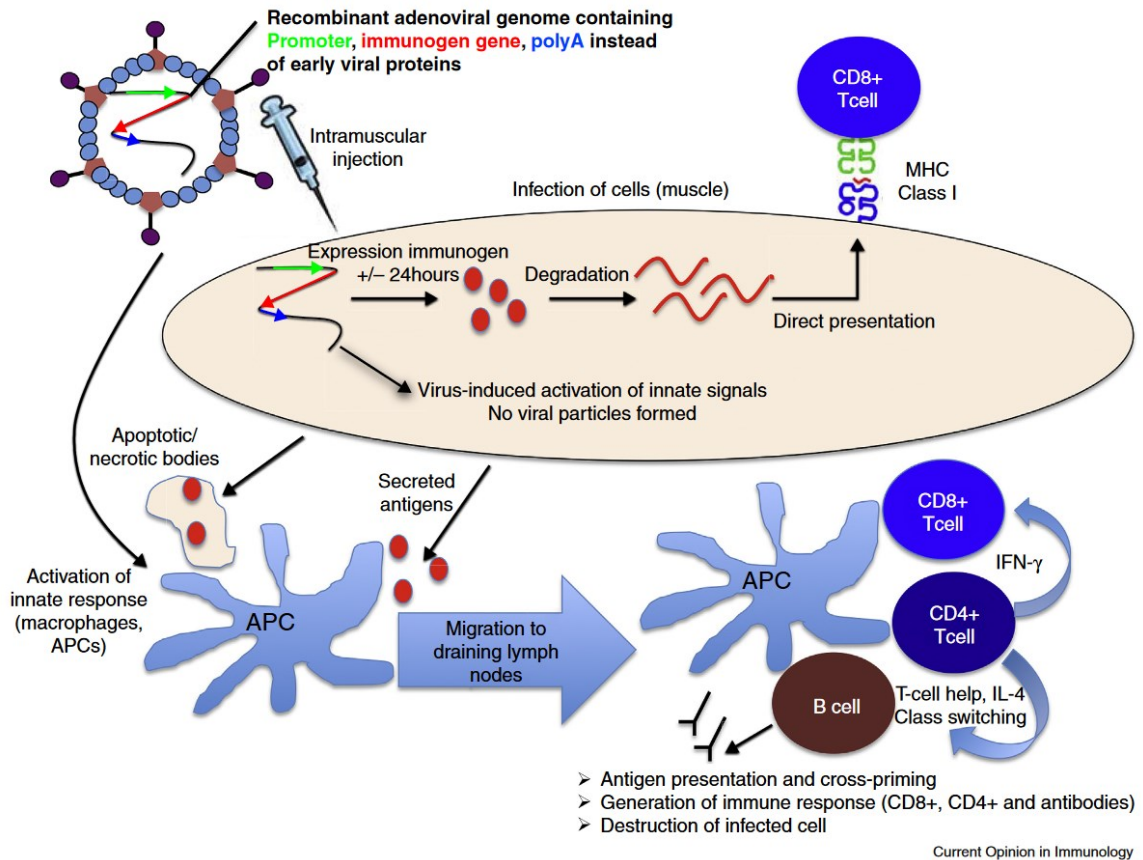


Figure 1.4.3 Mechanism of Induction of Transgene Specific Immune Responses Following Viral Vector Vaccine Administration

Administration of a recombinant adenovirus vaccine by intramuscular injection results in infection of muscle cells (non-productive in the case of replication-defective viral vectors) followed by expression of the transgene within 24 hours, together with triggering of innate immune responses via interactions between viral nucleic acids and pathogen recognition receptors. Expressed proteins undergo proteasomal degradation and presentation to CD8+ T cells in association with MHC class I molecules or may be secreted and taken up by professional antigen presenting cells (APC). APC may also acquire vaccine antigens as apoptotic or necrotic bodies or may be directly activated by interaction with the viral vector. Antigen-loaded APC migrate to draining lymph nodes

where they are able to prime CD8+ and CD4+T cells and B cells. Reprinted with permission from Ewer *et al.*, 2016 [356].

Genome translation in the transduced cells enables expression of these antigens for immune system recognition. Initial attempts utilized replication competent Ad5 E3 deleted vectors, using either the endogenous E3 or major late promoter to drive expression of the inserted transgene [362, 363]. While these approaches induced immunity to the delivered antigen, questions existed about the safety and toxicity of these vectors, especially in children, older adults, and immunocompromised individuals. These concerns led to a larger use of 1st generation replication incompetent E1 deleted vectors, either with or without an E3 deletion. Although Ad5 vectors are common in pre-clinical studies, globally high seroprevalence is a pervasive issue and alternative serotypes for clinical use are commonly studied. These include human serotypes with reduced seroprevalence (e.g. huAd26, huAd35, huAd48) or serotypes from different species (e.g. chimpanzee Ad3, chimpanzee Ad63, canine Ad2, etc) [364-369]. These studies have identified that differential immune responses can be elicited based on the serotype used.

An expanding target with Ad vectors has been in the development of prophylactic human immunodeficiency virus (HIV) vaccines. One of the most well-known trials was the Merck STEP and Phambili trial that utilized a combination of three Ad5 vectors expressing *gag*, *pol*, and *env* with two boosting injections at 1 and 6 months after the initial dose. Although there were promising data from pre-clinical and phase I trials, the large multicenter phase II trial identified that while the vectors

were able to elicit T cell immunogenicity vaccination increased rates of infection in men who were either uncircumcised or had pre-existing Ad5 immunity [370]. These findings led to the termination of both studies [371-373]. The mechanisms behind this phenomenon are still unclear. Hypotheses include that vaccination may have boosted Ad specific T cell response resulting in more activated T cells susceptible to HIV infection, that pre-existing Ad5 immunity may have skewed immune responses towards anti-Ad rather than anti-HIV, or that elicited HIV specific antibodies may have resulted in antibody-dependent enhancement of HIV infection [373]. Alternative HIV vaccination attempts incorporated three injections of plasmid DNA containing HIV genes followed by an Ad5 boost. This approach was again able to stimulate robust immune responses, but one clinical trial found that this vaccination regimen had no effect on HIV acquisition or viral loads post acquisition [374-376]. For these reasons, non Ad5 serotypes have been sought for continued HIV vaccine development [365, 377, 378].

Ad vectors have also been studied for vaccine applications against other prominent disease-causing viruses that pose global threats and/or lack effective mitigation approaches. These have included, among others, rabies virus, hemorrhagic filoviruses, tropical diseases, and pandemic coronaviruses [379-382]. Development of rabies vaccines has focused on pre-exposure prophylactic regimens for humans, as well as on oral administration to animal species with high susceptibility to infection (e.g. fox, raccoon, skunk, and dog) [380-382]. Rabies is globally distributed and results in ~59,000 yearly deaths, with significant disease

burden in poor and undeveloped nations where vaccination of domestic dog populations is lacking. As such, improved vaccination approaches could lead to a dramatic reduction in human exposure and subsequent deaths due to the near 100% fatality rate among infected individuals [383]. Expression of the rabies glycoprotein by Ad vectors has yielded strong immunogenic responses in pre-clinical settings with doses amenable to large scale production and administration [380-382].

Vaccine development for hemorrhagic fevers has been complicated by the inability to produce attenuated or inactivated vaccines based on concerns of incomplete inactivation and/or reactivation of the virus. Further, evaluated vaccines have struggled to elicit strong immunogenic responses following administration [384, 385]. Although strategies involving DNA plasmid priming vaccinations followed by Ad boosting have proven effective, the time course for these vaccinations limits the amenability to deploy rapid vaccination during outbreaks or potential bioterror incidents, largely restricting them to prophylactic administration [386, 387]. For this reason, approaches with just Ad vectors have been pursued, and application of a single dose Ad vaccine treatment has displayed effective immune stimulation [388]. Many approaches have utilized expression of both the Ebola glycoprotein and/or nuclear proteins from Sudan (SEBOV) and/or Zaire (ZEBOV) strains of Ebola virus and have identified protective immunity in non-human primate challenge models [386, 388, 389]. These combination vaccines typically utilize two or more vectors to express the viral proteins and are optimal due to a lack of cross-

protection conferred from vaccination against a single Ebola species. An additional approach has used single or multiple vectors expressing the glycoprotein antigens from ZEBOV, SEBOV, and Marburg virus in a single injection [390]. Clinical administration of chimpanzee Ad3 encoding the ZEBOV and SEBOV identified that the vaccine was able to elicit high antibody titers and immune responses previously shown to be protective in pre-clinical challenge models [391]. Additional studies have utilized combinations of Ad and modified Vaccinia virus vectors to increase the number of Ebola antigens that can be expressed. Some of these approaches have also included the expression of antigens from Marburg virus [392].

Development of vaccination approaches for tropical diseases has been spurred on following the recent Zika outbreak in the Americas. Zika virus was first detected in a rhesus monkey in Uganda in 1947 and over the last half-century has spread to Asian and Pacific Ocean island nations. This was followed by pandemic spread to the Americas. Although fatalities were rare and most of the infected suffered from characteristic symptoms of flavivirus infection (e.g. fever, rash, joint and muscle pain) a small number of patients experienced severe side effects. These included ocular complications such as bilateral posterior uveitis, neurological complications such as Guillain-Barrè, and congenital Zika syndromes characterized by spontaneous abortion or microcephaly of fetuses from infected mothers [393]. Candidate vectors expressing the pre-membrane and envelope proteins have emerged as potential efficacious approaches in flavivirus vaccination [394-396]. Similar efforts in developing Ad vaccine vectors have also been invested against

dengue virus, a related flavivirus with global distribution, and alphaviruses [397-402]. Vaccine development against alphaviruses will be further discussed in section 1.5. Additionally, although a plasmodium and not a virus, malaria has also been an Ad vaccine target due to considerable global risk, disease burden, and fatality rate. Insertion of epitopes of the *Plasmodium falciparum* circumsporozoite protein into the Ad capsid structure, such as the hypervariable region of hexon, elicited potent immune responses and increased the immunogenicity of the vaccine compared to transgene expression of the protein [403, 404].

In the last two decades, three highly pathogenic coronaviruses have emerged: severe acute respiratory syndrome (SARS-CoV) in November 2002, Middle East respiratory syndrome (MERS-CoV) in April 2012, and severe acute respiratory syndrome coronavirus 2 (SARS-CoV-2) in January 2020. Although global spread and infections attributed to SARS-CoV and MERS-CoV were relatively low (8422 SARS cases in 29 countries, 11% case fatality rate; 2494 MERS cases in 27 countries, 34.4% fatality rate), SARS-CoV-2 has had significant global ramifications to date, with the long-term consequences still to be determined. As of November 2020, by World Health Organization reporting, SARS-CoV-2 has spread to 235 Countries, areas, or territories, with over 50 million reported cases and 1.25 million reported deaths [405]. Cough and fever are shared symptoms among the three coronaviruses, although differential diagnosis criteria do exist, with shortness of breath and chill symptoms less prevalent in SARS-CoV-2 patients [406]. Following the outbreaks of SARS and MERS a number of studies

examined the potential of Ad vaccine vectors to protect against re-emergence. These studies found that expression of structural proteins elicited robust immune responses in pre-clinical small animal and rhesus macaque models, as well as humans in a phase I clinical trial of a MERS Ad vector vaccine [407-413]. Evaluation of a SARS-CoV Ad vector vaccine in mice identified that intranasal administration elicited stronger IgA responses than intramuscular injections and resulted in reduced levels of viral RNA in lung tissues. This data suggested that routes of administration could affect immune responses to the vaccine and in turn disease course and outcomes post-infection [408]. The noted success in stimulating protective immune responses to SARS-CoV and MERS-CoV has catapulted similar approaches to clinical trials against SARS-CoV-2 using Ad5 and chimpanzee Ad vectors expressing the viral spike protein. Vaccine vectors from CanSino (Ad5-nCOV) and Oxford (ChAdOx1 nCoV-19) have progressed rapidly to phase III clinical trials and preparation for global vaccination efforts as of November 2020 [414, 415].

1.4.2 Adeno-Associated Virus vectors

Adeno-associated virus (AAV) vectors have seen a significant increase in gene therapy applications in the 21st century. AAV vectors are advantageous vehicles for gene therapy due to the minimal inflammatory responses they elicit; the capability to transduce a wide array of tissues including cells of the nervous system, eye, lung, muscle, heart, etc; are non-integrating in the absence of Rep; and can provide prolonged expression of the transgene in cells with low division

[256]. While they are limited by their small transgene packaging capacity (~4.7 kb), recent strategies have worked to increase the length of genomes that can be efficiently packaged through capsid or genome modifications [416, 417]. Although AAV2 has been the predominant serotype for research on AAV, it is not the only serotype pursued for clinical applications. This is largely due to issues with high seroprevalence of pre-existing immunity to AAV2, as well as the different tropisms offered by alternative serotypes and engineered novel capsids [418-420].

1.4.2.1 Production of Adeno-associated Virus Vectors

Due to the constraints of AAV requiring the presence of a helper virus for productive replication, early strategies for vector production relied on co-infection of cells with infectious Ad, a vector plasmid containing the transgene of interest, and a helper plasmid containing the AAV *rep* and *cap* genes [421, 422]. In these approaches, the transgene plasmid would contain the AAV ITRs to facilitate packaging, while the AAV helper plasmid either lacked ITRs or were replaced with Ad ITRs to prevent packaging of the wild type genome. While these approaches were able to exclusively package the recombinant AAV genome containing the transgene of interest, questions remained about the potential for Ad helper virus contamination in the resulting vector stocks. One approach to address this concern relied on the use of multiple 1st generation Ad vectors. In this system, one vector delivered the AAV vector transgene genome, a second vector expressed AAV *rep* and *cap* under a tetracycline inducible and CMV immediate early promoter (CMV-

IE), respectively, and a third vector expressed tetracycline [423]. By placing the *rep* genes under an inducible promoter, cytotoxic effects could be limited.

To circumvent the issues of wildtype Ad contamination and simplify the process of vector production, Ad virus and vector free methods were developed that instead utilized plasmid transfection to deliver the requisite Ad genes [424, 425]. Using HEK293 or other cells that express the Ad E1 genes, these triple plasmid transfection systems express the E2, complete E4 or E4orf6, and VA Ad genes required for AAV replication from one plasmid, the AAV *rep* and *cap* genes from a second, and the vector genome from a third plasmid. Two plasmid systems combine the expression of the Ad and AAV genes onto a single plasmid. Alternative approaches included the production of cell lines with integrated *rep* and *cap* genes in order to reduce the number of plasmids required for transfection and production of AAV vectors [426-428]. Herpes virus complementation, baculovirus-insect cell expression systems, and yeast production systems also exist, although these are utilized far less than plasmid based Ad virus production systems [429].

1.4.2.2 Design of Recombinant AAV Vector Capsids

While initial vector development involved production of native AAV serotypes, considerable effort has recently been invested in the design and production of new capsid variants. These efforts aim to improve or modify vector tropism, enhance transduction, and/or evade vector stimulated immune responses. Attempts to construct these new vectors have largely relied upon directed evolution

mutagenesis, natural discovery of novel vectors, rational design, and *in silico* rational design (Figure 1.4.4) [430].

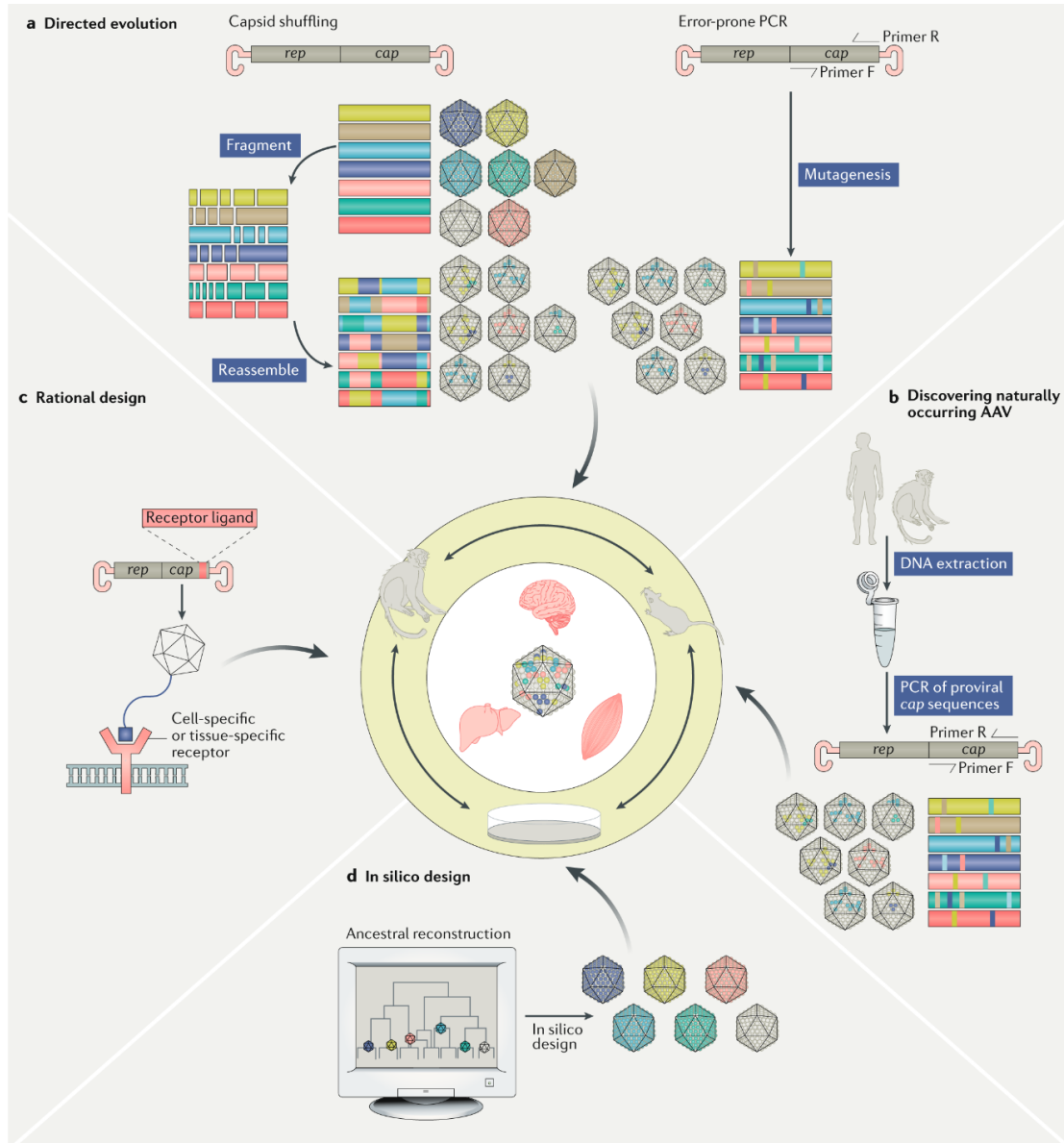


Figure 1.4.4 Four Predominant Methods for the Discovery of New AAV Capsids

(A) Directed evolution approaches heavily rely on capsid shuffling between serotypes after fragmentation and/or error prone PCR to introduce random mutations to create new vectors. (B) Population sampling and discovery of novel AAVs that can be combined with directed evolution approaches. (C) Rational design approaches utilize knowledge of desired properties to tailor make

AAVs. This can include desired tissue and cell receptors, as well as designs to reduce the immunogenicity to evade host immune responses. **(D)** *In silico* rational design-based approaches can be used to tailor specific attributes to vectors not observed in naturally occurring AAVs or to recreate phylogenetic ancestral AAV species. Designed mutants are then screened *in vitro* for their ability to produce virus and for initial studies prior to further *in vivo* assessment. Reprinted with permission from Wang *et al.*, 2019 [430].

Directed Evolution

Directed evolution approaches are heavily based on error-prone PCR and capsid shuffling techniques to identify novel capsid variants without *a priori* knowledge of structural domains of interest. Whereas rational design involves specific residue or sequence editing, error prone PCR relies on suboptimal PCR conditions and/or error prone polymerases to introduce random point mutations throughout the *cap* sequence. The pool of resulting *cap* products can then be used to create libraries of recombinant vectors to screen for preferential phenotypes [431, 432]. Capsid shuffling relies on the recombination of capsid sequences following fragmentation of the *cap* sequence, commonly through DNase I digestion. Fragments are then reassembled in random fashion through self-priming PCR reactions that result in diverse full-length capsid sequences. Subsequent amplification by traditional or error-prone PCR methods enables these capsids to be evaluated for their ability to assemble into functional packaged virions and for any novel capabilities they possess [433-435]. A prominent example of capsid shuffling technology is AAV-DJ. Following the shuffling of capsid sequences from eight AAV serotypes, mutants were selected that displayed enhanced transduction of human hepatocytes while avoiding neutralization by human intravenous immunoglobulin.

This resulted in the identification of an AAV2/8/9 chimera (AAV-DJ) with the desired phenotype [420].

Although these techniques are robust in producing large quantities of novel capsid mutants for researchers to evaluate, the identification of +1-frame shifted AAP and MAAP ORFs in the *cap* reading frame complicate their design and selection. As AAP is known to play an integral role in capsid assembly, novel capsid mutants with either sense or non-sense mutations of AAP could be disadvantaged in their ability to assemble capsids and achieve high titers. As such, these mutants may be wittingly or unwittingly selected against during evaluation of novel capsid mutant libraries, even if they do in fact contain the desired phenotypes. Since these approaches commonly utilize head-to-head production and evaluation of the novel capsid mutants, it is common that the highest titer and most prevalent mutants will be carried forward during refinement of the library. It is possible that some novel capsids with AAP mutations could be supported through *cis* acting functions of AAP from another capsid mutant in co-transfected cells during initial library evaluation. Though, as the library undergoes iterative rounds of refinement this support is likely to be lost, either through lack of co-transfected cells, or upon individual assessment of mutants. These issues are of concern especially for error-prone PCR approaches where randomly introduced mutations have a high likelihood to disturb the *cap* +1-reading frame [197]. Similarly, while capsid shuffling approaches may have a reduced risk of introducing non-sense mutations to AAP, and chimeric AAP sequences may still be able to assemble functional

capsids to some level, selection of novel capsids could still be influenced [198, 436]. One approach to overcome these potential biases would be to supplement broadly active AAP through an additional plasmid during transfection. This would remove the variable of AAP expression and allow for better evaluation based on desired phenotypes alone. Further studies are required to fully assess the effects of mutagenesis in the MAAP ORF as little is known regarding its properties and cross-complementation abilities.

Natural Discovery

Identification of naturally occurring non-human AAVs has been pursued to identify serotypes with reduced seroprevalence in human populations. These efforts have largely focused on isolation from vertebrate species. Non-human primates are the most commonly studied, and have yielded serotypes such as AAVrh.8, AAVrh.10, and AAVrh.43 [177, 430, 437]. Alternatively, groups have also studied and identified AAVs from species such as birds, pigs, and bats [438-440]. These discoveries aid in the identification of novel naturally occurring AAVs that may be useful in gene therapy approaches, or as substrates to create novel AAV capsids by the other described methods.

Rational Design

Rational design approaches have largely focused on capsid design to improve tissue tropism or to alter the primary cell binding receptor [441-443]. For example, a recombinant AAV2 capsid, AAV2.5, was created when five conserved residues

from AAV serotypes with high skeletal muscle tropism were substituted into the AAV2 capsid sequence. While the parental AAV2 is inefficient at skeletal muscle transduction, AAV2.5 displayed increased transduction, as well as decreased immune response to AAV2 neutralizing antibodies as changes also altered antigenic domains [443]. Similar effects have been observed with other hybrid recombinant vectors, such as AAV2G9 and AAV2i8. AAV2G9 was created by grafting the galactose binding domain from AAV9 onto AAV2, resulting in the ability to bind both galactose and heparan sulfate proteoglycan [441]. Similarly, AAV2i8 was designed by replacing the key heparan sulfate proteoglycan binding residues from AAV2 with amino acids corresponding to the same position in AAV8. This change enabled higher levels of skeletal muscle transduction while decreasing hepatocyte transduction [444].

Along with altering the primary receptor through domain swapping, approaches have also utilized peptide display libraries through insertions into the variable region of surface loops. In this approach, animals are injected with mutant libraries and bio-panning is used to identify vectors with phenotypes of interest, particularly tissue specificity [445-448]. For example, Dalkara *et al.* identified that the insertion of a 7mer peptide, LALGETTRP, at position 588 in the AAV2 capsid resulted in enhanced transduction of photoreceptor and retinal pigment epithelial cells, notoriously difficult targets for AAV vectors [448]. Recent techniques have evolved that utilize the *Cre/loxP* system to purify mutant vectors with desired phenotypes using a 3' floxed polyadenylation sequence. In this approach, mutated capsid

libraries are injected into mice expressing Cre recombinase and capsid sequences are purified from tissues of interest. A reverse primer designed to only amplify the sequence in Cre⁺ cells where recombination has occurred enables selection of variants that displayed enrichment in the Cre⁺ cells of interest [449]. While this approach identified a mutant AAV9 capsid, AAV-PHP.B, which displayed enhanced CNS tropism in the Cre⁺ C57BL/6J mice, such results have not been recapitulated in other animal models. These findings indicate that evaluation of mutant capsids could be constrained by model organisms and systems used for identification [450-452].

***In silico* Design**

Similar outcomes have been obtained through computationally directed design of ancestral capsids. Utilizing phylogenetic analysis of AAV clades, capsids can be designed that represent a common ancestor from nodes where divergence originated. These derived serotypes are advantageous due in part to increased immune evasion from neutralizing antibodies against the common outgroups, as well as altered tropism [453-455]. The best known examples from this approach are the computationally predicted Anc series of ancestral AAV mutants created by the Vandenberghe group [454]. One of these, Anc80, was a predicted ancestor to AAV serotypes 1, 2, 8, and 9. Early pre-clinical studies have found it to be a highly potent gene therapy vector for liver, muscle, and retinal gene therapy applications.

1.4.2.3 Genome Modifications for Transgene Expression

Alterations to the AAV genome itself have also been pursued in order to create optimized vectors. One approach has been to increase the size of transgenes that can be delivered by AAV vectors. Although the packaging capacity of AAV is ~4.7 kb, studies in the early 2000s examined the possibility of using dual vector approaches – so called split vectors. These approaches enabled the delivery of large transgenes that would undergo homologous recombination or trans-splicing following transduction. This recombination would enable the expression of the full length transgene sequence [456-459]. While these approaches utilized the co-transduction of two independent vectors that were within the packaging limit of AAV, studies also examined the absolute limit of genome lengths that could be published. A report published by Allocca *et al.* indicated that AAV5 vectors could express transgenes at least 8.9 kb in length [460]. Many believed that differences between AAV5 and other serotypes could be related to a genotype that lends itself to form an independent outgroup in the phylogenetic tree (**Figure 1.3.1**). It was soon identified though that these vectors did not in fact contain full length genomes. Rather a mixture of capsids were produced that carried genome fragments no larger than ~5 kb [461-463]. These fragments were then able to assemble into full length products in transduced cells through homologous recombination or concatemerization. Studies on split-vectors and capsid modifications to increase packaging size are still pursued, although the reliance on reestablishing the complete transgene in transduced cells decreases their efficiency compared to smaller vectors. Some issues have been reported where

the upstream transgene may express unintended protein products due to cryptic stop codons and polyA sites if recombination does not occur [416, 464, 465].

Alternatively, groups have examined methods to increase transgene expression through genome modifications. Following transduction a crucial rate-limiting step in the expression of the vector transgene is the requirement to convert the ssDNA genome into dsDNA [466]. While delivery approaches that involved co-transduction with helper Ad containing E1 and E4 genes, or treatment with DNA damaging agents were identified as methods to overcome this limitation, they are suboptimal approaches due to safety concerns [467-469]. The major pathway in unaided dsDNA conversion involves the annealing of complimentary ssDNA genomes with plus and minus polarity [470]. Building on this knowledge, self-complementary AAV vectors (scAAV) were developed to optimize this process. This system uses an internal inverted terminal repeat (ITR) with a deletion of the terminal resolution site (TRS) that enables it to act as a hairpin-like structure. This modification enables the genome to fold back upon itself and form dsDNA following transduction. This dimerization cannot occur during capsid packaging due to capsid packaging constraints and the dynamic differences between ssDNA and dsDNA genomes. The ability to overcome the dsDNA conversion step required for traditional ssDNA vector genomes results in dramatic increases in transgene expression and transduction efficiency, but the significantly reduced transgene capacity ($\leq \sim 2.2$ kb) further decreases the potential targets for therapeutic applications [419, 471-475].

1.4.2.4 Therapeutic Applications of Adeno-Associated Vectors

Owing to the safety and broad tissue tropism of AAV serotypes, they have been consistently used in a wide variety of gene therapy applications. As of late 2020, clinicaltrials.gov lists 152 registered ongoing studies evaluating AAV vectors, with AAV2 based approaches continuing to dominate the field. Although AAV can infect both replicating and non-replicating cell types, it is primarily used in non-dividing/slowly-dividing cell types to achieve prolonged expression without requiring integration. Designing vectors that contain regions of homology to genetic loci along with elements to introduce double-strand breaks can enable higher rates of integration. Zinc-finger nucleases, transcription activator-like effector nucleases, or Clustered Regularly Interspaced Short Palindromic Repeat/Cas (CRISPR/Cas) are common and enable long term transgene expression through the mechanisms of homology-directed repair [476-478].

Monogenic disorders are primary targets of AAV gene therapy and have covered a wide breadth of diseases across tissue and organ types. These include hemophilia A & B, retinal degeneration diseases, muscular dystrophy, Parkinson's disease, heart disease, and cystic fibrosis [479-485]. While some of these treatments are amenable to non-systemic delivery, such as retinal gene therapy and cystic fibrosis, a number of approaches entail systemic delivery. Those that require systemic delivery can be plagued by issues with natural pre-existing immunity or, in cases where more than one injection is required, acquired immunity from the initial treatment. For this reason, the development of the aforementioned

novel recombinant capsids that either reduce the immunogenicity of the vector and/or improve on tissue specific tropism can significantly increase the efficacy of these treatments.

To date, three AAV vector products have been approved for commercial development and use, although the cost of the treatments are severely limiting factors [486]. Alipogene tiparvoved (Glybera), an AAV1 based treatment for lipoprotein lipase deficiency, was approved in 2012 by the European Medicines Agency, becoming the first AAV vector-based gene therapeutic on the market. At a cost of \$1 million and limited use its production was halted in 2017. In 2017, an AAV2 vector treatment for Leber's congenital amaurosis, Voretigene Neparvoveczyl (Luxterna), became the first gene therapy product approved by the Food and Drug Administration at a cost of ~\$425,000 per eye. Onasemnogene Apeparvovec (Zolgensma), an AAV9 based treatment for spinal muscular atrophy was approved by the Food and Drug Administration for the treatment of children under two. With a treatment cost of \$2.125 million, the availability of this treatment is also severely constrained.

1.5 Alphaviruses

1.5.1 Classification

Alphaviruses are members of the family *Togaviridae*. The genus *Alphavirus* consists of approximately 30 species. They are enveloped viruses, ~70 nm in size, with an icosahedral capsid of $T = 4$ symmetry composed of 240 monomers, and a ~10 – 12 kb single-stranded positive sense RNA genome. Alphaviruses

are largely mosquito-borne arboviruses and utilize a variety of vertebrate hosts including non-human primates, equids, birds, amphibians, reptiles, rodents, pigs, and humans, although some have aquatic hosts [487-489]. They are classed in seven broad antigenic complexes – Barmah Forest, Eastern Equine Encephalitis, Middleburg, Ndumu, Semliki Forest, Venezuelan Equine Encephalitis, and Western Equine Encephalitis [122]. The genome contains two open reading frames. The first encodes nonstructural proteins (nsP1 – nsP4) in the N-terminal half of the genomic RNA, while the second encodes the structural proteins (Capsid, E3, E2, 6K/TF, E1) from a subgenomic promoter in the C-terminal half of the genome [490]. Both are translated with a 5' cap and 3' polyA tail.

Alphaviruses have a world-wide distribution, with detection on all continents, including Antarctica [488, 491]. The viruses are classified based on phylogenetic composition and clinical manifestations of disease as either New World, Old World, or Aquatic. Old World alphaviruses (e.g. Mayaro [MAYV], Chikungunya [CHIKV], and Semliki Forest virus [SFV]) are colloquially known as arthritogenic alphaviruses. They are characterized by typically mild disease symptoms that consist of fever and rash along with myalgia and arthralgia. In some cases, myalgia and arthralgia can persist for ≥ 1 year [492]. New World alphaviruses (e.g. Venezuelan, Eastern, and Western Equine Encephalitis virus [VEEV, EEEV, and WEEV]) are typically more virulent owing to the encephalitis that they induce in infected patients. For this reason they are designated as encephalitic alphaviruses, although they do share clinical symptoms including arthralgia and myalgia with the Old World alphaviruses [493]. Through phylogenetic

construction and analysis of member species multiple explanations have arisen regarding the geographic origin of the *Alphavirus* genus. While early proposals indicated the likelihood that they originated in the New World, it is still unclear. All current proposals rely on transoceanic spreads to result in the current distribution of viruses [494-499]. Phylogenetic analysis has led to proposals on origins and transoceanic introduction of New and Old World viruses. One such example is shown in **Figure 1.5.1**.

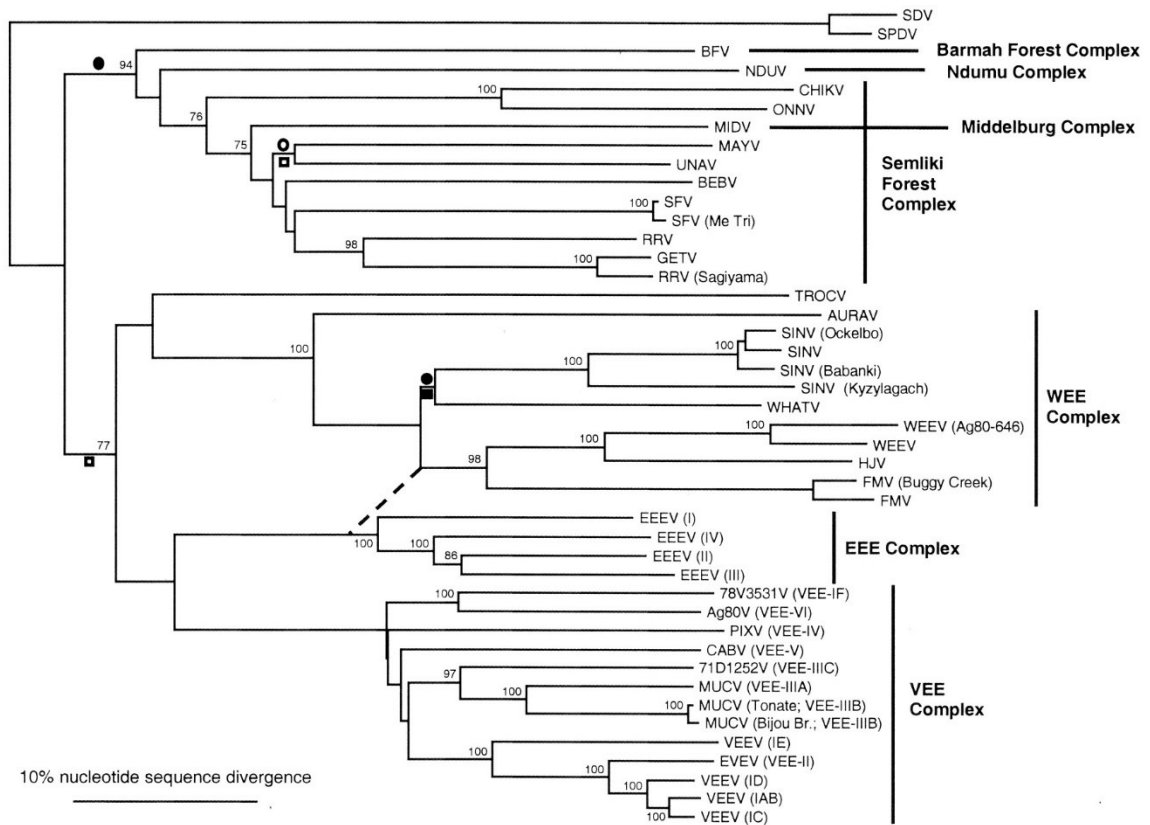


Figure 1.5.1 Phylogenetic relationship of Alphaviruses and Antigenic Complexes

Phylogenetic arrangement was completed by partial E1 glycoprotein gene sequences reconstruction. Numbers refer to bootstrap values for clades defined by the adjacent node. The open circle adjacent to a branch indicates hypothetical Old to New World introduction, and the closed circle indicates New to Old World introduction, assuming a New World origin; the open square indicates Old to New World introduction, and the closed square indicates New to Old World introduction, assuming an Old World origin of the non-fish *Alphavirus* clade. Abbreviations: SDV – sleeping disease virus; SPDV – salmon pancreatic disease virus; BFV – Barmah forest virus; NDUV – Ndumu virus; CHIKV – Chikungunya virus; ONNV – O’nyong’nyong virus; MIDV – Middelburg virus; MAYV – Mayaro virus; UNAV – Una virus; BEBV – Bebaru virus; SFV – Semliki Forest virus; RRV – Ross River virus; TROCV – Trocara virus; AURAV – Aura virus; SINV – Sindbis virus; WHATV – Whataroa virus; WEEV – Western Equine Encephalitis Virus; HJV – Highlands J virus; FMV – Fort Morgan Virus; EEEV – Eastern Equine Encephalitis Virus; PXV – Pixuna virus; CABV – Cabasou virus; MUCV – Mucambo virus; VEEV – Eastern Equine Encephalitis Virus. Reprinted with permission from Powers, *et al.* 2001 [497].

1.5.2 Genome and Viral Proteins

Alphavirus genomes are ~10 – 12 kb and consist of two open reading frames that encode the non-structural proteins (nsP1 – 4) and structural proteins (Capsid, E3, E2, 6K/TF, E1) (**Figure 1.5.2**) [500]. These proteins are synthesized as polyproteins, although the non-structural proteins are synthesized as two species, either p123 or p1234. The process of synthesis and cleavage will be discussed in the next section. The genomic RNA as well as the mRNA and subgenomic mRNA (sgmRNA) possess 5' 7-methyl-GpppA caps and 3' polyA tails [501, 502]. The genome also contains a number of important structural elements for replication and packaging. The genome is flanked by 5' and 3' untranslated regions (UTR) that play important roles in replication, suitable host range, and host cell interactions [503]. The length of the UTRs and sequence vary between different member species. A third UTR exists between the ORFs and contains the enhancer and promoter sequences for sgmRNA synthesis [504, 505]. There are four cis-acting conserved sequence elements (CSE) in the genome. Two are near the 5'

end, one between the non-structural and structural gene cassettes, and one upstream of the 3' polyA tail. They function to promote replication, transcription, and packaging of the viral RNA [506]. The first CSE is located at the 5' end and forms a stem loop like structure that serves as a promoter for positive-strand synthesis. The downstream second CSE is located within the coding sequence for nsP1 and has been identified to enhance both plus- and minus-strand synthesis. It may function as a promoter for minus-strand synthesis [507]. The third CSE, located between the non-structural and structural gene ORFs in the UTR, contains the subgenomic promoter required for synthesis of the structural gene products from the minus-strand genome product [506]. The fourth CSE located in the 3' untranslated region upstream of the polyA tail acts similarly to the first two CSEs, serving as a promoter for initiation of minus-strand synthesis [508]. Finally, packaging signals are present in the 5' end of the genome in order to direct faithful packaging of only the 49S genomic RNA rather than the 26S sgmRNA. These packaging signals have been detected in both nsP1 for viruses such as VEEV, WEEV, and SINV, and nsP2 for viruses such as CHIKV, ONNV, SFV [501, 509, 510].

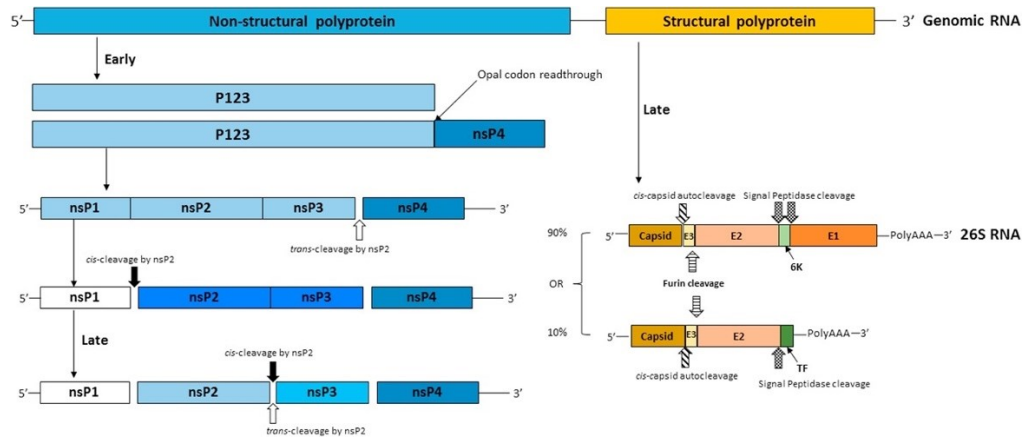


Figure 1.5.2 Organization of Alphavirus Genome

The Alphavirus genome is composed of non-structural and structural protein ORFs. The non-structural ORF is translated early in infection, yielding a polyprotein consisting of either 3 or 4 non-structural proteins (nsP123 or nsP1234 respectively). The presence of a leaky opal stop codon in some viruses is responsible for this phenomenon. Proteolytic cleavage by nsP2 results in the processing of the nsPs in a processive manner over the course of infection. Structural protein synthesis occurs late in infection, following negative strand synthesis, a subgenomic promoter is responsible for the transcription of the structural gene ORF and subsequent translation. Five structural proteins (Capsid, E3, E2, 6K/TF, and E1) are translated as a single polyprotein. Capsid autoproteolytically cleaves itself and the remain polyprotein is localized to the Endoplasmic Reticulum for further cleavage into single proteins. Reprinted with permission from Carey *et al.*, 2019 [500]

The nsP1 protein is ~60 kDa and encodes a capping enzyme with combined methyltransferase-guanylyltransferase activity [511-513]. It has been shown to play an important role in minus-strand synthesis. While it is structurally related to Rossman fold cellular methyltransferases, it instead methylates GTP prior to its addition to the 5' end of the viral RNA. nsP1 also contains an amphipathic peptide segment that serves to facilitate membrane binding, an important feature in the formation of viral replication complexes that will be discussed later [501, 514, 515]. Interactions between nsP1 with nsP3 and nsP4 have been implicated through co-precipitation assays.

The nsP2 protein is ~90 kDa and serves multiple roles in the virus life cycle. It has been shown to regulate the synthesis of sgRNA, acting as a co-factor that either binds to, or associates with the promoter for recruitment of the synthesis complex [501, 516]. The N-terminus contains a domain with helicase activity that is required for RNA unwinding during replication and transcription, as well as RNA triphosphatase and nucleoside triphosphatase activity [517, 518]. This triphosphatase activity is required and precedes the GTP capping activity of nsP1 [519]. The C-terminal domain encodes a novel papain like protease as well as an enzymatically non-functional methyltransferase domain. The protease domain is critical for the processing of P123 and P1234 into individual proteins through both *cis* and *trans* activity. nsP2 is also characterized by the presence of NLS domains that enables localization to the nucleus. This is important for Old World alphaviruses, as nsP2 induces host cell transcriptional shut-off through degradation of DNA-directed RNA polymerase II [520]. Mutations to the NLS domains has been shown to restrict nsP2 to the cytoplasm, preventing the transcriptional shutoff observed in Old World viruses, and reducing the observed cytopathogenicity [521].

The role of nsP3 in alphavirus replication and virus life cycle is less clear and is still under investigation. The protein is ~60 kDa and is composed of 3 domains – a highly conserved N-terminal macrodomain, an alphavirus-unique central zinc-binding domain, and a C-terminal hypervariable domain. The macrodomain has been shown to exhibit phosphatase activities and has been indicated in host-

protein interactions [522, 523]. It has also been implicated as serving as the recognition site for cleavage of nsP3 from nsP2, as well as facilitating ssRNA binding and minus-strand synthesis following phosphorylation [524, 525]. The precise role of the zinc-binding domain is still unclear, but studies have identified that mutations in this region negatively affect minus-strand and sgRNA synthesis, polypeptide processing, and neurovirulence [524, 526, 527]. A region of basic amino acids close to the zinc binding domain may be integral in the RNA binding activities exhibited by nsP3 [522]. The hypervariable region in the C-terminus is poorly conserved between alphavirus species and its exact role has not been fully defined. It appears to play a role in virus-host interactions and replication, with mutations in phosphorylation sites altering the replication permissiveness in cell culture and altering pathogenicity in mice [501, 526, 527]. The C-terminus also contains degradation signals that are believed to be involved in achieving the correct stoichiometric ratio of non-structural proteins during early alphavirus replication [522, 528].

Viral RNA replication is coordinated by the RNA dependent RNA polymerase (RdRp) activity possessed by nsP4, an ~70 kDa protein. The initial ~100 residues are unique to alphaviruses, although the remaining ~500 residues exhibit the traditional characteristics of RdRps [501]. A conserved N-terminal tyrosine residue has been shown to interact with nsP1 for minus-strand synthesis. Mutation of the N-terminus inhibited promoter binding activity for both the genomic and subgenomic promoters, altering either minus- or plus-strand synthesis [529, 530].

Alphavirus structural proteins are also synthesized as a single polypeptide. The capsid protein (Cap) autoproteolytically cleaves itself from the polypeptide shortly after synthesis through a serine protease domain in its C-terminus [531]. This proteolytic activity is conserved to the liberation of Cap and does not extend to further processing of the structural proteins. The N-terminus of Cap contains two distinct regions. Region I is highly positively charged and is believed to be involved in capsid dimerization through a helical secondary structure, while region II interacts with the genome packaging signal to facilitate nucleocapsid packaging [531-533]. Following the cleavage of Cap, a signal sequence is exposed that directs the remaining structural polypeptide to the ER for further processing and cleavage by host peptidases [534]. This processing results in the liberation of E1 and 6K/TF from E2 and E3, known as pE2 [535]. Following this activity, pE2 can then form heterodimers with E1 in the ER. Processing by furin in the Golgi results in cleavage of E3 from pE2, and enables the formation of 80 trimeric spikes of E1-E2 heterodimers [506, 536]. Cleavage of E3 from pE2 is required to generate infectious viral particles. Both E1 and E2 contain short cytosolic C-terminal domains, a transmembrane domain, and a large N-terminal ectodomain domain [506]. While the ectodomain of E1 possesses three β -sheet rich domains (I, II, and III), E2 is composed entirely of β -sheets and has three immunoglobulin domains referred to as A, B, and C [537]. The role of E1 and E2 in cell entry are discussed in the next section.

Finally, although 6K has been the canonical remaining protein, bioinformatic analysis was responsible for identifying the presence of a sparsely produced alternative protein, TransFrame (TF), from the 6K domain. TF is a small ~8 kDa protein product that shares the N-terminal domain with 6K, but the presence of a conserved UUUUUUA codon motif enables ribosomal shifting to the -1 reading frame at a frequency of ~10 – 18%. This results in the production of an approximately 15 aa extended C-terminus [538]. Although 6K has both N- and C-terminal transmembrane domains, the unique C-terminal extension of TF results in cytoplasm retention of the C-terminus. Both 6K and TF have been implicated in facilitating the budding of virus particles from infected cells and that the shared N-terminus is involved in ion-channel activity [535]. Analysis of TF deleted mutants with retained 6K activity identified a significant decrease in the production of infectious viral particles and severely attenuated pathogenesis in mouse models [535]. Similar approaches have been conducted with 6K mutations. It is believed that 6K may play a role in the proper folding, assembly, and transport to the plasma membrane of the E1-E2 spike heterodimers [539, 540]. Although both 6K and TF have been identified in small amounts in fully assembled virions, it is TF, rather than 6K, that is predominantly incorporated into virions [538].

1.5.3 Mechanisms of Cellular Entry, Trafficking, & Replication

Infection of host cells by alphaviruses relies on the binding of the viral E2 spike glycoprotein to host cell receptors. Although a great deal of effort has been expended, a clear predominant binding factor/receptor has not been identified. A

number of putative cellular proteins have been considered. These include heparan sulfate proteoglycan, major laminin receptor, DC-sign, L-sign, MHC-I, and prohibitin-1 [541-545]. The identification of primary receptors has been complicated by the wide host range for alphaviruses and as such suggests that either ubiquitous or multiple binding factors/receptors are utilized. Recently, a genome-wide CRISPR/Cas9 screen in mouse 3T3 fibroblasts identified that the adhesion molecule *Mxra8* played a key role in Old-World alphavirus cell infection. Assessment of CHIKV, MAYV, SFV, O'nyong'nyong virus (ONNV), and Ross River virus (RRV), all displayed decreased infectivity of cells modified by guide RNAs against *Mxra8*. Conversely, ectopic expression of mouse or human *Mxra8* increased infectivity [546]. Following E2 receptor binding, the virus is internalized primarily through clathrin-coated pits or caveolae-derived vesicles, although the virus does not promote increased production and internalization of these vesicles [544, 547-549]. As the endosome matures and acidifies, the E1/E2 heterotrimer dissociates, which exposes the E1 fusion domain [550]. The pH required for this conformational reorganization and subsequent membrane fusion varies between species and strains. Although CHIKV, MAYV, and SFV all fuse between pH ~5.9 – 6.2, VEEV requires the lower pH of late endosomes for viral fusion [551-554]. These differences are likely related to the sequence of the envelope proteins. Such an effect has previously been identified as the reason why some alphaviruses, such as CHIKV, SFV, and SINV require the presence of cholesterol and sphingolipids for E1 membrane fusion, while VEEV does not [490, 547, 551]. A P226S mutation in SFV was able to overcome the cholesterol fusion dependence,

and, as this mutation is already present in VEEV, this observation suggests that entry mechanisms vary slightly between New and Old World species [490, 551, 555]. It is also possible that the presence of cholesterol in endosomal vesicles may act to inhibit VEEV membrane fusion. As endosomes acidify they lose cholesterol and may indicate that cholesterol inhibits this process of membrane fusion to some degree [551].

Following nucleocapsid escape into the cytoplasm, disassembly occurs rapidly in ~1 minute. This process is facilitated through the binding of the large 60S ribosomal subunit to a ribosome binding site between the N-terminal basic region and C-terminal protease domain of Cap [556, 557]. The exact position of this region varies between the species (SINV from aa94-105, VEEV from aa105-116, and SFV from aa101-110), although the function is conserved [557, 558]. Once liberated from the nucleocapsid, the genomic RNA can then be translated by cellular ribosomes. Translation begins from the 5' end at an AUG codon and proceeds through the nsP ORF, producing P123 and/or P1234 polyproteins. The majority of alphaviruses contain a leaky opal stop codon between nsP3 and nsP4. At a readthrough rate of ~10% this enables production of both polyproteins. Some, such as ONNV, lack the opal stop codon and solely produce the P1234 polyprotein [522, 559, 560]. Following translation, the protease domain in nsP2 functions to process the polyprotein into individual proteins. Cleavage first occurs in *cis* at the P3/4 junction, resulting in P123 and nsP4. Next, nsP2 cleaves in *cis* between the P1/2 junction, resulting in nsP1 and P23 [561, 562]. The cleavage of nsP1 from

the P123 polyprotein is absolutely required for the final cleavage between P23. This final cleavage by nsP2 occurs in *trans* [563]. During the processing of the nsPs, the synthesis of viral RNA is temporally regulated. The P123+nsP4 product strongly favors synthesis of minus-sense RNA, while the nsP1+P23+nsP4 products favor positive-sense over minus-sense RNA synthesis. Once fully cleaved, the nsPs are only able to synthesize positive-sense RNA but strongly favor sgRNA synthesis [563, 564].

The replication of viral RNA by these nsP intermediate cleavage products is membrane-associated and relies on the formation of plasma membrane invaginations and type-1 cytopathic vacuoles, termed spherules. These are formed through interaction with the replication complex. They can be formed by the partially processed nsP polyproteins, although they are less morphologically structured than those formed during active RNA synthesis [565]. These spherules serve to protect the dsRNA intermediates from host cell cytoplasmic immune sensors and DNA degradation processes [566]. Viral replication proceeds in these spherules through the previously described nsP functions. The resulting RNA products are released into the cytoplasm through a narrow neck-like structure. As sgRNA becomes the favored replication product, the structural polyprotein can then be translated. During translation, Cap is autoproteolytically cleaved and able to dimerize and package the newly synthesized full length positive-sense viral RNA. The resulting nucleocapsid then proceeds towards the plasma membrane for budding. Following Cap cleavage, the remaining structural polyprotein is

transited to the ER and Golgi for processing by host peptidases and furin resulting in the cleavage of the polyprotein to individual proteins. Each virion contains 80 trimeric spikes of E1-E2 heterodimers. Although E3 is cleaved from the E1-E2 heterodimers by furin, it remains in a complex with them as they transit from the Golgi to the cell membrane. Due to the acidic environment of the cytoplasm, E3 prevents early triggering of E1 that would otherwise result in non-infectious virions [567]. Once at the plasma membrane, E3 is lost and the glycoprotein spikes and 6K/TF insert into the plasma membrane. The cytoplasmic domain of E2 is then able to associate with a hydrophobic pocket on the assembled nucleocapsid cores, enabling budding of the virus with a portion of the host cell membrane for subsequent rounds of infection. Transmission to neighboring cells can also occur through membrane projections that enables new virions to avoid immune detection and neutralization [568, 569].

1.5.4 Epidemiology, Hosts, & Vectors

Alphavirus transmission largely occurs through the bite of insects, the most frequent vectors are mosquitoes. The viruses are maintained and circulate in both sylvatic and urban cycles. Alphaviruses have a broad host range, infecting numerous vertebrate species including rodents, birds, reptiles, equids, non-human primates, and humans, as well as arthropods. Female mosquitoes acquire infections through feeding on viremic hosts, which results in midgut infection with persistent viral replication. The virus can then disseminate through the body, leading to infection of the salivary glands and ovaries. Mosquito vector

competence varies between member species, although *Aedes* and *Culex* species are predominant vectors of alphaviruses [570-572]. For example, while CHIKV is predominantly spread by *Aedes* species, *Culex* mosquitoes have been found to carry CHIKV but are currently considered a poor vector for spread. Vector competency can be affected by multiple viral intrinsic and extrinsic factors.

Tissue barriers in the mosquito are a primary obstacle for virions in establishing infection. After bloodmeal feeding, mosquitoes secrete a peritrophic matrix that envelopes the bloodmeal. Viruses must either infect prior to this secretion, or must be able to pass through it to access the midgut epithelium [571, 573]. For viruses that can bypass this first barrier, the virions must then penetrate the basal lamina following infection and replication to access the hemolymph system for dissemination. Evidence has shown that virions can take an alternative route to the hemolymph by infecting tracheal cells following midgut replication [573, 574]. Following entry into the hemolymph, the virions encounter a similar basal lamina that surrounds the salivary gland. While this barrier also functions to prevent infection of the salivary gland, it acts as a major limiting factor in virion escape during bloodmeal feeding. Although mosquitoes that consumed infected bloodmeal had detectable virus in the salivary glands as early as 2 dpi and achieved maximal titers after 4 dpi, only approximately one-third of the mosquitoes had detectable virus in their saliva at 7 dpi [575]. Although these barriers can be restrictive and limit the permissiveness of certain host species to infection, coinfection of mosquitoes with parasites and their microfilariae can entail damage

to these barriers. The parasites can damage the epithelial midgut resulting in increased midgut infection and can damage the basal lamina leading to increased shedding of virions into the mosquito hemolymph.

Ambient temperature has also been shown to affect the competency of mosquitoes for alphaviruses. During studies with *A. taeniorhyncus* mosquitoes it was identified that regardless of temperature after virus exposure, mosquitoes reared at 19 °C were significantly more susceptible to infection with Rift Valley Fever virus and VEEV than counterparts reared at 26 °C [576]. This same study did identify that regardless of rearing temperature, mosquitoes maintained at 26 °C had increased virus dissemination following infection than those maintained at 19 °C. Comparatively, Westbrook *et al.* identified a similar relationship between *A. albopictus* mosquitoes and CHIKV [577]. Rearing at 18 °C again resulted in significantly increased rates of infection compared to those reared at 24 °C or 32 °C. Rainfall and humidity are other environmental factors that have been associated with higher rates of infection and outbreaks [578, 579].

Vector competency is also affected by viral adaptations that enable broader host ranges and/or infectivity. The high mutation rate of approximately 10^{-4} mutations per copied nucleotide in RNA viruses is due to their RdRp [580]. The ability to rapidly evolve through adaptive mutations and purifying selection of mutants enables the emergence of novel strains that can display increased fitness and potentially new host ranges [581]. This was observed during the 2005 – 2006 Indian Ocean CHIKV outbreak where *A. albopictus* mosquitoes were responsible

for spread. It was observed that although viruses responsible for early infections from March – June 2005 all had an Alanine residue at position 226 of E1, by September a Valine mutation at this position (E1 A226V) emerged and grew to predominance. After September, greater than 90% of sampled viral sequences displayed this mutation [582]. Later studies identified that this mutation resulted in significant increases in vector competency of *A. albopictus* mosquitoes without affecting the viral fitness in *A. aegypti* mosquitoes [583]. Studies with the E1 A226V mutant found that it possessed an increased ability to overcome the mosquito midgut barrier and establish infection. The exact mechanisms behind the increased vector competency are unresolved [571, 584].

While outbreaks have largely been geographically restricted over the last century, the last few decades have seen an expansion in the global range of alphaviruses, notably for CHIKV. The global range of alphaviruses has increased for a number of reasons, including vector adaptation, global climate change, and host travel patterns. Although many viruses typically circulate within sylvatic cycles with forest-dwelling mosquitoes, adaptation to urban mosquitoes increases the risk for epidemic outbreaks. Such outbreaks could be precipitated from workers and travelers entering forests and returning to urban centers, a factor in recent global occurrences of MAYV and CHIKV in North America and Europe [585-587]. Deforestation and urban encroachment into environments where the viruses circulate are also influencing factors. Along with this, increased geographic range of host species, such as birds and mosquitoes, has influenced the increased range

of these viruses [588]. As global temperatures continue to increase, the range of hospitable temperatures for mosquito vectors outside of the tropics will enable further spread into new geographic regions, which the United States and Northern hemisphere is currently experiencing [589, 590]. Currently, the range of *A. aegypti* encompasses approximately half of the global population, creating a significant risk for transmission of alphaviruses, flaviviruses, and other arboviral diseases [591, 592].

Since the late nineteenth century when mosquitoes were recognized as a vector capable of transmitting pathogens to humans, control strategies have been employed to reduce outbreak potential. Petroleum-based larvicidal agents were among the first vector control approaches and continue to be utilized in some areas to this day. These agents are able to kill exposed larvae through direct toxicity and/or suffocation [593-595]. Chemical agents, such as dichloro-diphenyl-trichloroethane (DDT), have also been employed, but their use has been thwarted due to regulations and ecological/environmental damage. Pyrethroids, a family of synthetic organic compounds that are similar to naturally occurring pyrethrins, were then used as an alternative to the organophosphate compounds. Recently though, a growing trend in mosquito resistance has been noted [596, 597]. Insecticides offer a distinct advantage in their breadth of applications, including outdoor airborne dispersal, mosquito net coating, and indoor residual spraying. For these reasons they continue to be developed and utilized. Traps are another common strategy. Baited attractive lethal OviTraps are often used to kill egg-

bearing females, significantly reducing the *Aedes* population when employed in the field. Studies in Puerto Rico observed a 79% reduction in population densities of female *Aedes* mosquitoes, and in Iquitos, Peru dengue transmission was reduced by 75% in neighborhoods with traps versus control neighborhoods [598, 599].

Vector control has also relied on biological strategies, such as the use of the mosquito larvae predator *Poecilia reticulata*. The effectiveness and concerns on the introduction of potentially invasive foreign aquatic species, raises questions regarding this approach [600]. Alternative strategies have attempted to use the release of *Wolbachia*-infected mosquitoes. This strategy limits the ability of fertilized eggs to develop and protects against infection by some viral pathogens [601-603]. Recently, biological approaches have relied on the ability to introduce genetic mutants to the mosquito population. Genetically engineered OX513A *A. aegypti* mosquitoes pass on a dominant lethal gene to larvae, suppressing population growth. A field study noted that this approach did not result in species replacement by *A. albopictus* mosquitoes [604-606]. Recently, the FDA approved a field trial of a second generation OX5304 *A. aegypti* strain in Florida to combat Dengue following effective proof-of-principle studies in Brazil (unpublished data). Similar approaches have utilized gene drive technology to limit mosquito populations. Such an approach has been used against *Anopheles gambiae*, a vector of malaria. Using a CRISPR/Cas9 cassette, researchers were able to create sterile intersex rather than female mosquitoes. This resulted in complete

population suppression in a controlled environment [607]. Approaches are being developed for *A. aegypti* and are likely to provide similar efficacy as seen in previous applications of gene drives in other mosquito species [591, 608].

1.5.5 Pathogenesis

Host infection occurs following the bite of an infected arthropod, predominantly via mosquitoes. During blood meal feeding, the virus and mosquito salivary gland proteins are introduced into the dermis, enabling infection. The mosquito salivary proteins play an important role in the infection process as they facilitate blood feeding and are composed of numerous factors with immunomodulating, anti-inflammatory, and anti-hemostatic properties. These salivary proteins facilitate the local edema through upregulated expression of neutrophil attracting chemokines and cytokines. Expression of IL-1 β has been determined to play a significant role in the cutaneous inflammatory response to mosquito bites [609]. These immune responses create an environment that enables enhanced viral infection and replication. The effects of mosquito bites on viral infections have been observed in mouse studies where mice were either challenged at the site of a mosquito bite or in non-bitten locations. Mice challenged with SFV at the site of mosquito bites displayed markedly higher levels of viral RNA at the site of infection. A majority of these mice would later succumb to infection. Additionally, significant differences in the rate of viral RNA detection in the draining lymph node (dLN) post infection has been observed. When mice were challenged at mosquito-bite free sites, viral RNA was detected at ~3 – 6 hpi while those challenged at the site of mosquito bites had

undetectable viral RNA levels until 24 hpi [609]. The rapid draining of virus from the challenge site in control group animals resulted in decreased viral spread to other tissues and organs, as well as reduced viremia.

This transit of virus to the dLN occurs either through infected resident Langerhans and dendritic cells or as cell free virus. CHIKV infection of the dLN has been shown to result in lymphocyte depletion through inhibited accumulation of naïve lymphocytes, failure to develop germinal centers, and fibrosis [610]. Virus can then spread via the lymphatic system into the bloodstream for dissemination to distant organs and tissues. Although CHIKV has not been shown to productively replicate in the dLN, detected replication may be the result of infiltration of infected monocytes and macrophages. Comparatively, the dLN has been indicated as a primary site for VEEV replication [610-612]. VEEV begins to replicate upon introduction to the draining lymph node and enters the circulation within 12 hours of infection. Observed dissemination indicates a strong preference for lymph tissues and organs, replicating favorably within mononuclear phagocytes in these locations [613, 614].

1.5.5.1 Immunological Response

Both the adaptive and innate immune response play critical roles in controlling alphavirus infections. Following infection, the replication of the genomic RNA results in the accumulation of partially double-stranded RNA intermediates with pathogen associated molecular patterns (PAMPs) that are recognized by pattern recognition receptors (PRRs). The receptors include membrane bound toll-like

receptors (TLR), such as TLR3 and TLR7, cytosolic retinoic acid-inducible gene I (RIG-I), and RIG-I-like receptors such as melanoma differentiation-associated protein 5 (MDA5) to activate innate immune responses to infection [615-617]. Upon PRR activation, a cascade of ubiquitination- and phosphorylation-driven signaling events results in the activation of transcription factors such as IRF3/7 and NF- κ B. These drive the production of inflammatory cytokines, chemokines, and type I interferon (IFN) [618]. Her *et al.* found that TLR3, which signals through TRIF for IRF3 activation and IFN- β transcription, plays a fundamental role in the adaptive immune response in controlling CHIKV infection [619]. Similarly, TLR7 activation leads to NF- κ B and AP-1 mediated expression of inflammatory cytokines and chemokines through IRF7 mediated type I IFN signaling [618, 620].

PRRs RIG-1 and MDA5 are composed of 2 N-terminal Caspase recruitment domain adaptors (2CARD), a central DEAD-box helicase, and a C-terminal regulatory domain. Upon recognition and binding to dsRNA, the 2CARD domain is exposed, enabling activation of the mitochondrial antiviral signaling protein (MAVS). This results in a signaling cascade in which IKK-I and TBK1 kinases are stimulated and activate NF- κ B and IRF3 respectively [618]. IRF3 and NF- κ B signaling is also stimulated through the cGAS/STING pathway. This pathway is activated by the presence of cytosolic dsDNA, such as mitochondrial DNA released during cellular damage from infection. Evidence has found that RIG-1 and MAV5 are able to associate with STING, resulting in IRF3 activation [621]. Similarly, RIG-1 and MAVS signal through protein kinase R (PKR) for IRF3

activation. While this results in production and stabilization of type I IFN mRNA, PKR expression results in the inhibition of both viral and cellular protein synthesis through the phosphorylation of cellular eIF-2 [622].

The type I IFN response, including 13 alpha IFNs (IFN- α) and 1 beta IFN (IFN- β) in humans, is a critical component of the antiviral response to alphavirus infection. Upon infection, IFN- α/β results in autocrine and paracrine stimulation of the IFN- α/β receptors (IFN α R), activating the receptor associated Janus kinase (JAK1) and tyrosine kinase 2 (TYK2) [623]. Once activated, JAK1 and TYK2 phosphorylate signal transducers and activators of transcription (STAT) 1 and 2, enabling the formation of heterodimers. STAT1/2 heterodimers then associate with IFN regulatory factor (IRF9) and translocate to the nucleus. There they associate with IFN-stimulated response elements (ISREs) to activate the transcription of hundreds of IFN-regulated genes [623, 624]. These stimulated IFN genes are responsible for induction of the antiviral state that inhibits the required processes for viral transcription, replication, and translation. They also function to degrade viral nucleic acids and alter the cellular lipid metabolism processes. Studies with IFN α R^{-/-} and STAT1^{-/-} knockout mice have identified that this pathway is invariably required for control of alphavirus infection. These mice quickly succumb to infection and perish, while WT mice typically do not [624-626]. Similarly, IRF3/7^{-/-} knockout mice failed to produce detectable levels of IFN- α/β and quickly succumbed to infection [627].

Along with coordinating intracellular antiviral processes, IFN- α/β signaling plays integral roles in the innate and adaptive immune response, although they appear to act in separate pathways. Cook *et al.* identified that in the course of disease infection in various knockout mouse models, that IFN- α/β play differential roles: IFN- α limits the replication and dissemination of CHIKV while IFN- β limits pathogenesis and inflammation mediated by infiltrating neutrophils [628]. Following the activation of IFN and PRR signaling, pro-inflammatory cytokines and chemokines are robustly produced, resulting in the recruitment of innate and adaptive immune cells to the site of infection. Human cohort studies have identified a broad array of cytokines and chemokines displaying upregulation during infection, including CCL2, IL-6, IFN- α , TNF- α , and IL-1 β [629-632]. Recruitment of monocytes, macrophages, dendritic cells, and natural killer cells to the infection site occurs shortly after infection. Although their early actions are to aid in clearing the infection, their presence also correlates with inflammation-associated pathogenesis. Infiltration also enables the infection of macrophages, resulting in the prolonged detection of virus in lymphoid tissues and organs [632]. Intriguingly, recruitment and immune mediated pathogenesis of natural killer cells has been observed to be virus strain dependent [633]. Antigen presentation results in the activation of cytotoxic CD8⁺ and helper CD4⁺ T cells in order to mediate destruction of infected cells and support the modulation of the immune response. In the case of CHIKV infection, anti-CHIKV IgM antibodies are initially detected after B cell activation, but by the second week of infection IgM production wanes and IgG responses increase [632]. Elicited neutralizing antibodies predominantly target the

E2 protein, enabling inhibitory effects on virus attachment, fusion to the endosomal membrane, assembly and release of new virions, and cell-to-cell spread [632]. Additional effector properties of elicited antibodies to limit alphavirus infection may include antibody mediated cellular cytotoxicity, complement activation, and virus opsonization. Several studies, including the data presented in chapter 2, have identified that antibodies elicited from vaccination and natural infection are cross-protective against related alphavirus species. Most notably this has been observed for CHIKV, MAYV, and UNA, indicating that conserved antigenic domains exist (**Supplemental Figure 1**) [634-636].

As differences in viral dissemination and pathology exist between New and Old World alphaviruses they will be discussed separately below.

1.5.5.2 Old World Alphaviruses

Following infection and early replication, the virus enters the blood system and achieves high viremic titers. For Old World alphaviruses, such as MAYV and CHIKV, circulating virus is predominantly observed to infect muscle, joint, and tendon tissues (**Figure 1.5.3**). Following infection, symptoms typically present within 3 – 10 days, with a relatively short 4 – 7 day viremic period. The majority of symptoms typically resolve within 1 – 2 weeks and fatalities are exceedingly rare [614, 637]. Old World alphaviruses present with common symptoms of arthralgia and myalgia, and can be accompanied by acute fever, skin rash, malaise, retro-orbital pain, and headache. These symptoms can vary based on the virus species.

Arthralgia typically presents initially in the small joints such as the fingers, wrists, and tarsus, but later progresses to large joints such as the knees and shoulders [614, 638]. These symptoms are the result of viral tropism for musculoskeletal tissues, with primary cellular targets being fibroblasts, mesenchymal cells, osteoblasts, and muscle satellite cells [639, 640]. Lymphoid organs and tissues, liver, and the heart are additional targets of the virus following infection [637]. While historically rare, neurological complications associated with CHIKV infection were reported following the recent Indian Ocean outbreak. Viral RNA has also been detected in the vitreous fluid of the eye [641, 642]. As these reported effects are still rare, CHIKV is not considered a neurotropic virus. While other characteristic symptoms are transient and quickly resolve following infection, patients can experience prolonged arthralgia and myalgia. In some cases this can last upwards of one year [492, 614, 643]. A population study of La Réunion island residents that were seropositive for CHIKV infection found that ~43 – 75% of infected individuals reported prolonged symptoms two years post infection [644]. Infiltration of monocytes, macrophages, NK cells, CD4⁺ and CD8⁺ T lymphocytes are primary cellular components of inflammation and the associated arthralgia and myalgia experienced in patients.

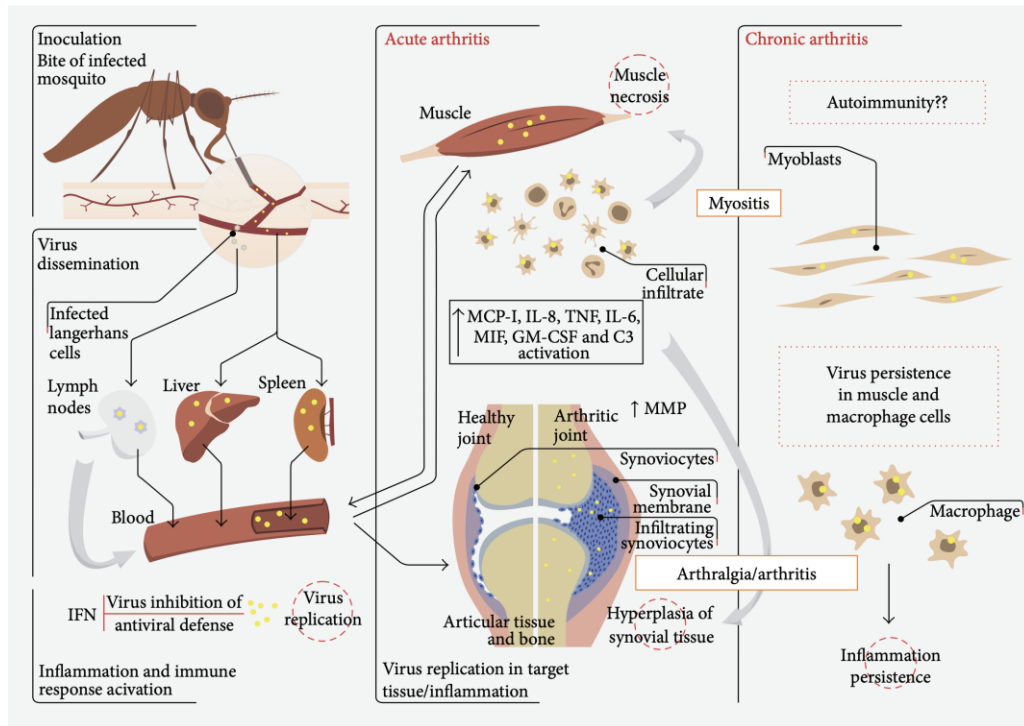


Figure 1.5.3 Infection Pathway and Pathogenesis of Arthritic Alphaviruses

Following the bite of an infected mosquito, virus is introduced into the dermis, enabling infection of resident Langerhans and dendritic cells. These can then transit to the draining lymph node for further dissemination by the circulatory system. Virus can also enter the circulatory system from the site of infection. Infection of muscle and joint tissues results in elevated production of pro-inflammatory cytokines and chemokines, attracting monocytes, macrophages, dendritic cells, and natural killer cells to the site of infection. These cellular infiltrates exacerbate inflammation and the associated arthralgia and myalgia. Chronic persistent arthralgia and myalgia can occur and can be caused by persistent virus/viral genomes in the tissues and macrophages. Reprinted with permission from Assunção-Miranda *et al.*, 2013 [614].

Following cellular infection nsP2 plays a critical role in shutoff of host cell transcription. The presence of a C-terminal NLS in nsP2 allows translocation to the nucleus where it induces the degradation of RNA polymerase II (RNAPII) subunit RBP1 within 6 hours of infection. The degradation does not occur by the innate nsP2 protease function, but rather through nsP2 directed ubiquitination of RBP1 and RNAPII-associated proteasome activity [520]. Mutational analysis identified that ubiquitination is facilitated by helicase and SAM-dependent methyltransferase

like domains of nsP2, as point mutations were able to abrogate RBP1 degradation activity [520]. This process is similar to the events of RPB1 ubiquitination in the transcription-coupled repair pathway. Rapid control and shutdown of host cell transcription is integral to counteract the stimulated antiviral response and subsequent production of interferon stimulated genes (ISGs). Frolova *et al.* identified that murine cells infected with nsP2 mutated SINV displayed higher levels of IFN and subsequent activation of 170 cellular genes induced by IFN expression and/or virus replication [645]. Subsequent research by Fros *et al.* established that nsP2 from CHIKV and SINV blocks STAT1 phosphorylation and/or nuclear translocation and in turn inhibits the JAK-STAT signaling pathway [646].

Coupled with transcription shutoff, alphaviruses also coordinate the inhibition of host cell translation. During infection and the induction of the cellular antiviral state, PKR is able to phosphorylate the alpha subunit of eIF2 to prevent GDP to GTP recycling by eIF2B [647]. This phosphorylation can also be regulated through PKR-like ER kinase (detects unfolded proteins in the ER), GCN2 (senses nutrient starvation), and heme-regulated inhibitor (detects heme deficiency) [648]. Although eIF2 α phosphorylation is a well-established function of alphavirus infection, Rathore *et al.* found that CHIKV nsP4 expressed under the control of a CMV promoter was able to inhibit this phosphorylation. Non-endogenous expression levels due to the CMV promoter may have influenced this observation [649, 650]. Gorchakov *et al.* found that SINV can inhibit translation in a PKR-independent mechanism, and Akhrymuk *et al.* later identified that the mono-ADP-

ribosylhydrolase activity of the nsP3 macrodomain was capable of driving this inhibition [651, 652]. As translational shutoff coincides temporally with the need to translate sgRNA into the structural proteins, alphaviruses have evolved a process to circumvent the requirement of eIF2. The presence of a downstream loop (DLP) structure in SFV and SINV serves as a translation enhancer and enables translation initiation in the absence of functional eIF2 [653]. The presence of the DLP has not been observed as a universal feature as RNA folding prediction software has been unable to determine the presence of such a structure in CHIKV, ONNV, VEEE, and WEEV, although eIF2 α phosphorylation does not inhibit translation of their sgRNA (**Figure 1.5.4**) [624, 650, 654]. Instead, similar structural features are likely present that act in a similar manner but do not conform to a canonical DLP structure. Evidence has suggested that the DLP functions to enable sgRNA translation by capturing the 40S ribosomal subunit in a position favorable for initiation at the AUG codon [655]. While the DLP is required for efficient translation initiation in mammalian cells, it is dispensable in insect cells where no PKR ortholog has been identified [654]. Ventoso found that culturing of SINV with a mutant DLP in a murine cell line led to the evolution of a DLP structure through recombination. This data indicated that this structure may have naturally evolved to counteract the effects of PKR activation and eIF2 α phosphorylation in mammalian cells [654].

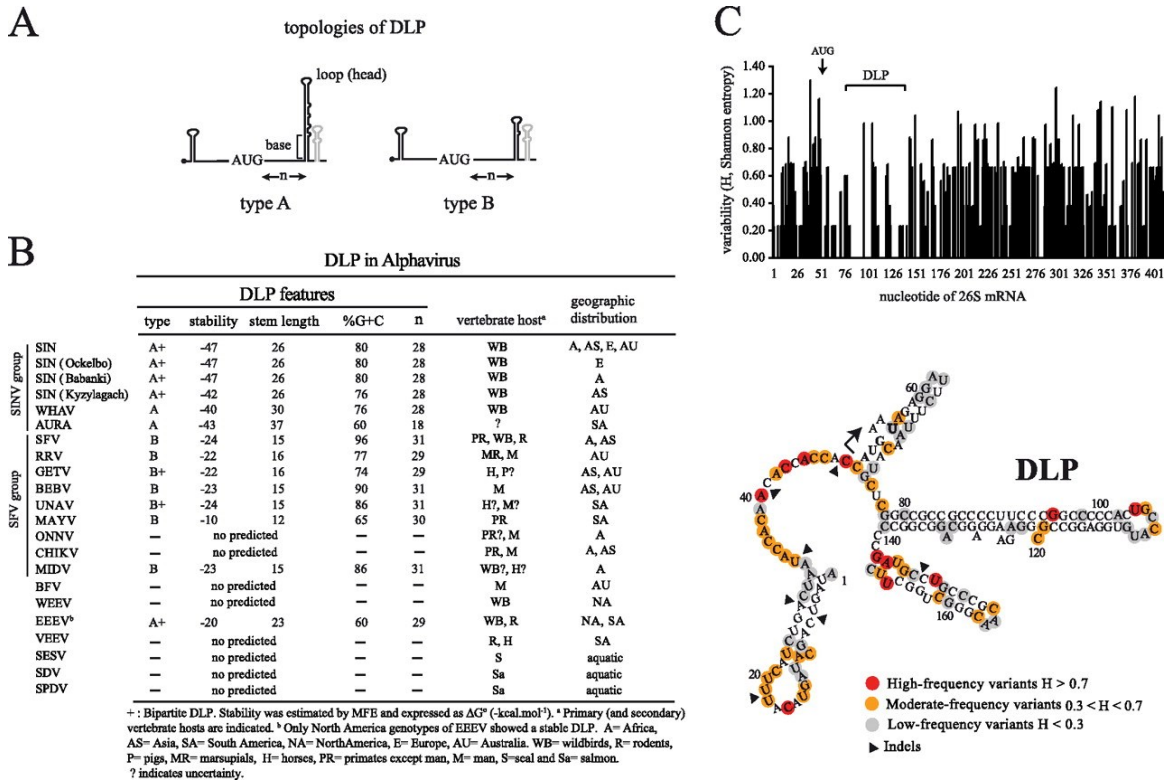


Figure 1.5.4 Structural Features and Presence of DLPs in Alphavirus Species

(A) Topologies of identified stem loops determined they consist of a large or compact spiral, sometimes with the presence of a secondary downstream loop (light grey). (B) Features of DLPs among analyzed species. N represents the number of bases between the AUG codon and the base of the DLP structure. Vertebrate hosts and geographic distribution are shown. (C) The DLP loop sequence is relatively well conserved with the bar chart indicating calculated variability of the first 400 bp of the 26S RNA by the Shannon entropy (H) method. Topology of the DLP is shown and variant positions and score are indicated. The AUG codon is marked by an arrow, and arrowheads indicate positions where indels were identified. Reprinted with permission from Ventoso, 2012 [654].

1.5.5.3 New World Alphaviruses

New World alphavirus infections are also facilitated by the bite of an infected mosquito. Patients typically begin experiencing symptoms within 2 – 5 days of infection, with febrile illness lasting on average between 4 – 6 days. The febrile infection symptoms share similarity to Old World alphaviruses, with patients

experiencing fever, headache, nausea, and myalgia. Approximately 5 – 15% of VEEV patients, especially children, progress to severe neurological symptoms shortly after onset of the febrile illness. These symptoms can include encephalitis, disorientation, convulsions, seizures, coma, and death [498]. Although mosquito bite acquired WEEV and VEEV infections have low-case fatality reports in humans (~0.5 – 1% and ~3 – 4% respectively), EEEV is substantially higher (~35 – 70%) [656, 657]. In contrast to humans, equine infections present serious veterinary medicine concerns and commonly result in death from encephalitis (~20 – 80% from VEEV, ~3 – 50% from WEEV, and ~70 – 90% from EEEV) [657, 658].

Central nervous system (CNS) penetration occurs primarily through the olfactory neuroepithelium and trigeminal nerve [659]. As aerosolized New World alphaviruses have been shown to infect patients, they are at increased risks of CNS penetration due to the direct access to the olfactory neuroepithelium. Patients infected by aerosolized virus have displayed a uniformly increased risk of death [498]. Access to the CNS can also be achieved through interferon responses that result in permeability of the blood brain barrier. Following entry, the virus progresses throughout the CNS by way of neuronal tracts and limbic structures [659, 660]. Neurons and glial cells are predominant targets, and infection results in subsequent degeneration of these cells [661]. Encephalitis is mediated through the host immune response and influx of macrophages, lymphocytes, and neutrophils [660, 662, 663]. Infected microglial cells play an important role in the

production of cytokines and chemokines through the activation of PRRs and their previously described downstream signaling pathways [664]. Mouse models of CNS adapted SINV infection have noted prolonged B cell secretion of IgG and IgA specific SINV antibodies in the CNS up to a year post infection. Although infectious virus is typically cleared within 7 dpi, viral RNA persists at a low level in some cells. It is likely that viral proteins are still shed and provide prolonged expression of antigens [665, 666].

In contrast to Old World alphaviruses, the capsid protein from New World alphaviruses is responsible for host cell transcriptional shutoff. This activity is mediated by two distinct domains (aa 32 – 51 and aa 64 – 68) in the capsid N-terminus. The first domain folds into an α -helix secondary structure and contains a leucine-rich supraphysiological nuclear export signal (NES), while the second domain acts as a nuclear localization signal (NLS) [667-669]. Together these function to inhibit transcription of genes under RNAPI and RNAPII promoters, as well as to inhibit nuclear import and export processes [669, 670]. The supraphysiological NES binds CRM1 in the absence of RanGTP, while the NLS domain binds to α/β importin. Upon binding these export/import factors, the complex binds to nucleoporins and accumulates in the nuclear pore complex. The formation of this tetrameric complex blocks further export/import activities of transcribed genes, reducing cytoplasmic mRNA levels [668]. Further direct inhibition of host cell translation follows the aforementioned eIF2 α phosphorylation process, although this again has no impact on viral sgRNA translation.

1.5.6 Mayaro Virus

Mayaro virus (MAYV) was first isolated from five symptomatic patients in 1954 in the Mayaro province of Trinidad and Tobago. It is an Old World alphavirus endemic to South and Central America [671]. MAYV is currently classified into three genotypes based on geographical distribution: (**D**) **D**istributed largely throughout South America and the Caribbean, (**L**) **L**imited to Brazil, and (**N**) **N**ewly identified, locally distributed in Peru [671, 672]. These geographical designations likely reflect a sampling bias rather than distinct geographical barriers to spread [673]. Between these genotypes there exists a narrow range of amino acid variability. Genotype D is the most prevalent and viruses within this group share structural protein amino acid divergence of less than 3%. Slightly higher variability exists between genotypes L and D, although divergence is still less than 10% [673]. MAYV is closely related phylogenetically to regionally co-circulating Una virus and CHIKV, and shares antigenic domains as described in chapter 2.

MAYV persists in sylvatic cycles, and numerous canopy dwelling mosquito genera have been identified as vectors with varying degrees of competency. These include *Haemagogus*, *Aedes*, *Culex*, and *Psorophora* mosquitoes [671, 673, 674]. A diverse number of vertebrate hosts are known, including non-human primates, rodents, birds, and sloths. Animals that occupy trees during the day display a significantly higher predisposition to infection [675]. Sporadic urban outbreaks have occurred but are typically restricted to rural areas near tropical forests and coincide with the onset of the rainy season [585]. Workers and forest visitors are

at elevated risk for exposure and upon returning to urban centers can facilitate the urban spread of the disease. Serosurveillance studies in Ecuador found that indigenous peoples of the Amazonian forests were at sustainably elevated risk for MAYV infection when compared to populations from Coastal and Andean zones [585]. Coupled with the expansion of urban areas adjacent to endemic locales increases the risk of outbreaks. Although historically contained to Central and South America, MAYV genotypes L and D were recently detected among a cohort of school age children in Haiti in 2014 – 2015, and infections have been diagnosed in global travelers returning to North America and Europe [671, 676].

Owing to the close similarity in symptoms and overlapping geographic circulation with CHIKV, Dengue, and Zika virus, it is likely that MAYV infections are underreported and misdiagnosed. Some have termed this challenge in accurate diagnosis as “ChikDenMaZika syndrome” [677]. Antigenic similarity between CHIKV and MAYV further complicates differential diagnosis. These factors may be reflected in the low overall number of reported MAYV cases in the literature [678]. Use of PCR based methods may provide more accurate diagnoses in the future.

1.5.6.1 Animal Models of Mayaro Virus

Small animal mouse models are the canonical research vehicle for understanding the effects of MAYV and other alphaviruses [679]. These include both immunocompetent (e.g. C57BL/6J, SV129, and BALB/c) and immunocompromised (e.g. IFN α R^{-/-} and RAG^{-/-}) mice [680-682]. Challenge

inoculations typically occur via footpad or in the forelimb. In studies with WT SV129 mice, Figueiredo *et al.* found that while 21-day old adult mice did not display symptoms of MAYV infection, young mice (≤ 11 days old) displayed significant footpad swelling, weight decrease, and quick demise [682]. Symptoms observed in young mice mirrored those in adult IFN α R^{-/-} mice, indicating a differential ability to control infection and severity based on age and immune status. These findings were congruent with observations of infected humans and indicated that the competency of innate immune responses is critical for control of early infection before activation of an adaptive immune response.

Although non-human primates have not been routinely used for MAYV infection studies, they have been used for other alphaviruses such as CHIKV, VEEV, WEEV, and EEEV [612, 613, 683]. These models can provide long-term data on viral persistence and are optimal pre-clinical animal models for vaccine and therapeutic assessment. Binn *et al.* conducted a study in rhesus macaques in 1967 that provided early evidence of their applicability for CHIKV, ONNV, and MAYV infection studies. Data from this study determined that infection with these viruses was able to elicit antibodies with cross-protective effects [635].

1.5.7 Vaccines & Therapeutics in Development

To date, there are no licensed vaccines or anti-viral therapeutics for the prevention or treatment of alphavirus infections. As such there is continued interest in the development of such approaches, as evidenced by chapter 2. CHIKV has been a predominant target of research due to the global disease burden it is responsible

for. As previous studies have established that CHIKV infection is able to elicit cross-protective antibodies against MAYV, UNA, and ONNV, there is a high likelihood that developed vaccines may provide broad protection against alphaviruses within antigenic complexes [634-636, 684]. Epitopes within the N-terminus of E2 have been identified as an important target of the early adaptive immune response and support the development of strategies that display the E1/E2 heterotrimer for immune recognition [685, 686]. Considerable effort has also been expended on the development of therapeutic compounds to mediate the effects of infection, especially inflammation induced myalgia and arthralgia, as well as small molecule inhibitors to control viral replication.

1.5.7.1 Vaccines

Multiple vaccine platforms exist with inherent advantages and disadvantages, although many have displayed efficacy in CHIKV infection models. Broadly, vaccines typically fall into one of the five following categories: live attenuated virus (LAV), inactivated virus, virus-like particles (VLP), subunit, nucleic acid, and viral vectors. A non-comprehensive summary of published alphavirus vaccine approaches is outlined in the **Table 1.5.1**. The ability to stimulate both strong innate and adaptive immune responses is critical for efficacious vaccines.

LAV platforms have traditionally utilized multiple passages of the virus through tissue culture cells, resulting in the acquisition of genetic mutations that decrease viral fitness in hosts. These vaccines mimic those seen in natural infections and stimulate comparable immune responses. A significant drawback is that these

viruses have the potential to revert back to WT virus, posing a significant risk to immunocompromised individuals. A few LAVs against alphaviruses have been tested in humans but have demonstrated the potential for adverse effects. A LAV for CHIKV was derived from a Southeast Asian human isolate of strain AF15561. Designated 181/clone 25, it was produced through 18 plaque-to-plaque passages in a MRC-5 human fibroblast cell line [687]. Passaging resulted in 5 synonymous and 5 non-synonymous amino acid mutations, with the non-synonymous mutations located in nsP1, E2, 6K, and E1 [688]. Follow-up studies have identified that the two mutations in E2 are responsible for the attenuated phenotype [688]. Clinical trials found that although only one participant did not develop neutralizing antibodies at 28 dpv, 5 of the 58 trial participants (8%) developed transient arthralgia, leading to discontinuation of the study [689]. A LAV for VEEV, designated TC-83, was developed through subsequent passages of the virulent Trinidad donkey strain in fetal guinea pig heart cells resulting in the acquisition of 12 nucleotide mutations [690, 691]. Much like the CHIKV 181/clone 25 LAV, a mutation in E2 was primarily responsible for the attenuated phenotype. Attenuation was also supported by a 5' non-coding region mutation. In human trials, 12 – 37.5% of vaccinated individuals developed febrile symptoms, and only 82% seroconverted; it is no longer utilized for vaccination of at risk individuals [690, 692, 693]. An additional VEEV attenuated vaccine, V3526, was created through site directed mutagenesis of the pE2 furin cleavage site and a single amino acid change in the E1 glycoprotein [694, 695]. Pre-clinical tests in rodents, NHP, and horses found it to elicit potent neutralizing antibody responses, although mild

adverse events were noted [696-698]. During testing in phase I clinical trials similar data was obtained, but based on the presence of adverse events the trial was discontinued [698]. Similar attenuation was obtained through manipulation of SINV E2 through an S114R mutation [699]. Together, these studies indicate that mutation of the alphavirus E2 protein is sufficient for attenuation. Mutations in this region can function either to inhibit binding to viral receptors or to inhibit furin cleavage of pE2, resulting in immature non-infectious spike proteins [694, 700].

Recent advances with genetic engineering have enabled manipulation of the viral genome resulting in new LAV approaches. Scott Weaver and colleagues have explored the potential for chimeric alphaviruses as vaccine candidates. In this approach, the non-structural proteins from one virus were combined with the structural proteins of another. This was tested with non-structural/structural proteins for SINV/EEEV, SINV/VEEV, VEEV/CHIKV, EEEV/CHIKV, and SINV/CHIKV [701-703]. Although able to elicit robust neutralizing antibody responses they were not pursued beyond mouse models. The chimeric viruses maintained the ability to replicate in mosquito hosts and intact host interferon responses were found to be necessary for attenuated phenotypes. An alternative approach to overcome this issue relied on the replacement of the sgRNA promoter with an internal ribosomal entry site (IRES). In this approach, structural proteins are expressed at a reduced frequency from the genomic RNA, and the inability for insect ribosomes to recognize the IRES prohibits replication in insect cells. Vaccination with these variants has proven to be an effective strategy in

eliciting robust CHIKV, MAYV, and VEEV immune responses [680, 704-706]. Similarly, the addition of tags to structural proteins to alter their properties has been tested. An mCherry tag added to the N-terminus of the E2 structural protein of CHIKV strain 37997 resulted in an attenuated phenotype likely due to altered furin cleavage kinetics of the pE2 precursor protein [707].

Inactivated virus platforms typically rely on the use of treatments such as heat, pH, γ -irradiation, UV light, and/or compounds and chemicals such as formalin, tween 80, binary ethyleneimine, and ether to render the virus non-infectious. Treatment leads to alteration of surface exposed proteins which inhibits their capacity to infect cells. Although they can elicit neutralizing antibody responses, their inability to infect cells diminishes their stimulation of T cell responses. Elicited immune responses following vaccination can be short lived. Multiple approaches have been utilized to inactivate live virulent viruses as well as live-attenuated vaccines [693, 708-713]. The first attempt at a MAYV vaccine utilized formalin inactivation of the TRVL15537 strain and was shown to elicit neutralizing antibodies in mice [714]. Similar studies with multiple chemicals was tested on SINV and found that administration of inactivated vaccines were able to prevent death in mice following challenge with a lethal dose [715]. Formalin was also used to inactivate the TC-83 vaccine strain of VEEV. The resulting inactivated virus (C-84) was better tolerated with reduced incidence of adverse effects, although the immunogenicity was reduced [708, 709]. The United States Army Special Immunization program at the United States Army Medical Research Institute of

Infectious Diseases utilized C-84 as a booster vaccination for individuals that failed to seroconvert following vaccination with TC-83 [693].

Viral-like particles are an alternative strategy that relies on the production of virions that lack a viral genome. While they resemble the conformational structure of wild type virions and maintain the associated immunogenic epitopes, they are unable to replicate following administration. This increases their safety profile and applicability for immunocompromised individuals. Multiple systems exist for the production of VLPs and include bacteria, yeast, insect, and mammalian cells. Proteins are commonly expressed through recombinant plasmid DNA or viral vectors and following translation are able to self-assemble into the canonical virion structure. Prior to administration, the vaccine preparation is commonly mixed with adjuvants in order to stimulate localized immune responses to facilitate elevated immunogenicity [716]. Based on their safety and ability to stimulate neutralizing antibody responses, VLP vaccines have been explored for multiple alphavirus members, including CHIKV, WEEV, VEEV, and EEEV [717-720].

Subunit vaccines rely on the production and vaccination of recombinant viral proteins that express antigenic domains. Although these have a high safety profile they are unable to infect cells and generate only incomplete immune responses. Kumar *et al.* produced a recombinant CHIKV E2 subunit vaccine (rE2p) in bacterial culture and after purification vaccinated mice in combination with a panel of adjuvants. Upon challenge, the elicited neutralizing antibody response from vaccination provided sterilizing immunity [721]. Similarly, a recombinant CHIKV E1

and E2 subunit vaccine was also tested in mice in combination with various adjuvants. This vaccine also stimulated robust production of neutralizing antibodies [722]. Alternatively, *in silico* prediction has been used to identify antigenic epitopes from the MAYV structural proteins. Using flexible linker sequences, this vaccine would be able to express multiple predicted antigenic epitopes [723]. No animal model data has been published to verify the ability of this construct to elicit immune responses.

Nucleic acid platforms utilize either plasmid-based DNA or mRNA vaccinations. As with VLP and subunit vaccines, they also suffer from issues with immunogenicity and immunity that can quickly wane. Prior to administration these vaccines are commonly mixed with adjuvants to help elicit immune responses and/or as carrier systems to improve the stability of the vaccine. Multiple avenues have been tested for the delivery of these vaccines with varying efficacy. These include microinjection, electroporation, ultrasound mediated microbubble delivery, and particle bombardment via gene-gun technology [724]. Following vaccine uptake, cells are then able to produce the encoded viral proteins for expression and immune presentation as would be seen in the case of a natural infection. Choi *et al.* published the first MAYV plasmid based synthetic DNA vaccine (scMAYV-E) in 2019 [725]. The plasmid construct contained codon and RNA optimized sequences for the structural glycoproteins and 6K/TF (capsid was not included in the design) and an IgE-leader sequence was added to the 5' end to increase protein expression after cellular uptake. Wildtype C57BL/6J and IFN α R^{-/-} mice

were vaccinated with scMAYV-E by injection and subsequent electroporation at the injection site. The vaccine elicited strong neutralizing antibody responses, as well as cellular immune responses to peptides from E3+E2 and E1 peptide pools. Similar approaches have been used with CHIKV, either with individual plasmids expressing the capsid, E1, or E2 proteins, or with a single plasmid expressing all three glycoproteins. Both approaches were able to elicit neutralizing antibodies and cellular immune responses [726, 727]. Similarly, a full length VEEV structural protein DNA vaccine driven off of a CMV-IE promoter elicited both cellular and humoral immune responses in mice, rabbits, and non-human primates [728].

Viral vectors utilize replication incompetent viruses to deliver a heterologous transgene that encodes antigenic proteins from the vaccine target. This approach allows for cellular infection and subsequent expression of viral antigens. Pre-existing immunity to the viral vector is a concern as it can limit the vaccine efficacy through inhibition of the viral vector and/or delivered transgene. Whereas the immunogenicity of vectors is a drawback in therapeutic gene transfer applications, the innate and adaptive immune responses they stimulate are desirable in vaccine applications. These properties augment the immunogenicity of the encoded antigens and stimulate elevated immune responses. Viral vectors are amenable to large scale production and yield high viral titers. The development of strategies to stabilize vectors in liquid formats or through lyophilization increases their utility in field settings, alleviating the need for cold-chain storage [729, 730]. This is of

particular importance in underdeveloped regions where access to electricity and proper storage is lacking.

As mentioned in section 1.4.1.3, replication-incompetent adenovirus vectors have shown promise in vaccine applications. Multiple Ad based vaccines have been tested against alphaviruses. An $\Delta E1/E3/E4orf6$ Ad vector expressing the full length structural proteins from CHIKV displayed protective immunity in mice following challenge [401]. Similar effects were observed with a $\Delta E1/E3$ chimpanzee Ad vector expressing the envelope glycoproteins (with or without capsid), and a $\Delta E1/E3$ Ad5 vector expressing either the full length or combinations of the CHIKV structural proteins. Both vaccines conferred immunity to mice and protected against lethal CHIKV challenge [399, 731]. Recently, a MAYV and CHIKV based vaccine expressed by the chimpanzee derived vector ChAdOx1 was able to elicit cross-protective neutralizing antibodies that provided partial protection against heterologous challenge (ChAdOX1-MAY vs CHIKV, ChAdOx1-CHIK vs MAYV) [400, 732, 733]. Intranasal administration of a $\Delta E1a$ Ad5 vector expressing the E3, E2, and 6K sequences from VEEV was also effective in protecting mice from aerosol challenge with VEEV [402, 734].

Vector platforms other than Ad have been investigated for their potential use as alphavirus vaccine vectors. A pseudotyped Vesicular stomatitis vector was created by deletion of the endogenous VSV glycoprotein and expression of the CHIKV envelope glycoproteins. Mice vaccinated with this pseudotyped vector developed both humoral and cellular immune responses that protected against lethal CHIKV

challenge [735]. Recombinant measles virus vectors encoding the structural proteins from the La Reunion strain 06-46 stimulated neutralizing antibody and T cell immune responses in IFN α R^{-/-} mice. A phase I clinical trial identified that it stimulated neutralizing antibody production in humans [736, 737]. Similar effects have included the use of mouse cytomegalovirus expressing antigenic peptides from CHIKV. This platform was able to simulate robust T cell responses following administration to mice [686].

Table 1.5.1 Published Alphavirus Vaccine Approaches

Platform	Virus Target	Vaccine Name	Species Tested	Elicited Immunity	Cross Protection	Ref(s).
Live-Attenuated Virus (LAV)	CHIKV	181/clone 25	Mice NHP Human	Neutralizing antibodies	Untested	[687, 689]
	VEEV	TC-83	Mice NHP Humans	Neutralizing antibodies	Untested	[690, 692, 693]
	VEEV	V3526	Rodents Horses NHP Humans	Neutralizing antibodies	Untested	[696-698]
	CHIKV	CHIKV/IRES	Mice	Neutralizing antibodies	ONNV	[704, 712,

			NHP	T cells	MAYV	713, 738]
	MAYV	MAYV/IRES	Mice	Neutralizing antibodies T cells	Untested	[680, 705]
	EEEV	SINV/EEEV	Mice	Neutralizing antibodies	Untested	[701]
	VEEV	SINV/VEEV	Mice	Neutralizing antibodies	Untested	[702]
	CHIKV	EEEV/CHIKV	Mice	Neutralizing antibodies	Untested	[703]
	CHIKV	SINV/CHIKV				
	CHIKV	EEEV/CHIKV				
	CHIKV	CHIKV 37997-mCherry	Mice	Neutralizing antibodies	Untested	[707]
Inactivated Virus	CHIKV	UV-CHIKV	NHP	Antibodies	Untested	[711]
	CHIKV	BEI-CHIKV	Mice	Neutralizing antibodies	Untested	[710]
	CHIKV	Formalin Inactivated CHIKV	Mice, NHP	Neutralizing antibodies T cells	Untested	[711, 721, 739]
	MAYV	Formalin Inactivated	Mice	Neutralizing antibodies	Untested	[714]
	VEEV	C-84 (Formalin inactivated TC-83)	Mice NHP	Neutralizing antibodies	Untested	[693, 708, 709]

			Humans			
	SINV	Subsequent treatments of: Formalin β -propiolactone hydroxylamine 2-ethylethlenimine	Mice	Protected against lethal challenge	Untested	[715]
Virus Like Particles (VLP)	CHIKV	Baculovirus-insect cell production	Mice	Neutralizing antibodies	Untested	[717]
	CHIKV	293 Human kidney cell production	Mice NHP Human	Neutralizing antibodies	Untested	[718, 719]
	WEEV VEEV EEEV	Mammalian and insect cell production of species specific VLPs	Mice NHP	Neutralizing antibodies	Tested against homotypic species and as a combined trivalent vaccine	[720]
Subunit	CHIKV	rE2p	Mice	Neutralizing antibodies	Untested	[721]
	CHIKV	rCHIKVE1/E2	Mice	Neutralizing antibodies	Untested	[722]
	MAYV	<i>In silico</i> prediction	Untested	Untested	Untested	[723]
DNA/RNA nucleic acid	MAYV	scMAYV-E	Mice	Neutralizing antibodies T cells	Untested	[725]

	CHIKV	CHIKV-E1 CHIKV-E2 CHIKV-Cap	Mice	Neutralizing antibodies T cells	Untested	[726]
	CHIKV	pMCE321	Mice NHP	Neutralizing antibodies T cells	Untested	[727]
	VEEV	VEEV _{co}	Mice Rabbits NHP	Neutralizing antibodies T cells	Untested	[728]
Viral Vectors	CHIKV	CAdVax-CHIK	Mice	Neutralizing antibodies T cells	Untested	[401]
	CHIKV	ChAdOX1	Mice	Neutralizing antibodies	Untested	[400, 733]
	CHIKV	Ad-CHIKV-SG Ad-CHIKV-E3/E2/6K Ad-CHIKV-E3/E2/E1	Mice	Neutralizing antibodies	Untested	[399]
	VEEV	rAD/ E3-E2-6K	Mice	Neutralizing antibodies	Untested	[402, 734]
	CHIKV	VSVΔG-CHIKV	Mice	Neutralizing antibodies T cells	Untested	[735]
	CHIKV	MV-CHIKV	Mice	Neutralizing antibodies	Untested	[736, 737]

			Humans	T cells		
	CHIKV	MCMV-CHKVf5 AdV-CHKVf5	Mice	T Cells	Untested	[686]
	CHIKV MAYV	ChAdOx1-CHIK ChAdOx1-MAY	Mice	Neutralizing antibodies	CHIKV MAYV	[732]

Published LAV, inactivated, VLP, subunit, nucleic acid, and viral vector vaccines that have been developed and tested against alphaviruses

1.5.7.2 Therapeutics

Along with vaccine development, research has also been focused on the development of therapeutic approaches to inhibit viral entry and/or replication, as well as those that provide benefit against the resultant symptoms following infection. Current strategies rely on the administration of steroidal or non-steroidal anti-inflammatory drugs (NSAID) and paracetamol to alleviate febrile symptoms. Methotrexate and other similar drugs have been used to treat long-term chronic inflammatory rheumatism. While they can alleviate symptoms, NSAIDs have been found to interfere with immune responses through inhibition of B cell IgG and IgM synthesis [740]. This can limit immune response and development of long-term immunity.

A large focus of drug development is to identify those with inhibitory effects on the synthesis and function of alphavirus proteins. A number of compounds have been identified that limit viral yield and replication through interference with the GTPase

and capping functions of CHIKV and VEEV nsP1. These include [1,2,3]triazolo[4,5-d]pyrimidin-7(6h)-ones (MADTP) series compounds, lobaric acid, pyrantel pamoate, and garcinolic acid [500, 741].

Identification of drugs that interfere with the nsP2 protease function has been pursued largely through *in silico* modeling [742]. *In vitro* analysis of a set of predicted compounds was shown to inhibit CHIKV protease function, viral RNA synthesis, and viral particle release [743]. Similarly, quinazolinone compounds displayed antiviral effects on VEEV and WEEV [500, 744]. Differences in the amino acid sequence and functions of nsP2 between New and Old World alphaviruses is likely to hamper the development of broad-spectrum antivirals against both classifications [744].

Determination of compounds with nsP3 inhibitory effects has focused on those that interfere directly with the macrodomain and ADP-ribose binding pocket, as well as those that disrupt virus-host protein interactions. *In silico* molecular docking studies have been used, and plant-derived polyphenolic flavonoids have shown anti-CHIKV activity [745]. The interactions of nsP3 with sphingosine kinase 2 (SK2), Hsp90B, PI3K-AKT-mTOR pathway, and Ikk β host-proteins are other potential anti-viral targets. Treatment with an IKK β inhibitor was shown to inhibit VEEV viral titers in glial and neuronal cell lines and mouse models [746].

Inhibition of nsP4 has largely focused on nucleoside analogs that target RdRp for chain termination. These have included β -d-N⁴-hydroxycytidine, sofosbuvir, and favipiravir [747-749]. Additional approaches have focused on inhibition of cellular

functions required for viral RNA synthesis and maturation. As previously mentioned, these have investigated viral-host cell kinase inhibitors to prevent interactions such as with IKK β , inhibitors of host cell protein chaperones, protease inhibitors to prevent furin cleavage of the viral structural proteins, and purine and pyrimidine synthesis inhibitors in order to prevent efficient viral replication [742]. Further development of compounds that not only prevent viral replication but also prevent the associated inflammatory effects will be important in effective treatment regimens.

Development of neutralizing antibody therapies has also been an area of great interest due to their observed efficacy. Passive transfer experiments in animal models have shown that administration of immune sera is capable of preventing infection for multiple alphaviruses [750-753]. Analysis of a panel of antibodies isolated from humans and mice by Fox *et al.* identified a subset of CHIKV antibodies which protected against CHIKV, MAYV, and ONNV in mouse challenge models. These antibodies were able to prevent multiple steps of the virus life cycle [634, 754, 755]. Application of monoclonal antibodies has proven effective when used prophylactically and post-exposure [754, 756]. Data by Broeckel *et al.* demonstrated that administration of a neutralizing human monoclonal antibody to rhesus macaques at 2 and 4 dpi prevented CHIKV dissemination and inflammation with no infectious virus detected in any of the surveyed tissues at 7 dpi [756]. This treatment reduced the levels of pro-inflammatory cytokines and chemokines but did not substantially reduce the associated B and T cell responses elicited

compared to those treated with an isotype control. Although questions remain on the longevity of protection provided by prophylactic treatments and efficacy of administration after the viremic period ends, neutralizing antibody therapies have shown clear benefits in challenge models.

1.6 Concluding Summary

In summary, viral vectors are of great utility in many healthcare applications. Since the 1980's research has continued on the development and use of robustly effective vector platforms. While this research has largely focused on the application of gene therapy against monogenic disorders, the utility of viral vectors as vaccine platforms has been an emerging field of research. The early research undertaken to understand the safety, immunogenicity, and tropism of vectors continues to play important roles in the progress for both of these applications.

Adenovirus vectors are highly desirable due to their large packaging capacity, wide tissue tropism, and their inability to integrate into the host genome, although their immunogenicity has challenged their use. Recently, the immunogenic properties of adenovirus vectors have been co-opted to increase the effectiveness of antigenic transgenes in vaccine applications. By removing the E1 and E3 genes from the virus genome, the adenovirus vector is rendered replication incompetent with space to insert transgenes up to ~8 kb while still retaining aspects of immunogenicity observed from wildtype adenovirus. These properties have resulted in the application of adenovirus vectors against multiple viral and protozoan pathogens. These efforts have involved a considerable focus on those

pathogens for which there are no effective therapeutics or vaccines approved for human use, and recent work against the recently emerged SARS-CoV-2 has highlighted the ability to rapidly develop safe and effective Ad vector-based vaccines. As alphaviruses are a persistent global pathogen with increasing geographic distributions, the need to develop safe and effective vaccines platforms is of critical importance for global health initiatives. To this end, we incorporated the knowledge of adenovirus vectors as vaccine platforms to develop a vaccine that proved highly effective in mouse models of alphaviruses that included Mayaro, Una, and Chikungunya virus (Chapter 2).

Additionally, continued research on viral vectors has also reshaped our understanding of the lifecycle of some viruses. The discovery of the assembly-activating protein (AAP) was a paradigm shift in our understanding of essential viral proteins involved in the process of adeno-associated virus (AAV) capsid assembly. As the field of research on AAV vectors has been intimately involved in developing novel vectors further understanding the properties of this protein will play important roles in identifying and selecting vectors with preferential features. These efforts underscore the need to understand the mechanistic properties of AAP. Such work will be covered in Chapter 3 and Supplemental Chapter 1.

Chapter 2.

Non-Replicating Adenovirus Based Mayaro Virus Vaccine Elicits Protective Immune Responses and Cross Protects Against Other Alphaviruses

John M. Powers^{1,2}, Nicole N. Haese¹, Michael Denton¹, Takeshi Ando¹, Craig Kreklywich¹, Kiley Bonin¹, Cassilyn E. Streblow¹, Nicholas Kreklywich¹, Patricia Smith¹, Rebecca Broeckel^{1*}, Victor DeFilippis¹, Thomas E. Morrison³, Mark T. Heise⁴, Daniel N. Streblow^{1,5}

¹ Vaccine and Gene Therapy Institute, Oregon Health and Science University, Beaverton, Oregon, USA, ² Department of Molecular and Medical Genetics, Oregon Health and Science University, Portland, Oregon, USA, ³ Department of Immunology and Microbiology, University of Colorado School of Medicine, Aurora, Colorado, USA, ⁴ Department of Genetics, Department of Microbiology and Immunology, The University of North Carolina at Chapel Hill, Chapel Hill, North Carolina, USA, ⁵ Division of Pathobiology and Immunology, Oregon National Primate Research Center, Beaverton, Oregon, USA

* Current address: Rocky Mountain Laboratories, NIH/NIAID, Hamilton, Montana, USA

Most data was generated and analyzed by John Powers. Nicole Haese and Takeshi Ando vaccinated and challenged the mice, and Craig Kreklywich performed qRT-PCR analysis on samples. Michael Denton aided in plaque reduction neutralization assays. Rebecca Broeckel aided in the production of viruses, and Nicholas Kreklywich aided in vector cloning. Nicole Haese, Michael Denton, Takeshi Ando, Craig Kreklywich, Patricia Smith, and Daniel Streblow aided in processing and titering of mouse tissues. John Powers, Nicole Haese, and Daniel Streblow were responsible for experimental design.

2.1 Abstract

Mayaro virus (MAYV) is an alphavirus endemic to South and Central America associated with sporadic outbreaks in humans. MAYV infection causes severe joint and muscle pain that can persist for weeks to months. Currently, there are no approved vaccines or therapeutics to prevent MAYV infection or treat the debilitating musculoskeletal inflammatory disease. In the current study, a

prophylactic MAYV vaccine expressing the complete viral structural polyprotein was developed based on a non-replicating human adenovirus serotype 5 (AdV) platform. Vaccination with AdV-MAYV elicited potent neutralizing antibodies that protected WT mice against MAYV challenge by preventing viremia, reducing viral dissemination to tissues and mitigating viral disease. The vaccine also prevented viral-mediated demise in IFN α R1^{-/-} mice. Passive transfer of immune serum from vaccinated wild-type mice similarly prevented infection and disease in WT mice as well as virus-induced demise of IFN α R1^{-/-} mice, indicating that antiviral antibodies are protective. Immunization with AdV-MAYV also generated cross-neutralizing antibodies against two related arthritogenic alphaviruses – chikungunya and Una viruses. These cross-neutralizing antibodies were protective against lethal infection in IFN α R1^{-/-} mice following challenge with these heterotypic alphaviruses. These results indicate AdV-MAYV elicits protective immune responses with substantial cross-reactivity and protective efficacy against other arthritogenic alphaviruses. Our findings also highlight the potential for development of a multivalent targeting vaccine against alphaviruses with endemic and epidemic potential in the Americas.

2.2 Introduction

Mayaro virus (MAYV) is a mosquito-transmitted alphavirus that circulates in zoonotic cycles in non-human primates, birds, and rodents with occasional spillover into human populations that can lead to urban spread [675]. The ability of the virus to infect both *Aedes* and *Culex* mosquitos and a wide range of vertebrate

hosts permits both enzootic and urban transmission cycles [614]. MAYV is endemic to Central and South America and was first discovered in 1954 in Trinidad and Tobago [671]. Forest workers or visitors to forested areas are at increased risk of becoming infected. Upon returning to urban areas, this can lead to human outbreaks through the urban cycle of mosquito-human-mosquito transmission [671]. Human infection with MAYV leads to fever, myalgia, arthralgia, and rash, which are common symptoms of infection with other arthritogenic alphaviruses. MAYV febrile symptoms typically last for 3-5 days, although joint and muscle pain can persist for up to one year [614, 671]. Based on similarity to other more prevalent alphaviruses, reduced reporting of MAYV infections could be due to misdiagnosis, most commonly as dengue fever or chikungunya disease [757].

The alphavirus genome is a positive single-stranded RNA approximately 11.5 kb in length that encodes 4 non-structural proteins (nsP1, 2, 3, 4) and 6 structural proteins (C, E3, E2, 6K, TF, E1). The structural proteins are translated as a single polyprotein from the subgenomic viral mRNA. First, the capsid protein (C) undergoes autoproteolytic cleavage, and the resultant C oligomerizes around the viral genome forming nucleocapsid structures. The remaining portion of the structural polyprotein is processed in the ER and cleaved into pE2 (E3-E2), 6K, and E1. E1 and pE2 form non-covalent heterodimers, and during trafficking through the Golgi secretory pathway pE2 is processed into E2 and E3 [742, 758]. Processed glycoproteins are transported to the plasma membrane and encapsulated viral genomes are recruited for budding of viral particles. There are

3 genotypic strains of MAYV that have a narrow range of amino acid variability in the structural proteins. Genotype D is the most prevalent and viruses within this group have structural protein amino acid divergence of less than 3%. Slightly higher variability exists between genotypes L and D, although divergence is still less than 10% [673]. Such high amino acid similarity greatly increases the likelihood of shared antigenic domains, enabling a vaccine to cross-protect against most, if not all, MAYV strains [671, 673]. However, to date there are no approved vaccines for humans against any alphaviruses. Previous MAYV vaccination attempts have included live-attenuated virus and DNA based vaccines [680, 714, 725, 759]. Therapeutic approaches to limit disease severity have been another area of research interest. For example, the use of adenovirus vectors expressing an IFN- α transgene have shown efficacy in reducing the inflammatory response in mice challenged with CHIKV, indicating a role for adenovirus vectors as permissive approaches for therapeutics [760].

To this end, the development of a vaccine that elicits protective immunity against MAYV is of significant interest to public health initiatives. Recent studies have suggested that a number of mosquito species are capable of transmitting MAYV and that they have broadening distributions, thus increasing the potential for global spread of the virus to more distant geographical regions [761]. There are numerous vaccine platforms from which to choose when designing a MAYV vaccine including: Live-attenuated viruses (LAV), recombinant proteins, self-assembled virus-like particles (VLP), and other viral vectors. We chose to combine VLP and

Adenovirus vectors as our approach to develop a MAYV vaccine since LAV alphavirus vaccines can be contraindicated in immune compromised individuals, such as the elderly, and recombinant protein vaccines are plagued by rapidly waning immunity [689, 716, 762, 763]. Previous studies have shown that expression of full-length alphavirus structural proteins, either through direct DNA transfection of cells or by viral vectors, results in self-assembly of VLPs. These VLPs are structurally similar to native virus particles but are devoid of infectious viral genomes [719, 764]. Adenovirus-based vectors have previously shown vaccination potential against alphaviruses. Earlier studies discovered the potential of an Ad5 vaccine expressing CHIKV structural proteins that protected mice from disease following virulent CHIKV challenge [399-401]. Therefore, a recombinant adenovirus vector vaccine platform was utilized in the current study because adenovirus vectors have the capacity to accept the entire structural protein from MAYV and have considerable efficacy as gene therapy vectors due to their ability to stimulate both innate and adaptive immune responses due to high transgene expression [379, 765]. As outbreaks of these related alphaviruses have occurred in the same regions due to their overlapping circulation, a multivalent vaccine would be of great benefit to the region [766-768]. Previous studies have indicated the existence of conserved antigenic epitopes between these viruses, with groups reporting on the presence of cross-neutralizing antibodies following infection with CHIKV or MAYV in rhesus macaques, and that humans infected with CHIKV possessed antibodies against CHIKV, MAYV, and Una virus (UNAV) (**Supplemental Figure 1**) [634-636]. Similar data on the ability of alphavirus

vaccines to cross-protect against heterotypic viruses has also been noted in mouse models [684, 712, 738, 769, 770]. Therefore, in addition to evaluating the efficacy of AdV-MAYV against MAYV, we also cross-examined its vaccine potency against CHIKV and UNAV, two related members of the Semliki Forest complex [497].

2.3 Results

Adenovirus Mediated Expression of Mayaro Structural Proteins

The Mayaro (MAYV) structural protein ORF from a Buenos Aires isolate (BeAr505411) was cloned into a replication-defective adenovirus serotype 5 expression vector (AdV-MAYV) as previously described [686]. The CMV-IE promoter drives expression of the structural ORF (**Figure 2.1A**). Western blotting was used to confirm expression of the MAYV ORF in lysates from THF-CAR cells infected with a range of MOI's ranging from 0.1 to 1,000 PFU/cell. Lysates from uninfected and MAYV-infected Vero cells were included as negative and positive controls, respectively. Robust protein expression was observed for the vector in a dose-dependent manner. Blotting using an anti-alphavirus capsid antibody detected a band at ~30 kDa, which is the expected size of processed capsid protein [771] (**Figure 2.1B**). To determine whether transduction of cells with AdV-MAYV resulted in the production of intact virus-like particles (VLPs), THF-CAR cells were infected with a multiplicity of infection (MOI) equal to 100 PFU/cell and VLPs were purified from clarified supernatants by ultracentrifugation [719]. Resuspended VLPs were fixed with 4% PFA, counterstained with uranyl acetate

and EM analysis identified particles of ~60-70 nm in size with the correct alphavirus morphology indicating that transduction of cells with AdV-MAYV generated virus-like particles [772](Figure 2.1C).

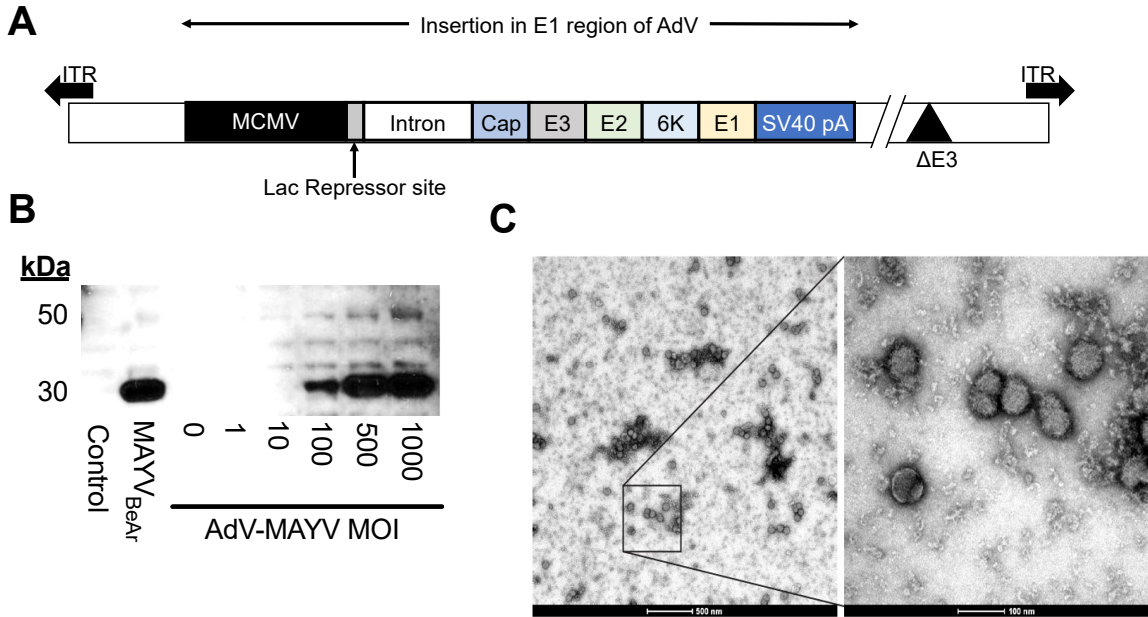


Figure 2.1 AdV-MAYV Vaccine Vector Expression of MAYV Structural Proteins

(A) The MAYV structural protein ORF was inserted into the replication defective huAdV expression vector under the control of the MCMV-IE2 promoter containing a Lac repressor to specifically modulate expression during reconstitution and stock production of the virus. (B) AdV-MAYV expression of the structural protein was evaluated in THF-CAR cells infected with increasing MOIs. Cell lysates were analyzed at 72 hpi for capsid expression by western blotting for the viral capsid protein. Shown is a representative image of two independent experiments. (C) Electron microscopy image of 4% PFA fixed AdV-MAYV VLPs from clarified supernatants of AdV-MAYV infected THF-CAR cells (MOI = 100 PFU/cell). Representative images are shown of 500 nm (left) and 100 nm (right) magnifications. Shown is a representative image of three biological replicates.

AdV-MAYV Vaccination Elicits Neutralizing Antibodies and T cell Responses

To determine optimal dose and dosing regimen, WT C57BL/6 mice were vaccinated intramuscularly (n = 5 per group) with single doses of 10^6 , 10^7 , or 10^8 PFU AdV-MAYV. An additional cohort of animals for each group received a booster vaccination at 14 days post vaccination (dpv) with the same vaccine and at the same dosage. Negative control animals were vaccinated with an AdV-GFP vector, and positive control animals were infected in the footpad with 10^4 PFU MAYV_{BeAr}. Serum was harvested and heat inactivated for use in plaque reduction neutralization assays (PRNT) with MAYV_{CH} on Vero cells as indicated in the experimental timeline (**Figure 2.2A**). All animals that received the AdV-MAYV vaccination generated neutralizing antibodies to a higher degree than the AdV-GFP control group ($P < 0.0001$) (**Figure 2.2B**). Increasing the AdV-MAYV dose, as well as providing a boost at 14 dpv, increased levels of neutralizing antibodies substantially. Only the prime + boost animals receiving the 10^8 PFU dose of AdV-MAYV developed neutralizing antibody levels higher than those observed in the serum from MAYV-infected mice (PRNT₅₀ of 4,123 vs 853). A dose of 10^7 PFU AdV-MAYV prime + boost provided near equivalent neutralizing antibody production relative to MAYV-infected mice (PRNT₅₀ of 795 vs 853) (**Figure 2.2B**). Serum was tested to assess whether neutralization of infection occurred pre- or post-viral binding to the cell using modified neutralization assays. For this assay, serum neutralizing antibody levels from mice vaccinated with AdV-MAYV (10^8 prime + boost) was compared to serum from naïve, PBS control, or AdV-MAYV

10⁸ prime + boost + challenged mice. In pre-attachment assays, a series of diluted serum was mixed with MAYV and pre-incubated for 1 h and then the mixture was added to confluent monolayers of Vero cells to allow for plaque formation. For post-attachment assays, Vero cells were incubated with MAYV at 4°C to allow attachment prior to incubation with a similar dilution series of serum. The greatest amount of neutralization occurred for serum in the pre-binding assay, indicating that the neutralizing antibodies stimulated from vaccination functioned to prevent virus binding to the cell. This was observed in serum from both the AdV-MAYV 10⁸ prime + boost mice and AdV-MAYV 10⁸ prime + boost challenged mice with greater than an 80% reduction in plaques at a serum dilution of 1:80 and PRNT₅₀'s of 1358 & 385, respectively (**Figure 2.2C**). Comparatively, post-binding analysis identified minimal neutralization and plaque reduction, with serum from vaccinated animals presenting a PRNT₅₀ dilution of only 66, while no other samples had plaque reduction above 50% (**Figure 2.2D**).

non-linear regression. (C and D) Pre- and post-attachment neutralization assays were performed to explore the mechanism of inhibition. For pre-attachment neutralization assays, aliquots of a known concentration of virus were mixed with serial dilutions of serum for one hour prior to application to confluent monolayers of Vero cells. For post-attachment treatments, virus was incubated with Vero cells at 4°C for one hour to allow binding and then serial dilutions of antibody were added for one additional hour at 4°C. Triplicate biological replicates and representative curves determined by variable slope non-linear regression are shown. Error bars represent SEM representative of 4 biological replicates.

Based on the presence of strongly neutralizing antibodies, we next used ELISA to evaluate serum from naïve, MAYV_{BeAr} infected, AdV-MAYV prime or prime + boost vaccinated mice for the presence of binding antibodies. Inactivated MAYV_{BeAr} was bound to 96-well high-binding ELISA plates. Serial dilutions of each serum were added to the plates and then probed with secondary antibodies directed against mouse IgG1, IgG2b, IgG3, or total IgG/M to determine the isotype of the MAYV specific antibody responses. Vaccinated mice and MAYV-infected mice showed elevated levels of antiviral antibodies for all isotypes compared to negative controls (**Figure 2.3A**). AdV-MAYV prime + boost resulted in the production of higher levels of total antiviral antibodies (IgG/M) relative to AdV-MAYV prime only, which is consistent with the increase levels of neutralizing antibodies following vaccination booster (**Figure 2.2B**). While AdV-MAYV prime + boost vaccinated animals had similar levels of antibody subclass responses compared to the MAYV-infected group, the total IgG/M response was significantly higher for the MAYV infected group (**Figure 2.3A**). Western blotting was used to confirm MAYV antigen specificity and binding of the vaccine-elicited antibodies (**Figure 2.3B**, panels 1-4). Serum from non-vaccinated controls did not detect MAYV proteins (**Figure 2.3B**, panel 3). In contrast, serum from vaccinated mice detected MAYV E1/E2

glycoproteins (Fig 3B, panel 4) comparable to those detected by anti-CHIKV monoclonal antibodies 87.H1 and 133.B4 (Fig 3B, panels 1 and 2). In addition, serum from vaccinated animals also bound to the MAYV capsid protein (**Figure 2.3B**, panel 4).

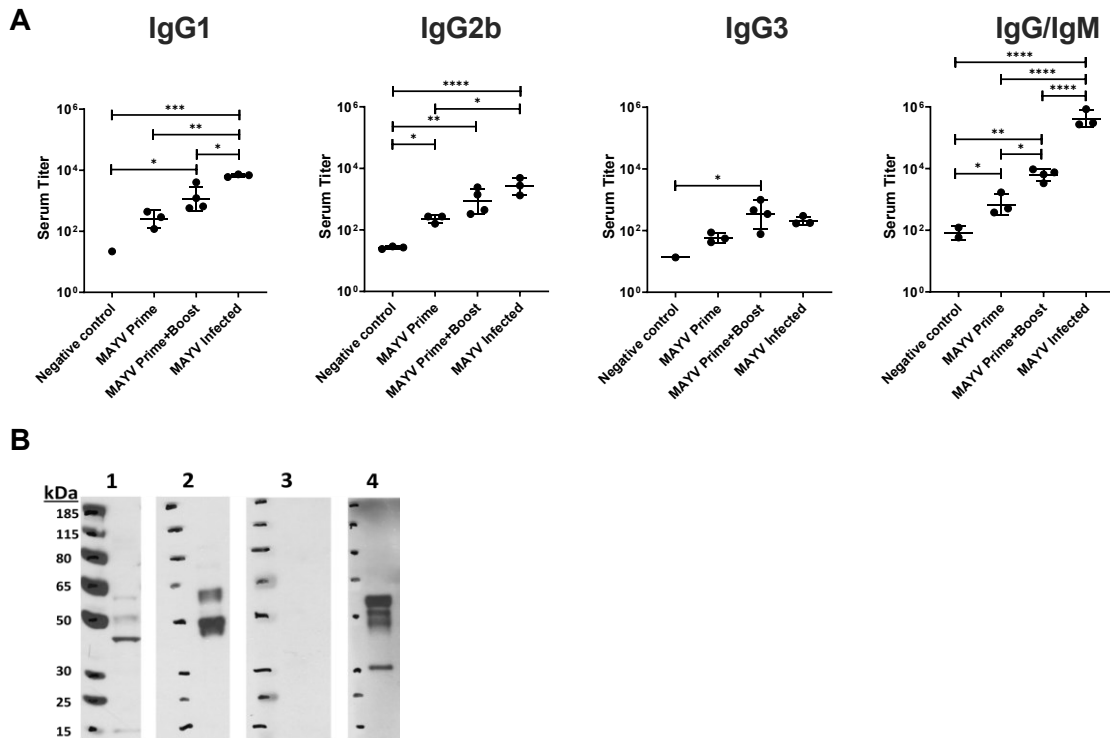


Figure 2.3 Characterization of Anti-MAYV Antibody Responses

(A) Isotype specific ELISAs were performed to characterize and measure the MAYV_{BeAr} binding antibodies in sera from naïve, AdV-MAYV prime vaccinated, AdV-MAYV prime + boost vaccinated, and MAYV infected mice. Preparations of heat inactivated whole MAYV stocks were bound to high affinity 96-well plates. Serial dilutions of mouse sera were plated in order to calculate binding dilution titer. Binding antibodies were detected by secondary antibodies specific for mouse IgG1, IgG2a, and IgG3 as well as a pan IgG/IgM. Error bars represent SD representative of quadruplicate biological replicates. Statistical analysis was performed on log transformed data by a one-way ANOVA (*P < 0.05, **P < 0.005, ***P = 0.0001, P < 0.0001). (B) Western blot analysis was used to determine antigen specificity of antibodies in serum from vaccinated mice. Protein lysates containing purified MAYV_{TrVI} were separated by SDS-PAGE and transferred to immunoassay membranes for western blotting. Cross-reactive anti-CHIKV E1 (panel 1) and E2 (panel 2) monoclonal antibodies were used to identify MAYV envelop proteins. Serum derived from naïve

mice (panel 3) and AdV-MAYV prime + boost vaccinated mice (panel 4) demonstrate the presence of envelope and capsid specific antibodies to MAYV_{TM1} following vaccination. The blots shown are representative images of 3 independent experiments.

We previously demonstrated the positive effect that pre-formed CD8⁺ T cell responses have on CHIKV induced disease, and therefore, next determined whether AdV-MAYV also induced virus-specific T cell responses [686]. T cell IFN γ -ELISPOT assays were performed using peptides predicted to be MAYV T cell receptor epitopes (IEDB analysis resource) for C57BL/6 mice [773]. Lymphocytes were prepared from spleens harvested from WT and interferon alpha receptor knockout (IFN α R1^{-/-}) mice vaccinated with AdV-MAYV and the cells were plated onto IFN- γ ELISpot plates in the presence of 18mer peptides derived from the MAYV structural proteins, DMSO, or the positive control PMA/Ionomycin. After 48 h, plates were stained for the presence of IFN- γ and spots counted using an automated ELISpot reader. A peptide derived from sequences present in the N-terminal domain of MAYV E2 (LAKCPPGEVISVSFV) stimulated the strongest T cell production of IFN- γ in mice vaccinated with AdV-MAYV (**Figure 2.4**). This response was significantly increased in response to AdV-MAYV vaccination relative to DMSO control (**Figure 2.4**). There was a slight increase in the T cell response present in vaccinated IFN α R1^{-/-} mice versus WT mice. Epitopes in E2 have been identified as prominent targets of early T cell responses in CHIKV infection and support the N-terminus of E2 as an important target of the early adaptive immune response [685, 686].

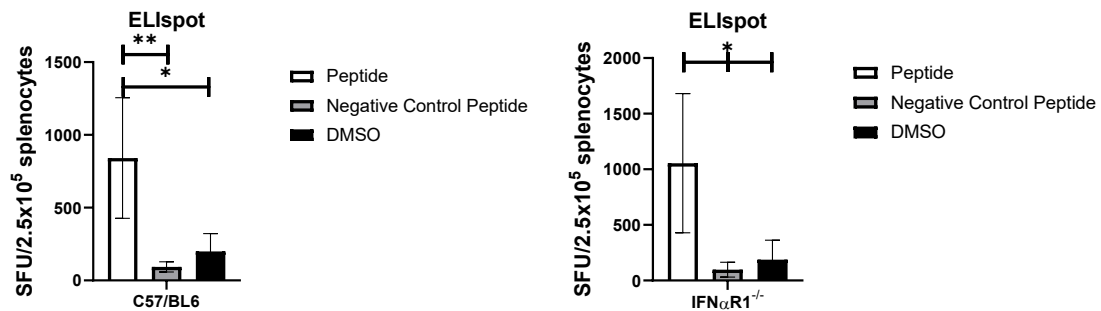


Figure 2.4 AdV-MAYV Vaccination Elicits Robust T-cell Response Against MAYV E2 Glycoprotein in Wild Type and IFN α R^{-/-} Mice

C57BL/6J or IFN α R^{-/-} mice were vaccinated with AdV-MAYV or AdV-GFP by i.m. injection followed by a booster vaccination 14 days later. At day 28 post vaccination, spleens were collected and processed for lymphocytes. IFN- γ ELISpot assays were performed by stimulating 2.5×10^5 splenocytes with 18mer peptides from the MAYV structural proteins incorporated, DMSO (vehicle negative control) or PMA/ionomycin (positive control). At 2 days post stimulation the plates were developed for the presence of IFN- γ and spots were counted using an automated microscope with computer interface. Two independent experiments were performed with 4 biological replicates. Statistical analysis was performed by paired one-way ANOVA and error bars represent SD (* P < 0.05, ** P < 0.01).

AdV-MAYV Vaccine Elicits Protective Efficacy & Reduces Inflammatory Chemokine Production

To test the efficacy of AdV-MAYV against MAYV infection, vaccinated WT mice were challenged by footpad injection with 10^4 PFU MAYV_{BeAr} at 28 dpv (**Figure 2.5A**). A second group of vaccinated mice was assessed for vaccine durability by challenge at 84 dpv. Blood collected at two days prior to challenge (26 and 82 dpv) displayed robust neutralizing antibody titers (PRNT₅₀ equal to 1,791 and 4,826; respectively) for AdV-MAYV vaccinated mice while control animals had no

neutralization activity ($P < 0.0001$) (**Figure 2.5B**). After challenge, mice were monitored daily for footpad swelling and other signs of disease. At 2 dpi, blood was collected from the animals and sera was processed for viremia measurement. At experimental end point 4 dpi (for 28 dpv challenge group) and 7 dpi (for 84 dpv challenge group), ipsilateral and contralateral hind limb tissues (ankles, calves, and quadriceps), spleen, and blood were harvested. Tissues were homogenized in 1 mL of PBS, debris was pelleted, and lysates were titered along with sera for the presence of infectious virus on Vero cells by limiting dilution plaque assay. For both short- and long-term vaccine groups, AdV-MAYV vaccination prevented the development of viremia; no infectious MAYV was detectable in serum at 2 dpi while AdV-GFP control animals had a mean viral titer of 8.39×10^4 and 1.31×10^5 PFU/ml, respectively ($P < 0.0001$) (**Figure 2.5C-D**). Similarly, infectious virus was undetectable in any of the tissues from both groups of AdV-MAYV vaccinated mice but virus was present in all tested tissues from AdV-GFP vaccinated mice ($P < 0.0001$) (**Figure 2.5E-F**). Total RNA was extracted from a portion of the tissue homogenates for qRT-PCR quantification of viral RNA. Control AdV-GFP treated animals all contained viral genomes in each of the surveyed tissues while the majority of animals from the AdV-MAYV vaccinated groups had below detectable levels of viral RNA ($P < 0.0001$) (**Figure 2.5G-H**). These data indicate that the AdV-MAYV vaccination elicits durable potent neutralizing antibodies that limit viremia and widespread viral tissue distribution.

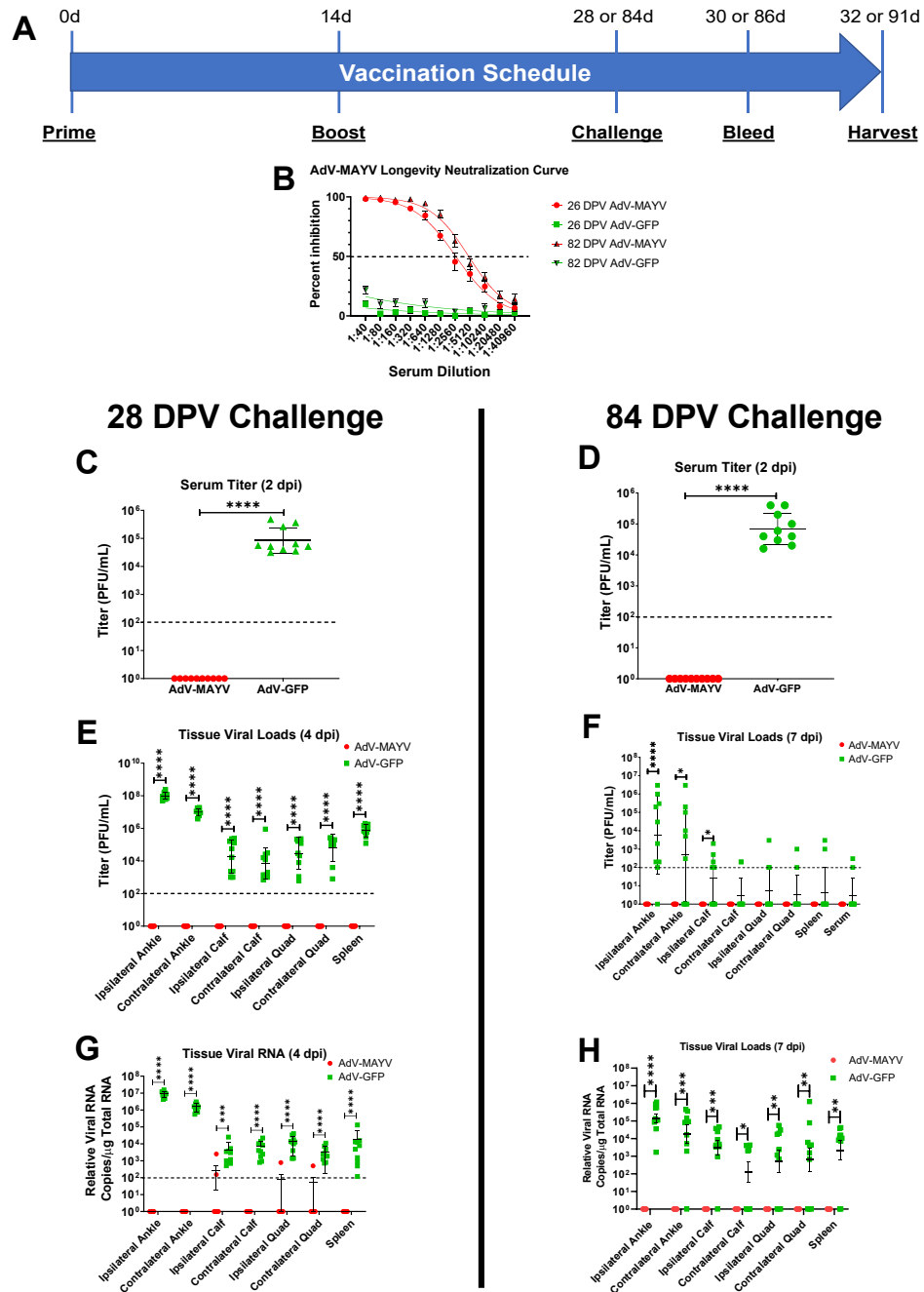


Figure 2.5 AdV-MAYV Vaccination Protects WT Mice from MAYV challenge

(A) WT C57BL/6 mice were vaccinated with AdV-MAYV or AdV-GFP prime vaccination by i.m. injection followed by a booster vaccination at 14 days. At day 28 or 84 post prime, mice were challenged with 10^4 PFU/ml MAYV_{BeAr} in the right footpad. Blood was collected at 2 dpi and tissues and blood were harvested at 4 or 7 dpi. The data represent a single experiment performed with an n=10 mice per group. (B) Serum collected prior to challenge displayed robust neutralizing antibody titers for AdV-MAYV vaccinated mice at both 26 and 82 dpv compared to AdV-GFP controls.

PRNT₅₀ values calculated for each group by variable slope non-linear regression. Error bars represent SEM. (C and D) Serum viremia at 2 dpi was measured by limiting dilution plaque assay on Vero cells. Viral titers in the serum from AdV-MAYV vaccinated animals was below the detection limit (100 PFU/ml of serum) for all animals. Statistical analysis was performed on log-transformed data using an unpaired Mann-Whitney U test (**** P < 0.0001). (E and F) Infectious viral loads in lysates derived from the ankles, calves, quads, spleen tissues and serum were measured by limiting dilution plaque assays at 4 dpi. Infectious viral loads in AdV-MAYV vaccinated animals were below the detection limit for the assay (100 PFU/ml of lysate). Statistical analysis was performed on log-transformed data using unpaired Mann-Whitney U tests (* P < 0.05, **** P < 0.0001). (G and H) Total RNA was extracted from mouse tissue lysates and viral RNA levels were measured by qRT-PCR using primers and probes directed against the virus. Statistical analysis was performed on log-transformed data using unpaired Mann-Whitney U tests (* P < 0.05, ** P < 0.005, *** P = 0.0001, **** P < 0.0001). Black dotted line indicates limit of detection (100 copies per µg of total RNA). Viral RNA was below the detection limit for most AdV-MAYV vaccinated animals following challenge. Error bars in panels C-H represent SD.

Next, we determined whether 10⁸ PFU prime + boost AdV-MAYV vaccination affects the inflammatory immune environment in the joint following MAYV challenge. Following challenge, tissue homogenates from vaccinated WT mice were collected and prepared at 4 dpi for analysis of cytokine and chemokine levels using a magnetic bead multiplex assay. Both contralateral and ipsilateral ankles from AdV-MAYV vaccinated, MAYV-challenged mice had significantly lower levels of MCP-1, MIP-1 α , RANTES, Eotaxin, and MIP-2 α when compared to control AdV-GFP vaccinated, MAYV-challenge mice (**Figure 2.6**). In fact, for most chemokines there was no statistical difference in chemokine levels between AdV-MAYV vaccinated mice challenged with MAYV and the naïve control mice. The lower levels of inflammatory chemokines following MAYV challenge in AdV-MAYV vaccinated mice correlates with the ability of the vaccination platform to diminish infection. To further evaluate the effects of vaccination and the elicited antibodies on tissue inflammation, we challenged groups of WT mice one day after passive transfer of naïve or immune sera from vaccinated mice and compared them to a

mock challenged group. At 7 dpi mice in the naïve serum transfer group had significant increases in footpad swelling compared to the immune sera group ($P < 0.05$) (**Figure 2.7A**). H&E staining of lower hind limbs harvested from mice at 7 dpi revealed significantly increased pathologic changes in both ipsilateral and contralateral lower leg tissues for the naïve serum group when compared to the MAYV vaccine immune sera group (**Figure 2.7B**). Representative images from the ankle joint, footpad muscle, and tibia muscle are shown in **Figure 2.7C**.

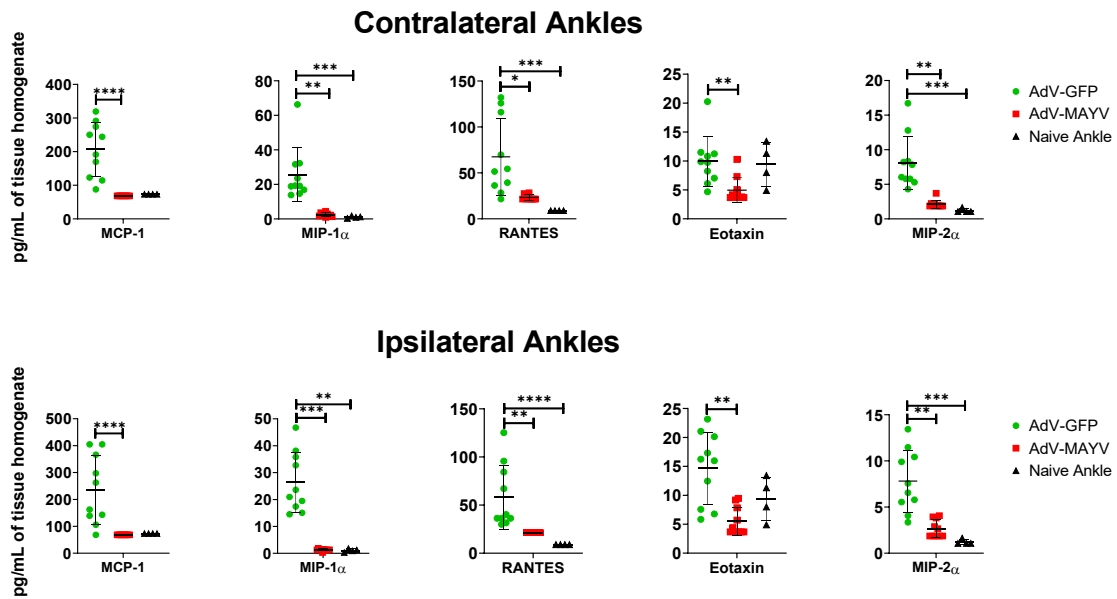


Figure 2.6 AdV-MAYV Vaccination Reduces Inflammatory Mediators in the Joint

Levels of cytokines and chemokines in control mice and mice challenged with MAYV following vaccination with AdV-GFP and AdV-MAYV. WT C57BL/6 mice were vaccinated with AdV-MAYV or AdV-GFP by i.m. injection followed by a booster vaccinated at 14 days. At day 28 post vaccination, mice were challenged with 1×10^4 PFU/ml MAYV_{BeAr} in the right footpad (n=10 mice per group). Ankle tissue homogenates collected from mice at 4 dpi were analyzed for cytokine and chemokines by a 26-plex cytokine multiplex kit and compared to naïve tissues. Statistical analysis was performed using Kruskal-Wallis tests and error bars represent SD (* $P < 0.05$, ** $P < 0.005$, *** $P = 0.0001$, **** $P < 0.0001$).

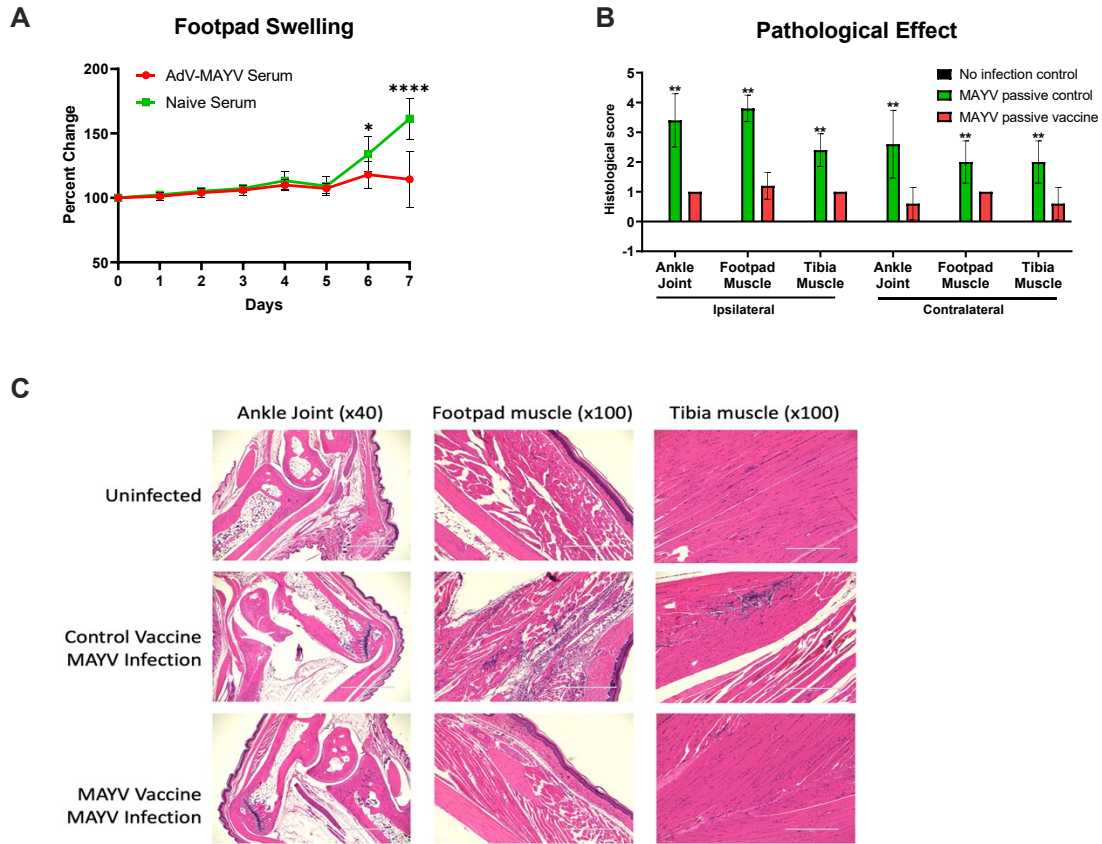


Figure 2.7 Passive Transfer of AdV-MAYV Immune Sera Protects Against Pathological Effects of Infection

Naïve or immune sera was passively transferred to groups of five-week-old female WT C57BL/6 mice one day prior to challenge with 10^4 PFU MAYV_{BeAr} in the right hind limb footpad. A second group of naïve five-week-old female WT C57BL/6 were mock inoculated with PBS. (A) Footpad swelling was monitored by digital calipers throughout the experiment. Statistical analysis was performed by paired repeated measures ANOVA (* $P < 0.05$, **** $P < 0.0001$). (B) Whole hind legs were harvested at 7 dpi and sectioned for histopathology by hematoxylin and eosin staining. Tissue sections were scored on a 0 – 5 scale: 0 absent (no lesions), 1 minimal (1~10% of tissues affected), 2 mild (11~25% affected), 3 moderate (26~50% affected), 4 marked (51~75% affected), 5 severe (>75% affected). Statistical analysis was performed by two-way ANOVA (** $P < 0.005$). (C) Representative images of gross pathology for the ankle joint, footpad muscle, and tibia muscle between the three groups. Error bars represent SD.

Based on the strong protective immunity afforded by AdV-MAYV vaccination to WT mice, we next evaluated vaccine efficacy in IFN α R1^{-/-} mice, which have greatly reduced innate immune responses making them highly susceptible to MAYV

infection [625, 774]. An initial group of IFN α R1^{-/-} mice (n=4) were vaccinated using the AdV-MAYV 10⁸ prime + boost regimen and 28 dpv serum was analyzed for neutralizing antibodies. Neutralization assays identified a PRNT₅₀ of 3,678, mirroring the strong neutralizing antibody response identified in the WT mice (Figure 2.8).

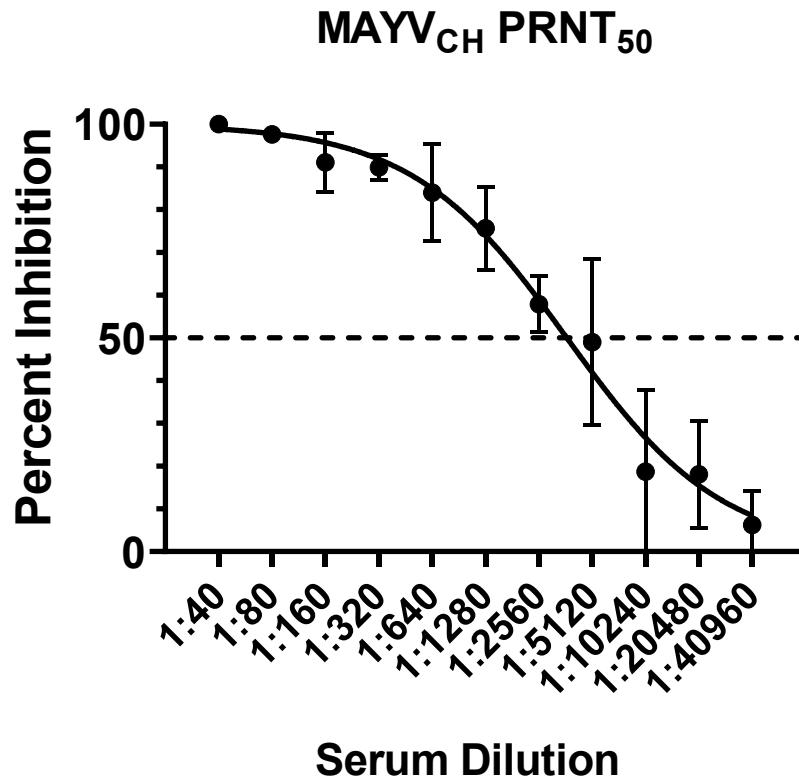


Figure 2.8 AdV-MAYV Vaccination of IFN α R^{-/-} Mice Induces Strong Neutralizing Antibody Responses

A group of IFN α R^{-/-} mice (n=4) were vaccinated with AdV-MAYV and at 28 dpv blood was collected and serum analyzed for neutralizing antibodies. Neutralization assays identified a PRNT₅₀ of 3678 by variable slope non-linear regression, mirroring the similarly strong neutralizing antibody response identified in the WT mice. Error bars represent SEM.

A second group of AdV-MAYV vaccinated IFN α R1^{-/-} mice (n=7) displayed pre-challenge levels of neutralizing activity against MAYV_{CH} (PRNT₅₀ = 1,115) (**Figure 2.9A**). At 28 dpv the mice were challenged with 10⁴ PFU MAYV_{BeAr} in the right posterior footpad. At 2 dpi, serum viremia was below detection in AdV-MAYV vaccinated mice in contrast to the viremia level in AdV-GFP vaccinated and PBS control mice (5.6x10⁷ and 1.2x10⁸ PFU/ml, respectively; P < 0.0001) (**Figure 2.9B**). Mice were monitored daily for morbidity and mortality until 7 dpi. All AdV-GFP and PBS control mice succumbed to infection by 5 dpi, while AdV-MAYV mice survived without physical signs of infection until the study endpoint at 7 dpi (P < 0.0001) (**Figure 2.9C**). The AdV-MAYV vaccine elicited similar levels of neutralizing antibodies in both WT mice and IFN α R1^{-/-} mice, which afforded the highly susceptible IFN α R1^{-/-} mice protection against lethal challenge.

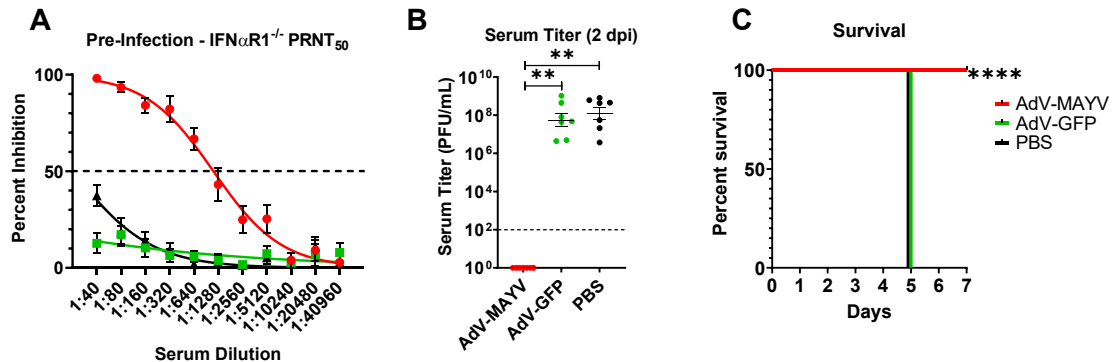


Figure 2.9 AdV-MAYV Vaccination Protects IFN α R1^{-/-} Mice from Lethal Challenge

Male and female IFN α R1^{-/-} mice were vaccinated with 10⁸ PFU AdV-MAYV, AdV-GFP, or PBS by i.m. injection followed by a booster vaccination 14 days later. At day 28, mice were challenged with 1x10⁴ PFU/ml MAYV_{BeAr} in the right footpad. The data presented represents one independent experiment (n=7 mice per vaccine). (A) Prior to challenge, blood was collected to measure neutralizing titers against MAYV_{CH} by PRNT assay using variable slope non-linear regression. AdV-MAYV elicited robust neutralizing antibodies in IFN α R1^{-/-} mice. Error bars represent SEM. (B) Limiting dilution plaque assays were used to measure viremia for blood serum samples collected at 2 dpi. Black dotted line indicates limit of detection (100 PFU/ml). Statistical analysis was performed on log-transformed data using a Kruskal-Wallis test (** P < 0.005). Error bars represent SD. (C) Mouse morbidity and mortality was monitored daily for 7 days post infection with Kaplan-Meier survival curve analysis (**** P < 0.0001).

Passive Transfer of AdV-MAYV Vaccinated Serum Provides Protective Immunity

To assess the ability of circulating antibodies to protect IFN α R1^{-/-} mice against MAYV infection, sera collected from AdV-MAYV 10⁸ prime + boost vaccinated WT mice at 28 dpv was i.p. injected into IFN α R1^{-/-} mice one day prior to lethal challenge with 10⁴ PFU MAYV_{BeAr} and mice were monitored daily for signs of infection and survival for 7 days (Experimental design is shown in **Figure 2.10A**). Blood collected at 2 dpi was used to measure differences in serum viremia levels using plaque assays. IFN α R1^{-/-} mice receiving serum from AdV-MAYV vaccinated mice had significantly reduced levels of infectious virus compared to IFN α R1^{-/-} mice receiving serum from PBS control mice (P = 0.008) (**Figure 2.10B**). In concordance with reductions in levels of serum viremia, IFN α R1^{-/-} mice receiving serum from AdV-MAYV WT mice maintained their starting body weights in contrast to the PBS control group, which lost 14% from their starting weights the day prior to death (P << 0.0001) (**Figure 2.10C**). As shown in **Figure 2.10D**, control serum transfer IFN α R1^{-/-} mice survived only to 4 dpi while IFN α R1^{-/-} mice receiving serum

from AdV-MAYV vaccinated WT mice all survived until study endpoint at 7 dpi ($P < 0.0001$). Tissue viral RNA levels at 7 dpi in IFN α R1^{-/-} mice receiving serum from AdV-MAYV vaccinated WT mice were detectable only in the ipsilateral ankle, except for one mouse with viral RNA detected in the contralateral ankle (**Figure 2.10E**). These data demonstrate the protective nature of the strongly neutralizing antibodies in the serum of AdV-MAYV vaccinated mice.

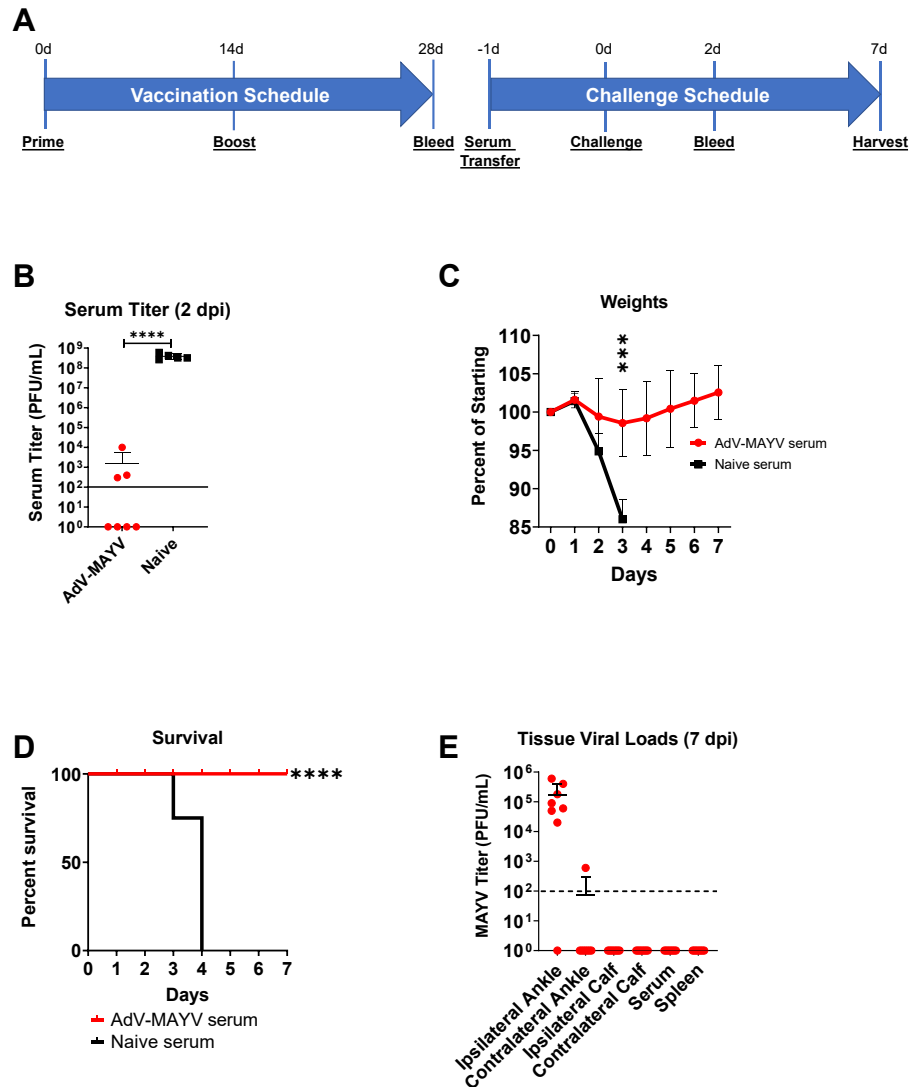


Figure 2.10 Passive Transfer of Immune Serum Protects $IFN\alpha R1^{-/-}$ Mice from Lethal MAYV Challenge

(A) Six WT C57BL/6 mice were vaccinated with 10^8 PFU of AdV-MAYV following the prime + boost regimen; at 28 days post-prime total blood was collected and serum pooled from all mice. A bolus of 200 μ l of pooled serum from AdV-MAYV vaccinated or naive mice was administered to $IFN\alpha R1^{-/-}$ mice by intraperitoneal injection 1 day before challenge with 1×10^4 PFU $MAYV_{BeAr}$. The data represents one experiment with $n=7$ per condition. (B) Blood collected at 2 days post-challenge was used to measure viremia by limiting dilution plaque assays. While all 7 animals receiving control serum had high levels of virus, only three of the seven animals receiving passive transfer of immune sera had detectable virus, which was 5-6 logs lower than controls. Statistical analysis was performed on log-transformed data using a Mann-Whitney test (** $P < 0.005$). (C) Mice were weighed daily after challenge until experiment endpoint at 7 dpi. Statistical analysis was performed using multiple repeated measures mixed-effects ANOVA (** $P = 0.0001$). (D) Mouse survival following MAYV challenge was graphed. Statistical analysis was performed using Kaplan-Meier

survival curve analysis (**** $P < 0.0001$). (E) Tissue viral RNA levels were determined by qRT-PCR for mice that survived until 7 dpi (those animals receiving AdV-MAYV vaccine sera only). Virus was detected in the ipsilateral ankles of challenged mice but very little was detected in other tissues. Black dotted line indicates limit of detection (100 viral RNA copies/ μg of total RNA). Error bars represent SD.

AdV-MAYV Vaccination Elicits Cross-Protection Against Other Alphaviruses

Previous studies have indicated the existence of cross-protection for related alphaviruses such as chikungunya virus (CHIKV) and MAYV [634, 635]. Thus, we next evaluated the AdV-MAYV vaccine for protective immunity against CHIKV and UNAV, two related alphaviruses in the Semliki Forest complex [497]. Serum collected from WT mice vaccinated with AdV-MAYV was first tested for neutralizing activity against CHIKV and UNAV and shown by PRNT to reduce the levels of infection for both viruses (**Figure 2.11A&B**).

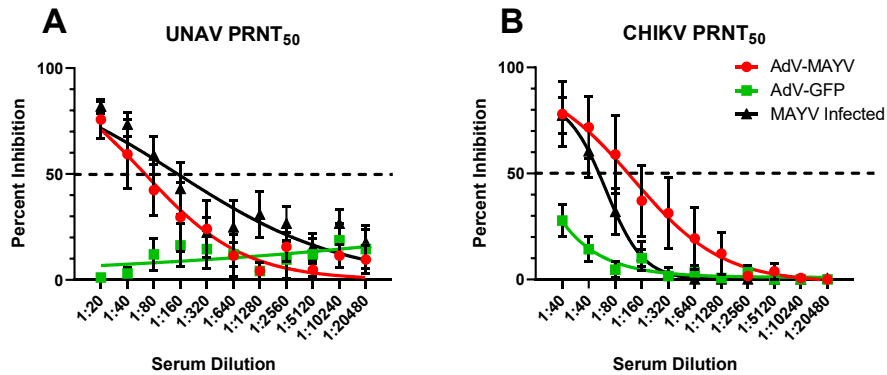


Figure 2.11 AdV-MAYV Elicits Cross Neutralizing Antibodies Against Una and Chikungunya Viruses

In order to determine whether the AdV-MAYV elicited cross-protection against related alphaviruses, PRNT₅₀ assays were performed on serum from WT C57BL/6 mice vaccinated with AdV-MAYV,

AdV-GFP vaccinated, and compared to serum from mice infected with MAYV. Shown are the average PRNT₅₀ values calculated for each group (n=5). PRNT₅₀ assays for (A) Una virus and (B) CHIKV indicate cross-species neutralization is elicited in serum from mice vaccinated with AdV-MAYV as well as mice infected with MAYV but not for serum collected from AdV-GFP vaccinated controls. Curves were calculated using a variable slope non-linear regression analysis. Error bars representing SEM from 5 biological replicates.

Based on this data, *in vivo* cross-protection experiments in lethally challenged IFN α R1^{-/-} mice were conducted to evaluate the protective efficacy of AdV-MAYV immunization against CHIKV or UNAV infection. IFN α R1^{-/-} mice were vaccinated and challenged at 28 dpv with either 10³ PFU CHIKV_{SL15649} or 10⁴ PFU UNAV_{Mac150} in the right footpad. Blood collected at 2 dpi from control mice showed high levels of CHIKV and UNAV viremia while viremia in the AdV-MAYV vaccinated groups was below the level of detection (P < 0.0001 for both groups) (**Figure 2.12A**). Animals were monitored daily until 7 dpi for the presence of ipsilateral footpad swelling, weight loss and other signs of morbidity. All of the control vaccinated animals developed weight loss and clear signs of morbidity; these animals were euthanized at 4 or 5 dpi. AdV-MAYV vaccinated animals did not display weight loss and survived until the study endpoint at 7 dpi (P < 0.0001) (**Figure 2.12B & C**). One mouse in the AdV-MAYV CHIKV challenge group died of reasons unrelated to infection. Control animals challenged with CHIKV had remarkable footpad swelling starting at 2 dpi until death at 5 dpi (**Figure 2.12D**). CHIKV disease, weight loss, and associated death in IFN α R1^{-/-} mice was completely abrogated by AdV-MAYV vaccination (**Figure 2.12B-D**). There was no detectable footpad swelling in mice challenged with UNAV, but the onset on UNAV induced footpad swelling may be delayed and take longer than what is observed following

CHIKV challenge (**Figure 2.12C**). Tissues and sera were collected from the surviving AdV-MAYV vaccinated IFN α R1^{-/-} mice at 7 dpi to measure infectious virus and viral genomes (**Figure 2.12E-G**). For both CHIKV and UNAV challenged mice the ipsilateral ankle was the only tissue with detectable infectious virus with 4 of 5 mice in the CHIKV challenge and 1 out of 6 mice in the UNAV challenge groups having viral titers above the limit of detection (**Figure 2.12E**). CHIKV or UNAV vRNA RT-qPCR analysis of tissues identified the presence of low levels of viral genomes in the ankle and calf tissues of surviving vaccinated challenge group mice. UNAV challenged IFN α R1^{-/-} mice had equivalent levels in viral genomes on both contralateral and ipsilateral tissues, indicating that proximity to the injection site did not have an influence on viral RNA levels at 7 dpi, although ankle tissues had mean values approximately 2 logs higher than calf tissues (**Figure 2.12F**). In CHIKV challenged IFN α R1^{-/-} mice there was a notable difference in viral genomes based upon proximity to infection site. The ipsilateral ankle had a mean approximately 3.2 logs higher than the contralateral ankle, and while viral genomes were detected in the ipsilateral calf, no genomes were detected on the contralateral calf (**Figure 2.12G**). These findings replicate the previous results in the vaccinated MAYV challenged mice and indicate that the vaccine platform generates cross-protective immunity against related alphaviruses.

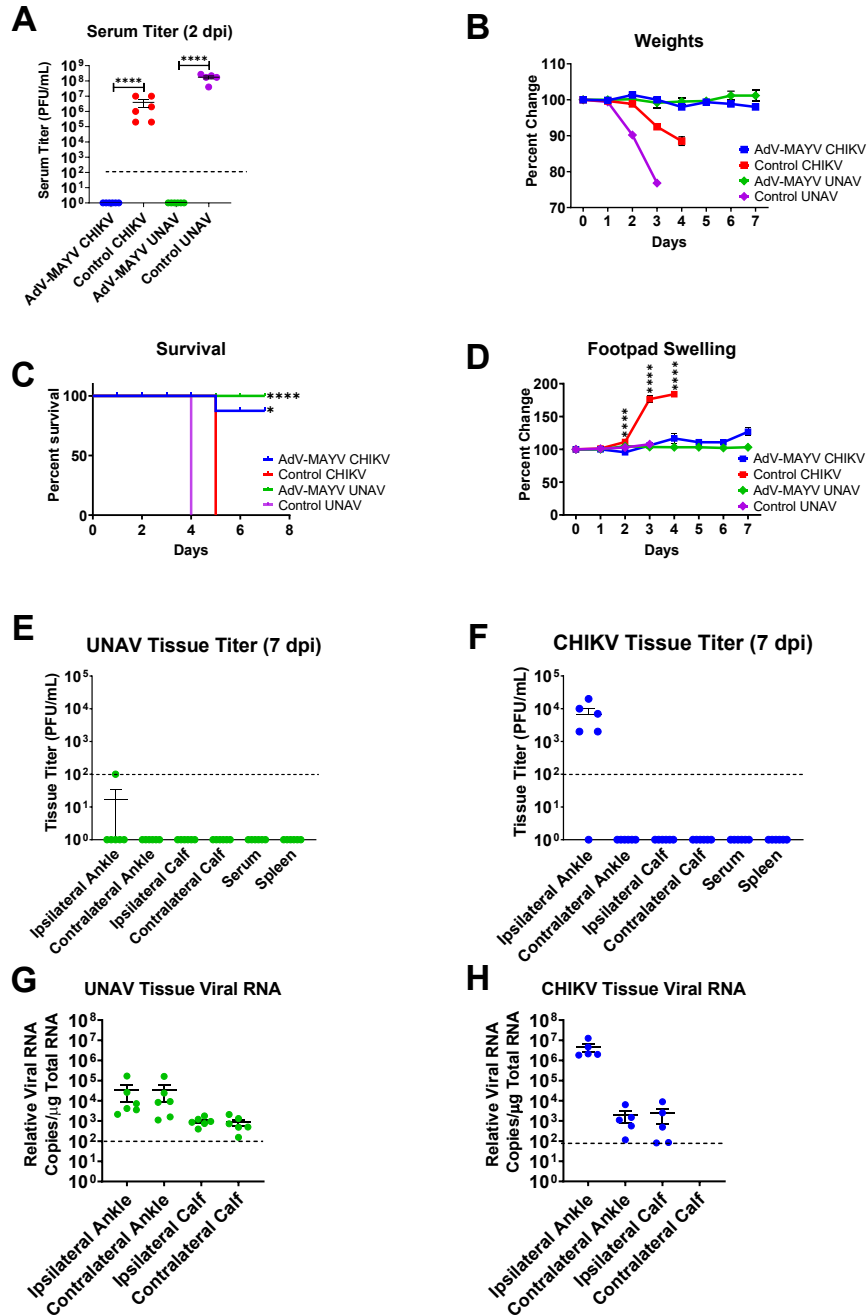


Figure 2.12 AdV-MAYV Vaccination Cross-Protects $IFN\alpha R1^{-/-}$ Mice Against Lethal Challenge with CHIKV and Una Virus

$IFN\alpha R1^{-/-}$ mice vaccinated by intramuscular injection of AdV-MAYV, using the prime-boost vaccination regimen, were challenged with 1×10^4 PFU CHIKV or UNAV in the right footpad. Serum was collected at 2 dpi and animals were monitored for clinical signs for 7 days. Experimental timeline is similar to that in Figure 4A. Data represents one independent experiment performed with $n = 5$ mice per group for vaccinated animals and $n = 6$ for controls. (A) Viremia was measured by

limiting dilution plaque assay on confluent monolayers of Vero cells. Statistical analysis was performed within groups by Mann-Whitney tests (** $P < 0.005$). Following challenge mice were monitored daily until experiment endpoint for (B) weight loss (C) morbidity and mortality (D) changes in right posterior footpad swelling as measure by caliper. Statistical analysis was performed using multiple T-tests and Kaplan-Meier survival curve analysis. Error bars represent SD (* $P < 0.05$, ** $P < 0.005$, **** $P < 0.0001$). At 7 dpi tissues were harvested and ankle, calf, and spleen infectious viral loads for Una virus (E) and CHIKV virus (F) were measured in tissue homogenates by limiting dilution plaque assays. Black dotted line indicates limit of detection (100 copies of viral RNA/ μg of total RNA). Total RNA was extracted from ankle and calf tissue homogenates to quantify Una virus (G) and CHIKV virus (H) RNA loads by qRT-PCR. Error bars represent SD.

2.4 Discussion

Mayaro virus (MAYV) is an emerging viral disease currently endemic to South and Central America, although some recent cases have been observed globally. The Netherlands, France, and numerous other nations in Europe and North America have reported infections over the last two decades in citizens that have travelled to South and Central America [671, 775-777]. MAYV infection causes a febrile illness for 3-5 days, while joint and muscle pain can last for up to a year. Based on the similarity of disease symptoms between Old-World alphaviruses and serological cross-reactivity, infections with MAYV are commonly misdiagnosed [671]. Currently, there are no FDA-approved vaccines for humans against MAYV or any other alphaviruses; therefore, the development of effective treatments or vaccines would be of great international benefit. In this study, we demonstrate that a non-replicating human adenovirus serotype 5 based vaccine platform expressing the MAYV structural protein (AdV-MAYV) generated potent immunogenicity. AdV-MAYV generated virus-like particles were shed from transduced cells, which may be an important attribute that leads to robust neutralizing antibody generation. As such, in a mouse MAYV challenge model, AdV-MAYV vaccination resulted in a

significant decrease in viremia at 2 dpi to levels that were below the detection limit when compared to AdV-GFP vaccine control mice. This finding was confirmed during testing for infectious virus and viral genomes in tissues at 4 dpi. Upon challenge, IFN α R1^{-/-} mice vaccinated with AdV-MAYV also had undetectable levels of viremia at 2 dpi and all survived to the study endpoint at 7 dpi. This demonstrated that even in a very stringent challenge model, the vaccine elicited highly efficacious immunity. Mechanism of protection studies identified that AdV-MAYV vaccination elicited highly neutralizing and binding MAYV specific antibodies as well as E2 protein specific T cell responses. Interestingly, the AdV-MAYV vaccine also protected IFN α R1^{-/-} mice from challenge with UNAV or CHIKV, other Old-World alphaviruses, indicating cross protection elicited by the vaccine.

IFN α R^{-/-} mice are a highly stringent model as they display increased arbovirus replication and tissue damage compared to wildtype mice [774]. Previous studies have indicated a high susceptibility of IFN α R1^{-/-} mice to members of the alphavirus family with lethality achieved using doses of as little as 3 PFU CHIKV or approximately 10² – 10⁴ PFU when challenged with other family members including ONNV and VEEV [625, 774]. Thus, they are highly effective models to understand the protective effects of vaccination approaches [626, 774, 778]. Passive transfer experiments demonstrated robust and transferrable antibody production in AdV-MAYV vaccinated mice, protecting recipient mice from viremia at 2 dpi and enabling survival until study endpoint, as well as the ability to largely reduce or entirely ablate the presence of infectious virus and/or viral RNA in the

muscle and joint tissues of vaccinated and challenged mice. Joint and muscle tissues are known to be reservoirs for arthritogenic alphavirus replication. Fibroblasts, mesenchymal, and osteoblast cells have been identified as predominant and preferential locations for CHIKV replication, and muscle satellite cells have also been identified as selective targets in human muscle tissues [639, 640]. Infection of joints typically leads to arthralgia in small joints (e.g. fingers, wrist, tarsus) prior to larger joints (e.g. knees and shoulders) but can and typically does involve multiple joints simultaneously [614]. High levels of viral replication and persistence in these tissues as well as immune cell infiltration and long-term inflammation are both responsible for the prolonged arthralgia and myalgia experienced by patients. We demonstrate that the AdV-MAYV vaccine can play an important role in diminishing the myalgia and arthralgia experienced following infection by restricting viral dissemination and replication in these tissues and thus limiting the associated inflammatory response. It has previously been shown that adult $IFN\alpha R^{-/-}$ mice challenged with $MAYV_{TR4675}$ exhibit high levels of infectious virus in the footpad, knee, gastrocnemius, and thigh muscle, while adult C57BL/6 had high levels in their thigh, spleen, and gastrocnemius [682]. Our findings agree with these data and also suggest the spleen is a reservoir permissive to high levels of MAYV replication in the absence of innate immunity. Further, while vaccination was able to prevent viral dissemination, passive transfer of immune serum was capable of significantly reducing the pathological symptoms of infection when we surveyed lower hind limb ankle joints, and footpad and tibia muscles (**Figure 2.7**).

A previous study by *Webb et al.*, in which mice vaccinated with a CHIKV/IRES vector, as well as CHIKV infected mice, produced MAYV cross-reactive antibodies, thus implicating shared antigenic epitopes between MAYV and CHIKV [738]. That study did, however, indicate that a minimum level of CHIKV neutralizing antibody titer must be reached in order to confer cross-protection, supporting the idea that robust stimulation of neutralizing antibodies is key for broad protective effects. Our AdV-MAYV vaccination regimen also supports these findings and provides confirmatory evidence that shared antigenic domains exist between these related alphavirus member species. Upon testing serum from vaccinated mice, it was determined that the elicited antibodies bore close similarity to antibody types and levels produced in MAYV infected mice, although total Ig was significantly decreased between MAYV infected and prime + boosted AdV-MAYV vaccinated mice (**Figure 2.3**). IgG3 was the only subclass induced by prime/boost vaccination that displayed higher binding levels than those observed in infected mice. IgG3 is the only IgG subclass that is T cell independent and primarily is targeted against carbohydrates and repeating protein aggregates [779-781]. Studies have previously indicated that IgG3 subclass antibodies were the predominant anti-E2 glycoprotein response in mice vaccinated with CHIKV VLP and appeared shortly after vaccination [782]. It also can serve as an intermediary between IgM and IgG2b. IgG2b antibodies work with IgG3 in the early T cell independent response but function to elicit early Fc γ R-mediated effector functions [781]. This partnership could explain why even if IgG3 primarily binds to E2 epitopes the expression is diminished at 7 dpi while IgG2b is elevated in order to direct ADCC and CDC

functional responses. The strong levels of IgG1 and IgG2b are also in line with previous studies that utilized AdV vectors in 129Sv/Ev and IFN α R^{-/-} mice where significant production of these subclasses was noted [783]. The ability to stimulate both strong humoral and cellular immune responses correlates with evidence presented by Choi *et al.* in their DNA based vaccine against MAYV [705, 714, 725]. Surveying mouse ankles identified that there were elevated levels of MCP-1, MIP-1 α , RANTES, Eotaxin, and MIP-2 α . Recently, the analysis of spleens from MAYV/IRES vaccinated and challenged mice had a significant reduction in MCP-1, MIP-1 α , and RANTES, among others, compared to MAYV infected at 3 dpi [680]. We previously identified these among a group of elevated chemokines in sampled ipsilateral ankle tissues in control mice following infection with CHIKV, and others have found that MCP-1 and MIP-1 α were both elevated in tissues of Ross River virus infected mice by qRT-PCR [686, 784]. Thus, the reduction in these inflammatory chemokines could be important factors in reducing the sequelae of inflammatory responses in infected individuals. Our balanced cellular and humoral immune response elicited by the AdV-MAYV provides robust neutralizing antibodies but also T cell responses that we have previously shown are important for limiting inflammation following alphavirus challenge [686].

Adenovirus based vaccine vectors have advantages when compared to live-attenuated and recombinant protein vaccines with their ability to stimulate both strong humoral and cellular immune responses, elicit strong persistent immunity, and the ability to be used in susceptible populations such as the elderly and

immunocompromised [379, 785-787]. They can be readily produced to high titer, do not integrate, and can be administered safely. The novel AdV-MAYV vaccine approach reported here is the fourth reported vaccine approach against MAYV and is the only MAYV vaccine approach that has shown the ability to cross-protect against both CHIKV and UNAV [705, 714, 725, 738]. CHIKV and UNAV circulate in the same geographical region as MAYV, so providing multitarget protection would be beneficial to local inhabitants and travelers alike. There have been no previous studies on the development of UNAV vaccines, nor the indication that previously published pre-clinical alphavirus vaccines provide cross protection against UNAV, thus making our AdV-MAYV vaccine novel in this regard. Previous studies in macaques reported on the ability of antibodies produced during CHIKV infection to neutralize MAYV, and serum samples from humans indicated that convalescent CHIKV infected patient antibodies were capable of neutralizing both MAYV and UNAV [635, 636, 738]. These findings support our study findings on the elicitation of cross-protective antibodies against other Old-World alphaviruses following vaccination against MAYV. Similar vaccine studies in mice have also observed heterotypic protection against related alphaviruses, indicating that this phenomenon is a feature that should be studied alphavirus vaccine development [684, 712, 769, 770]. Together, the data from these studies confirms the findings that shared epitopes for neutralizing antibodies exist between these members of the Semliki Forest complex and supports the presented findings of cross protection from our AdV-MAYV vaccine. Additional pre-clinical studies with this vaccine

vector will provide important insight into new approaches to vaccinate at risk populations against MAYV, Una, and CHIKV.

2.5 Materials and Methods

Cells

Vero cells (ATCC) and 293-IQ cells (Microbix; HEK293 cells expressing the lac repressor [788]) were propagated at 37°C with 5% CO₂ in Dulbecco's Modified Eagle Medium (DMEM) supplemented with 5 or 10% Fetal Bovine Serum (FBS) and Penicillin-Streptomycin-L-Glutamine (PSG). Telomerized human fibroblasts stably expressing the coxsackie and adenovirus receptor (THF-CAR) were propagated in DMEM containing 10% FBS plus PSG. *Aedes albopictus* cells (C6/36 cells; ATCC CRL-1660) were propagated at 28°C with 5% CO₂ in DMEM supplemented with 10% FBS and PSG.

Viruses

Mayaro virus, CH was generated from an infectious clone received from Dr. Thomas Morrison (UC-Denver). The following reagents were obtained through BEI Resources, NIAID, NIH as part of the WRCEVA program: Mayaro virus, Guyane, NR-49911; Mayaro virus, TRVL 4675, NR-49913; Mayaro virus, BeAr505411, NR-49910; Mayaro virus, Uruma, NR-49914; Una virus, MAC 150, NR-49912. CHIKV SL15649 and vaccine strain CHIKV 181/25 were generated from their respective infectious clones as previously described [686]. Alphaviruses were grown in C6/36 cells. Viral stocks were prepared from clarified supernatants at 72 h post infection

(hpi) by ultracentrifugation over 10% sucrose (SW32Ti, 70 min at 76,755 x g). The virus pellets were resuspended in PBS and stored at -80°C. Viral limiting dilution plaque assays using Vero cells were performed on 10-fold serial dilutions of virus stocks or tissue homogenates. The infected cells were rocked continuously in an incubator at 37°C for 2 h, and then DMEM containing 5% FBS, PSG, 0.3% high viscosity carboxymethyl cellulose (CMC) (Sigma) and 0.3% low viscosity CMC (Sigma) was added to the cells. At 2 dpi, cells were fixed with 3.7% formaldehyde (Fisher) and stained with 0.5% methylene blue (Fisher). Plaques were visualized under a light microscope and counted.

Adenovirus Vaccine Vector

A replication-incompetent human Ad serotype 5 (AdV) vector (containing E1 and E3 deletions) expressing the MAYV structural polyprotein (Capsid, E3, E2, 6K/TF, E1) was generated using the AdMax HiIQ system (Microbix). Briefly, the structural gene from MAYV BeAr505411 was cloned into pDC316(io) by first amplifying the gene by PCR with forward (ATATGAATTCATGGACTTCCTACCAACTCAAGTG) and reverse (ATATAAGCTTTTACCTTCTCAAAGTCACACAAG) primers containing EcoRI and HindIII restriction sites, respectively. Resulting clones were sequence verified. For adenovirus rescue, 293-IQ cells were co-transfected with pDC316(io)-MAYVsp and pBHGlox Δ E1,3Cre plasmid using Lipofectamine 2000 [686, 788, 789]. A modified Cytomegalovirus immediate-early promoter containing a lac repressor binding site inserted between the promoter and the open reading frame was used to drive transgene expression in cells lacking the Lac repressor.

Adenovirus containing supernatants were collected at maximum cytopathic effect (CPE) and the virus vectors were passaged a total of four times in 293-IQ cells with the final production from the clarified supernatants of eleven infected T175 flasks. Virus was pelleted by ultracentrifugation at 79,520 x g for 70 minutes. The pellets were resuspended in a total of 1.5 mL of phosphate buffered saline (PBS) and stored at -80°C. Adenovirus stocks were titered by limiting dilution CPE assay on 293-IQ cells in 96 well plates.

Ethics Statement

Mouse experiments were performed in an ABSL3 laboratory, accredited by the Association for Accreditation and Assessment of Laboratory Animal Care (AALAC) International, in compliance with IACUC protocols.

Mouse Experiments

IFN α R1^{-/-} and WT C57BL/6 mice were housed in ventilated racks with free access to food and water and maintained on a 12 h light/dark cycle. WT C57BL/6 mice were purchased from Jackson Laboratories and IFN α R1^{-/-} were used from an established breeding colony at the VGTI/OHSU. Animals were vaccinated with 100 μ l AdV-MAYV (1x10⁶ to 1x10⁸ plaque forming units (PFU)) diluted in PBS injected into the posterior thigh with or without a boost at 14 days post-prime using the same viral dose used in the initial vaccination. At times listed in the figure legends, blood was collected from the facial vein and allowed to clot before centrifuging for 10 minutes at 9,391 x g in a microcentrifuge in order to collect serum. Vaccinated

mice were challenged with virus at either 28- or 84-days post-vaccination (dpv). A few groups of animals received passive transfer of 200 μ l of pooled serum from five AdV-MAYV or mock vaccinated mice by intraperitoneal injection at 24 h before infection. Mice were challenged with 10^4 PFU of MAYV_{BeAr}, UNV_{MAC 150}, or 10^3 PFU CHIKV_{SL15649}, via a 20 μ l injection into the right posterior footpad. Footpad swelling measurements were performed with digital calipers and health and weight were monitored daily following challenge. Serum was collected at 2 days post-infection (dpi) to measure viremia by plaque assay. These challenge studies were terminated at either 4 or 7 dpi at which time ankle, calf muscle, quadricep muscle, spleen, and serum were collected for use in plaque titration assays and qRT-PCR as previously described [686]. Tissue samples were collected into tubes with 0.5 mL of PBS and 2 mm beads (Propper Manufacturing Co., Inc.) for homogenization by bead beating. Cellular debris were pelleted and clarified lysate was used for infectious virus titration and cytokine multiplex assays. An additional 100 μ l aliquot of the tissue homogenate was added to Trizol for qRT-PCR analysis. Histological analysis was performed on groups of five-week-old female WT C57BL/6 mice that received passive transfer of naïve or immune serum from vaccinated animals. One day after transfer, animals were challenged with 10^4 PFU MAYV_{BeAr} in the right hind limb footpad. A second group of naïve five-week-old female WT C57BL/6 were mock inoculated with PBS.

Quantification of virus tissue burden

Tissues were harvested from infected mice into 500 µl PBS with approximately 20 glass beads in 2 mL Starstedt screw cap tubes. Tissues were bead beat in three 45 second cycles. Blood was collected and serum was collected from the clotted blood sample. A 20 µl sample of tissue lysates or sera were serially diluted in DMEM containing 5% FBS and 1x PSG and added to 48-well plates containing confluent monolayers of Vero cells and rocked at 37°C for 2 h. CMC in DMEM containing 5% FBS and 1x PSG (250 µl per well) was overlaid and plates were incubated for 2 days at 37°C and then the cells were fixed with 3.7% formalin diluted in 1x PBS and stained with 0.2% methyl blue dye for 15 minutes.

qRT-PCR

A 100 µl aliquot of homogenized tissue was added to 900 µl Trizol and used for RNA extraction. cDNA was synthesized with superscript IV. Taqman qRT-PCR was performed on a QuantStudio 7 flex Real-Time PCR system. MAYV probe (TGGACACCGTTTCGATAC) was used with forward (CCATGCCGTAACGATTG) and reverse (ATGGTGCCGGGCAGCCTGGAAG) primers, CHIKV probe (ACATACCAAGAGGCTGC) with forward (CCGTCCCTTTCCTGCTTAGC) and reverse (AAAGGTTGCTGCTCGTTCCA) primers, and UNAV probe (ACGGTACGCTTAAAAT) with forward (CGCGTTGGAGACGATCAGA) and reverse (TCCGATTTGGGCAGAGAACT) primers.

Western Blot Analysis

THF-CAR were transfected with varying MOI's from 0 to 1000. Cells were harvested 72 hpi after washing with PBS and were pelleted at 9,391 x g for 15 minutes at 4°C in a refrigerated microcentrifuge. Pelleted cells were lysed in 300 µl cell lysis buffer for 30 minutes on ice. Lysed cells and debris were pelleted at 16,363 x g for 15 minutes in a microcentrifuge and supernatant was transferred to a new tube. 20 µl of lysate was run on a 4-12% Bis/Tris polyacrylamide gel alongside MAYV infected Vero cells and control Vero cell lysate at 200 volts for 37 minutes. Semi-dry transfer was used to transfer proteins onto an activated PVDF membrane at 25 volts for 35 minutes. Membranes were blocked with 3% BSA/TBST, and probed with a 1:250 dilution of serum from 10⁸ prime + boost AdV-MAYV vaccinated mice. Membranes were then washed, and a secondary HRP conjugated rabbit α-Mouse IgG was used. Membranes were washed and then developed with ThermoFisher Pico chemiluminescent developer solution and exposed onto X-ray film. 1.7x10⁷ PFU of MAYV_{TrVI} was also run on a 4-12% Bis/Tris polyacrylamide gel, proteins were transferred, and membranes probed with a 1:250 dilution of serum from naïve or 10⁸ prime + boost AdV-MAYV following the above protocol.

Electron Microscopy

THF-CAR cells were infected with AdV-MAYV at an MOI = 100 PFU/cell. Media was harvested 72 hpi and cell debris was pelleted at 2,514 x g in a tabletop centrifuge for 10 minutes. Clarified media was then 0.22 µM filtered, and 10%

Sorbitol was underlaid. Tubes were spun at 110,527 x g for 2 h. Supernatant was poured off and pellets were resuspended in 250 μ l of PBS and 0.22 μ M filtered. Resuspended samples were brought to a final volume of 1 mL in 15% trehalose [790], and a 50 μ l sample was fixed in 4% PFA for 30 minutes and frozen at -80°C. Samples were stained with uranyl acetate and EM images were taken by the OHSU Multiscale Microscopy Core on a Krios G4 Cryo-TEM.

Neutralization Assays

Blood was collected from mice and allowed to clot at room temperature for 30 minutes before centrifuging for 5 minutes at 3,000 x g. Sera was transferred to a new tube and heat inactivated at 56°C for 30 minutes. A portion of sera was used for serial dilutions in DMEM supplemented with 5% FBS and 1% PSG. Diluted serum was mixed with media containing 50 PFU of MAYV_{CH}, MAYV_{BeAr}, CHIKV 181/25, or Una_{Mac150}. Media and virus were incubated for 2 h at 37°C while rocking. Serum and virus containing media was transferred to confluent 12 well plates of Vero cells and rocked for 2 h in a 37°C 5% CO₂ incubator. One milliliter of 5% FBS/DMEM/CMC was added to each well and the plate was incubated for 48 h. Plaques were fixed by adding 1 mL of 3.7% formaldehyde to each well for 15 minutes, washed with cold water and stained with 0.2% methyl blue dye for 15 minutes. Plates were washed with cold water and dried prior to counting plaques. PRNT₅₀ was calculated by non-linear regression after determining the percent of plaques at each dilution relative to the average plaques in virus only control wells.

Pre- and Post-Attachment Neutralization Assay

Two-fold serial dilutions of PBS or heat inactivated serum from PBS or AdV-MAYV vaccinated, as well as AdV-MAYV MAYV challenged mice were prepared in DMEM (1:80 to 1:81920). For pre-attachment assays, diluted serum was mixed with 11 PFU of MAYV_{BeAr} and rocked for 1 h at 4°C. Serum-virus complexes were then added to confluent 12-well plates of Vero cells and rocked for 1 h at 4°C. Non-adsorbed complexes were removed by 3 washes of DMEM and plates were moved to a 37°C incubator for 15 minutes to allow for internalization of bound virus. Plates were then overlaid with 1 mL of 5% FBS/DMEM/CMC. Post-attachment assays were conducted in a similar manner, but initially 11 PFU of MAYV_{BeAr} was added to 12-well plates and plates were rocked at 4°C for 1 h. After washing to remove unbound virus, serum dilutions were added to the wells. Plates were again rocked for 1 h at 4°C, followed by washing, and plates were moved to a 37°C incubator for 15 minutes and overlaid with 1 mL of 5% FBS/DMEM/CMC. At 48 hpi, cells were fixed with 3.7% formaldehyde, stained with 0.5% methylene blue, and virus plaques were counted.

Enzyme-Linked Immunoassay (ELISA)

MAYV_{BeAr} was heat inactivated at 56°C for 30 minutes and 9.4×10^4 PFU in 100 μ l PBS was added to each well of high binding flat bottom 96 well plates (Corning). Plates were sealed and incubated at 4°C for 4 days to allow for virus coating. Plates were blotted dry and blocked for 1 h with 5% milk in 1X TBS with 1% Tween-

20 (ELISA buffer). Heat-inactivated sera from mice was diluted 1:50 in ELISA buffer and serially diluted 1:3 for a total of 6 dilutions. 100 μ l of each dilution was added to wells and incubated for 1.5 h at room temperature. Plates were washed three times with ELISA wash buffer and blotted dry. Secondary antibodies were diluted 1:10,000 in ELISA buffer and 100 μ l was added to wells and incubated for 1 h at RT. Plates were then washed three times with ELISA buffer, blotted dry and developed with OPD substrate. The reaction was stopped with 1 M HCl 10 minutes after exposure. Plates were read at 490 nm on a BioTek plate reader.

Enzyme-Linked Immunospot Assay (ELISpot)

ELISpot assays were performed as previously described [686]. A single-cell suspension was created by grinding a whole spleen through a 70 μ m cell strainer and rinsing with 15 mL of RPMI with 10% FBS and 1% PSG (RPMI complete). Cells were pelleted at 650 x g for 10 minutes and red blood cells were lysed with 1x Red Blood Cell Lysis Buffer (Biolegend) for 3 minutes, after which 10 mL of complete RPMI was added and cells were pelleted. Cells were resuspended in 3 mL RPMI complete medium and counted. Splenocytes, 2.5×10^5 cells per well, were added to Mouse IFN- γ ELISpot plates (MabTech) in addition to 20 μ l of peptide (2 μ g/well), 2 μ l of DMSO, or 2 μ l of a phorbol 12-myristate 13-acetate/ionomycin stock at a 1:300 dilution as a positive control. 18mer peptides corresponding to predicted H2b epitopes present in the MAYV structural polypeptide were ordered from Thermo Scientific. Plates were incubated for 48 h, washed and incubated with anti-mouse IFN- γ biotin antibody for 2 h. Plates were

again washed and incubated with streptavidin-ALP antibody for 1 h following the manufacturer's protocol. Spots were visualized using BCIP/NPT-plus substrate, after which the plates were washed and dried prior to counting with the aid of an ELISpot plate reader.

Cytokine and Chemokine Analysis

A Milliplex MAP Mouse Cytokine Magnetic Bead Panel multiplex assay (Millipore Sigma) was used to detect 26 cytokines, chemokines, and growth factors in mouse tissue homogenates from vaccinated and control mice at 4 days post footpad MAYV_{BeAr} challenge. Cytokines from tissues of AdV-MAYV and AdV-GFP vaccinated mice were analyzed using a R&D Systems mouse magnetic Luminex[®] LXSANSN-26 assay. Briefly, 25 µl of clarified tissue homogenate from ipsilateral and contralateral ankles and quadriceps (N=10 per group), calf (N=8 per group), and naïve mouse calf and ankles (N=4 per tissue). The manufacturer's protocol was followed with minor alterations as previously described [686]. The plate was read on a Luminex 200™ Detection system (Luminex).

Histopathology

At 7 dpi, MAYV-infected mice were sacrificed and perfused with 4% paraformaldehyde in PBS. The lower hind legs were collected, embedded in paraffin, and 5-µm sections were prepared. Mounted sections of ipsilateral and contralateral legs were stained with H&E and evaluated for inflammation and tissue

disease by light microscopy (Olympus VS120 Virtual Slide Microscope). Anatomic pathology specialists blindly scored the presence, distribution and severity of histological lesions, using a scoring system of 0-5: 0 absent (no lesions), 1 minimal (1~10% of tissues affected), 2 mild (11~25% affected), 3 moderate (26~50% affected), 4 marked (51~75% affected), 5 severe (>75% affected). All data were analyzed using GraphPad Prism 8 software.

Statistical analysis

Statistics and graphs were created with GraphPad Prism 8. Normalized variable slope non-linear regression using upper and lower limits of 100 and 0, respectively, was used to calculate neutralizing antibody titers. T tests were used to compare normally distributed pairwise data sets and Mann-Whitney was used for pairwise comparison on non-normally distributed and/or when data points were below the assays limit of detection. ANOVA was used for data sets with three or more groups with normally distributed data and Kruskal-Wallis ANOVA was used for data sets of three or more groups with non-normally distributed and/or data points that were below the assays limit of detection.

Chapter 3.

Adeno-associated Virus (AAV) Assembly-Activating Protein Is Not an Essential Requirement for Capsid Assembly of AAV Serotypes 4, 5, and 11

Lauriel F. Earley¹, John M. Powers², Kei Adachi², Joshua Baumgart², Nancy L. Meyer³, Qing Xie³, Michael S. Chapman³, Hiroyuki Nakai^{2,4}

Departments of Molecular Microbiology & Immunology¹, Molecular and Medical Genetics², and Biochemistry & Molecular Biology³, Oregon Health & Science University School of Medicine, Portland, Oregon 97239; Division of Neuroscience⁴, Oregon National Primate Research Center, Beaverton, Oregon 97006, United States of America.

John Powers conducted cross-complementation transduction studies in figures 3.4, 3.8 and 3.9; analyzed relative molecular weights for table 3.1; performed a portion of the immunofluorescence microscopy for figures 3.3 and table 3.2; and assisted with the production of virus for electron microscopy. Lauriel Earley conducted western blots and ELISA for figure 3.1, AAP sequence alignment, and conducted immunofluorescence microscopy for figure 3.5 and a portion of the immunofluorescence microscopy for figure 3.3 and table 3.2. Lauriel Earley produced and purified virus for infection assay for figure 3.7. Lauriel Earley and Hiroyuki Nakai performed biochemical analysis of AAP in tables 3.3 and 3.4. Kei Adachi purified virus with assistance from John Powers and Lauriel Earley for electron microscopy that was conducted by Qing Xie and Nancy Meyer. Kei Adachi performed barcode sequencing library preparation and analysis for cross-complementation analysis. Plasmids for the experiments were made by John Powers, Lauriel Earley, Joshua Baumgart, and Hiroyuki Nakai. Experimental design was conducted by John Powers, Lauriel Earley, and Hiroyuki Nakai, with Michael Chapman providing assistance and advice.

3.1 Abstract

Adeno-associated virus (AAV) vectors have made great progress in their use for gene therapy; however, fundamental aspects of AAV's capsid assembly remain poorly characterized. In this regard, the discovery of assembly-activating protein (AAP) sheds new light on this crucial part of AAV biology and vector production.

Previous studies have shown that AAP is essential for assembly; however, how its mechanistic roles in assembly might differ among AAV serotypes remains uncharacterized. Here, we show that biological properties of AAPs and capsid assembly processes are surprisingly distinct among the AAV serotypes 1 to 12. In the study, we investigated subcellular localizations and assembly-promoting functions of AAP1 to -12 (i.e., AAPs derived from AAV1 to -12, respectively) and examined the AAP dependence of capsid assembly processes of these 12 serotypes using combinatorial approaches that involved immunofluorescence and transmission electron microscopies, barcode-Seq (i.e., a high-throughput quantitative method using DNA barcodes and a next-generation sequencing technology), and quantitative dot blot assay. This study revealed that AAP1 to -12 are all localized in the nucleus with serotype-specific differential patterns of nucleolar association; AAPs and assembled capsids do not necessarily colocalize; AAPs are promiscuous in promoting capsid assembly of other serotypes, with the exception of AAP4, -5, -11, and -12; assembled AAV5, -8, and -9 capsids are excluded from the nucleolus, in contrast to the nucleolar enrichment of assembled AAV2 capsids; and, surprisingly, AAV4, -5, and -11 capsids are not dependent on AAP for assembly. These observations highlight the serotype-dependent heterogeneity of the capsid assembly process and challenge the current notions about the role of AAP and the nucleolus in capsid assembly.

Importance

Assembly-activating protein (AAP) is a recently discovered adeno-associated virus (AAV) protein that promotes capsid assembly and provides new opportunities for research in assembly. Previous studies on AAV serotype 2 (AAV2) showed that assembly takes place in the nucleolus and is dependent on AAP and that capsids colocalize with AAP in the nucleolus during the assembly process. However, through the investigation of 12 different AAV serotypes (AAV1 to -12), we find that AAP is not an essential requirement for capsid assembly of AAV4, -5, and -11, and AAP, assembled capsids, and the nucleolus do not colocalize for all the serotypes. In addition, we find that there are both serotype-restricted and serotype-promiscuous AAPs in their assembly roles. These findings challenge widely held beliefs about the importance of the nucleolus and AAP in AAV assembly and show the heterogeneous nature of the assembly process within the AAV family.

3.2 Introduction

Capsid assembly of icosahedral viruses has been an important area of research with an impact on multiple fields. Foremost is the basic biology behind how pathogenic viral proteins hijack the host cell to aid in their assembly and how viral capsid proteins fit together with the ultimate end of devising antiviral therapies [791]. While there are a multitude of morphologies that viruses can have, icosahedral symmetry is found broadly in perhaps half of the known viral families [792]. A model icosahedral virus with $T = 1$ symmetry is adeno-associated virus (AAV), a parvovirus that belongs to the genus *Dependoparvovirus* of the family *Parvoviridae* [73]. AAV has recently become a well-regarded vector for *in vivo* gene

therapy with successful clinical trials for hemophilia B, lipoprotein lipase deficiency, and Leber congenital amaurosis, among others (reviewed by Mingozzi and High, [793]), thus making the study of its capsid assembly an attractive pursuit both for gene therapy applications and for furthering our knowledge of parvovirus biology [481, 793-796].

AAV is a small, nonenveloped virus with a single-stranded DNA genome of 4.7 kb containing two genes, *rep* and *cap*, between two inverted terminal repeats. The *rep* gene produces nonstructural Rep proteins essential for viral genome replication and packaging. The *cap* gene produces the three structural proteins VP1, VP2, and VP3, translated from different start codons in a single open reading frame (ORF). Alternative mRNA splicing and the combined use of an ATG codon and an alternative start codon for the initiation of VP protein translation lead to appropriate capsid stoichiometry at a VP1/VP2/VP3 ratio of approximately 1:1:10 [193, 797]. It was long believed that the AAV genome encodes only the Rep and VP proteins, until 2010, when a second +1-frameshifted open reading frame (ORF) that encodes a 204-amino-acid-long nonstructural protein was identified within the *cap* gene of AAV serotype 2 (AAV2) [197]. This new AAV protein has been named assembly-activating protein (AAP), after the role that it plays in capsid assembly [197].

The AAP ORFs have been found in all parvoviruses that belong to the genus *Dependoparvovirus*, and among them, AAP derived from AAV2 (i.e., AAP2) has been the main focus of the studies to date [197, 201]. AAP2 is a nucleolus-

localizing protein essential for AAV2 capsid assembly [197, 202]. When the AAV2 VP proteins are expressed in cultured cells in the absence of AAP, the VP proteins can be found in both the cytoplasm and the nucleus but are excluded from the nucleolus, and there is no detectable capsid assembly [197, 202]. When the AAV2 VP proteins and AAP2 are coexpressed in cells, the VP proteins translocate to and accumulate in the nucleolus together with AAP2 and assemble into capsids [197, 202]. AAP2 can form high-molecular-weight oligomers and change the conformation of a wide range of VP protein oligomer intermediates, leading to the formation of capsid-specific antibody-positive oligomers before the capsids are fully assembled [200]. This, together with the demonstration of AAP2-AAV2 VP3 interactions through hydrophobic regions, may suggest that AAP functions as a scaffolding protein in the capsid assembly reaction as well as a transporter, targeting VP proteins to the nucleolus for assembly [200, 798]. As for the role of AAPs derived from other AAV serotypes, Sonntag et al. demonstrated that AAP is essential for AAV1, -8, and -9 assembly by showing that the expression of VP3 alone does not yield capsids but that assembly can be restored by the coexpression of heterologous AAP2 [201]. They also showed that such a cross-complementation of capsid assembly with heterologous AAP2 does not easily extend to AAV5, one of the most divergent serotypes [201]. In addition, those researchers found that AAP1, -2, and -5 protein expression levels could be significantly affected by the nature of the coexpressed homologous and heterologous VP proteins [201]. While these findings are intriguing, a number of

questions remain about the roles of AAP in capsid assembly and elsewhere in the life cycle.

In this study, to further understand the roles of AAPs in AAV capsid assembly, we comprehensively characterized AAPs derived from AAV1 to -12 (AAP1 to -12, respectively). To this end, we investigated the subcellular localizations of AAP1 to -12 and their assembly-promoting abilities for homologous and heterologous AAV VP3 proteins derived from all 12 serotypes by immunofluorescence microscopy, a comprehensive AAP-VP3 cross-complementation assay, and transmission electron microscopy (TEM). These analyses revealed AAP's various capabilities for nucleolar enrichment and heterologous capsid assembly among the serotypes and serotype-dependent differences in the sites of capsid assembly inside the nucleus. The most striking finding was that VP proteins derived from AAV4, -5, and -11 could assemble without requiring AAP, in contrast to the VP proteins from the other nine serotypes, which required AAP for assembly. A recombinant AAV5 vector, produced in the absence of AAP, was found to be infectious and capable of transducing cells, indicating that AAP is not a necessary component for the production of infectious virions for some AAV serotypes.

3.3 Results

Successful expression of AAP1 to -12 in cultured cells

Initial work by Sonntag *et al.* found that the expression level of AAP in transfected cells depended on the serotype and was especially low for AAP5. In an effort to try and increase AAP production in our transfections, we used the 750-bp

cytomegalovirus immediate early (CMV-IE) enhancer-promoter fused with the 132-bp intervening sequence (IVS) that is known to enhance the stability of mRNA to drive the expression of FLAG-tagged codon-optimized AAP2 [799]. We also changed the native non-ATG start codon to the strong ATG start codon. Previously, we found that this expression plasmid construction led to strong steady-state levels of AAP2 [202]. Prompted by this observation, we constructed a panel of FLAG-tagged AAP expression plasmids for the AAPs from AAV1 to -12, pCMV3-FLAGcmAAPx (where x is 1 to 12), using the same plasmid backbone. All the AAPs were readily detected by Western blot analysis of plasmid-transfected human embryonic kidney 293 (HEK 293) cells in the absence of coexpressed VP proteins, with each AAP showing primarily a discrete single band, except for AAP8, -9, and -10, which had faint secondary bands (**Figure 3.1**). Interestingly, the molecular masses of FLAG-tagged AAPs that were experimentally determined by Western blot analysis were higher than the theoretical molecular masses by 14% to 63%, with AAP4 showing the largest discrepancy (**Table 3.1**). An increase of the molecular masses by the addition of a FLAG tag, which is only 1 kDa, does not account for this discrepancy. Such a discrepancy was previously observed for AAP5 [201]. The slower-than-expected migration might be due simply to differences in amino acid sequences, although the possibility of posttranslational modification has not been ruled out.

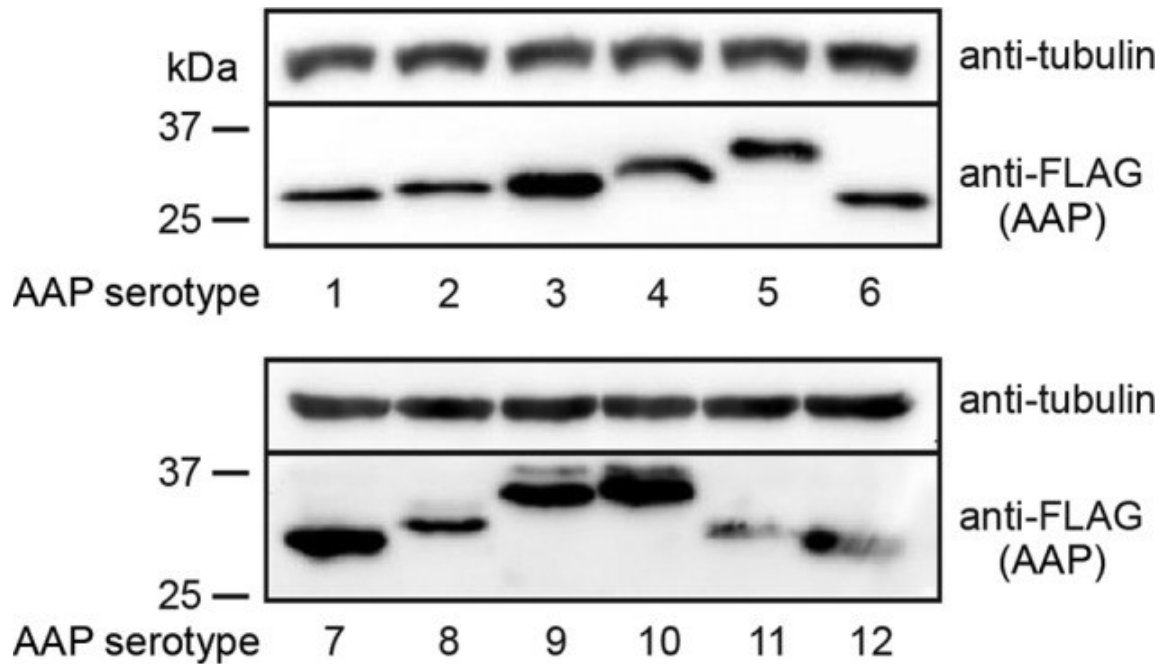


Figure 3.1 Expression of AAP1 to -12 in HEK 293 Cells

HEK 293 cells were transiently transfected with a plasmid expressing the respective FLAG-tagged AAPs indicated below each panel, and AAP expression in transfected cells was analyzed by Western blotting using anti-FLAG antibody. α -Tubulin was used as a loading control. Molecular mass markers (kilodaltons) are shown at the left.

Table 3.1 Theoretically and Experimentally Determined Molecular Masses of FLAG-Tagged AAPs

AAP	Theoretical molecular mass (kDa)	Mean experimentally determined molecular mass (kDa) \pm SD^a	% difference between theoretical and experimentally determined molecular masses^b
1	22	27.3 \pm 1.7	24
2	24	27.3 \pm 1.6	14
3B	23	28.5 \pm 1.2	24
4	19	31.0 \pm 1.1	63
5	22	33.2 \pm 0.9	51
6	22	27.3 \pm 1.3	24
7	22	27.8 \pm 1.7	26
8	22	30.4 \pm 1.5	38
9	22	33.7 \pm 0.7	53
10	22	34.4 \pm 0.7	56
11	20	29.7 \pm 0.6	48
12	20	28.6 \pm 0.7	43

(a) The molecular mass of each FLAG-tagged AAP was determined by Western blot analysis in four biological replicate experiments.

(b) Percent increase of the molecular mass as determined by Western blot analysis compared to the theoretical molecular mass.

AAPs show various subnuclear localizations

Our previous work on identifying amino acids involved in AAP2 nuclear and nucleolar localization identified five clusters of basic amino acids (AAP2 basic region 1 [BR1] to AAP2 BR5) near its C-terminus that contained overlapping

nuclear and nucleolar localization signals (NLS-NoLS) [202]. While these regions are generally well conserved among the AAPs of different AAV serotypes (AAP BR1 to AAP BR5) (**Figure 3.2**), certain AAPs lack some or nearly all of the lysine and arginine residues found in their corresponding protein sequences (**Figure 3.2**). For instance, AAP5 has more proline residues and fewer basic residues than does AAP2 in these regions, leading us to hypothesize that AAP5 might be excluded from the nucleolus, as discussed in our previous publication [202]. To test this hypothesis and determine the subcellular localization of AAP1 to -12, HeLa cells were transiently transfected with each FLAG-tagged AAP-expressing pCMV3-FLAG-cmAAPx plasmid (where x is 1 to 12) individually, and localization was determined 48 h later by using an anti-FLAG antibody. To assess statistically the degree of nucleolar association of AAP1 to -12, we counted 50 nuclei with the anti-FLAG antibody signal and categorized the nuclear staining patterns into the following two groups: “No+,” showing nucleolar association, and “No-,” showing decreased or no nucleolar association. All of the AAPs were found in the nucleus, but their nucleolar localization varied by serotype (**Figure 3.3**). AAP5 and AAP9, which have the least basic charge between BR1 and BR5, exhibited a substantially decreased nucleolar association compared to those of the other 10 serotypes (adjusted P value of 0.001 for all possible pairwise comparisons by using Fisher’s exact test) (**Tables 3.2 – 3.4**). The other 10 AAPs showed unambiguous nucleolar localization to various degrees (**Figure 3.3**). In a random model in which only two AAPs show a distinctively decreased nucleolar association among a total of 12 AAPs, the probability that the 2 AAPs showing the lowest pI values are also the 2

AAPs that exhibit a distinctively decreased nucleolar association is 0.015. This indicates a strong correlation between low pI values and decreased nucleolar association. There is another basic amino-acid rich region further down toward the C-terminus (AAP BR6); however, such a strong relationship between low pI and decreased nucleolar association was not observed in the larger segment containing AAP BR6 (**Table 3.4**). Therefore, the amino acid stretch containing only AAP BR1 to AAP BR5 is the most likely determinant of nucleolar localization. These results demonstrate that, while all 12 AAPs are localized to the nucleus, the strong nucleolar association observed for AAP2 is not a general characteristic of AAPs and that AAPs with lower pI values in the well-conserved basic amino-acid-rich region near the C-terminus show decreased nucleolar association.

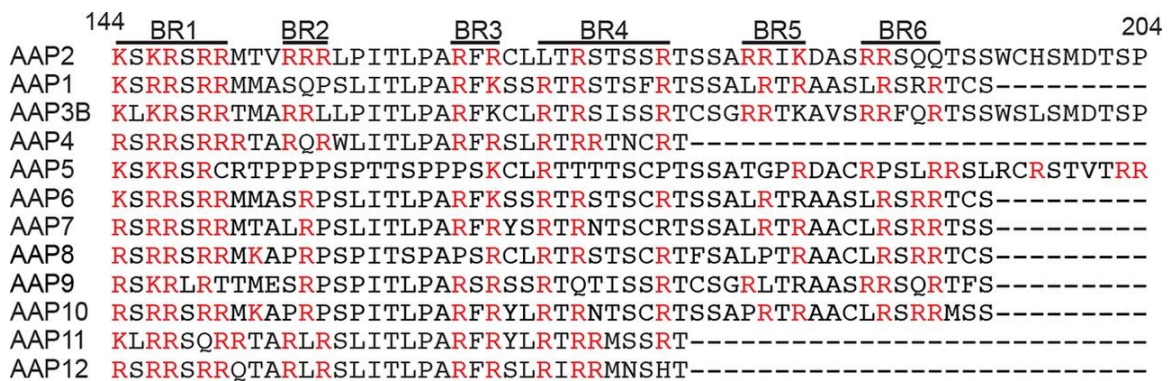


Figure 3.2 Sequence alignment of the C-termini of AAP1 to -12
Sequences of the basic amino-acid-rich C-termini of AAP1 to -12 are aligned. The basic amino-acid-rich regions BR1 to BR6 are indicated with overlines. Positively charged lysine (K) and arginine (R) residues are indicated with red letters. These 6 BRs are defined arbitrarily based on sequence alignment data. BR1 to BR5 were previously identified as the NLS-NoLS in the context of AAP2.

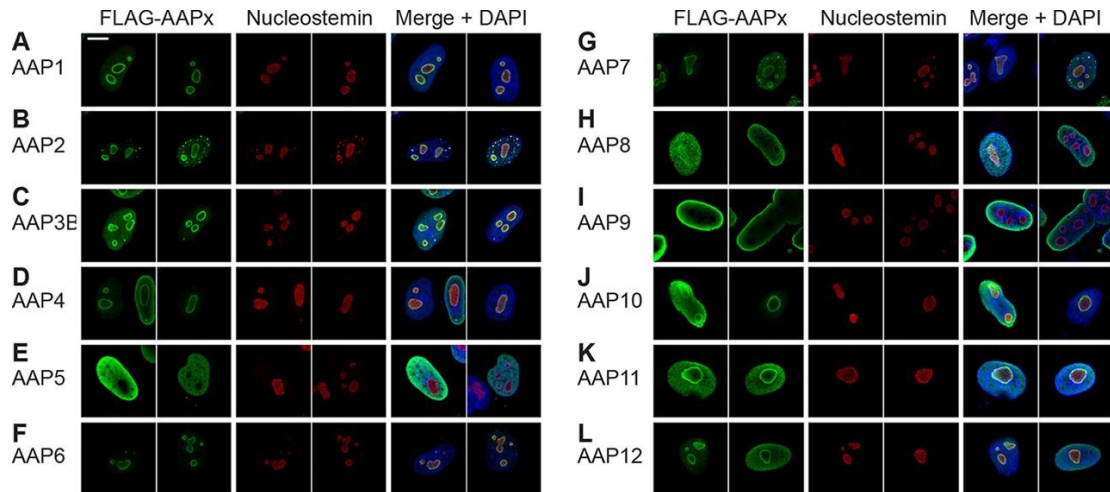


Figure 3.3 Intracellular Localization of AAP1 to -12

HeLa cells were transiently transfected with a plasmid expressing the respective FLAG-tagged AAPs indicated in each panel. The cells were fixed at 48 h posttransfection, immunostained with anti-FLAG antibody (green) and antinucleostemin antibody (red), and counterstained with DAPI (blue) before being imaged on a Zeiss LSM 710 confocal microscope with a 100×/1.46-NA objective. Two representative fields of view are shown for each AAP. (A) AAP1; (B) AAP2; (C) AAP3B; (D) AAP4; (E) AAP5; (F) AAP6; (G) AAP7; (H) AAP8; (I) AAP9; (J) AAP10; (K) AAP11; (L) AAP12. All AAPs are enriched in the nucleus. AAP5 and -9 show a pattern of decreased nucleolar association, while nucleolar signals are observed with other AAPs to various degrees. Note that the ring-shaped anti-FLAG antibody staining pattern with a central hollow (A to D, F, G, and J to L) is most likely a staining artifact caused by the overexpression of a nucleolus-localizing protein and does not necessarily indicate that nucleolar expression is enriched in the nucleolar periphery [202].

Table 3.2 Nucleolar Association of AAPs

AAP ^a	% No ^{+b} (no. of nuclei counted)
AAP5	36 (50)
AAP9	46 (50)
AAP6	88 (50)
AAP1	96 (50)
AAP7	96 (50)
AAP10	96 (50)
AAP2	98 (50)
AAP3B	100 (50)
AAP4	100 (50)
AAP8	100 (50)
AAP11	100 (50)
AAP12	100 (50)

(a) The order of AAPs is sorted by the No⁺ percentage. (b) % No⁺ is the percentage of the nuclei showing a nucleolar association of AAP among the total nuclei counted that were stained with the anti-FLAG antibody (for detection of FLAG-tagged AAP).

Table 3.3 Biochemical Properties of AAP BR1 to BR5

AAP ^a	No. of residues ^b		pI
	H, K, or R	D or E	
AAP5	8	0	11.45
AAP9	11	1	12.37
AAP3B	15	0	12.43
AAP8	12	0	12.43
AAP7	13	0	12.52
AAP10	14	0	12.52
AAP6	13	0	12.65
AAP2	15	0	12.70
AAP11	13	0	12.70
AAP4	14	0	12.78
AAP1	12	0	12.96
AAP12	13	0	13.04

Table 3.4 Biochemical Properties of AAP BR1 to BR6 Toward the C-Terminus

AAP ^a	No. of residues ^b		pI
	H, K, or R	D or E	
AAP5	15	1	11.86
AAP2	18	2	12.26
AAP8	15	0	12.26
AAP3B	18	1	12.40
AAP7	16	0	12.48
AAP10	17	0	12.48
AAP9	14	1	12.52
AAP6	16	0	12.57
AAP11	13	0	12.70
AAP1	15	0	12.74
AAP4	14	0	12.78
AAP12	13	0	13.04

(a) The order of AAPs is sorted by pI (lowest to highest). pI values were determined by using BioPerl pI Calculator.]

(b) D, aspartic acid; E, glutamic acid; H, histidine; K, lysine; R, arginine.

Investigation of assembly of capsids of various serotypes without AAP

It is well established that AAV2 capsid assembly requires AAP [197, 202]. As for other serotypes, Sonntag *et al.* previously reported that AAV1, -5, -8, and -9 capsid

assembly also requires AAP [201]. To reproduce the observations by Sonntag *et al.* and investigate AAP-independent assembly for other serotypes, we expressed AAV1 to -12 VP3 proteins from pCMV1-AAVxVP3 plasmids (where x is 1 to 12) in HEK 293 cells in the presence or absence of cognate AAP expressed from a separate plasmid. In this transfection system, we also provided the components necessary for the packaging of recombinant AAV genomes encoding enhanced green fluorescent protein (eGFP) into assembled capsids. We then quantified packaged viral genomes as surrogates of assembly by quantitative dot blotting in an experiment performed in biological duplicates. In the presence of AAP, all serotypes showed assembled capsids at readily detectable levels, as expected (**Figure 3.4**). Surprisingly, in the absence of AAP, the signals from AAV4, -5, and -11 were clearly beyond the background level, in contrast to the other serotypes (**Figure 3.4**). This result strongly indicates that AAV4, -5, and -11 could assemble without AAP. As for the other serotypes, signals were below the lowest standard signal and near or below the background signal. This indicates that capsid assembly of the other serotypes did not occur or was significantly impaired.

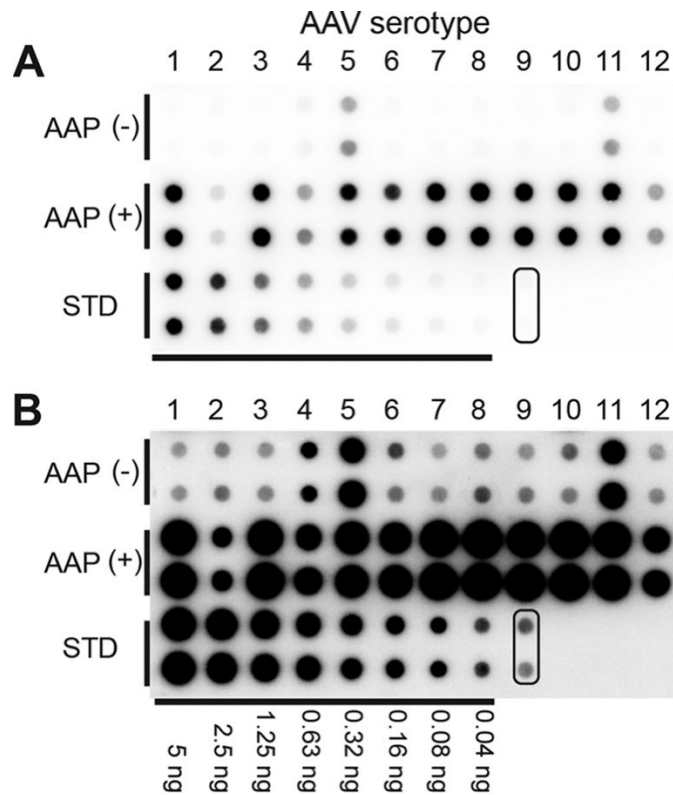


Figure 3.4 Quantitative Dot Blot Assay to Determine Titers of VP3 Capsids Produced in the Presence or Absence of AAP

(A) AAP-independent assembly of VP3 proteins of AAV1 to -12 assessed by a quantitative dot blot assay in an experiment performed in biological duplicates. VP3-only particles derived from AAV1 to -12 that contained a double-stranded AAV-CMV-GFP genome were produced in 6-well plates in the presence or absence of their cognate AAPs. Benzonase-resistant DNA was recovered from 7% of the samples obtained from each well, blotted onto a nylon membrane together with standards (STD) (i.e., linearized pEMBL-CMV-GFP plasmid), and probed with a ^{32}P -labeled GFP probe. Pairs of dots in each combination represent the results obtained from two separate transfections. The pair of dots indicated with a rounded rectangle are negative controls. (B) Same blot as the one shown in panel A. The signals were intensified equally across the entire image by using ImageJ.

AAV5 VP3 can assemble capsids without AAP

To examine potential AAP-independent assembly further, we chose to study AAV5 in depth because there are commercially available reagents for this serotype that allow verification of capsid assembly on multiple levels and because, contrary to

our experience, AAV5 assembly was previously reported to require cognate AAP5 [201]. In all the experiments described above, the VP3 plasmids used still retained the C-terminal 80% of the AAP ORFs. Without its start codon, AAP should not be expressed, but it was important to rule out any possibility that an unidentified cryptic start codon could have provided a functional phenotype through the expression of N-terminally truncated AAP5. To exclude this possibility, we created plasmids carrying codon-modified AAV2 (cmAAV2) and cmAAV5 VP3 ORFs (pCMV1-AAV2cmVP3 and pCMV1-AAV5cmVP3, respectively) and used them in subsequent experiments. These mutated AAP ORFs within the cmVP3 ORFs should not express any peptides that exhibit the capsid assembly-promoting function at detectable levels (see Discussion). To verify that the AAV5 cmVP3 proteins could also assemble capsids without AAP, we transiently transfected HeLa cells with pCMV1AAV2cmVP3 or pCMV1-AAV5cmVP3 together with either the cognate AAP-expressing plasmid (pCMV3-FLAG-cmAAP2 or pCMV3-FLAG-cmAAP5) or pCMV3-GFP, a GFP-expressing control plasmid devoid of AAP expression. Forty-eight hours after transfection, the cells were stained with anti-FLAG and anti-AAV capsid antibodies (A20 to detect assembled AAV2 VP3 capsids and ADK5a to detect assembled AAV5 VP3 capsids). As previously shown, AAV2 VP3 was able to assemble capsids only when AAP2 was supplied in trans (**Figure 3.5A**)[197]. In contrast, AAV5 VP3 was able to produce capsid antibody-positive staining regardless of the presence or absence of AAP5 (**Figure 3.5A**). The ADK5a antibody is an anti-AAV5 antibody that should be specific for only intact AAV5 capsids and not monomers or oligomers of AAV5 VP proteins

[800]. Thus, positive staining with ADK5a strongly indicates that AAV5 VP3 can assemble into capsids without a need for AAP. The same approach was used to investigate capsid assembly for AAV8 VP3 and AAV9 VP3 in the presence or absence of the cognate AAP. For this analysis, we used pCMV1-AAV8VP3 or pCMV1-AAV9VP3 together with the cognate AAP-expressing plasmids. Assembled capsid-specific signals were readily detected in cells expressing AAP; however, none of the cells had assembled AAV8 or AAV9 VP3 capsid signals in the absence of AAP expression (**Figure 3.5A**). These observations complement the dot blot results and strongly support that capsid assembly requires AAP for the AAV2, AAV8, and AAV9 VP3 proteins.

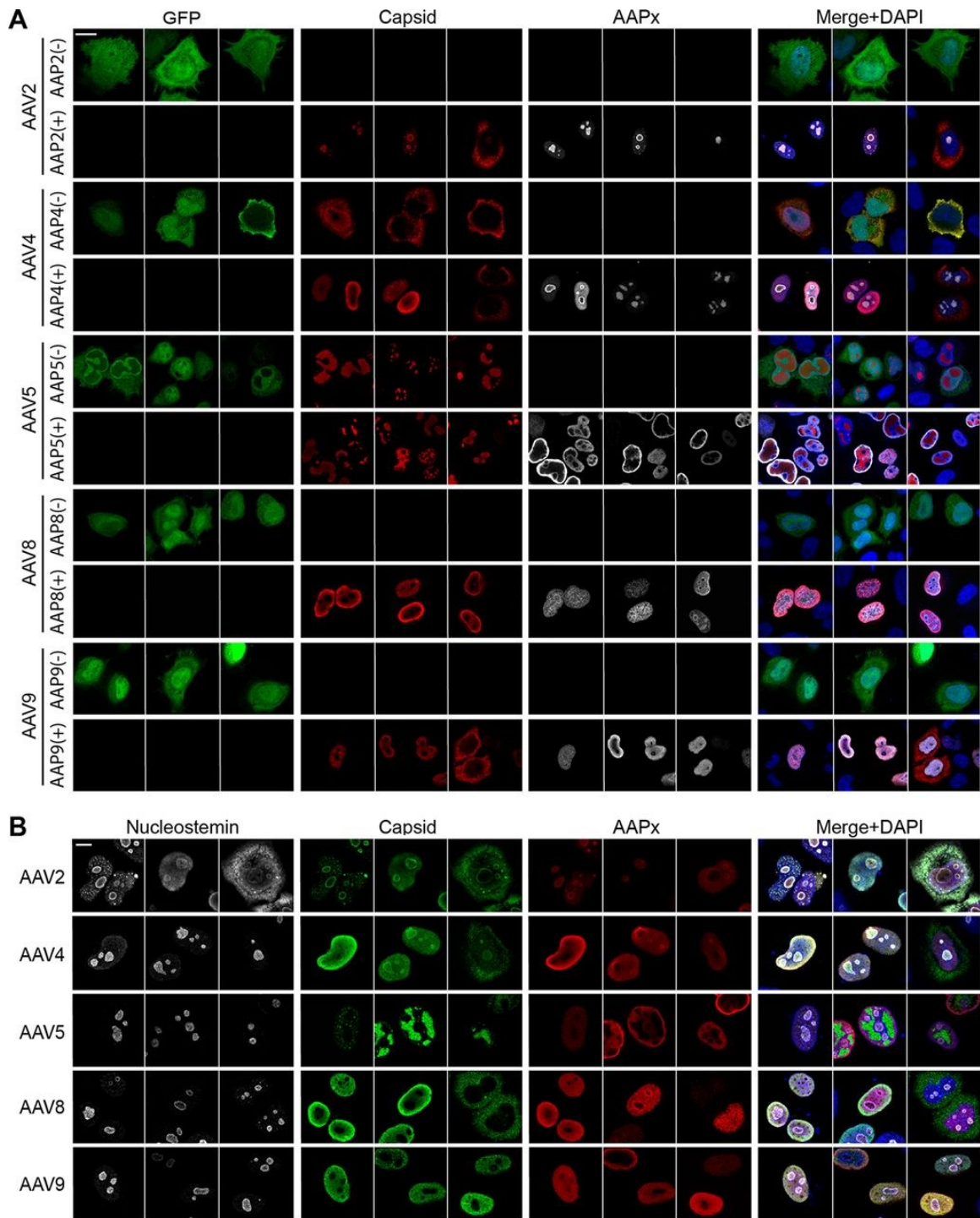


Figure 3.5 Capsid Assembly of AAV2, -4, -5, -8, and -9 in HeLa cells

HeLa cells were transiently transfected with plasmids expressing VP3 proteins derived from AAV2, -4, -5, -8, or -9 in the presence (+) or absence (-) of a cotransfected plasmid expressing their cognate AAP. The groups that received no AAP-expressing plasmid were transfected with pCMV3-

GFP instead to ensure successful transfection and maintain the total quantity of transfected DNA constant across the groups. The cells were fixed at 48 h posttransfection, immunostained with the antibodies indicated in each panel, and counterstained with DAPI. The images were obtained by using a Zeiss LSM 710 confocal microscope with a 63×/1.4-NA objective. Three representative fields of view are shown for each condition. (A) Cells were stained with anti-AAV capsid antibody (A20 for AAV2, ADK4 for AAV4, ADK5a for AAV5, ADK8 for AAV8, and ADK8/9 for AAV9) (red) and anti-FLAG antibody (white). (B) Cells were stained with antinucleostemin antibody (white), anti-AAV capsid antibodies (green), and anti-FLAG antibody (red). Bar, 10 μ m.

Finally, TEM was used to visualize directly the assembly (or not) of the AAV5 “VP3-only” capsid in the presence or absence of AAP5. HEK 293 cells were transfected by using either plasmid pCMV1-AAV2cmVP3, with or without pCMV3-FLAG-cmAAP2, or pCMV1-AAV5cmVP3, with or without pCMV3-FLAG-cmAAP5. At 5 days posttransfection, the medium and cells were harvested and subjected to three rounds of purification by cesium chloride (CsCl) density gradient ultracentrifugation to prepare samples for TEM. In the final round, a discrete band was found at refractive indices (RIs) of 1.3640 to 1.3645, except for AAV2 VP3 without AAP2 (**Figure 3.6A** and **D**). After fractions were collected, an enzyme-linked immunosorbent assay (ELISA) specific for intact capsids was performed on each fraction to confirm the presence of assembled AAV2 or AAV5. Assembled AAV2 capsids were not detected in the absence of AAP2 but were present when AAP2 was coexpressed (**Figure 3.6B**), consistent with the observed CsCl banding and results of immunofluorescence microscopy. AAV5 capsids were detected in samples of both AAV5 VP3 without AAP5 and AAV5 VP3 with AAP5 by an ELISA (**Figure 3.6E**). An analysis of TEM images of the fractions showing high ELISA optical density (OD) values confirmed the presence of assembled capsids, while the sample of AAV2 VP3 without AAP2 with the corresponding RI (1.3640) did not

contain any capsids (**Figure 3.6C** and **F**). AAV5 VP3 capsids produced in the absence of coexpressed AAP5 were morphologically indistinguishable from those produced in the presence of AAP5 (**Figure 3.6F**). Thus, we concluded that the AAV5 VP3 proteins are capable of forming capsids in the absence of AAP.

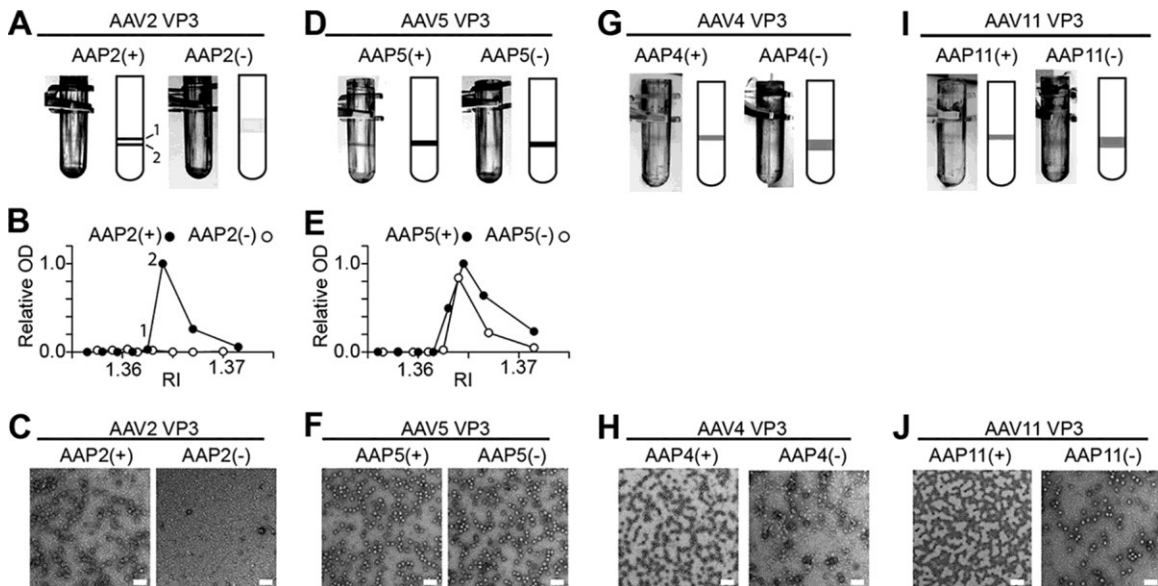


Figure 3.6 Transmission Electron Microscopy of AAV VP3-Only Capsids Produced With or Without AAP

HEK 293 cells were transfected with plasmids expressing VP3 proteins and AAP proteins as indicated. At 5 days posttransfection, capsids were purified by three rounds of CsCl density gradient ultracentrifugation. (**A**, **D**, **G**, and **I**) Negative-image photos and accompanying cartoons showing bands formed after the third CsCl ultracentrifugation. AAV2 VP3 with AAP2 [AAP2(+)] contained two bands at RIs of 1.3630 and 1.3645. The following ELISA indicated that the heavier of the two bands contained more capsids, and this was the band used for TEM imaging. (**B** and **E**) Assembled AAV capsids positive for anti-AAV capsid antibody in each CsCl fraction were assessed by an AAV capsid-specific ELISA. Relative optical density (OD) values at 450 nm are plotted against RIs of CsCl fractions. The OD at 450 nm obtained in the peak fraction was set to 1.0. (**C**, **F**, **H**, and **J**) Representative TEM images of samples prepared with or without AAP. The CsCl fractions showing RIs of 1.3645, 1.3640, 1.3645, 1.3640, 1.3635, 1.3640, 1.3635, and 1.3640 were used for TEM imaging of samples of AAV2 VP3 with and without AAP2 [AAP2(+)] and AAP2(-), respectively], AAV5 VP3 with and without AAP5 [AAP5(+)] and AAP5(-), respectively], AAV4 VP3 with and without AAP4 [AAP4(+)] and AAP4(-), respectively], and AAV11 VP3 with and without AAP11 [AAP11(+)] and AAP11(-), respectively]. Bar, 100 nm. (**A** to **C**) AAV2; (**D** to **F**) AAV5; (**G** and **H**) AAV4; (**I** and **J**) AAV11.

Infectious AAV5 virions can be produced without AAP

While AAV capsids can be composed entirely of VP3, VP1 is required for viral infectivity and cell transduction [223, 801, 802]. Having established that AAV5 VP3 could assemble capsids in the absence of coexpressed AAP, we sought to determine if infectious AAV5 virions could be produced by expressing all of the AAV5 VP proteins, VP1, VP2, and VP3, without supplying the AAP5 protein. To this end, we utilized two types of AAV5 helper plasmids, pHLPAAV5(AAP5) and pHLP-AAV5(AAP5). The pHLP-AAV5(AAP5) plasmid is our standard AAV5 helper plasmid for vector production that expresses AAV2 Rep and the AAV5 VP1, VP2, VP3, and AAP5 proteins. pHLP-AAV5(AAP5) expresses all the AAV proteins except AAP5 due to extensive codon modification of the AAP-VP-overlapping ORFs (**Figure 3.7A**). Western blot analysis of the cell lysates obtained from HEK 293 cells transfected with pHLP-AAV5(AAP5) or pHLP-AAV5(AAP5) with or without pCMV3-FLAGcmAAP5 showed that the AAV5 VP3 protein was detectable in small amounts when AAP5 was not expressed and that the steady-state level of expression of AAV5 VP proteins could be increased substantially when AAP5 was coexpressed (**Figure 3.7B**). Using the adenovirus-free plasmid transfection method with pHLP-AAV5(AAP5), we successfully produced AAV5 vectors containing a recombinant AAV vector genome in the absence of AAP5 expression, although the vector yield was an order of magnitude lower than the yields that could be obtained when AAP5 was expressed (**Figure 3.7C**)[425].

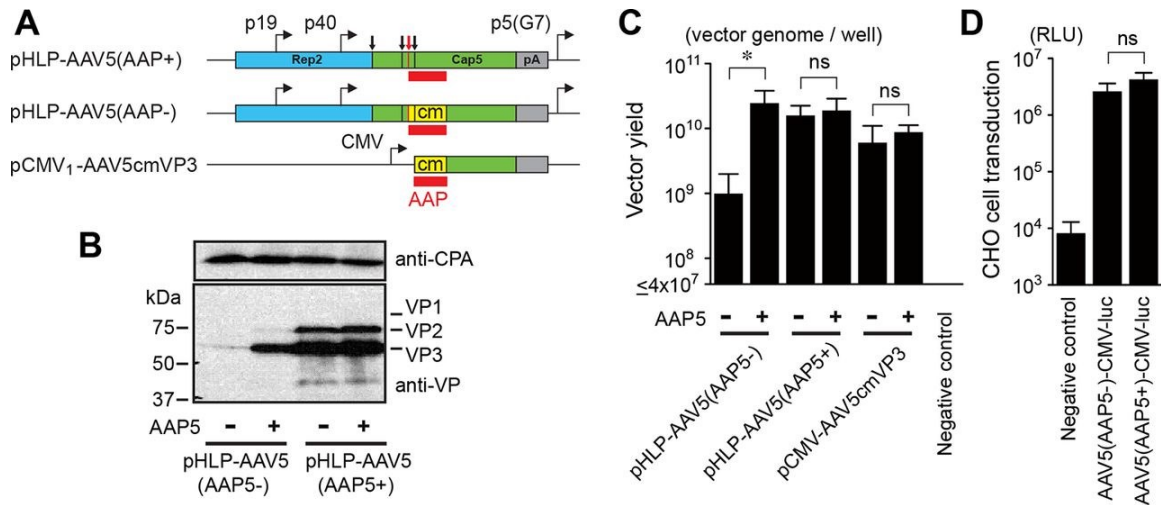


Figure 3.7 Production and Characterization of AAV5 VP1/VP2/VP3 Particles Produced With and Without AAP5

(A) Schematic representation of plasmids expressing AAV5 VP proteins. These plasmids were used for the experiments shown in panels B – D. The VP1, VP2, and VP3 translation start sites are indicated with black vertical lines and arrows from left to right. The AAP translation start site is indicated with red vertical lines and a red arrow. The AAP ORF is shown with red boxes. The codon-modified region is indicated with yellow boxes. pA, polyadenylation signal; p5(G7), AAV2 p5 promoter with the TATA box sequence TATTTAA replaced with GGGGGG. (B) HEK 293 cells were transiently transfected with an AAV5 helper plasmid, pHLP-AAV5(AAP5+) or pHLP-AAV5(AAP5-), with or without a plasmid expressing AAP5. All the groups were also transfected with an adenovirus helper plasmid, pHelper, to induce protein expression from the AAV5 helper plasmids. At 48 h posttransfection, the AAV5 VP1, VP2, and VP3 proteins were probed with anti-AAV VP antibody (B1) by Western blotting. Cyclophilin A (CPA) was used as a loading control. (C) HEK 293 cells were transfected with the plasmids indicated to produce AAV5 VP1/VP2/VP3 particles or VP3-only particles containing a double-stranded AAV-CMV-GFP vector genome in the presence or absence of AAP5 expressed from a separate plasmid, pCMV₃-FLAG-cmAAP5. At 5 days posttransfection, the medium and cells were harvested, and Benzonase-resistant viral genomes in each sample were quantified by a dot blot assay in an experiment performed in biological triplicates. The y axis shows the AAV vector titers (vector genomes) per well in a 6-well-plate format. (D) CHO-K1 cells were infected with either the AAV5(AAP5+)-CMV-luc or AAV5(AAP5-)-CMV-luc vector, which was produced with or without AAP5, respectively, at an MOI of 10⁶. Luciferase activity was measured at 46 h postinfection in an experiment performed in biological triplicates. The negative-control group received the luciferase-containing samples prepared in the same manner except for the absence of AAV5 VP protein expression, which provides a measure of pseudotransduction. For the pseudotransduction control, the same sample volume as that for the AAV5(AAP5-)-CMV-luc vector preparation was used. The y axis shows relative light units (RLUs). Error bars represent standard deviations. An asterisk indicates statistical significance with a *P* value of <0.05 (two-tailed Welch's *t* test). ns, not significant.

We then produced two types of recombinant AAV5 vectors expressing firefly luciferase, AAV5(AAP5)-CMV-luc and AAV5(AAP5)-CMV-luc, using pHLP-AAV5(AAP5) and pHLPAAV5(AAP5), respectively, without supplying AAP5 in trans from the pCMV3-FLAGcmAAP5 plasmid. The two vector preparations were added to Chinese hamster ovary K1 (CHO-K1) cells at a multiplicity of infection (MOI) of 106, and luciferase activity was measured at 46 h postinfection in an experiment performed in biological triplicates. The results showed that the AAV5(AAP5)-CMV-luc vector was able to transduce CHO-K1 cells, and there was no statistically significant difference in transduction efficiency between the AAV5(AAP5)-CMV-luc and AAV5(AAP5)-CMV-luc vectors ($P = 0.18$ by two-tailed Welch's t test) (**Figure 3.7D**). Taken together, our data demonstrate that AAV5 does not require AAP5 for the assembly of infectious virions containing a recombinant viral genome.

AAV4 and -11 can assemble capsids without AAP

Having determined that AAV5 was capable of assembling infectious virions in the absence of AAP, we next sought to determine conclusively if AAV4 and AAV11 could also assemble capsids without AAP. AAV4 has a commercially available mouse monoclonal antibody against the assembled AAV4 capsid, ADK4, and thus, we were able to use immunofluorescence microscopy to determine if capsids could be made from AAV4 VP3 without AAP4. However, this approach was not applicable to AAV11 because an antibody specific for the assembled AAV11 capsid is currently not available.

In the immunofluorescence microscopy approach, we transfected HeLa cells with pCMV1-AAV4VP3 and either pCMV3-FLAG-cmAAP4 or pCMV3-GFP. At 48 h posttransfection, the cells were fixed and stained with an anti-FLAG antibody or anti-AAV4 capsid antibody (ADK4). This analysis confirmed that AAV4 VP3 was also able to assemble antibody-positive capsids regardless of whether AAP4 was coexpressed (**Figure 3.5A**). In the TEM approach, we followed the same procedure as the one that we used for the AAV5 TEM experiment described above. In brief, to completely abolish any possible functional AAP expression, we constructed pCMV1-AAV4cmVP3 and pCMV1-AAV11cmVP3, in which the AAP-VP-overlapping ORFs were extensively codon modified compared to the native nucleotide sequences. These mutated AAP ORFs within the cmVP3 ORFs should not retain the AAP function at detectable levels (see Discussion). These two plasmids were used to produce viral capsids in HEK 293 cells in the presence or absence of coexpressed AAP, and the TEM samples were then prepared by three rounds of CsCl density gradient ultracentrifugation. In the final round of ultracentrifugation, a discrete band could be seen in each tube for both AAV4 and AAV11 regardless of the presence or absence of coexpressed AAP (**Figure 3.6G and I**). TEM analysis revealed that these bands contained capsid structures of the expected size and shape for AAV (**Figure 3.6H and J**). These observations provide direct evidence that AAV4 and AAV11 VP3s are capable of assembling capsids without AAP.

Heterologous AAPs efficiently promote capsid assembly, except for AAP4, -5, -11, and -12

The promiscuity of AAPs in assembling capsids of heterologous AAV serotypes was previously shown with combinations of AAPs and AAV VP3 proteins derived from AAV1, -2, -5, -8, and -9 [201]. In that study, Sonntag *et al.* reported that AAP2 could stimulate the assembly of heterologous AAV1, -8, and -9 capsids but not the AAV5 capsid; AAP1 could stimulate AAV2 capsid assembly; and AAP5 could weakly support AAV1 capsid assembly. While the observations obtained from these limited combinations have given us a glimpse of the nature of AAP-VP compatibility in capsid assembly, more expansive investigation of numerous different AAP and VP3 combinations for heterologous capsid assembly is imperative for a deeper understanding of the role of AAP. In order to fill this knowledge gap, we performed an AAP-VP3 cross-complementation study in which we investigated all 121 possible combinations of AAP1 to -11 and the VP3 proteins of AAV1 to -11 in an experiment performed in biological triplicates. Including the no-AAP controls used to determine the background levels for the assay, a total of 396 assessments of capsid formation was required for this comprehensive experiment. For this reason, we applied a massively parallel capsid assembly assay using an Illumina sequencing-based AAV barcode-Seq approach reported previously [803]. In this approach, packaged viral genomes were quantified as surrogates of assembly (see Materials and Methods). A subset of 7 combinations was validated by quantitative dot blotting in an experiment performed in biological

replicates (n = 2 to 4). This validation experiment revealed that the results obtained by these two different methods were primarily concordant (**Figure 3.8**).

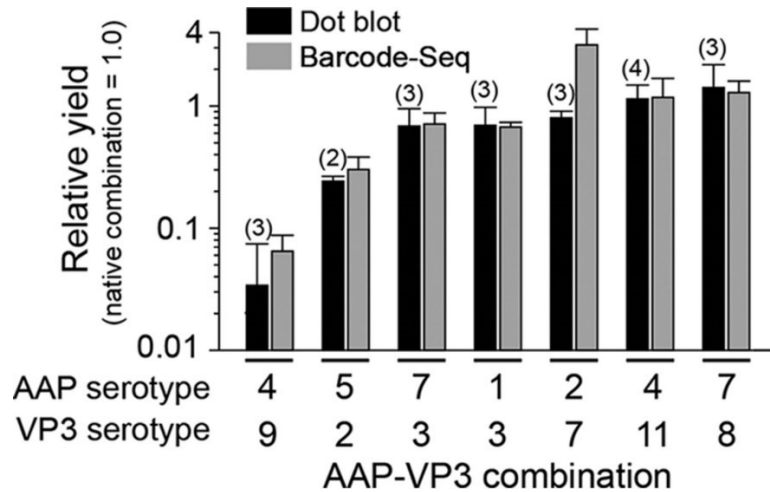


Figure 3.8 AAP-VP3 Cross-Complementation Analysis by a Quantitative Dot Blot Assay

A total of 7 AAP-VP3 combinations were analyzed for cross-complementation of capsid assembly by a quantitative dot blot assay in an experiment performed in biological replicates. The numbers of replicates for each AAP-VP combination are indicated in parentheses. The results were compared to those obtained by AAV barcode-Seq, as shown in **Figure 3.9**. Values represent relative AAV VP3-only particle yields with each AAP-VP combination relative to those obtained with the native AAP-VP3 combination. Error bars represent standard deviations, except for the AAP5-AAV2 VP3 combination. For the AAP5-AAV2 VP3 combination, the error bar represents the difference between each value and the mean value because the data were collected from samples in biological duplicates.

As for AAP12, which was not included in this analysis, we determined the yields by quantitative dot blot analysis. The results showed that AAPs derived from AAV1, -2, -3B, -6, -7, -8, -9, and -10 could promote heterologous serotype capsid assembly at least 30% as efficiently as the native combinations (**Figure 3.9**). As observed in the previous study, AAP5 also weakly supported the assembly of

many heterologous VP3 proteins. AAP4, -11, and -12 were found to be least efficient for heterologous capsid assembly (**Figure 3.9**)[201]. In particular, AAP12 supported assembly efficiently only for AAV11 besides its cognate capsid. AAV12 VP3, which could not assemble without AAP, formed capsids exclusively with AAP4 or AAP11 besides its cognate AAP12 (**Figure 3.9**). The capsid assembly-promoting role of heterologous AAPs was difficult to assess for the AAV4, -5, and -11 VP3 proteins because of the high background signals due to AAP-independent assembly (**Figure 3.9**). Nonetheless, the decreased ability of AAP4, -5, -11, and -12 to promote the assembly of VP3 capsids of heterologous serotypes is congruent with previously reported data showing that AAP4, -5, -11, and -12 were the most phylogenetically dissimilar AAPs compared to the other AAPs derived from AAV1 to -13 [200]. These observations establish that the AAPs promiscuously promote the efficient assembly of capsids among wide groups of closely related serotypes but that promiscuity does not extend to more distantly related serotypes such as AAV4, -5, -11, and -12.

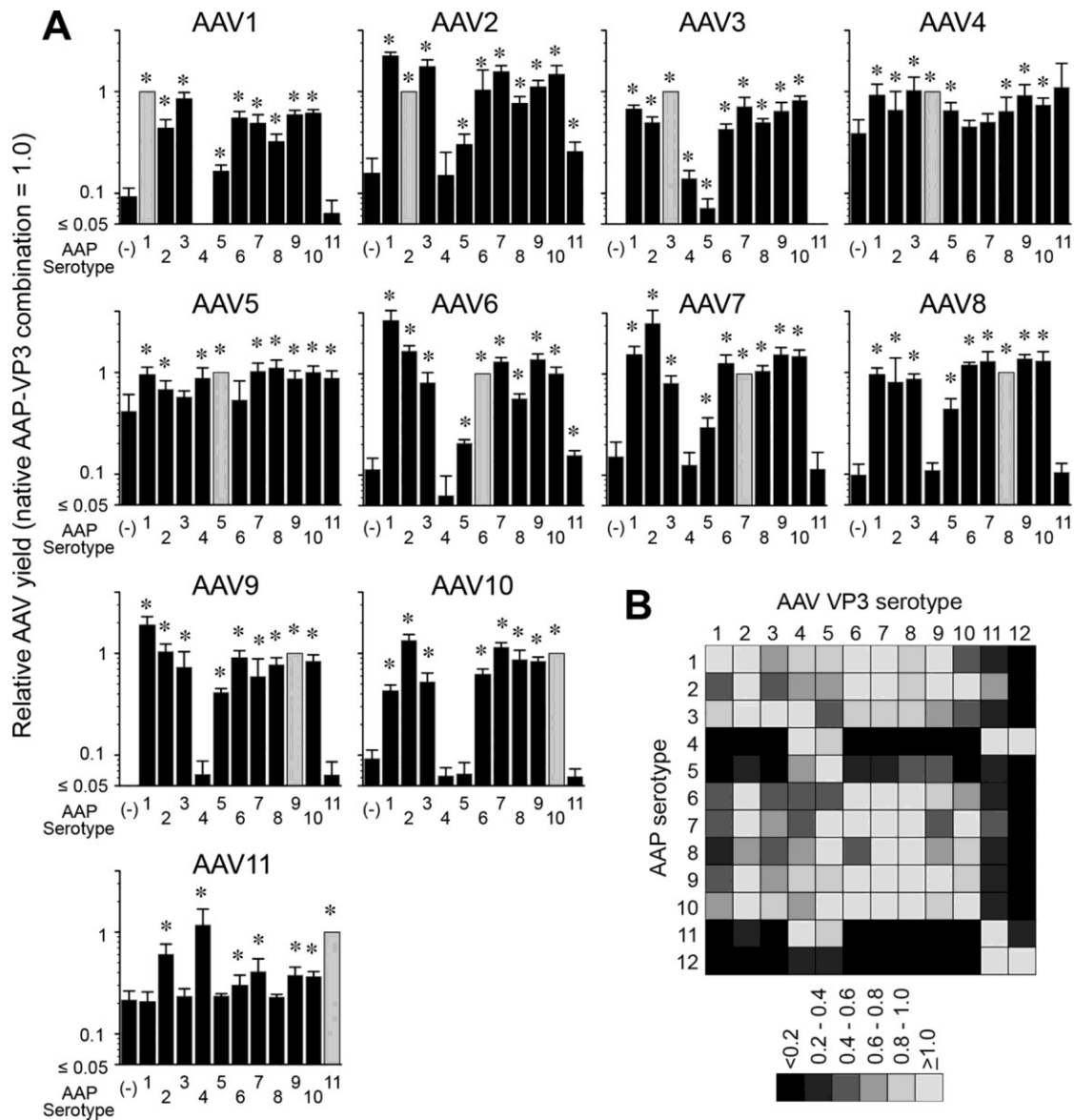


Figure 3.9 AAP-VP3 Cross-Complementation Among 12 Different AAV Serotypes

(A) Data from AAV barcode-Seq analysis showing the ability of each AAP to assemble homologous and heterologous VP3 proteins derived from AAV1 to -11. No-AAP controls are shown as AAP (-) to the left of each panel. The y axis shows AAV VP3-only particle yields in each AAP-VP combination relative to the yields obtained with the native AAP-VP3 combination. The values obtained with the native combination are set as 1.0. The data were collected from an experiment performed in biological triplicates. Error bars represent standard deviations. Asterisks indicate that values are higher than those for the no-AAP controls with a P value of <0.05 (one-tailed Mann-Whitney U test). (B) Matrix heat map showing the ability of each AAP to cross-complement assembly. The data for AAV1 to -11 were obtained from the data shown in panel A. The data for AAV12 were obtained by a quantitative dot blot assay in an experiment performed in biological duplicates. The values obtained by the native combination are set as 1.0.

Concordant and discordant subnuclear localization between AAPs, capsids, and nucleostemin

During microscopic analyses, we observed both concordant and discordant subcellular localization patterns between AAPs, assembled capsids, and nucleostemin. In the case of AAV2, AAP2, assembled AAV2 VP3 capsids, and nucleostemin were tightly associated with each other and localized to the nucleoli and subnuclear bodies (**Figure 3.5B**). AAP, assembled capsids, and nucleostemin were also colocalized in the case of AAV4 (**Figure 3.5B**). In contrast, in the case of AAV5, AAP, assembled capsids, and nucleostemin were localized in different subnuclear compartments (**Figure 3.5B**). The AAV5 VP3 capsid signals formed discrete spheres and globules, while the AAP5 signals were diffuse and different from the AAV5 VP3 capsid localization, and nucleostemin was not associated with these viral elements. AAV8 and AAV9 VP3 capsids also showed no association with nucleostemin (**Figure 3.5B**). These observations demonstrate that the sites of AAP enrichment do not necessarily correspond to the sites of capsid assembly. In addition, our data presented here challenge a long-believed notion that tight association with the nucleolus is a hallmark of AAV capsid assembly. Because assembled capsids for certain serotypes such as AAV5, -8, and -9 are found outside the nucleolus and are not associated with the nucleolar protein nucleostemin, the involvement of the nucleolus and nucleolar proteins seen with AAV2 capsid assembly is not generalizable to all AAV serotypes.

3.4 Discussion

In this study, we comprehensively analyzed AAPs derived from 12 AAV serotypes, AAV1 to -12, for their subcellular localization and their ability to promote the assembly of capsids derived from homologous and heterologous serotypes. For nearly a half-century, AAV2 has been the prototype for studies of the AAV life cycle, including infection, replication, and assembly, and much of what is currently known about AAV comes from experiments with this serotype. Although all the currently known AAV serotypes and variants display significant similarity to each other in their viral protein amino acid sequences and virion structures, studies of AAVs as gene delivery vectors for the last 2 decades have delineated that there are substantial differences in their biological properties, including cell and tissue tropisms [804]. This has raised the possibility that certain aspects of fundamental AAV biology are also diverse among different serotypes, and what we had learned from the prototype AAV2 might not be applicable to the basic biology of the entire AAV family, including the process of capsid assembly. In this regard, the study reported here has clearly demonstrated that (i) AAP, which had been believed to be essential for capsid assembly based on observations obtained with AAV2, -8, and -9, is not necessarily essential for capsid assembly for other serotypes; (ii) a tight association between AAP and assembled capsids in the nucleolus during or after assembly, which has been shown for AAV2, is not always the case for other serotypes; and (iii) targeting to the nucleolus, which serves as an indispensable organelle for many viruses, including AAV2, may not be required for certain AAV serotypes [197, 201, 226, 227, 798, 805-808]. To be more concrete, we

demonstrated here the dispensability of AAP for the assembly of AAV4, -5, and -11 capsids and for the production of infectious virions, at least for AAV5; serotype-specific concordant (in the cases of AAV2, -4, -8, and -9) and discordant (in the case of AAV5) associations between AAP and assembled capsids; and nucleolar exclusion of assembled AAV5, -8, and -9 capsids as opposed to the tight nucleolar association observed for AAV2 capsids.

The structural organization of AAP has been partially revealed in previous studies [200, 202]. AAP has two hydrophobic domains of 15 amino acids near the N-terminus. The first domain closer to the N-terminus consists of four short hydrophobic motifs that are evolutionarily highly conserved among AAV1, -2, -3B, -6, -7, -8, -9, -10, and -13 and partially conserved among AAV4, -5, -11, and -12. The second domain, which is closer to the C-terminus, is highly conserved across AAV1 to -13 and termed the “conserved core” of AAP [200]. A coimmunoprecipitation analysis using a panel of AAP2 and AAV2 VP3 mutants showed that these two hydrophobic domains in the AAP proteins play a crucial role in interacting with the capsid VP proteins through a highly conserved hydrophobic patch near the VP C-terminus that includes I682 (note that this amino acid position is based on the AAV2 capsid protein)[200]. This high level of conservation of amino acids that constitute the interface of the AAP-VP interaction might allow an AAP derived from one serotype to assist in the assembly of AAV capsids of other serotypes. Therefore, the promiscuity of AAPs in cross-complementing the assembly of heterologous capsids that we observed in this study conforms well to

the inference drawn from the evolutionarily conserved interfaces in the AAP-VP complex. Although the mechanism underlying why AAP4, -5, -11, and -12 show no or limited promiscuity in heterologous capsid assembly has yet to be elucidated, the decreased hydrophobicity in the first hydrophobic region found only in these four AAPs might correspondingly decrease the ability of the AAPs to interact with the hydrophobic C-terminal regions in VP proteins. A note of interest in the context of AAV capsid engineering by DNA shuffling is that while, overall, AAPs are generally able to cross-complement many different serotypes, capsid libraries that include AAV4, -5, -11, and -12 might benefit from providing their cognate AAPs during capsid assembly reactions [804].

To our surprise, our study convincingly demonstrated that AAV4, -5, and -11 can assemble capsids without a need for AAP. This was not anticipated, because a previous study had shown that AAV5 capsid assembly required AAP [201]. Although the reasons for this discrepancy are still unknown, there are a few possible explanations. First, there was a difference in the AAV5 VP3 expression plasmid constructs used in these studies. The plasmid used in the previous study contained an extra 154 bp after the stop codon derived from the AAV5 genome. Second, in our experiment, AAV5 VP3 might have been expressed in cells at a higher level than that in the previous study. As detailed in Materials and Methods, we used a strong CMV-IE enhancer-promoter with an enhancing element to express VP proteins. Taking this into account, a higher concentration of AAV5 VP3 proteins might allow AAP-independent capsid assembly. Interestingly, AAV12 VP3

was found to require AAP for assembly. This was also unexpected because AAV12 VP3 is evolutionarily closely related to AAV4 and AAV11, which exhibit AAP-independent assembly, and because the subcellular localization and specificity in the cross-complementation of capsid assembly of heterologous serotypes are conserved among these serotypes [201]. Further studies will be needed to delineate the AAP-independent assembly properties seen in the AAV4 and AAV11 VP3 proteins, which will lead to a better understanding of AAV assembly mechanisms.

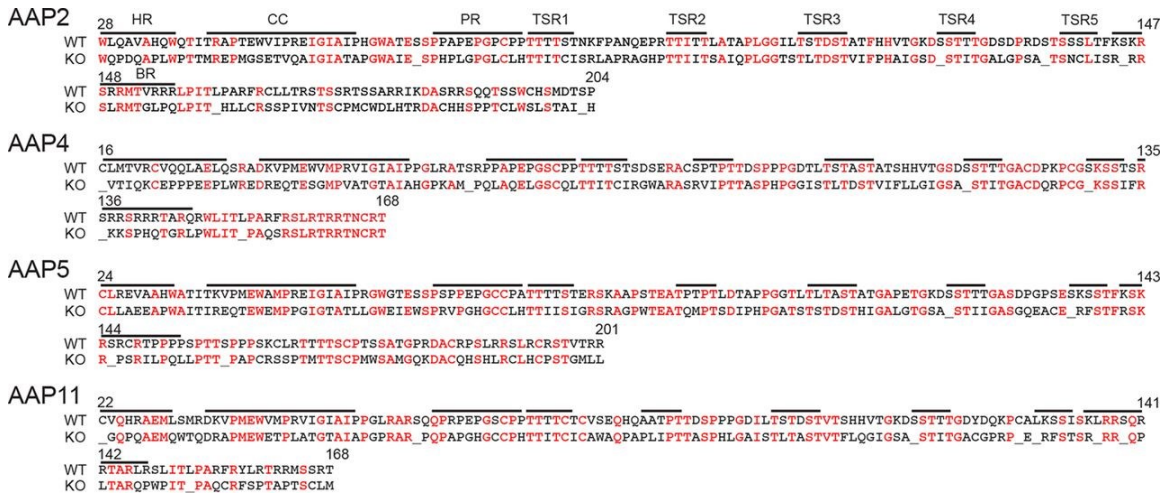


Figure 3.10 Sequence Alignment of Wild-Type AAPs and the Mutated AAPs Encoded by the AAP ORFs Within the cmVP3 ORFs

Amino acid sequences encoded by the mutated AAP ORFs in the pCMV₁-AAVxcmVP3 plasmids (where x is 2, 4, 5, and 11) (knockout [KO]) are aligned with the wild-type (WT) AAPs, showing extensive amino acid alterations with new stop codons in the mutated AAP ORFs within the cmVP3 ORFs. Black and red letters indicate amino acids with and without changes, respectively. Underlining indicates stop codons. Annotations and the indicated amino acid positions were described previously by Naumer *et al.* [200]. HR, hydrophobic region; CC, conserved core; PR, proline rich; TSR, T/S rich; BR, basic region.

One might argue that the +1-frameshifted mutated AAP ORFs within the cmVP3 ORFs could still express peptides that promote capsid assembly, allowing AAV4, AAV5, and AAV11 to assemble even in the absence of AAP supplied in trans. Naumer *et al.* showed that (i) a C-terminal deletion of AAP2 including the right half of the basic region (BR) (**Figure 3.10**) can abolish capsid assembly, (ii) the left half of the hydrophobic region of AAP2 (**Figure 3.10**) is essential for capsid assembly, and (iii) amino acid mutations within the conserved region (CC) (**Figure 3.10**) impair capsid assembly [200]. When those previously reported observations are taken into account, one can conclude that the mutations in the AAP ORF should be sufficient to abrogate or impair assembly substantially, because the encoded peptides embody the deleterious alterations described above (**Figure 3.10**). Complete abrogation of the AAP function by the codon modification has been proven experimentally by using a plasmid carrying the AAV2 cmVP3 ORF since no assembled AAV2 VP3 capsids were observed for AAV2 cmVP3 (**Figure 3.5** and **3.6**). The amino acid sequences of the essential regions identified previously by Naumer *et al.* are well conserved across AAPs derived from various serotypes; therefore, it is extremely unlikely that the mutated AAP ORFs in our cmVP3 plasmid constructs retain the assembly-promoting function [200].

It is worth noting that despite the dispensable nature of AAP5 for infectious AAV5 virion formation, the capsid assembly-promoting role of AAP5 is still obvious, as the abrogation of AAP5 expression from the capsid gene substantially decreased AAV5 vector production (**Figure 3.7C**). AAP4 and AAP11 also shared this role

(**Figure 3.9**), although they were also not essential for capsid formation. These observations led us to speculate that AAP might contribute to the promotion of capsid assembly through mechanisms other than its above-described essential role. In this respect, it is intriguing that when we used the pCMV1-AAV5cmVP3 plasmid to express AAV5 VP3 in HEK 293 cells (**Figure 3.7A**), we were able to produce assembled AAV5 VP3 capsids at equivalent levels irrespective of the presence or absence of coexpressed AAP5 (**Figure 3.7C**), while this was not the case when we used the pCMV1-AAV5VP3 plasmid (**Figure 3.4**). The pCMV1-AAV5cmVP3 plasmid differs from the pCMV1-AAV5VP3 plasmid in that the AAV5 VP3 ORF had been codon optimized for human cell expression. Hence, the concentration of VP proteins in cells may be rate limiting in the AAP-independent assembly process of the AAV5 capsid. At a lower concentration, the AAV5 VP3 proteins might require the presence of AAP5 to become stabilized and accumulate at the sites where capsids assemble through the interaction with AAP5. Therefore, it is plausible to propose a stabilization-accumulation mechanism via AAP-VP interactions, through which capsid assembly could be further enhanced. Such a mechanism might be postulated not only for AAV5 but also for other serotypes, although AAP-dependent serotypes still require AAP for its essential role in the assembly of capsids.

For many years, the nucleolus has been viewed as an organelle important for the AAV2 life cycle. Early work showed that AAV2 capsids are first seen in the nucleolus and subnuclear bodies during replication [227, 798]. Several studies

have found a close association between nucleolar proteins and AAV2 capsids [226, 227], and it was found that AAV2 capsids are trafficked to the nucleolus following infection [808]. These observations led the field to speculate a role for the nucleolus or nucleolar proteins in AAV2 replication. A proposed hypothesis is that AAV capsid assembly occurs in the nucleolus and that capsids are subsequently moved to the nucleoplasm for genome packaging in a Rep-dependent manner [227]. The identification of the nucleolus as the site of AAV2 capsid assembly was further supported by the identification of the nucleolus-localizing AAP2 protein [197]. However, the role of the nucleolus had not been examined for other AAV serotypes. Our study addressed this question and revealed that AAP5 and AAP9 display a markedly decreased association with the nucleolus and that AAV5, -8, and -9 capsids do not accumulate in the nucleolus or associate with nucleostemin. Thus, the question arises as to whether the nucleolus plays an important role in capsid assembly for only a subset of AAV serotypes. It is possible that certain AAV serotypes require only a transient interaction with the nucleolus for capsid assembly and that the assembled capsids leave the nucleolus for packaging viral genomes in the nucleoplasm. Alternatively, for certain serotypes such as AAV5, assembly of the capsid may not have to rely upon factors in the nucleolus. Thus, our observations challenge the generalized view on the significance of roles of the nucleolus in the AAV life cycle and highlight a potential heterogeneity of the mechanisms of viral capsid assembly and replication among different AAV serotypes.

In summary, we show that capsid assembly in the nucleolus and its strict dependence on AAP are not universal phenomena applicable to all AAV serotypes. A potential caveat of our study is that we used an artificial plasmid transient-transfection system to study AAPs, which might not necessarily mimic the AAV infection and replication that take place in nature. Nonetheless, this study reveals that the processes and mechanisms involved in the AAV life cycle are more heterogeneous among different serotypes than previously thought. Further study into the roles and functions of AAPs in the AAV life cycle will advance our foundational knowledge of icosahedral capsid assembly mechanisms and lead to improved methods for the production of AAV vectors for gene therapy.

3.5 Materials and Methods

Plasmid construction

The pCMV3-FLAG-cmAAPx plasmids (where x is 1 to 12) are plasmids expressing codon-modified versions of AAP with an N-terminal FLAG tag under the control of the human CMV-IE gene enhancer-promoter and an ATG start codon. Each AAP ORF was codon modified to optimize expression in human cells and cloned into the pCMV3-FLAG-cmAAP2 parental plasmid used in our previous study by replacing the cmAAP2 ORF with a new cmAAPx ORF [202]. Plasmid pCMV3-FLAG-AAP2 carries the native AAP2 ORF sequence in place of the cmAAP2 ORF. Plasmid pCMV3-GFP is a plasmid expressing eGFP under the control of the same CMV-IE enhancer-promoter. The pCMV1-AAVxVP3 plasmids (where x is 1 to 12) are plasmids expressing each VP3 protein from the native ORF initiating at the

ATG start codon. The pCMV1-AAV_xcmVP3 plasmids (where x is 2, 4, 5, and 11) are plasmids expressing each VP3 protein from a codon-modified ORF in which the AAP-VP-overlapping ORFs were codon modified to optimize VP3 expression in human cells. The modification resulted in extensive changes in amino acids encoded by each AAP ORF, with identities and numbers of new stop codons being 37% and 6 for AAP2, 48% and 5 for AAP4, 47% and 4 for AAP5, and 44% and 8 for AAP11, respectively. Each VP3 ORF was cloned in the pCMV1-AAV2VP3 parental plasmid used in our previous study by replacing the AAV2VP3 ORF with a new VP3 ORF [202]. The CMV-IE enhancer-promoters that we used in this study contained an intervening sequence (IVS) consisting of a splice donor, an intron, and a splice acceptor from pIRES (Clontech, Mountain View, CA) for the AAP-expressing plasmids or the IVS from pAAV-MCS (Agilent, Santa Clara, CA) for the VP3-expressing plasmids. An adenovirus helper plasmid, pHelper, was purchased from Agilent. pHLP-AAV5(AAP5+) and pHLP-AAV5(AAP5-) are AAV5 helper plasmids carrying the AAV2 rep gene and the AAV5 cap gene. pHLP-AAV5(AAP5+) is the same as pHLP19-5, which has been used for recombinant AAV5 vector production in our laboratory [809]. In the pHLP19-5 helper plasmid, the AAV2 p5 promoter is moved from the native location to the downstream region of the AAV2 polyadenylation signal, and the TATA box sequence in the p5 promoter, TATTTAA, is replaced with the sequence GGGGGGG to reduce the expression of the large Rep proteins. pHLP-AAV5(AAP5-) is a derivative of pHLP-AAV5(AAP5+) that carries the codon-modified AAP-VP ORFs, which abolishes functional AAP5 expression while preserving the expression of the wild-type AAV5

VP1, VP2, and VP3 proteins. The identity of AAP5 amino acids encoded by the native and codon-modified AAP-VP ORFs is 44% with 4 new stop codons being introduced into the AAP5 ORF. pHLP-Rep is a plasmid that expresses all the AAV2 Rep proteins in HEK 293 cells in the presence of cotransfected pHelper. pHLP-Rep was constructed by removing a 1.8-kb XhoI-XcmI fragment from the wild-type AAV2 genome contained in our standard AAV2 helper plasmid pHLP19-2 and expressed only AAV2 Rep proteins [809]. pEMBL-CMV-GFP is an AAV vector plasmid for the production of a double-stranded AAV vector expressing eGFP under the control of the CMV-IE enhancer-promoter and was a gift from X. Xiao. pAAV-CMV-luc is an AAV vector plasmid for the production of a single-stranded AAV vector expressing firefly luciferase under the control of the CMV-IE enhancer-promoter and was created from pAAV-MCS. The pdsAAV-U6-VBCx plasmids (where x is an integer identification number indicating each different DNA barcode contained in each pdsAAV-U6-VBCx plasmid) are all double-stranded AAV vector plasmids carrying a 135-bp DNA fragment (nucleotide positions 4445 to 4579 of pAAV9-SBBANN-VBCLib [GenBank accession number KF032296]) that harbors a pair of 12-nucleotide-long DNA barcodes (virus barcodes [VBCs]). Besides the DNA barcodes and flanking PCR primer binding sites, the pdsAAV-U6-VBCx vector plasmids contain a human U6 snRNA promoter-driven nonfunctional noncoding RNA expression cassette of 0.6-kb and a 1.0-kb stuffer DNA derived from the bacterial lacZ gene between the two AAV2 inverted terminal repeats. The pdsAAV-U6-VBCx vector plasmids were designed and created for a separate study, and their feature of noncoding RNA expression was not utilized in this study. We

confirmed that the expression of noncoding RNA from the pdsAAV-U6-VBCx plasmids does not affect AAV vector production in HEK 293 cells. pCMV1 and pCMV3 are control empty plasmids carrying no transgene in the pCMV1 and pCMV3 backbones, respectively. The native capsid ORFs used for plasmid construction were derived from pHLP19-1 to -6; AAV7, -8, and -9 helper plasmids were provided by J. M. Wilson and G. Gao; AAV10 and AAV11 helper plasmids were provided by S. Mori; and a plasmid containing a de novo-synthesized AAV12 cap ORF was provided by Voyager Therapeutics [809]. The codon-modified AAP and VP3 ORFs were synthesized by GenScript.

Cells

HEK 293 cells (AAV293) were purchased from Stratagene. The HeLa human cervical cancer cell line and the CHO-K1 cell line were obtained from the American Type Culture Collection (ATCC). HEK 293 cells and HeLa cells were grown in Dulbecco's modified Eagle's medium (DMEM) (Lonza, Basel, Switzerland) supplemented with 10% fetal bovine serum (FBS), L-glutamine, and penicillin-streptomycin. CHO-K1 cells were grown in F-12K medium supplemented with 10% FBS.

AAV particle production

AAV VP1/VP2/VP3 particles and VP3-only particles were produced in HEK 293 cells by using an adenovirus-free plasmid transfection method [425], with modifications. In brief, we changed the complete culture medium to serum-free

medium immediately before transfection, transfected cells with a mixture of the required amount of each plasmid DNA with polyethylenimine (PEI) at a DNA:PEI weight ratio of 1:2, and harvested both medium and cells for viral particle recovery at 5 days posttransfection. The plasmids used for the production of each viral particle preparation are described in each relevant section. The AAV5(AAP5⁻)-CMV-luc and AAV5(AAP5⁺)-CMV-luc vectors were produced by using one 225-cm² flask and concentrated from an initial volume of 25 mL to a final volume of 250 μ L using Amicon Ultra Centrifugal Filter units with a molecular mass cutoff of 100 kDa. For TEM, we produced VP3-only virus-like particles using 15 225-cm² flasks. The harvested medium and cells underwent one cycle of freezing and thawing, and the cell debris was removed by centrifugation at 10,000 \times g for 15 min. The culture medium supernatants were made with 8% polyethylene glycol 8000 (PEG 8000) and 0.5 M NaCl, incubated on ice for 3 h, and spun at 10,000 \times g for 30 min to precipitate viral particles. The pellets were resuspended in a buffer containing 50 mM Tris-HCl (pH 8.5) and 2 mM MgCl₂, treated with Benzonase (EMD Millipore, Darmstadt, Germany) at a concentration of 200 U per mL for 1 h, and subjected to purification by three rounds of CsCl density gradient ultracentrifugation followed by dialysis with a buffer (25 mM HEPES, 150 mM NaCl [pH 7.4]) for TEM [809].

Cell infection

CHO-K1 cells seeded onto a 96-well plate were infected with AAV5(AAP5⁻)-CMV-luc or AAV5(AAP5⁺)-CMV-luc at an MOI of 10⁶ in the absence of a helper virus.

At 46 h postinfection, luciferase activity was quantified by using the Bright-Glo luciferase assay system (Promega, Madison, WI) and the CentroXS LB960 plate reader (Berthold, Bad Wildbad, Germany). The data were collected from an experiment performed in biological triplicates.

Immunofluorescence microscopy

HeLa cells were seeded onto coverslips in 12-well plates and transfected with plasmid DNA by using PEI. Forty-eight hours after transfection, the cells were fixed with 4% paraformaldehyde at room temperature, permeabilized with 0.2% Tween 20, and blocked with 8% bovine serum albumin (BSA). For AAP localization, the cells were stained with mouse monoclonal anti-FLAG M2 antibody (catalog number F1804; Sigma-Aldrich, St. Louis, MO) and rabbit polyclonal antinucleostemin antibody (catalog number sc-67012; Santa Cruz Biotechnology, Dallas, TX), followed by DAPI (4',6-diamidino-2-phenylindole), Alexa Fluor 488-AffiniPure goat anti-mouse IgG antibody (catalog number 115-545-166; Jackson ImmunoResearch, West Grove, PA), and Cy3-AffiniPure goat anti-rabbit IgG antibody (catalog number 111-165-144; Jackson ImmunoResearch). For imaging of AAV capsids, cells were stained with mouse monoclonal anti-AAV2 capsid antibody (A20 clone, catalog number 03-61055; American Research Products Inc., Waltham, MA), mouse monoclonal anti-AAV4 capsid antibody (ADK4 clone, 03-610147; American Research Products Inc.), mouse monoclonal anti-AAV5 capsid antibody (ADK5a clone, catalog number 03-61048; American Research Products Inc.), mouse monoclonal anti-AAV8 capsid antibody (ADK8 clone, catalog number

03-651160; American Research Products Inc.), or mouse monoclonal anti-AAV8/9 capsid antibody (ADK8/9 clone, catalog number 03-651161; American Research Products Inc.) and rat monoclonal anti-DYKDDDDK (FLAG) antibody (catalog number NBP106712; Novus Biological, Littleton, CO), followed by DAPI, Alexa Fluor 488-AffiniPure goat anti-mouse IgG antibody (catalog number 115-545-166; Jackson ImmunoResearch), and Cy3-AffiniPure donkey anti-rat IgG antibody (catalog number 712-165-153; Jackson ImmunoResearch). The nucleolus was visualized by using rabbit polyclonal antinucleostemin antibody (catalog number sc-67012; Santa Cruz Biotechnology) and Alexa Fluor 647-AffiniPure goat anti-rabbit IgG antibody (catalog number 111-605-144; Jackson ImmunoResearch). GFP was directly visualized by fluorescence microscopy. The cells were imaged on a Zeiss LMS 710 laser scanning confocal microscope using either a 63×/1.4-numerical-aperture (NA) or a

100×/1.46-NA objective. To perform a quantitative assessment of the degree of nucleolar association of AAP1 to -12, cells were imaged on a Zeiss Axio Imager 2 microscope using a 40/1.3-NA objective, and a virtual large image was reconstructed from 49 individual image tiles by using an ApoTome.2 device attached to the microscope. We categorized the nuclear staining patterns into the following two groups: No⁺ and No⁻. The nuclei of the No⁺ group have nucleoli that are stained with the anti-FLAG antibody at the same level as that of the nucleoplasm or show a pattern of nucleolar enrichment. The nucleoli that do not

belong to the No⁺ group are categorized as No⁻. We counted 50 nuclei for each AAP serotype for a statistical comparison.

Quantitative dot blotting

HEK 293 cells were seeded onto 6-well plates 1 day before transfection. We changed complete culture medium to serum-free medium before transfection and transfected cells with 0.4 µg each of the following 5 plasmids using PEI: pCMV3-FLAG-cmAAPx (where x is 1 to 12) or pCMV3 (an empty plasmid as a no-AAP control), pCMV1-AAVxVP3 (where x is 1 to 12), pEMBL-CMV-GFP, pHLP-Rep, and pHelper. At 5 days posttransfection, we harvested both medium and cells, disrupted cells by one cycle of freezing and thawing, and released viral particles into the culture medium. After cell debris was removed by centrifugation at 21,100 × g for 5 min, 200 µL of the culture medium supernatant was subjected to nuclease treatment with 200 U per mL of Benzonase at 37°C for 4 h, followed by proteinase K treatment at 55°C for 1 h. Viral genome DNA was purified by phenol-chloroform extraction, ethanol precipitated, and dissolved in 1 x Tris-HCl-EDTA (TE) buffer (pH 8.0). The viral DNA and linearized standard plasmid DNA were then denatured with 0.4 N NaOH, blotted onto a Zeta Probe nylon membrane (Bio-Rad, Hercules, CA), and hybridized with a ³²P-labeled GFP probe. The hybridized signals were imaged and quantified by using a Typhoon FLA7000 scanner (GE Healthcare Bio-Science, Uppsala, Sweden). The negative control contained double-stranded AAV-CMV-GFP genomes that had undergone AAV2 Rep-mediated replication but were not protected by viral capsids. The negative control ensured efficient

nuclease digestion in the assay. However, the Benzonase-treated negative control still generates a low level of background signal; therefore, the dot blot assay by itself cannot completely rule out the possibility of the presence of viral particles at very low levels. To create dot blot images for figures, the tiff images were imported to ImageJ, and the dot intensities were adjusted equally across the entire image by using the ImageJ Brightness & Contrast function.

AAP-VP cross-complementation analysis

For AAP-VP cross-complementation analysis, we used two methods: Illumina sequencing-based AAV barcode-Seq and the conventional quantitative dot blot assay as described above [803]. For AAV barcode-Seq, HEK 293 cells were seeded onto 12-well plates 1 day before transfection, and VP3-only particles containing a DNA-barcoded viral genome were produced essentially in the same manner as described above except that we used 0.24 μg of each plasmid, pdsAAV-U6-VBCx in place of pEMBL-CMV-GFP, and pCMV3-FLAG-AAP2 in place of pCMV3-FLAG-cmAAP2. There were a total of 132 AAP and VP combinations, and each combination received a different DNA-barcoded AAV vector plasmid, pdsAAV-U6-VBCx (where x is 1 to 132). At 5 days posttransfection, we harvested both medium and cells and pooled them in a bottle. We performed this procedure in triplicate and produced three pooled samples. Viral genome DNA was extracted from 200 μL of each pooled sample, purified by phenol-chloroform extraction, ethanol precipitated, and dissolved in 20 μL of 1 \times TE buffer (pH 8.0). We then PCR amplified both the left VBCs (lt-VBCs) and the right VBCs (rt-VBCs)

separately using two different sets of PCR primers and 2 μ L each of the resulting DNA solution. The PCR primers are as follows: It-VBC-For (frameshifting nucleotide [FSN]-sample-specific barcode [SBC]-ACCTACGTACTTCCGCTCAT), It-VBC-Rev (FSN-SBC-TCCCGACATCGTATTTCCGT), rt-VBC-For (FSN-SBC-ACGGAAATACGATGTCGGGA), and rt-VBC-Rev (FSN-SBC-CTTCTCGTTGGGGTCTTTGC). Each primer contained a 7-nucleotide-long SBC and 1 to 5 FSNs at the 5' end. The primer combinations of It-VBC-For plus It-VBC-Rev and rt-VBC-For plus rt-VBC-Rev were used to amplify the It-VBCs and rt-VBCs, respectively, in each of the biological triplicates of the experiment. The resulting six PCR products were mixed at an equimolar ratio and subjected to multiplexed Illumina sequencing as previously described), together with other PCR products prepared in the same manner in separate AAV barcode-Seq studies [803]. One to five micrograms of PCR products attached to Illumina sequencing adaptors was sent to Elim Biopharmaceuticals Inc. (Hayward, CA) and sequenced with a 50-cycle single-end run on an Illumina HiSeq 2500 instrument. The quality measures of Illumina raw sequence reads determined by FastQC (i.e., per-base sequence quality, per-sequence quality scores, per-base N content, and sequence length distribution) were all met in the data set used in this study. We analyzed the Illumina sequencing data at the Pittsburgh Supercomputing Center using an algorithm that we developed. In this experimental scheme, a pair of the DNA barcodes carried by each AAV vector plasmid could provide a measure of AAV vector yield from each individual transfection by means of AAV barcode-Seq.

Barcode-Seq data analysis

We determined relative viral particle yields in each of the triplicate sets of the experiment using the same principle as that used for our previous study [803]. First, we globally normalized Illumina raw sequence read numbers for all the 132 VBCs to obtain relative read number data for each of the It-VBCs and rt-VBCs. We then adjusted the relative read number data for each of the It-VBCs and rt-VBCs by each VBC-specific PCR amplification efficiency factor. The VBC-specific PCR amplification efficiency factor was determined in the following manner. We created two sets of an equimolar mixture of 379 pdsAAV-U6-VBCx plasmids (where x is 1 to 379) independently. The 132 pdsAAV-U6-VBCx plasmids (where x is 1 to 132) used in this study were included in each equimolar plasmid mixture. We then PCR amplified 379 It-VBCs together using primers It-VBC-For and It-VBC-Rev and PCR amplified 379 rt-VBCs together by using primers rt-VBC-For and rt-VBC-Rev, in each of the two equimolar plasmid mixtures. The resulting four PCR products were mixed at an equimolar ratio and subjected to multiplexed Illumina sequencing together with other PCR products prepared in the same manner in separate AAV barcode-Seq studies as described above. This gave us raw sequence read numbers for all 132 It-VBCs and 132 rt-VBCs in each set. We then globally normalized the sequence read numbers and determined a relative quantity value for each It-VBC and each rt-VBC in each set. The relative quantity values for each VBC obtained from the duplicate sets of the experiment were averaged and used as the PCR amplification efficiency factor. Since the experiment was done in

triplicate and two DNA barcodes, lt-VBC and rt-VBC, were used, we obtained a total of 6 relative quantity values that could quantify the AAV vector yield with each AAP-VP3 combination. Among the 6 values for each AAP-VP3 combination, we excluded outliers showing values more than three times the interquartile range beyond the upper and lower quartiles. The AAV vector yield of each AAP-VP3 combination relative to the native combination was determined for each serotype. The AAV vector yield for the native AAP-VP3 combination was set as 1.0. It should be noted that Benzonase-treated samples containing replicated AAV vector genomes unprotected by capsid coats generate positive barcode PCR signals due to the high sensitivity of this PCR-based assay. This often generates a background signal higher than that of the quantitative dot blot assay described above. We have found that the background signals can be as high as ~0.2; therefore, positive values of up to ~0.2 do not necessarily indicate capsid assembly. This represents the limitation of this assay.

Transmission electron microscopy

Viral particle preparations, purified by three rounds of CsCl density gradient ultracentrifugation followed by dialysis, were spun at $6,100 \times g$ for 10 min to remove any viral precipitate. Carbon-coated copper grids (Cu-300CN; Pacific Grid-Tech, San Francisco, CA) were glow discharged for 25 s at 15 mA by using the Pelco easiGlow glow discharge cleaning system (Ted Pella Inc., Redding, CA) immediately prior to use. Four microliters of each sample was placed onto the grids for 3 min and manually blotted with Whatman filter paper (catalog number 1001-

125; GE Healthcare, Pittsburg, PA). The grids were then placed face down onto 45 μ L drops of a buffer (50 mM HEPES, 25 mM MgCl₂, 50 mM NaCl [pH 7.4]) for 30 s, washed three times similarly with distilled water, and then blotted. The samples on the grids were stained with 5.5 μ L of 0.75% uranyl formate (pH 4.5) for 30 s and washed with distilled water, followed by blotting. The grids were allowed to dry and then stored at room temperature in a petri dish sealed with Parafilm until imaging.

Enzyme-linked immunosorbent assay

After viral particle preparations were purified by three rounds of CsCl density gradient ultracentrifugation, 0.04 μ L of each fraction was subjected to a capsid-specific ELISA using the AAV2 Titration ELISA kit or the AAV5 Titration ELISA kit (Progen, Heidelberg, Germany) according to the manufacturer's instructions.

Western blotting

We seeded HEK 293 cells onto 6-well plates and transfected them with a total of 2 μ g of a plasmid or a mixture of plasmids using PEI. The plasmids used in each experiment are described in each relevant section. At 48 h posttransfection, we lysed HEK 293 cells in radioimmunoprecipitation assay (RIPA) buffer containing protease inhibitors (Complete Mini; Roche, Indianapolis, IN), sonicated the cells, and determined protein concentrations in the cell lysates with a DC Protein Assay kit (Bio-Rad, Hercules, CA). The same amount of total cell lysates (40 μ g per lane) along with a molecular weight marker were separated on a 10% SDS-PAGE gel,

transferred onto a polyvinylidene difluoride (PVDF) membrane, and reacted with mouse monoclonal anti-FLAG M2 antibody and mouse anti- α -tubulin antibody (catalog number sc-32293; Santa Cruz Biotechnology) or mouse monoclonal anti-AAV VP1/VP2/VP3 antibody (B1) (catalog number 03-61058; American Research Products) and rabbit polyclonal anti-cyclophilin A antibody (Cell Signaling Technology, Danvers, MA) followed by goat polyclonal anti-mouse IgG antibody (catalog number sc-2055; Santa Cruz Biotechnology) or goat polyclonal anti-rabbit IgG antibody (catalog number sc-2004; Santa Cruz Biotechnology) conjugated to horseradish peroxidase (HRP). The signals on the blots were visualized with the Immobilon Western chemiluminescent HRP substrate (EMD Millipore) and imaged on X-ray films or by using the FluorChem M system (ProteinSimple, Santa Clara, CA). Molecular weights of FLAG-tagged AAP1 to -12 were determined in quadruplicate Western blots. In brief, tiff images of the blots were imported into ImageJ, and the positions of the peak of each AAP band were identified by densitometry and used for the calculation of the migration distance for each AAP. The molecular weights of AAPs were then determined by interpolation using the migration distances of molecular weight markers and their log-transformed molecular weights. The Western blot images for figures were created in the same manner as described above for the dot blot images by using ImageJ.

Statistics

In the cross-complementation study using AAV barcode-Seq, the null hypothesis that there was no enhancement of assembly by AAP was examined by a one-tailed

Mann-Whitney U test for each serotype. For the quantitative assessment of the nucleolar association of AAPs, we used Fisher's exact test. Because 12 AAPs were compared pairwise, P values were adjusted by Bonferroni correction. In the AAV5 vector production and infection assays, we used two-tailed Welch's t test to assess differences in the mean values between two groups. P values of < 0.05 were considered statistically significant.

ACKNOWLEDGMENTS

We thank Xiao at the University of North Carolina at Chapel Hill for providing us with the pEMBL-CMV-GFP plasmid; Guangping Gao and James M. Wilson for helper plasmids for AAV7, -8, and -9; Seiichiro Mori for the helper plasmid for AAV10 and AAV11; Voyager Therapeutics for a plasmid containing the de novo-synthesized AAV12 cap gene ORF; and Christoph Kahl and Michelle Gomes for technical assistance.

Chapter 4.

Discussion and Future Directions

4.1 Novel Viral Vector Vaccination Strategies Against Alphaviruses

Due to the epidemic potential of alphaviruses and their continued spread to new regions and urban environments, the development of effective vaccines and therapeutics is of great interest to public health initiatives. Chapter 2 reports on the development of a replication-incompetent adenovirus serotype 5 (Ad5) vaccine that expresses the full-length structural gene cassette from the Old-World alphavirus Mayaro virus (AdV-MAYV). Compared to other vaccination approaches, the ability for Ad vectors to stimulate long-lasting innate and adaptive immune responses is advantageous for vaccine development. Infection of cultured cells with the AdV-MAYV vaccine resulted in the expression of the structural genes from a CMV-IE promoter and formation of viral like particles (VLP) that conformed to the size and structure of native infectious alphaviruses (**Figure 2.1**). Intramuscular vaccination of mice with the AdV-MAYV vaccine identified that a prime + boost vaccination regimen with 10^8 PFU delivered intramuscularly at day 0 (prime) and 14 (boost) resulted in robust neutralizing antibody activity. Elicited neutralizing antibodies were protective in both wild type and severely immunocompromised IFN α R1^{-/-} mouse models. Protection was maintained through at least 84 days post vaccination (dpv) when evaluated in wild type mice (**Figure 2.5**). Similar data was also obtained when mice were vaccinated with an AdV vector that expressed the structural gene cassette from Una (AdV-UNAV) virus (**Supplemental Figure 2**). T

cell responses in WT and IFN α R1^{-/-} AdV-MAYV vaccinated mice were elevated against an 18-mer peptide from the N-terminal domain of MAYV E2 (LAKCPPGEVISVSFV) at 28 dpv. Epitopes from this region have previously been identified as prominent targets for early T cell responses in CHIKV infection and support the N-terminus of E2 as an important target of the early adaptive immune response [685, 686]. Due to homology between different alphaviruses, it is likely that vaccines may provide protection against heterologous alphavirus species. Along with our data in chapter 2 that identified this phenomena with AdV-MAYV, cross-protection has also been observed for vaccines that other groups have developed and tested against Chikungunya (CHIKV) as well as after natural infection with CHIKV (**Figure 2.10**) [634-636, 738]. Recently, we have tested plasma samples of individuals from Ponce, Puerto Rico and observed similar instances of cross-protective antibodies in convalescent plasma samples from CHIKV infected patients (**Supplemental Figure 1**). Although MAYV is currently believed to be regionally restricted to South America and infections are less common than CHIKV, the difficulties in accurate differential diagnosis from other alphaviruses due to sero-cross-reactivity and shared physical symptoms (“ChikDenMaZika” syndrome) complicates positive identification. As such, a broadly protective vaccine is of importance to the region, but would also be of importance on a global scale do to the increasing geographic range.

We have also evaluated adenovirus vector vaccines against other alphavirus species, including O’nyong’nyong (ONNV), UNAV (**Supplemental Figure 2**), and

CHIKV (**Supplemental Figure 3 & 4**). In these approaches, native Ad5 capsids have been used to package the structural protein transgenes, but the AdV-CHIKV studies also included a panel of modified capsids designed to target vectors for dendritic cells (DC) to increase antigen presentation and stimulated immune responses. These vectors have displayed the ability to stimulate neutralizing antibodies similar to what was observed with AdV-MAYV. Similarly, ELISpot analysis identified peptide specific T cell responses following vaccination. (**Supplemental Figure 3**). These findings support the utility of Ad-vectored vaccines against alphavirus species and provide evidence that single vaccines may be able to protect against co-circulating viruses, such as MAYV, UNAV, and CHIKV. Assessment of the cross-protection entailed from these other Ad-based alphavirus vaccine vectors is planned and will further the understanding of shared antigenic domains between these species. Development of DC-targeting adenoviruses may prove helpful in eliciting immune responses similar to those observed during natural infections due to the importance of antigen presentation from infected DCs during the normal course of alphavirus infection. Follow-up studies with these vaccines in a rhesus macaque model would provide important data on vaccine efficacy and protection in large animal models. Moreover, they would provide novel data on MAYV and UNAV disease course and immune response following infection in a large animal model system. Only one such study in 1967 has published on non-human primate infection with MAYV, but no data on pathology was included [635]. To date no data exists on vaccination attempts for these viruses in non-human primates.

We also attempted to create an adenovirus vector vaccine expressing the structural proteins for Venezuelan Equine Encephalitis Virus (VEEV) but were unsuccessful. The VEEV capsid may interfere with protein translation as it has been shown to induce host shutoff by targeting of transcription factors in the nucleus. To circumvent this issue, we utilized a mutant capsid with a deletion of aa64 – 68, disrupting the NLS domain [669]. This region was previously identified as important in the inhibition of nuclear import through binding to CRM1, importin α , and importin β [668]. Even with this deletion, it is possible that the capsid protein may have retained some undesirable functions. Two alternative approaches to circumvent this issue could be attempted. An alanine replacement of aa64 – 68 if the deletion somehow affected the ability of the capsid to fold correctly, although it is unlikely as published data exists that VLP could form with these bases deleted. Alternatively, we could explore mutation of the NES domain (aa32 – 51), which has known effects on host transcription through a leucine-rich supraphysiological nuclear export signal that inhibits RNAPI and RNAPII, with or without mutations in the NLS domain [667-669]. It is possible that mutagenesis of both domains could support higher titer virus production while limiting the cytopathic effects from capsid expression in the HEK293 production cell line.

Based on the current predominance of alphaviruses in tropical forests and remote locations, the ability to deliver vaccines to the most affected populations is critically important in limiting the spill-over from the sylvatic cycle to humans. As viral vectors are thermolabile and rely on cold chain storage to maintain activity the ability to

deploy them to remote sites and facilities without modern infrastructure is complicated. Evaluation of lyophilized or thermostabilized vector compounds would be important follow-up studies. Studies with Ad vectors and other vector-based vaccines has indicated that such approaches are viable without significant effects on viral titer and transgene expression [729, 730]. Additionally, due to the seroprevalence of anti-Ad5 antibodies globally, evaluation of the AdV-MAYV vaccine platform using alternative adenovirus serotypes may enable wider distribution and limit concerns of vector-induced immune responses. Alternative options include bovine (BAd-3), Canine (CAd-2), and multiple simian (SAd) serotypes [369]. The recent publication of ChAdOx1 MAYV and CHIKV vectored vaccines displayed similar results, but elicited levels of neutralizing antibodies was decreased from what we observed and protection from heterotypic challenge did not provide complete protection [732]. These differences could be related either to the ChAdOx1 vector and/or the expression of a codon optimized structural protein that reportedly did not express the transframe (TF) protein. As previous studies have identified that viral particles produced from TF deleted mutants displayed severely attenuated pathogenesis and that TF, rather than 6K, is predominantly incorporated into the viral particle this could have altered the ability to form more immunogenic VLP [535, 538].

Isolation of the neutralizing antibodies elicited by vaccination is another future avenue that could be pursued. This would help provide important evidence on predominant antigenic domains and provide potential therapeutic options.

Evidence presented by Broeckel *et al.* identified the applicability of such an approach, showing that broadly neutralizing anti CHIKV mAbs were effective in limiting disease in macaque models of CHIKV infection [756].

4.2 Functional Role and Importance of Assembly-Activating Protein

With the increasing use of AAV vectors in therapeutic gene therapy applications, further characterization of the genome has led to the identification of +1 frame shifted protein AAP and MAAP. Studies on AAP, a +1 frame shifted protein from the *cap* ORF, have uncovered important information on the mechanism of capsid assembly and have led to a further understanding of basic AAV biology. Intriguingly, while AAP is present in all studied AAVs, the absolute requirement of its presence in capsid assembly is not conserved. Our experiments with AAP in chapter 3 identified a disparity between serotypes in the requirement of this esoteric protein across twelve human AAV serotypes (AAV1 – 12). While it was identified that AAP plays a critical role in efficient capsid assembly for the majority of evaluated serotypes, AAV4, 5 and 11 capsid assembly was determined to be AAP-independent. This identification helped to broaden the understanding of the functions of AAP, as previous studies had largely focused on the function of AAP in the context of AAV2 capsid assembly. Intriguingly, although AAV5 is in an isolated individual phylogenetic outgroup, AAV4 and 11 are contained in a clade with AAV12. While AAV4 and 11 are AAP independent, AAV12 was found to require AAP for capsid assembly. As such, the requirement for AAP-supported

assembly does not appear to be related to currently defined ancestral branch points.

While our data in chapter 3 defined strict requirements for full length AAP in capsid assembly, recent data has indicated an even broader divergence. Data presented by Maurer *et al.* found that some of the serotypes previously designated as AAP dependent were able to assemble capsids when minimal N-terminal sequences from AAP2 were expressed [199]. Like our data, these findings again identified that this phenomenon was not shared among members of a phylogenetic clade. Although we both have identified serotypes that possess either complete or C-terminal AAP independence, all of these serotypes achieve higher titers when AAP is present. Thus, AAP appears to play a supportive role in capsid assembly for all assayed serotypes since no evidence has been presented on the existence of a serotype that is negatively affected by the presence of AAP. One current theory on the function of AAP is that it exists in order to enable a wider range of non-truncating mutations to the *cap* proteins without affecting their ability to assemble [199]. With the data presented by Maurer *et al.* that N-terminally truncated AAP is functional for some serotypes, AAP itself may have evolved to tolerate mutations to its reading frame.

During the production of AAV, the production of viral proteins (VP) in the correct stoichiometric ratio of 1:1:10 for VP1:VP2:VP3 respectively is critical to the assembly of functional virions. Studies on the production of AAV2 VP proteins found that while the synthesis and abundance of VP monomers was unaffected in

the absence of AAP, oligomerization and full capsid formation was facilitated by AAP [200]. These results suggested a scaffolding role in the surface interactions at the 3- and 5-fold axes, although binding would be transient as assembled capsids lack AAP. Additional studies on the functional role of AAP by Maurer *et al.* confirmed the presence of twelve residues in the *cap* sequence that varied between AAP dependent and independent serotypes [199]. When these point mutations were grafted onto AAP dependent serotypes, capsid assembly could then occur in an AAP independent manner. Structural mapping identified that seven residues mapped to the 3-fold axis and could form salt bridges, hydrogen bonds, and reduced hydrophobic interactions between VP trimers. These residues and binding interactions would then support intermolecular bonds between VP trimers to enable oligomerization and full capsid assembly binding interactions in the absence of AAP. These findings supported the aforementioned hypothesis proposed by Maurer *et al.*, as scaffolding functions may be able to stabilize acquired mutations that would otherwise prevent self-assembly [199]. Further studies on functional domains within AAP will help provide a better understanding of its role and the divergent requirements between serotypes.

Further studies on the properties of AAP in capsid assembly will aid in the design of new recombinant capsids with beneficial phenotypes such as refined tissue tropism, decreased immunogenicity, and increased half-life following systemic delivery. A significant issue in these approaches is the potential that the AAP reading frame could be disturbed, destroying its function. Along with this, insertion

of peptides at hypervariable loops may also impose restrictions on oligomerization that would require the presence of an efficient AAP to provide scaffolding support. Data in Supplemental Chapter 1 found that disparities existed when AAPs were tested for their ability to assemble homologous and heterologous VP3 only capsids. Thus, production of AAV capsid mutants may be skewed depending on what AAP is encoded or supplemented in *trans*. This could dramatically affect the type of mutants selected during head-to-head pooled mutant library productions. AAP disadvantaged mutants (such as those mutants without a functional/full length AAP reading frame or where the AAP does not adequately support VP sequences) would likely be lost over library refinement as the chance of *trans* supplementation from mutants with functional AAPs is diminished. Instead, the identification of a broadly acting AAP that could be supplemented in *trans* could alleviate selection biases. This approach could lead to the identification of mutants with desired phenotypes that would otherwise be selected against/overlooked. In fact, work by Maurer *et al.* suggests that rational mutagenesis approaches with AAP may be an approach to create a broadly acting AAP [205]. Using an N-terminal AAP2 mutant they identified that a double mutant AAP2 H34L/R50Q was able to rescue viral titers for AAVs that were unable to efficiently assemble when native AAP2 was supplemented in *trans*. Intriguingly, evidence from *trans*-complementation assays has identified another interesting phenomenon. Plasmids expressing FLAG-tagged AAP have shown improved function in *trans* complementation assays when compared to native AAP [205]. The properties behind this observed phenomenon are unclear and further investigation of what role manipulations such as tagging

may have on stability and function are warranted. Continued research on the biology and function of AAP across serotypes will be of great importance to the development of novel designer capsids, enabling increased efficacy and the breadth of potential applications.

4.3 Concluding Summary

Since its inception, the field of gene therapy has continually evolved. The discovery of the utility of viral vectors ushered in a new era of effective approaches to deliver exogenous DNA to patient solid organs and tissues, an approach not feasible by transfection. While viral vectors continue to be effective tools for the treatment of monogenic disorders, they have seen increased interest as platforms for cancer treatment and as vaccines. Increasing evidence has shown the utility of Ad vectors as vaccine platforms due in part to their wide tissue tropism, innate immunogenicity, and large transgene packaging capacity (section 1.4.1.3). In our hands, we have observed the efficacy of Ad serotype 5 (Ad5) vector vaccines against multiple alphavirus species to elicit both humoral and cellular immunity (Chapter 2, Supplemental Figures 2 – 4). Further evaluation of antigenic domains and potential targets for monoclonal neutralizing antibodies will expand potential vaccine and therapeutic approaches against alphaviruses. While Ad5 vectors have been a predominant research vehicle, further evaluation of alternative serotypes with decreased human seroprevalence will be of importance. Identification of alternative naturally occurring serotypes or the design of novel vectors will enable

widespread global use and the implementation of Ad vaccine vectors against numerous pathogens.

Additionally, the use of adeno-associated virus vectors in gene therapy applications against monogenic disorders has flourished with the discovery and design of novel serotypes. Although AAV2 vectors have dominated the field and continue to provide important information on AAV biology, the discovery of the assembly-activating protein (AAP) and the integral role it plays in capsid assembly has presented the need to develop a broader of the biology of genus *Dependoparvovirus* members. Our findings in Chapter 3 and Supplemental Chapter 1 identified that the absolute requirement of AAP for capsid assembly varies between serotypes, as well as the ability of AAP to support the capsid assembly of heterologous serotypes. With the recent push towards identification and design of novel, non-naturally occurring serotypes with desirable phenotypes there exists a need to develop a further understanding of the functional mechanism of AAP and optimal naturally occurring or rationally designed AAPs that can broadly support capsid assembly of non-homotypic serotypes. Continued research by other groups has expanded on our findings and provided important data that could aid in the rational design of AAP(s) with the ability to broadly support AAV capsid assembly across serotypes [199, 205]. This knowledge would be of great importance in helping researchers effectively and efficiently achieve high titer vector productions. Further research on the functional domains, mechanism of

action, and phylogenetic conservation of AAP will be of significant benefit in the pursuit of novel AAV vectors.

Taken together, the data presented herein provides additional evidence on the utility and biology of viral vectors. With the continued use of vectors in approaches for treatment of monogenic disorders, cancer, and a burgeoning interest as vaccine platforms, the information presented provides important insight into the production of effective AAV vectors and efficacy of Ad vectored vaccines. Along with this, the observations with our AdV-MAYV vaccine indicate the likelihood that vaccination and natural infection with alphaviruses within the Semliki Forest complex are capable of eliciting broadly neutralizing antibodies. This finding indicates the importance of evaluating the cross-protective effects that vaccines against alphaviruses within this complex may elicit and whether developed vaccines function to provide multivalent protection.

References

1. Tatum EL. Molecular biology, nucleic acids, and the future of medicine. *Perspect Biol Med.* 1966;10(1):19-32. Epub 1966/01/01. doi: 10.1353/pbm.1966.0027. PubMed PMID: 6002665.
2. Sinsheimer RL. The prospect for designed genetic change. *Am Sci.* 1969;57(1):134-42. Epub 1969/01/01. PubMed PMID: 5781400.
3. Davis BD. Prospects for genetic intervention in man. *Science.* 1970;170(3964):1279-83. Epub 1970/12/18. doi: 10.1126/science.170.3964.1279. PubMed PMID: 5479007.
4. Pinsky L. Inborn errors of metabolism: principles and their applications. *Can Med Assoc J.* 1972;106(6):677 passim. Epub 1972/03/18. PubMed PMID: 4551928; PubMed Central PMCID: PMC1940485.
5. Berry SA, Brown C, Grant M, Greene CL, Jurecki E, Koch J, et al. Newborn screening 50 years later: access issues faced by adults with PKU. *Genet Med.* 2013;15(8):591-9. Epub 2013/03/09. doi: 10.1038/gim.2013.10. PubMed PMID: 23470838; PubMed Central PMCID: PMC3938172.
6. MacDonald A, van Rijn M, Feillet F, Lund AM, Bernstein L, Bosch AM, et al. Adherence issues in inherited metabolic disorders treated by low natural protein diets. *Ann Nutr Metab.* 2012;61(4):289-95. Epub 2012/12/05. doi: 10.1159/000342256. PubMed PMID: 23208158.
7. Das AM. Pharmacotherapy of inborn errors of metabolism illustrating challenges in orphan diseases. *J Pharmacol Toxicol Methods.* 2016;81:9-14. Epub 2016/02/28. doi: 10.1016/j.vascn.2016.02.182. PubMed PMID: 26921514.
8. Rogers S. Induction of arginase in rabbit epithelium by the Shope rabbit papilloma virus. *Nature.* 1959;183:1815-6. Epub 1959/06/27. doi: 10.1038/1831815b0. PubMed PMID: 14438381.
9. Rogers S, Lowenthal A, Terheggen HG, Columbo JP. Induction of arginase activity with the Shope papilloma virus in tissue culture cells from an argininemic patient. *J Exp Med.* 1973;137(4):1091-6. Epub 1973/04/01. doi: 10.1084/jem.137.4.1091. PubMed PMID: 4348278; PubMed Central PMCID: PMC2139227.
10. Munyon W, Buchsbaum R, Paoletti E, Mann J, Kraiselburd E, Davis D. Electrophoresis of thymidine kinase activity synthesized by cells transformed by herpes simplex virus. *Virology.* 1972;49(3):683-9. Epub 1972/09/01. doi: 10.1016/0042-6822(72)90525-9. PubMed PMID: 4342081.

11. Sambrook J, Westphal H, Srinivasan PR, Dulbecco R. The integrated state of viral DNA in SV40-transformed cells. *Proceedings of the National Academy of Sciences of the United States of America*. 1968;60(4):1288-95. Epub 1968/08/01. doi: 10.1073/pnas.60.4.1288. PubMed PMID: 4299943; PubMed Central PMCID: PMC224916.
12. Jr. HMS. Virus Is Injected Into 2 Children In Effort to Alter Chemical Trait. *The New York Times*. 1970.
13. Brody JE. GENETIC AID FAILS IN TEST ON HUMANS. *The New York Times*. 1975.
14. Friedmann T, Roblin R. Gene therapy for human genetic disease? *Science*. 1972;175(4025):949-55. Epub 1972/03/03. doi: 10.1126/science.175.4025.949. PubMed PMID: 5061866.
15. Friedmann T. The future for gene therapy--a reevaluation. *Annals of the New York Academy of Sciences*. 1976;265:141-52. Epub 1976/01/01. doi: 10.1111/j.1749-6632.1976.tb29328.x. PubMed PMID: 1066080.
16. Morrow JF. The prospects for gene therapy in humans. *Annals of the New York Academy of Sciences*. 1976;265:13-21. Epub 1976/01/01. doi: 10.1111/j.1749-6632.1976.tb29316.x. PubMed PMID: 1066078.
17. Jackson DA, Symons RH, Berg P. Biochemical method for inserting new genetic information into DNA of simian virus 40: circular SV40 DNA molecules containing lambda phage genes and the galactose operon of *Escherichia coli*. *Biotechnology*. 1972;24:11-6. Epub 1992/01/01. PubMed PMID: 1330117.
18. Yoshimori R, Roulland-Dussoix D, Boyer HW. R factor-controlled restriction and modification of deoxyribonucleic acid: restriction mutants. *J Bacteriol*. 1972;112(3):1275-9. Epub 1972/12/01. PubMed PMID: 4565538; PubMed Central PMCID: PMC251559.
19. Maniatis T, Kee SG, Efstratiadis A, Kafatos FC. Amplification and characterization of a beta-globin gene synthesized in vitro. *Cell*. 1976;8(2):163-82. Epub 1976/06/01. doi: 10.1016/0092-8674(76)90001-5. PubMed PMID: 61066.
20. Graham FL, van der Eb AJ. A new technique for the assay of infectivity of human adenovirus 5 DNA. *Virology*. 1973;52(2):456-67. Epub 1973/04/01. doi: 10.1016/0042-6822(73)90341-3. PubMed PMID: 4705382.
21. McCutchan JH, Pagano JS. Enhancement of the infectivity of simian virus 40 deoxyribonucleic acid with diethylaminoethyl-dextran. *J Natl Cancer Inst*. 1968;41(2):351-7. Epub 1968/08/01. PubMed PMID: 4299537.

22. Warden D, Thorne HV. The infectivity of polyoma virus DNA for mouse embryo cells in the presence of diethylaminoethyl-dextran. *J Gen Virol*. 1968;3(3):371-7. Epub 1968/12/01. doi: 10.1099/0022-1317-3-3-371. PubMed PMID: 4304101.
23. Cline MJ. Gene therapy. *Mol Cell Biochem*. 1984;59(1-2):3-10. Epub 1984/01/01. doi: 10.1007/bf00231302. PubMed PMID: 6584732.
24. MacMillan P. The Cline affair. *Nurs Times*. 1982;78(9):383. Epub 1982/03/03. PubMed PMID: 6950366.
25. Sun M. Cline loses two NIH grants. *Science*. 1981;214(4526):1220. Epub 1981/12/11. doi: 10.1126/science.7302590. PubMed PMID: 7302590.
26. Goff SP, Berg P. Construction of hybrid viruses containing SV40 and lambda phage DNA segments and their propagation in cultured monkey cells. *Cell*. 1976;9(4 PT 2):695-705. Epub 1976/12/01. doi: 10.1016/0092-8674(76)90133-1. PubMed PMID: 189942.
27. Hamer DH, Leder P. Splicing and the formation of stable RNA. *Cell*. 1979;18(4):1299-302. Epub 1979/12/01. doi: 10.1016/0092-8674(79)90240-x. PubMed PMID: 229971.
28. Hamer DH, Leder P. Expression of the chromosomal mouse Beta maj-globin gene cloned in SV40. *Nature*. 1979;281(5726):35-40. Epub 1979/09/06. doi: 10.1038/281035a0. PubMed PMID: 233122.
29. Ginn SL, Amaya AK, Alexander IE, Edelstein M, Abedi MR. Gene therapy clinical trials worldwide to 2017: An update. *The journal of gene medicine*. 2018;20(5):e3015. Epub 2018/03/27. doi: 10.1002/jgm.3015. PubMed PMID: 29575374.
30. Goswami R, Subramanian G, Silayeva L, Newkirk I, Doctor D, Chawla K, et al. Gene Therapy Leaves a Vicious Cycle. *Front Oncol*. 2019;9:297. Epub 2019/05/10. doi: 10.3389/fonc.2019.00297. PubMed PMID: 31069169; PubMed Central PMCID: PMC6491712.
31. Rowe WP, Huebner RJ, Gilmore LK, Parrott RH, Ward TG. Isolation of a cytopathogenic agent from human adenoids undergoing spontaneous degeneration in tissue culture. *Proc Soc Exp Biol Med*. 1953;84(3):570-3. Epub 1953/12/01. doi: 10.3181/00379727-84-20714. PubMed PMID: 13134217.
32. Dhingra A, Hage E, Ganzenmueller T, Bottcher S, Hofmann J, Hamprecht K, et al. Molecular Evolution of Human Adenovirus (HAdV) Species C. *Sci Rep*. 2019;9(1):1039. Epub 2019/02/02. doi: 10.1038/s41598-018-37249-4. PubMed PMID: 30705303; PubMed Central PMCID: PMC6355881.

33. Seto D, Chodosh J, Brister JR, Jones MS, Members of the Adenovirus Research C. Using the whole-genome sequence to characterize and name human adenoviruses. *Journal of virology*. 2011;85(11):5701-2. Epub 2011/04/01. doi: 10.1128/JVI.00354-11. PubMed PMID: 21450823; PubMed Central PMCID: PMC3094998.
34. Ismail AM, Lee JS, Lee JY, Singh G, Dyer DW, Seto D, et al. Adenoviromics: Mining the Human Adenovirus Species D Genome. *Front Microbiol*. 2018;9:2178. Epub 2018/09/27. doi: 10.3389/fmicb.2018.02178. PubMed PMID: 30254627; PubMed Central PMCID: PMC6141750.
35. Abbink P, Maxfield LF, Ng'ang'a D, Borducchi EN, Iampietro MJ, Bricault CA, et al. Construction and evaluation of novel rhesus monkey adenovirus vaccine vectors. *Journal of virology*. 2015;89(3):1512-22. Epub 2014/11/21. doi: 10.1128/JVI.02950-14. PubMed PMID: 25410856; PubMed Central PMCID: PMC4300752.
36. Lukashev AN, Ivanova OE, Eremeeva TP, Iggo RD. Evidence of frequent recombination among human adenoviruses. *J Gen Virol*. 2008;89(Pt 2):380-8. Epub 2008/01/17. doi: 10.1099/vir.0.83057-0. PubMed PMID: 18198368.
37. Ahi YS, Mittal SK. Components of Adenovirus Genome Packaging. *Front Microbiol*. 2016;7:1503. Epub 2016/10/11. doi: 10.3389/fmicb.2016.01503. PubMed PMID: 27721809; PubMed Central PMCID: PMC5033970.
38. Davison AJ, Benko M, Harrach B. Genetic content and evolution of adenoviruses. *J Gen Virol*. 2003;84(Pt 11):2895-908. Epub 2003/10/24. doi: 10.1099/vir.0.19497-0. PubMed PMID: 14573794.
39. Biasiotto R, Akusjarvi G. Regulation of human adenovirus alternative RNA splicing by the adenoviral L4-33K and L4-22K proteins. *Int J Mol Sci*. 2015;16(2):2893-912. Epub 2015/01/31. doi: 10.3390/ijms16022893. PubMed PMID: 25636034; PubMed Central PMCID: PMC4346872.
40. Fessler SP, Young CS. Control of adenovirus early gene expression during the late phase of infection. *Journal of virology*. 1998;72(5):4049-56. Epub 1998/04/29. PubMed PMID: 9557693; PubMed Central PMCID: PMC109633.
41. Siekierka J, Mariano TM, Reichel PA, Mathews MB. Translational control by adenovirus: lack of virus-associated RNAi during adenovirus infection results in phosphorylation of initiation factor eIF-2 and inhibition of protein synthesis. *Proceedings of the National Academy of Sciences of the United States of America*. 1985;82(7):1959-63. Epub 1985/04/01. doi: 10.1073/pnas.82.7.1959. PubMed PMID: 3856874; PubMed Central PMCID: PMC397459.
42. Andersson MG, Haasnoot PC, Xu N, Berenjian S, Berkhout B, Akusjarvi G. Suppression of RNA interference by adenovirus virus-associated RNA. *Journal*

- of virology. 2005;79(15):9556-65. Epub 2005/07/15. doi: 10.1128/JVI.79.15.9556-9565.2005. PubMed PMID: 16014917; PubMed Central PMCID: PMC1181602.
43. Hearing P, Shenk T. The adenovirus type 5 E1A transcriptional control region contains a duplicated enhancer element. *Cell*. 1983;33(3):695-703. Epub 1983/07/01. doi: 10.1016/0092-8674(83)90012-0. PubMed PMID: 6871991.
 44. Nevins JR, Ginsberg HS, Blanchard JM, Wilson MC, Darnell JE, Jr. Regulation of the primary expression of the early adenovirus transcription units. *Journal of virology*. 1979;32(3):727-33. Epub 1979/12/01. PubMed PMID: 513202; PubMed Central PMCID: PMC525919.
 45. Pelka P, Ablack JN, Fonseca GJ, Yousef AF, Mymryk JS. Intrinsic structural disorder in adenovirus E1A: a viral molecular hub linking multiple diverse processes. *Journal of virology*. 2008;82(15):7252-63. Epub 2008/04/04. doi: 10.1128/JVI.00104-08. PubMed PMID: 18385237; PubMed Central PMCID: PMC2493305.
 46. Gallimore PH, Turnell AS. Adenovirus E1A: remodelling the host cell, a life or death experience. *Oncogene*. 2001;20(54):7824-35. Epub 2001/12/26. doi: 10.1038/sj.onc.1204913. PubMed PMID: 11753665.
 47. Frisch SM, Mymryk JS. Adenovirus-5 E1A: paradox and paradigm. *Nat Rev Mol Cell Biol*. 2002;3(6):441-52. Epub 2002/06/04. doi: 10.1038/nrm827. PubMed PMID: 12042766.
 48. Schaack J, Bennett ML, Colbert JD, Torres AV, Clayton GH, Ornelles D, et al. E1A and E1B proteins inhibit inflammation induced by adenovirus. *Proceedings of the National Academy of Sciences of the United States of America*. 2004;101(9):3124-9. Epub 2004/02/21. doi: 10.1073/pnas.0303709101. PubMed PMID: 14976240; PubMed Central PMCID: PMC365754.
 49. Sieber T, Dobner T. Adenovirus type 5 early region 1B 156R protein promotes cell transformation independently of repression of p53-stimulated transcription. *Journal of virology*. 2007;81(1):95-105. Epub 2006/10/20. doi: 10.1128/JVI.01608-06. PubMed PMID: 17050591; PubMed Central PMCID: PMC1797270.
 50. Nakajima T, Morita K, Tsunoda H, Imajoh-Ohmi S, Tanaka H, Yasuda H, et al. Stabilization of p53 by adenovirus E1A occurs through its amino-terminal region by modification of the ubiquitin-proteasome pathway. *J Biol Chem*. 1998;273(32):20036-45. Epub 1998/08/01. doi: 10.1074/jbc.273.32.20036. PubMed PMID: 9685342.

51. Lowe SW, Ruley HE, Jacks T, Housman DE. p53-dependent apoptosis modulates the cytotoxicity of anticancer agents. *Cell*. 1993;74(6):957-67. Epub 1993/09/24. doi: 10.1016/0092-8674(93)90719-7. PubMed PMID: 8402885.
52. See RH, Shi Y. Adenovirus E1B 19,000-molecular-weight protein activates c-Jun N-terminal kinase and c-Jun-mediated transcription. *Mol Cell Biol*. 1998;18(7):4012-22. Epub 1998/06/25. doi: 10.1128/mcb.18.7.4012. PubMed PMID: 9632786; PubMed Central PMCID: PMC108986.
53. Kim J, Cho JY, Kim JH, Jung KC, Yun CO. Evaluation of E1B gene-attenuated replicating adenoviruses for cancer gene therapy. *Cancer gene therapy*. 2002;9(9):725-36. Epub 2002/08/22. doi: 10.1038/sj.cgt.7700494. PubMed PMID: 12189522.
54. Martin ME, Berk AJ. Corepressor required for adenovirus E1B 55,000-molecular-weight protein repression of basal transcription. *Mol Cell Biol*. 1999;19(5):3403-14. Epub 1999/04/17. doi: 10.1128/mcb.19.5.3403. PubMed PMID: 10207064; PubMed Central PMCID: PMC84133.
55. Blackford AN, Grand RJ. Adenovirus E1B 55-kilodalton protein: multiple roles in viral infection and cell transformation. *Journal of virology*. 2009;83(9):4000-12. Epub 2009/02/13. doi: 10.1128/JVI.02417-08. PubMed PMID: 19211739; PubMed Central PMCID: PMC2668481.
56. Matsushita T, Okada T, Inaba T, Mizukami H, Ozawa K, Colosi P. The adenovirus E1A and E1B19K genes provide a helper function for transfection-based adeno-associated virus vector production. *J Gen Virol*. 2004;85(Pt 8):2209-14. Epub 2004/07/23. doi: 10.1099/vir.0.79940-0. PubMed PMID: 15269360.
57. Caravokyri C, Leppard KN. Human adenovirus type 5 variants with sequence alterations flanking the E2A gene: effects on E2 expression and DNA replication. *Virus Genes*. 1996;12(1):65-75. Epub 1996/01/01. doi: 10.1007/BF00370002. PubMed PMID: 8879122.
58. Chang LS, Shenk T. The adenovirus DNA-binding protein stimulates the rate of transcription directed by adenovirus and adeno-associated virus promoters. *Journal of virology*. 1990;64(5):2103-9. Epub 1990/05/01. PubMed PMID: 2157873; PubMed Central PMCID: PMC249367.
59. Swaminathan S, Thimmapaya B. Regulation of adenovirus E2 transcription unit. *Current topics in microbiology and immunology*. 1995;199 (Pt 3):177-94. Epub 1995/01/01. doi: 10.1007/978-3-642-79586-2_9. PubMed PMID: 7555076.
60. Lesokhin AM, Delgado-Lopez F, Horwitz MS. Inhibition of chemokine expression by adenovirus early region three (E3) genes. *Journal of virology*.

- 2002;76(16):8236-43. Epub 2002/07/23. doi: 10.1128/jvi.76.16.8236-8243.2002. PubMed PMID: 12134029; PubMed Central PMCID: PMC155150.
61. Lichtenstein DL, Toth K, Doronin K, Tollefson AE, Wold WS. Functions and mechanisms of action of the adenovirus E3 proteins. *Int Rev Immunol.* 2004;23(1-2):75-111. Epub 2003/12/24. doi: 10.1080/08830180490265556. PubMed PMID: 14690856.
 62. Tollefson AE, Scaria A, Hermiston TW, Ryerse JS, Wold LJ, Wold WS. The adenovirus death protein (E3-11.6K) is required at very late stages of infection for efficient cell lysis and release of adenovirus from infected cells. *Journal of virology.* 1996;70(4):2296-306. Epub 1996/04/01. PubMed PMID: 8642656; PubMed Central PMCID: PMC190071.
 63. Tauber B, Dobner T. Molecular regulation and biological function of adenovirus early genes: the E4 ORFs. *Gene.* 2001;278(1-2):1-23. Epub 2001/11/15. doi: 10.1016/s0378-1119(01)00722-3. PubMed PMID: 11707318.
 64. Leppard KN. E4 gene function in adenovirus, adenovirus vector and adeno-associated virus infections. *J Gen Virol.* 1997;78 (Pt 9):2131-8. Epub 1997/09/18. doi: 10.1099/0022-1317-78-9-2131. PubMed PMID: 9291998.
 65. Weinberg DH, Ketner G. Adenoviral early region 4 is required for efficient viral DNA replication and for late gene expression. *Journal of virology.* 1986;57(3):833-8. Epub 1986/03/01. PubMed PMID: 3485200; PubMed Central PMCID: PMC252812.
 66. Muller U, Kleinberger T, Shenk T. Adenovirus E4orf4 protein reduces phosphorylation of c-Fos and E1A proteins while simultaneously reducing the level of AP-1. *Journal of virology.* 1992;66(10):5867-78. Epub 1992/10/01. doi: 10.1128/JVI.66.10.5867-5878.1992. PubMed PMID: 1326648; PubMed Central PMCID: PMC241463.
 67. Ben-Israel H, Sharf R, Rechavi G, Kleinberger T. Adenovirus E4orf4 protein downregulates MYC expression through interaction with the PP2A-B55 subunit. *Journal of virology.* 2008;82(19):9381-8. Epub 2008/07/26. doi: 10.1128/JVI.00791-08. PubMed PMID: 18653458; PubMed Central PMCID: PMC2546959.
 68. Tauber B, Dobner T. Adenovirus early E4 genes in viral oncogenesis. *Oncogene.* 2001;20(54):7847-54. Epub 2001/12/26. doi: 10.1038/sj.onc.1204914. PubMed PMID: 11753667.
 69. Thai M, Graham NA, Braas D, Nehil M, Komisopoulou E, Kurdistani SK, et al. Adenovirus E4ORF1-induced MYC activation promotes host cell anabolic glucose metabolism and virus replication. *Cell Metab.* 2014;19(4):694-701.

Epub 2014/04/08. doi: 10.1016/j.cmet.2014.03.009. PubMed PMID: 24703700; PubMed Central PMCID: PMC4294542.

70. Andrade F, Bull HG, Thornberry NA, Ketner GW, Casciola-Rosen LA, Rosen A. Adenovirus L4-100K assembly protein is a granzyme B substrate that potently inhibits granzyme B-mediated cell death. *Immunity*. 2001;14(6):751-61. Epub 2001/06/23. doi: 10.1016/s1074-7613(01)00149-2. PubMed PMID: 11420045.
71. Zhao H, Chen M, Pettersson U. A new look at adenovirus splicing. *Virology*. 2014;456-457:329-41. Epub 2014/06/04. doi: 10.1016/j.virol.2014.04.006. PubMed PMID: 24889252.
72. Reddy VS, Nemerow GR. Structures and organization of adenovirus cement proteins provide insights into the role of capsid maturation in virus entry and infection. *Proceedings of the National Academy of Sciences of the United States of America*. 2014;111(32):11715-20. Epub 2014/07/30. doi: 10.1073/pnas.1408462111. PubMed PMID: 25071205; PubMed Central PMCID: PMC4136627.
73. Caspar DL, Klug A. Physical principles in the construction of regular viruses. *Cold Spring Harb Symp Quant Biol*. 1962;27:1-24. Epub 1962/01/01. doi: 10.1101/sqb.1962.027.001.005. PubMed PMID: 14019094.
74. Russell WC. Adenoviruses: update on structure and function. *J Gen Virol*. 2009;90(Pt 1):1-20. Epub 2008/12/18. doi: 10.1099/vir.0.003087-0. PubMed PMID: 19088268.
75. Burnett RM. The structure of the adenovirus capsid. II. The packing symmetry of hexon and its implications for viral architecture. *Journal of molecular biology*. 1985;185(1):125-43. Epub 1985/09/05. doi: 10.1016/0022-2836(85)90187-1. PubMed PMID: 4046035.
76. San Martin C. Latest insights on adenovirus structure and assembly. *Viruses*. 2012;4(5):847-77. Epub 2012/07/04. doi: 10.3390/v4050847. PubMed PMID: 22754652; PubMed Central PMCID: PMC3386624.
77. Crowther RA, Franklin RM. The structure of the groups of nine hexons from adenovirus. *Journal of molecular biology*. 1972;68(1):181-4. Epub 1972/07/14. doi: 10.1016/0022-2836(72)90273-2. PubMed PMID: 5050362.
78. Roberts MM, White JL, Grutter MG, Burnett RM. Three-dimensional structure of the adenovirus major coat protein hexon. *Science*. 1986;232(4754):1148-51. Epub 1986/05/30. doi: 10.1126/science.3704642. PubMed PMID: 3704642.
79. Valentine RC, Pereira HG. Antigens and structure of the adenovirus. *Journal of molecular biology*. 1965;13(1):13-20. Epub 1965/08/01. doi: 10.1016/s0022-2836(65)80076-6. PubMed PMID: 4955344.

- 80.** van Raaij MJ, Mitraki A, Lavigne G, Cusack S. A triple beta-spiral in the adenovirus fibre shaft reveals a new structural motif for a fibrous protein. *Nature*. 1999;401(6756):935-8. Epub 1999/11/30. doi: 10.1038/44880. PubMed PMID: 10553913.
- 81.** Nicklin SA, Wu E, Nemerow GR, Baker AH. The influence of adenovirus fiber structure and function on vector development for gene therapy. *Molecular therapy : the journal of the American Society of Gene Therapy*. 2005;12(3):384-93. Epub 2005/07/05. doi: 10.1016/j.ymthe.2005.05.008. PubMed PMID: 15993650.
- 82.** Saban SD, Silvestry M, Nemerow GR, Stewart PL. Visualization of alpha-helices in a 6-angstrom resolution cryoelectron microscopy structure of adenovirus allows refinement of capsid protein assignments. *Journal of virology*. 2006;80(24):12049-59. Epub 2006/09/29. doi: 10.1128/JVI.01652-06. PubMed PMID: 17005667; PubMed Central PMCID: PMC1676273.
- 83.** Liu H, Jin L, Koh SB, Atanasov I, Schein S, Wu L, et al. Atomic structure of human adenovirus by cryo-EM reveals interactions among protein networks. *Science*. 2010;329(5995):1038-43. Epub 2010/08/28. doi: 10.1126/science.1187433. PubMed PMID: 20798312; PubMed Central PMCID: PMC3412078.
- 84.** Prage L, Pettersson U, Hoglund S, Lonberg-Holm K, Philipson L. Structural proteins of adenoviruses. IV. Sequential degradation of the adenovirus type 2 virion. *Virology*. 1970;42(2):341-58. Epub 1970/10/01. doi: 10.1016/0042-6822(70)90278-3. PubMed PMID: 4099069.
- 85.** van Oostrum J, Burnett RM. Molecular composition of the adenovirus type 2 virion. *Journal of virology*. 1985;56(2):439-48. Epub 1985/11/01. PubMed PMID: 4057357; PubMed Central PMCID: PMC252598.
- 86.** Colby WW, Shenk T. Adenovirus type 5 virions can be assembled in vivo in the absence of detectable polypeptide IX. *Journal of virology*. 1981;39(3):977-80. Epub 1981/09/01. PubMed PMID: 7288921; PubMed Central PMCID: PMC171335.
- 87.** Ma HC, Hearing P. Adenovirus structural protein IIIa is involved in the serotype specificity of viral DNA packaging. *Journal of virology*. 2011;85(15):7849-55. Epub 2011/06/03. doi: 10.1128/JVI.00467-11. PubMed PMID: 21632753; PubMed Central PMCID: PMC3147925.
- 88.** Russell WC, Precious B. Nucleic acid-binding properties of adenovirus structural polypeptides. *J Gen Virol*. 1982;63 (Pt 1):69-79. Epub 1982/11/01. doi: 10.1099/0022-1317-63-1-69. PubMed PMID: 7175505.

- 89.** Matthews DA, Russell WC. Adenovirus protein-protein interactions: hexon and protein VI. *J Gen Virol.* 1994;75 (Pt 12):3365-74. Epub 1994/12/01. doi: 10.1099/0022-1317-75-12-3365. PubMed PMID: 7996131.
- 90.** Benevento M, Di Palma S, Snijder J, Moyer CL, Reddy VS, Nemerow GR, et al. Adenovirus composition, proteolysis, and disassembly studied by in-depth qualitative and quantitative proteomics. *J Biol Chem.* 2014;289(16):11421-30. Epub 2014/03/05. doi: 10.1074/jbc.M113.537498. PubMed PMID: 24591515; PubMed Central PMCID: PMC4036278.
- 91.** Vayda ME, Rogers AE, Flint SJ. The structure of nucleoprotein cores released from adenovirions. *Nucleic acids research.* 1983;11(2):441-60. Epub 1983/01/25. doi: 10.1093/nar/11.2.441. PubMed PMID: 6828374; PubMed Central PMCID: PMC325724.
- 92.** Lee TWR, Lawrence FJ, Dauksaite V, Akusjarvi G, Blair GE, Matthews DA. Precursor of human adenovirus core polypeptide Mu targets the nucleolus and modulates the expression of E2 proteins. *J Gen Virol.* 2004;85(Pt 1):185-96. Epub 2004/01/14. doi: 10.1099/vir.0.19352-0. PubMed PMID: 14718634.
- 93.** Ostapchuk P, Hearing P. Minimal cis-acting elements required for adenovirus genome packaging. *Journal of virology.* 2003;77(9):5127-35. Epub 2003/04/15. doi: 10.1128/jvi.77.9.5127-5135.2003. PubMed PMID: 12692215; PubMed Central PMCID: PMC153973.
- 94.** Ostapchuk P, Hearing P. Control of adenovirus packaging. *J Cell Biochem.* 2005;96(1):25-35. Epub 2005/07/01. doi: 10.1002/jcb.20523. PubMed PMID: 15988756.
- 95.** Wu K, Guimet D, Hearing P. The adenovirus L4-33K protein regulates both late gene expression patterns and viral DNA packaging. *Journal of virology.* 2013;87(12):6739-47. Epub 2013/04/05. doi: 10.1128/JVI.00652-13. PubMed PMID: 23552425; PubMed Central PMCID: PMC3676125.
- 96.** Mangel WF, San Martin C. Structure, function and dynamics in adenovirus maturation. *Viruses.* 2014;6(11):4536-70. Epub 2014/11/26. doi: 10.3390/v6114536. PubMed PMID: 25421887; PubMed Central PMCID: PMC4246237.
- 97.** Mangel WF, McGrath WJ, Toledo DL, Anderson CW. Viral DNA and a viral peptide can act as cofactors of adenovirus virion proteinase activity. *Nature.* 1993;361(6409):274-5. Epub 1993/01/21. doi: 10.1038/361274a0. PubMed PMID: 8423855.
- 98.** Ostapchuk P, Suomalainen M, Zheng Y, Boucke K, Greber UF, Hearing P. The adenovirus major core protein VII is dispensable for virion assembly but is essential for lytic infection. *PLoS pathogens.* 2017;13(6):e1006455. Epub

2017/06/20. doi: 10.1371/journal.ppat.1006455. PubMed PMID: 28628648; PubMed Central PMCID: PMC5491326.

- 99.** Blainey PC, Graziano V, Perez-Berna AJ, McGrath WJ, Flint SJ, San Martin C, et al. Regulation of a viral proteinase by a peptide and DNA in one-dimensional space: IV. viral proteinase slides along DNA to locate and process its substrates. *J Biol Chem.* 2013;288(3):2092-102. Epub 2012/10/09. doi: 10.1074/jbc.M112.407460. PubMed PMID: 23043138; PubMed Central PMCID: PMC3548515.
- 100.** Mangel WF, Toledo DL, Ding J, Sweet RM, McGrath WJ. Temporal and spatial control of the adenovirus proteinase by both a peptide and the viral DNA. *Trends Biochem Sci.* 1997;22(10):393-8. Epub 1997/11/14. doi: 10.1016/s0968-0004(97)01123-7. PubMed PMID: 9357315.
- 101.** Ruzindana-Umunyana A, Imbeault L, Weber JM. Substrate specificity of adenovirus protease. *Virus research.* 2002;89(1):41-52. Epub 2002/10/09. doi: 10.1016/s0168-1702(02)00111-9. PubMed PMID: 12367749.
- 102.** Chatterjee PK, Vayda ME, Flint SJ. Identification of proteins and protein domains that contact DNA within adenovirus nucleoprotein cores by ultraviolet light crosslinking of oligonucleotides ³²P-labelled in vivo. *Journal of molecular biology.* 1986;188(1):23-37. Epub 1986/03/05. doi: 10.1016/0022-2836(86)90477-8. PubMed PMID: 3712442.
- 103.** Perez-Berna AJ, Ortega-Esteban A, Menendez-Conejero R, Winkler DC, Menendez M, Steven AC, et al. The role of capsid maturation on adenovirus priming for sequential uncoating. *J Biol Chem.* 2012;287(37):31582-95. Epub 2012/07/14. doi: 10.1074/jbc.M112.389957. PubMed PMID: 22791715; PubMed Central PMCID: PMC3438990.
- 104.** Perez-Berna AJ, Marabini R, Scheres SH, Menendez-Conejero R, Dmitriev IP, Curiel DT, et al. Structure and uncoating of immature adenovirus. *Journal of molecular biology.* 2009;392(2):547-57. Epub 2009/07/01. doi: 10.1016/j.jmb.2009.06.057. PubMed PMID: 19563809; PubMed Central PMCID: PMC2749003.
- 105.** Mangel WF, Baniecki ML, McGrath WJ. Specific interactions of the adenovirus proteinase with the viral DNA, an 11-amino-acid viral peptide, and the cellular protein actin. *Cell Mol Life Sci.* 2003;60(11):2347-55. Epub 2003/11/20. doi: 10.1007/s00018-003-2318-2. PubMed PMID: 14625681.
- 106.** Jiang H, White EJ, Gomez-Manzano C, Fueyo J. Adenovirus's last trick: you say lysis, we say autophagy. *Autophagy.* 2008;4(1):118-20. Epub 2007/11/23. doi: 10.4161/auto.5260. PubMed PMID: 18032923.

- 107.** Cohen CJ, Shieh JT, Pickles RJ, Okegawa T, Hsieh JT, Bergelson JM. The coxsackievirus and adenovirus receptor is a transmembrane component of the tight junction. *Proceedings of the National Academy of Sciences of the United States of America*. 2001;98(26):15191-6. Epub 2001/12/06. doi: 10.1073/pnas.261452898. PubMed PMID: 11734628; PubMed Central PMCID: PMC65005.
- 108.** Bergelson JM, Cunningham JA, Droguett G, Kurt-Jones EA, Krithivas A, Hong JS, et al. Isolation of a common receptor for Coxsackie B viruses and adenoviruses 2 and 5. *Science*. 1997;275(5304):1320-3. Epub 1997/02/28. doi: 10.1126/science.275.5304.1320. PubMed PMID: 9036860.
- 109.** Medina-Kauwe LK. Development of adenovirus capsid proteins for targeted therapeutic delivery. *Ther Deliv*. 2013;4(2):267-77. Epub 2013/01/25. doi: 10.4155/tde.12.155. PubMed PMID: 23343164; PubMed Central PMCID: PMC3645976.
- 110.** Cao C, Dong X, Wu X, Wen B, Ji G, Cheng L, et al. Conserved fiber-penton base interaction revealed by nearly atomic resolution cryo-electron microscopy of the structure of adenovirus provides insight into receptor interaction. *Journal of virology*. 2012;86(22):12322-9. Epub 2012/09/07. doi: 10.1128/JVI.01608-12. PubMed PMID: 22951835; PubMed Central PMCID: PMC3486510.
- 111.** Meier O, Boucke K, Hammer SV, Keller S, Stidwill RP, Hemmi S, et al. Adenovirus triggers macropinocytosis and endosomal leakage together with its clathrin-mediated uptake. *J Cell Biol*. 2002;158(6):1119-31. Epub 2002/09/11. doi: 10.1083/jcb.200112067. PubMed PMID: 12221069; PubMed Central PMCID: PMC2173207.
- 112.** Wiethoff CM, Wodrich H, Gerace L, Nemerow GR. Adenovirus protein VI mediates membrane disruption following capsid disassembly. *Journal of virology*. 2005;79(4):1992-2000. Epub 2005/02/01. doi: 10.1128/JVI.79.4.1992-2000.2005. PubMed PMID: 15681401; PubMed Central PMCID: PMC546575.
- 113.** Bremner KH, Scherer J, Yi J, Vershinin M, Gross SP, Vallee RB. Adenovirus transport via direct interaction of cytoplasmic dynein with the viral capsid hexon subunit. *Cell Host Microbe*. 2009;6(6):523-35. Epub 2009/12/17. doi: 10.1016/j.chom.2009.11.006. PubMed PMID: 20006841; PubMed Central PMCID: PMC2810746.
- 114.** Wodrich H, Henaff D, Jammart B, Segura-Morales C, Seelmeir S, Coux O, et al. A capsid-encoded PPxY-motif facilitates adenovirus entry. *PLoS pathogens*. 2010;6(3):e1000808. Epub 2010/03/25. doi: 10.1371/journal.ppat.1000808. PubMed PMID: 20333243; PubMed Central PMCID: PMC2841620.

- 115.** Cassany A, Ragues J, Guan T, Begu D, Wodrich H, Kann M, et al. Nuclear import of adenovirus DNA involves direct interaction of hexon with an N-terminal domain of the nucleoporin Nup214. *Journal of virology*. 2015;89(3):1719-30. Epub 2014/11/21. doi: 10.1128/JVI.02639-14. PubMed PMID: 25410864; PubMed Central PMCID: PMC4300731.
- 116.** Strunze S, Engelke MF, Wang IH, Puntener D, Boucke K, Schleich S, et al. Kinesin-1-mediated capsid disassembly and disruption of the nuclear pore complex promote virus infection. *Cell Host Microbe*. 2011;10(3):210-23. Epub 2011/09/20. doi: 10.1016/j.chom.2011.08.010. PubMed PMID: 21925109.
- 117.** Schreiner S, Martinez R, Groitl P, Rayne F, Vaillant R, Wimmer P, et al. Transcriptional activation of the adenoviral genome is mediated by capsid protein VI. *PLoS pathogens*. 2012;8(2):e1002549. Epub 2012/03/20. doi: 10.1371/journal.ppat.1002549. PubMed PMID: 22427750; PubMed Central PMCID: PMC3303589.
- 118.** Schreiner S, Wimmer P, Sirma H, Everett RD, Blanchette P, Groitl P, et al. Proteasome-dependent degradation of Daxx by the viral E1B-55K protein in human adenovirus-infected cells. *Journal of virology*. 2010;84(14):7029-38. Epub 2010/05/21. doi: 10.1128/JVI.00074-10. PubMed PMID: 20484509; PubMed Central PMCID: PMC2898266.
- 119.** Charman M, Herrmann C, Weitzman MD. Viral and cellular interactions during adenovirus DNA replication. *FEBS Lett*. 2019;593(24):3531-50. Epub 2019/11/26. doi: 10.1002/1873-3468.13695. PubMed PMID: 31764999; PubMed Central PMCID: PMC6928415.
- 120.** Hoeben RC, Uil TG. Adenovirus DNA replication. *Cold Spring Harb Perspect Biol*. 2013;5(3):a013003. Epub 2013/02/08. doi: 10.1101/cshperspect.a013003. PubMed PMID: 23388625; PubMed Central PMCID: PMC3578361.
- 121.** Condezo GN, San Martin C. Localization of adenovirus morphogenesis players, together with visualization of assembly intermediates and failed products, favor a model where assembly and packaging occur concurrently at the periphery of the replication center. *PLoS pathogens*. 2017;13(4):e1006320. Epub 2017/04/28. doi: 10.1371/journal.ppat.1006320. PubMed PMID: 28448571; PubMed Central PMCID: PMC5409498.
- 122.** Howley PM, Knipe DM, Fields BN. *Fields virology*. Place of publication not identified: Place of publication not identified Wolters Kluwer Health/Lippincott Williams & Wilkins; 2007.
- 123.** Chaitanya KV. *Genome and genomics : from archaea to eukaryotes*. 1st ed. 2019. ed. Gateway East, Singapore: Gateway East, Singapore : Springer; 2019.

- 124.** Chirmule N, Propert K, Magosin S, Qian Y, Qian R, Wilson J. Immune responses to adenovirus and adeno-associated virus in humans. *Gene therapy*. 1999;6(9):1574-83. Epub 1999/09/22. doi: 10.1038/sj.gt.3300994. PubMed PMID: 10490767.
- 125.** Mast TC, Kierstead L, Gupta SB, Nikas AA, Kallas EG, Novitsky V, et al. International epidemiology of human pre-existing adenovirus (Ad) type-5, type-6, type-26 and type-36 neutralizing antibodies: correlates of high Ad5 titers and implications for potential HIV vaccine trials. *Vaccine*. 2010;28(4):950-7. Epub 2009/11/21. doi: 10.1016/j.vaccine.2009.10.145. PubMed PMID: 19925902.
- 126.** Khanal S, Ghimire P, Dhamoon AS. The Repertoire of Adenovirus in Human Disease: The Innocuous to the Deadly. *Biomedicines*. 2018;6(1). Epub 2018/03/10. doi: 10.3390/biomedicines6010030. PubMed PMID: 29518985; PubMed Central PMCID: PMC5874687.
- 127.** Koneru B, Atchison R, Jaffe R, Cassavilla A, Van Thiel DH, Starzl TE. Serological studies of adenoviral hepatitis following pediatric liver transplantation. *Transplant Proc*. 1990;22(4):1547-8. Epub 1990/08/01. PubMed PMID: 2167527; PubMed Central PMCID: PMC2975978.
- 128.** Montone KT, Furth EE, Pietra GG, Gupta PK. Neonatal adenovirus infection: a case report with in situ hybridization confirmation of ascending intrauterine infection. *Diagn Cytopathol*. 1995;12(4):341-4. Epub 1995/06/01. doi: 10.1002/dc.2840120411. PubMed PMID: 7656759.
- 129.** Echavarria M. Adenoviruses in immunocompromised hosts. *Clin Microbiol Rev*. 2008;21(4):704-15. Epub 2008/10/16. doi: 10.1128/CMR.00052-07. PubMed PMID: 18854488; PubMed Central PMCID: PMC2570151.
- 130.** Arnberg N. Adenovirus receptors: implications for targeting of viral vectors. *Trends Pharmacol Sci*. 2012;33(8):442-8. Epub 2012/05/25. doi: 10.1016/j.tips.2012.04.005. PubMed PMID: 22621975.
- 131.** Harrach B. Family Adenoviridae. *Virus Taxonomy: 9th Report of the International Committee on Taxonomy of Viruses*. 2011:125-41.
- 132.** Vogels R, Zuijdgheest D, van Rijnsoever R, Hartkoorn E, Damen I, de Bethune MP, et al. Replication-deficient human adenovirus type 35 vectors for gene transfer and vaccination: efficient human cell infection and bypass of preexisting adenovirus immunity. *Journal of virology*. 2003;77(15):8263-71. Epub 2003/07/15. doi: 10.1128/jvi.77.15.8263-8271.2003. PubMed PMID: 12857895; PubMed Central PMCID: PMC165227.
- 133.** Kidd AH, Banatvala JE, de Jong JC. Antibodies to fastidious faecal adenoviruses (species 40 and 41) in sera from children. *J Med Virol*.

- 1983;11(4):333-41. Epub 1983/01/01. doi: 10.1002/jmv.1890110409. PubMed PMID: 6308143.
- 134.** Radke JR, Cook JL. Human adenovirus infections: update and consideration of mechanisms of viral persistence. *Curr Opin Infect Dis.* 2018;31(3):251-6. Epub 2018/03/31. doi: 10.1097/QCO.0000000000000451. PubMed PMID: 29601326; PubMed Central PMCID: PMC6367924.
- 135.** Jones MS, 2nd, Harrach B, Ganac RD, Gozum MM, Dela Cruz WP, Riedel B, et al. New adenovirus species found in a patient presenting with gastroenteritis. *Journal of virology.* 2007;81(11):5978-84. Epub 2007/03/16. doi: 10.1128/JVI.02650-06. PubMed PMID: 17360747; PubMed Central PMCID: PMC1900323.
- 136.** Radin JM, Hawksworth AW, Blair PJ, Faix DJ, Raman R, Russell KL, et al. Dramatic decline of respiratory illness among US military recruits after the renewed use of adenovirus vaccines. *Clinical infectious diseases : an official publication of the Infectious Diseases Society of America.* 2014;59(7):962-8. Epub 2014/07/06. doi: 10.1093/cid/ciu507. PubMed PMID: 24991024.
- 137.** Fu Y, Tang Z, Ye Z, Mo S, Tian X, Ni K, et al. Human adenovirus type 7 infection causes a more severe disease than type 3. *BMC infectious diseases.* 2019;19(1):36. Epub 2019/01/11. doi: 10.1186/s12879-018-3651-2. PubMed PMID: 30626350; PubMed Central PMCID: PMC6327436.
- 138.** Wold WS, Toth K. Adenovirus vectors for gene therapy, vaccination and cancer gene therapy. *Current gene therapy.* 2013;13(6):421-33. Epub 2013/11/28. doi: 10.2174/1566523213666131125095046. PubMed PMID: 24279313; PubMed Central PMCID: PMC4507798.
- 139.** Sudhindra P, Knoll B, Nog R, Singh N, Dhand A. Brincidofovir (CMX001) for the Treatment of Severe Adenoviral Pneumonia in Kidney Transplant Recipient. *Cureus.* 2019;11(8):e5296. Epub 2019/10/04. doi: 10.7759/cureus.5296. PubMed PMID: 31579636; PubMed Central PMCID: PMC6768614.
- 140.** Worgall S, Leopold PL, Wolff G, Ferris B, Van Roijen N, Crystal RG. Role of alveolar macrophages in rapid elimination of adenovirus vectors administered to the epithelial surface of the respiratory tract. *Human gene therapy.* 1997;8(14):1675-84. Epub 1997/10/10. doi: 10.1089/hum.1997.8.14-1675. PubMed PMID: 9322870.
- 141.** Zsengeller Z, Otake K, Hossain SA, Berclaz PY, Trapnell BC. Internalization of adenovirus by alveolar macrophages initiates early proinflammatory signaling during acute respiratory tract infection. *Journal of virology.* 2000;74(20):9655-67. Epub 2000/09/23. doi: 10.1128/jvi.74.20.9655-9667.2000. PubMed PMID: 11000238; PubMed Central PMCID: PMC112398.

- 142.** Shaw AR, Suzuki M. Immunology of Adenoviral Vectors in Cancer Therapy. *Mol Ther Methods Clin Dev.* 2019;15:418-29. Epub 2020/01/01. doi: 10.1016/j.omtm.2019.11.001. PubMed PMID: 31890734; PubMed Central PMCID: PMC6909129.
- 143.** Zhu J, Huang X, Yang Y. Innate immune response to adenoviral vectors is mediated by both Toll-like receptor-dependent and -independent pathways. *Journal of virology.* 2007;81(7):3170-80. Epub 2007/01/19. doi: 10.1128/JVI.02192-06. PubMed PMID: 17229689; PubMed Central PMCID: PMC1866082.
- 144.** Lam E, Falck-Pedersen E. Unabated adenovirus replication following activation of the cGAS/STING-dependent antiviral response in human cells. *Journal of virology.* 2014;88(24):14426-39. Epub 2014/10/10. doi: 10.1128/JVI.02608-14. PubMed PMID: 25297994; PubMed Central PMCID: PMC4249147.
- 145.** Lam E, Stein S, Falck-Pedersen E. Adenovirus detection by the cGAS/STING/TBK1 DNA sensing cascade. *Journal of virology.* 2014;88(2):974-81. Epub 2013/11/08. doi: 10.1128/JVI.02702-13. PubMed PMID: 24198409; PubMed Central PMCID: PMC3911663.
- 146.** Muruve DA, Petrilli V, Zaiss AK, White LR, Clark SA, Ross PJ, et al. The inflammasome recognizes cytosolic microbial and host DNA and triggers an innate immune response. *Nature.* 2008;452(7183):103-7. Epub 2008/02/22. doi: 10.1038/nature06664. PubMed PMID: 18288107.
- 147.** Reich N, Pine R, Levy D, Darnell JE, Jr. Transcription of interferon-stimulated genes is induced by adenovirus particles but is suppressed by E1A gene products. *Journal of virology.* 1988;62(1):114-9. Epub 1988/01/01. PubMed PMID: 2446013; PubMed Central PMCID: PMC250508.
- 148.** Zhao H, Granberg F, Elfineh L, Pettersson U, Svensson C. Strategic attack on host cell gene expression during adenovirus infection. *Journal of virology.* 2003;77(20):11006-15. Epub 2003/09/27. doi: 10.1128/jvi.77.20.11006-11015.2003. PubMed PMID: 14512549; PubMed Central PMCID: PMC224976.
- 149.** Ginsberg HS, Moldawer LL, Prince GA. Role of the type 5 adenovirus gene encoding the early region 1B 55-kDa protein in pulmonary pathogenesis. *Proceedings of the National Academy of Sciences of the United States of America.* 1999;96(18):10409-11. Epub 1999/09/01. doi: 10.1073/pnas.96.18.10409. PubMed PMID: 10468621; PubMed Central PMCID: PMC17901.
- 150.** Thacker EE, Timares L, Matthews QL. Strategies to overcome host immunity to adenovirus vectors in vaccine development. *Expert Rev Vaccines.*

- 2009;8(6):761-77. Epub 2009/06/03. doi: 10.1586/erv.09.29. PubMed PMID: 19485756; PubMed Central PMCID: PMC3700409.
- 151.** Windheim M, Southcombe JH, Kremmer E, Chaplin L, Urlaub D, Falk CS, et al. A unique secreted adenovirus E3 protein binds to the leukocyte common antigen CD45 and modulates leukocyte functions. *Proceedings of the National Academy of Sciences of the United States of America*. 2013;110(50):E4884-93. Epub 2013/11/13. doi: 10.1073/pnas.1312420110. PubMed PMID: 24218549; PubMed Central PMCID: PMC3864294.
- 152.** Leen AM, Sili U, Vanin EF, Jewell AM, Xie W, Vignali D, et al. Conserved CTL epitopes on the adenovirus hexon protein expand subgroup cross-reactive and subgroup-specific CD8+ T cells. *Blood*. 2004;104(8):2432-40. Epub 2004/07/22. doi: 10.1182/blood-2004-02-0646. PubMed PMID: 15265797.
- 153.** Tang J, Olive M, Pulmanausahakul R, Schnell M, Flomenberg N, Eisenlohr L, et al. Human CD8+ cytotoxic T cell responses to adenovirus capsid proteins. *Virology*. 2006;350(2):312-22. Epub 2006/02/28. doi: 10.1016/j.virol.2006.01.024. PubMed PMID: 16499941.
- 154.** Olive M, Eisenlohr L, Flomenberg N, Hsu S, Flomenberg P. The adenovirus capsid protein hexon contains a highly conserved human CD4+ T-cell epitope. *Human gene therapy*. 2002;13(10):1167-78. Epub 2002/07/23. doi: 10.1089/104303402320138952. PubMed PMID: 12133270.
- 155.** Heemskerk B, Veltrop-Duits LA, van Vreeswijk T, ten Dam MM, Heidt S, Toes RE, et al. Extensive cross-reactivity of CD4+ adenovirus-specific T cells: implications for immunotherapy and gene therapy. *Journal of virology*. 2003;77(11):6562-6. Epub 2003/05/14. doi: 10.1128/jvi.77.11.6562-6566.2003. PubMed PMID: 12743315; PubMed Central PMCID: PMC155022.
- 156.** Hutnick NA, Carnathan D, Demers K, Makedonas G, Ertl HC, Betts MR. Adenovirus-specific human T cells are pervasive, polyfunctional, and cross-reactive. *Vaccine*. 2010;28(8):1932-41. Epub 2010/03/02. doi: 10.1016/j.vaccine.2009.10.091. PubMed PMID: 20188249; PubMed Central PMCID: PMC2832841.
- 157.** Sumida SM, Truitt DM, Lemckert AA, Vogels R, Custers JH, Addo MM, et al. Neutralizing antibodies to adenovirus serotype 5 vaccine vectors are directed primarily against the adenovirus hexon protein. *Journal of immunology*. 2005;174(11):7179-85. Epub 2005/05/21. doi: 10.4049/jimmunol.174.11.7179. PubMed PMID: 15905562.
- 158.** Gahery-Segard H, Farace F, Godfrin D, Gaston J, Lengagne R, Tursz T, et al. Immune response to recombinant capsid proteins of adenovirus in humans: antifiber and anti-penton base antibodies have a synergistic effect on

- neutralizing activity. *Journal of virology*. 1998;72(3):2388-97. Epub 1998/03/14. PubMed PMID: 9499099; PubMed Central PMCID: PMC109538.
- 159.** Kagami H, Atkinson JC, Michalek SM, Handelman B, Yu S, Baum BJ, et al. Repetitive adenovirus administration to the parotid gland: role of immunological barriers and induction of oral tolerance. *Human gene therapy*. 1998;9(3):305-13. Epub 1998/03/21. doi: 10.1089/hum.1998.9.3-305. PubMed PMID: 9508048.
- 160.** Wohlfart CE, Svensson UK, Everitt E. Interaction between HeLa cells and adenovirus type 2 virions neutralized by different antisera. *Journal of virology*. 1985;56(3):896-903. Epub 1985/12/01. PubMed PMID: 4068145; PubMed Central PMCID: PMC252662.
- 161.** Smith JG, Cassany A, Gerace L, Ralston R, Nemerow GR. Neutralizing antibody blocks adenovirus infection by arresting microtubule-dependent cytoplasmic transport. *Journal of virology*. 2008;82(13):6492-500. Epub 2008/05/02. doi: 10.1128/JVI.00557-08. PubMed PMID: 18448546; PubMed Central PMCID: PMC2447115.
- 162.** Wohlfart C. Neutralization of adenoviruses: kinetics, stoichiometry, and mechanisms. *Journal of virology*. 1988;62(7):2321-8. Epub 1988/07/01. PubMed PMID: 3373570; PubMed Central PMCID: PMC253388.
- 163.** Kosulin K, Haberler C, Hainfellner JA, Amann G, Lang S, Lion T. Investigation of adenovirus occurrence in pediatric tumor entities. *Journal of virology*. 2007;81(14):7629-35. Epub 2007/05/12. doi: 10.1128/JVI.00355-07. PubMed PMID: 17494079; PubMed Central PMCID: PMC1933336.
- 164.** McAllister RM, Gilden RV, Green M. Adenoviruses in human cancer. *Lancet*. 1972;1(7755):831-3. Epub 1972/04/15. doi: 10.1016/s0140-6736(72)90812-4. PubMed PMID: 4111589.
- 165.** Mackey JK, Rigden PM, Green M. Do highly oncogenic group A human adenoviruses cause human cancer? Analysis of human tumors for adenovirus 12 transforming DNA sequences. *Proceedings of the National Academy of Sciences of the United States of America*. 1976;73(12):4657-61. Epub 1976/12/01. doi: 10.1073/pnas.73.12.4657. PubMed PMID: 1070016; PubMed Central PMCID: PMC431585.
- 166.** Atchison RW, Casto BC, Hammon WM. Adenovirus-Associated Defective Virus Particles. *Science*. 1965;149(3685):754-6. Epub 1965/08/13. doi: 10.1126/science.149.3685.754. PubMed PMID: 14325163.
- 167.** Hoggan MD, Blacklow NR, Rowe WP. Studies of small DNA viruses found in various adenovirus preparations: physical, biological, and immunological characteristics. *Proceedings of the National Academy of Sciences of the United*

- States of America. 1966;55(6):1467-74. Epub 1966/06/01. doi: 10.1073/pnas.55.6.1467. PubMed PMID: 5227666; PubMed Central PMCID: PMC224346.
- 168.** Goncalves MA. Adeno-associated virus: from defective virus to effective vector. *Virology journal*. 2005;2:43. Epub 2005/05/10. doi: 10.1186/1743-422X-2-43. PubMed PMID: 15877812; PubMed Central PMCID: PMC1131931.
- 169.** Georg-Fries B, Biederlack S, Wolf J, zur Hausen H. Analysis of proteins, helper dependence, and seroepidemiology of a new human parvovirus. *Virology*. 1984;134(1):64-71. Epub 1984/04/15. doi: 10.1016/0042-6822(84)90272-1. PubMed PMID: 6200995.
- 170.** Thomson BJ, Weindler FW, Gray D, Schwaab V, Heilbronn R. Human herpesvirus 6 (HHV-6) is a helper virus for adeno-associated virus type 2 (AAV-2) and the AAV-2 rep gene homologue in HHV-6 can mediate AAV-2 DNA replication and regulate gene expression. *Virology*. 1994;204(1):304-11. Epub 1994/10/01. doi: 10.1006/viro.1994.1535. PubMed PMID: 8091661.
- 171.** Buller RM, Janik JE, Sebring ED, Rose JA. Herpes simplex virus types 1 and 2 completely help adenovirus-associated virus replication. *Journal of virology*. 1981;40(1):241-7. Epub 1981/10/01. PubMed PMID: 6270377; PubMed Central PMCID: PMC256613.
- 172.** McPherson RA, Rosenthal LJ, Rose JA. Human cytomegalovirus completely helps adeno-associated virus replication. *Virology*. 1985;147(1):217-22. Epub 1985/11/01. doi: 10.1016/0042-6822(85)90243-0. PubMed PMID: 2998066.
- 173.** Schlehofer JR, Ehrbar M, zur Hausen H. Vaccinia virus, herpes simplex virus, and carcinogens induce DNA amplification in a human cell line and support replication of a helpervirus dependent parvovirus. *Virology*. 1986;152(1):110-7. Epub 1986/07/15. doi: 10.1016/0042-6822(86)90376-4. PubMed PMID: 3012864.
- 174.** You H, Liu Y, Prasad CK, Agrawal N, Zhang D, Bandyopadhyay S, et al. Multiple human papillomavirus genes affect the adeno-associated virus life cycle. *Virology*. 2006;344(2):532-40. Epub 2005/10/06. doi: 10.1016/j.virol.2005.08.039. PubMed PMID: 16203022.
- 175.** Srivastava A. In vivo tissue-tropism of adeno-associated viral vectors. *Curr Opin Virol*. 2016;21:75-80. Epub 2016/09/07. doi: 10.1016/j.coviro.2016.08.003. PubMed PMID: 27596608; PubMed Central PMCID: PMC5138125.
- 176.** Li Y, Ge X, Hon CC, Zhang H, Zhou P, Zhang Y, et al. Prevalence and genetic diversity of adeno-associated viruses in bats from China. *J Gen Virol*.

- 2010;91(Pt 10):2601-9. Epub 2010/06/25. doi: 10.1099/vir.0.020032-0. PubMed PMID: 20573859.
- 177.** Gao G, Vandenberghe LH, Alvira MR, Lu Y, Calcedo R, Zhou X, et al. Clades of Adeno-associated viruses are widely disseminated in human tissues. *Journal of virology*. 2004;78(12):6381-8. Epub 2004/05/28. doi: 10.1128/JVI.78.12.6381-6388.2004. PubMed PMID: 15163731; PubMed Central PMCID: PMC416542.
- 178.** O'Leary NA, Wright MW, Brister JR, Ciufu S, Haddad D, McVeigh R, et al. Reference sequence (RefSeq) database at NCBI: current status, taxonomic expansion, and functional annotation. *Nucleic acids research*. 2016;44(D1):D733-45. Epub 2015/11/11. doi: 10.1093/nar/gkv1189. PubMed PMID: 26553804; PubMed Central PMCID: PMC4702849.
- 179.** Srivastava A, Lusby EW, Berns KI. Nucleotide sequence and organization of the adeno-associated virus 2 genome. *Journal of virology*. 1983;45(2):555-64. Epub 1983/02/01. doi: 10.1128/JVI.45.2.555-564.1983. PubMed PMID: 6300419; PubMed Central PMCID: PMC256449.
- 180.** Feng D, Chen J, Yue Y, Zhu H, Xue J, Jia WW. A 16bp Rep binding element is sufficient for mediating Rep-dependent integration into AAVS1. *Journal of molecular biology*. 2006;358(1):38-45. Epub 2006/03/07. doi: 10.1016/j.jmb.2006.01.029. PubMed PMID: 16516232.
- 181.** Ling C, Wang Y, Lu Y, Wang L, Jayandharan GR, Aslanidi GV, et al. The Adeno-Associated Virus Genome Packaging Puzzle. *J Mol Genet Med*. 2015;9(3). Epub 2016/03/08. doi: 10.4172/1747-0862.1000175. PubMed PMID: 26949410; PubMed Central PMCID: PMC4778740.
- 182.** Wu J, Davis MD, Owens RA. Factors affecting the terminal resolution site endonuclease, helicase, and ATPase activities of adeno-associated virus type 2 Rep proteins. *Journal of virology*. 1999;73(10):8235-44. Epub 1999/09/11. PubMed PMID: 10482574; PubMed Central PMCID: PMC112841.
- 183.** Stutika C, Gogol-Doring A, Botschen L, Mietzsch M, Weger S, Feldkamp M, et al. A Comprehensive RNA Sequencing Analysis of the Adeno-Associated Virus (AAV) Type 2 Transcriptome Reveals Novel AAV Transcripts, Splice Variants, and Derived Proteins. *Journal of virology*. 2016;90(3):1278-89. Epub 2015/11/13. doi: 10.1128/JVI.02750-15. PubMed PMID: 26559843; PubMed Central PMCID: PMC4719636.
- 184.** Collaco RF, Kalman-Maltese V, Smith AD, Dignam JD, Trempe JP. A biochemical characterization of the adeno-associated virus Rep40 helicase. *J Biol Chem*. 2003;278(36):34011-7. Epub 2003/06/26. doi: 10.1074/jbc.M301537200. PubMed PMID: 12824181.

- 185.** Saudan P, Vlach J, Beard P. Inhibition of S-phase progression by adeno-associated virus Rep78 protein is mediated by hypophosphorylated pRb. *EMBO J.* 2000;19(16):4351-61. Epub 2000/08/16. doi: 10.1093/emboj/19.16.4351. PubMed PMID: 10944118; PubMed Central PMCID: PMC302033.
- 186.** Timpe JM, Verrill KC, Black BN, Ding HF, Trempe JP. Adeno-associated virus induces apoptosis during coinfection with adenovirus. *Virology.* 2007;358(2):391-401. Epub 2006/10/03. doi: 10.1016/j.virol.2006.08.042. PubMed PMID: 17011012; PubMed Central PMCID: PMC1839828.
- 187.** Maurer AC, Weitzman MD. Adeno-Associated Virus Genome Interactions Important for Vector Production and Transduction. *Human gene therapy.* 2020;31(9-10):499-511. Epub 2020/04/19. doi: 10.1089/hum.2020.069. PubMed PMID: 32303138.
- 188.** Penaud-Budloo M, Francois A, Clement N, Ayuso E. Pharmacology of Recombinant Adeno-associated Virus Production. *Mol Ther Methods Clin Dev.* 2018;8:166-80. Epub 2018/04/25. doi: 10.1016/j.omtm.2018.01.002. PubMed PMID: 29687035; PubMed Central PMCID: PMC5908265.
- 189.** Hastie E, Samulski RJ. Adeno-associated virus at 50: a golden anniversary of discovery, research, and gene therapy success--a personal perspective. *Human gene therapy.* 2015;26(5):257-65. Epub 2015/03/27. doi: 10.1089/hum.2015.025. PubMed PMID: 25807962; PubMed Central PMCID: PMC4442590.
- 190.** Weitzman MD, Kyostio SR, Kotin RM, Owens RA. Adeno-associated virus (AAV) Rep proteins mediate complex formation between AAV DNA and its integration site in human DNA. *Proceedings of the National Academy of Sciences of the United States of America.* 1994;91(13):5808-12. Epub 1994/06/21. doi: 10.1073/pnas.91.13.5808. PubMed PMID: 8016070; PubMed Central PMCID: PMC44086.
- 191.** Daya S, Cortez N, Berns KI. Adeno-associated virus site-specific integration is mediated by proteins of the nonhomologous end-joining pathway. *Journal of virology.* 2009;83(22):11655-64. Epub 2009/09/18. doi: 10.1128/JVI.01040-09. PubMed PMID: 19759155; PubMed Central PMCID: PMC2772704.
- 192.** Nash K, Chen W, Salganik M, Muzyczka N. Identification of cellular proteins that interact with the adeno-associated virus rep protein. *Journal of virology.* 2009;83(1):454-69. Epub 2008/10/31. doi: 10.1128/JVI.01939-08. PubMed PMID: 18971280; PubMed Central PMCID: PMC2612328.
- 193.** Trempe JP, Carter BJ. Alternate mRNA splicing is required for synthesis of adeno-associated virus VP1 capsid protein. *Journal of virology.*

- 1988;62(9):3356-63. Epub 1988/09/01. doi: 10.1128/JVI.62.9.3356-3363.1988. PubMed PMID: 2841488; PubMed Central PMCID: PMC253458.
- 194.** Agbandje-McKenna M, Kleinschmidt J. AAV capsid structure and cell interactions. *Methods in molecular biology*. 2011;807:47-92. Epub 2011/10/29. doi: 10.1007/978-1-61779-370-7_3. PubMed PMID: 22034026.
- 195.** Rose JA, Maizel JV, Jr., Inman JK, Shatkin AJ. Structural proteins of adenovirus-associated viruses. *Journal of virology*. 1971;8(5):766-70. Epub 1971/11/01. PubMed PMID: 5132697; PubMed Central PMCID: PMC376258.
- 196.** Popa-Wagner R, Porwal M, Kann M, Reuss M, Weimer M, Florin L, et al. Impact of VP1-specific protein sequence motifs on adeno-associated virus type 2 intracellular trafficking and nuclear entry. *Journal of virology*. 2012;86(17):9163-74. Epub 2012/06/15. doi: 10.1128/JVI.00282-12. PubMed PMID: 22696661; PubMed Central PMCID: PMC3416132.
- 197.** Sonntag F, Schmidt K, Kleinschmidt JA. A viral assembly factor promotes AAV2 capsid formation in the nucleolus. *Proceedings of the National Academy of Sciences of the United States of America*. 2010;107(22):10220-5. Epub 2010/05/19. doi: 10.1073/pnas.1001673107. PubMed PMID: 20479244; PubMed Central PMCID: PMC2890453.
- 198.** Earley LF, Powers JM, Adachi K, Baumgart JT, Meyer NL, Xie Q, et al. Adeno-associated Virus (AAV) Assembly-Activating Protein Is Not an Essential Requirement for Capsid Assembly of AAV Serotypes 4, 5, and 11. *Journal of virology*. 2017;91(3). Epub 2016/11/18. doi: 10.1128/JVI.01980-16. PubMed PMID: 27852862; PubMed Central PMCID: PMC5244341.
- 199.** Maurer AC, Pacouret S, Cepeda Diaz AK, Blake J, Andres-Mateos E, Vandenberghe LH. The Assembly-Activating Protein Promotes Stability and Interactions between AAV's Viral Proteins to Nucleate Capsid Assembly. *Cell Rep*. 2018;23(6):1817-30. Epub 2018/05/10. doi: 10.1016/j.celrep.2018.04.026. PubMed PMID: 29742436; PubMed Central PMCID: PMC5983388.
- 200.** Naumer M, Sonntag F, Schmidt K, Nieto K, Panke C, Davey NE, et al. Properties of the adeno-associated virus assembly-activating protein. *Journal of virology*. 2012;86(23):13038-48. Epub 2012/09/28. doi: 10.1128/JVI.01675-12. PubMed PMID: 23015698; PubMed Central PMCID: PMC3497687.
- 201.** Sonntag F, Kother K, Schmidt K, Weghofer M, Raupp C, Nieto K, et al. The assembly-activating protein promotes capsid assembly of different adeno-associated virus serotypes. *Journal of virology*. 2011;85(23):12686-97. Epub 2011/09/16. doi: 10.1128/JVI.05359-11. PubMed PMID: 21917944; PubMed Central PMCID: PMC3209379.

- 202.** Earley LF, Kawano Y, Adachi K, Sun XX, Dai MS, Nakai H. Identification and characterization of nuclear and nucleolar localization signals in the adeno-associated virus serotype 2 assembly-activating protein. *Journal of virology*. 2015;89(6):3038-48. Epub 2015/01/02. doi: 10.1128/JVI.03125-14. PubMed PMID: 25552709; PubMed Central PMCID: PMC4337552.
- 203.** Popa-Wagner R, Sonntag F, Schmidt K, King J, Kleinschmidt JA. Nuclear translocation of adeno-associated virus type 2 capsid proteins for virion assembly. *J Gen Virol*. 2012;93(Pt 9):1887-98. Epub 2012/06/15. doi: 10.1099/vir.0.043232-0. PubMed PMID: 22694902.
- 204.** Romanova L, Grand A, Zhang L, Rayner S, Katoku-Kikyo N, Kellner S, et al. Critical role of nucleostemin in pre-rRNA processing. *J Biol Chem*. 2009;284(8):4968-77. Epub 2008/12/25. doi: 10.1074/jbc.M804594200. PubMed PMID: 19106111; PubMed Central PMCID: PMC2643513.
- 205.** Maurer AC, Cepeda Diaz AK, Vandenberghe LH. Residues on Adeno-associated Virus Capsid Lumen Dictate Interactions and Compatibility with the Assembly-Activating Protein. *Journal of virology*. 2019;93(7). Epub 2019/01/18. doi: 10.1128/JVI.02013-18. PubMed PMID: 30651367; PubMed Central PMCID: PMC6430561.
- 206.** Earley LF. The Role of Assembly-Activating Protein in the Capsid Assembly of Different Adeno-Associated Virus Serotypes [Dissertation]: Oregon Health & Science University; 2016.
- 207.** Ogden PJ, Kelsic ED, Sinai S, Church GM. Comprehensive AAV capsid fitness landscape reveals a viral gene and enables machine-guided design. *Science*. 2019;366(6469):1139-43. Epub 2019/11/30. doi: 10.1126/science.aaw2900. PubMed PMID: 31780559; PubMed Central PMCID: PMC7197022.
- 208.** Pillay S, Zou W, Cheng F, Puschnik AS, Meyer NL, Ganaie SS, et al. Adeno-associated Virus (AAV) Serotypes Have Distinctive Interactions with Domains of the Cellular AAV Receptor. *Journal of virology*. 2017;91(18). Epub 2017/07/07. doi: 10.1128/JVI.00391-17. PubMed PMID: 28679762; PubMed Central PMCID: PMC5571256.
- 209.** Dudek AM, Pillay S, Puschnik AS, Nagamine CM, Cheng F, Qiu J, et al. An Alternate Route for Adeno-associated Virus (AAV) Entry Independent of AAV Receptor. *Journal of virology*. 2018;92(7). Epub 2018/01/19. doi: 10.1128/JVI.02213-17. PubMed PMID: 29343568; PubMed Central PMCID: PMC5972900.
- 210.** Pillay S, Carette JE. Host determinants of adeno-associated viral vector entry. *Curr Opin Virol*. 2017;24:124-31. Epub 2017/07/04. doi:

- 10.1016/j.coviro.2017.06.003. PubMed PMID: 28672171; PubMed Central PMCID: PMC5549665.
- 211.** Pillay S, Meyer NL, Puschnik AS, Davulcu O, Diep J, Ishikawa Y, et al. An essential receptor for adeno-associated virus infection. *Nature*. 2016;530(7588):108-12. Epub 2016/01/28. doi: 10.1038/nature16465. PubMed PMID: 26814968; PubMed Central PMCID: PMC4962915.
- 212.** Johnson JS, Li C, DiPrimio N, Weinberg MS, McCown TJ, Samulski RJ. Mutagenesis of adeno-associated virus type 2 capsid protein VP1 uncovers new roles for basic amino acids in trafficking and cell-specific transduction. *Journal of virology*. 2010;84(17):8888-902. Epub 2010/06/25. doi: 10.1128/JVI.00687-10. PubMed PMID: 20573820; PubMed Central PMCID: PMC2918992.
- 213.** Dudek AM, Zabaleta N, Zinn E, Pillay S, Zengel J, Porter C, et al. GPR108 Is a Highly Conserved AAV Entry Factor. *Molecular therapy : the journal of the American Society of Gene Therapy*. 2020;28(2):367-81. Epub 2019/12/01. doi: 10.1016/j.ymthe.2019.11.005. PubMed PMID: 31784416; PubMed Central PMCID: PMC7000996.
- 214.** Bartlett JS, Wilcher R, Samulski RJ. Infectious entry pathway of adeno-associated virus and adeno-associated virus vectors. *Journal of virology*. 2000;74(6):2777-85. Epub 2000/02/23. doi: 10.1128/jvi.74.6.2777-2785.2000. PubMed PMID: 10684294; PubMed Central PMCID: PMC111768.
- 215.** Sanlioglu S, Benson PK, Yang J, Atkinson EM, Reynolds T, Engelhardt JF. Endocytosis and nuclear trafficking of adeno-associated virus type 2 are controlled by rac1 and phosphatidylinositol-3 kinase activation. *Journal of virology*. 2000;74(19):9184-96. Epub 2000/09/12. doi: 10.1128/jvi.74.19.9184-9196.2000. PubMed PMID: 10982365; PubMed Central PMCID: PMC102117.
- 216.** Nonnenmacher M, Weber T. Adeno-associated virus 2 infection requires endocytosis through the CLIC/GEEC pathway. *Cell Host Microbe*. 2011;10(6):563-76. Epub 2011/12/20. doi: 10.1016/j.chom.2011.10.014. PubMed PMID: 22177561; PubMed Central PMCID: PMC3257174.
- 217.** Xiao PJ, Samulski RJ. Cytoplasmic trafficking, endosomal escape, and perinuclear accumulation of adeno-associated virus type 2 particles are facilitated by microtubule network. *Journal of virology*. 2012;86(19):10462-73. Epub 2012/07/20. doi: 10.1128/JVI.00935-12. PubMed PMID: 22811523; PubMed Central PMCID: PMC3457265.
- 218.** Meyer NL, Hu G, Davulcu O, Xie Q, Noble AJ, Yoshioka C, et al. Structure of the gene therapy vector, adeno-associated virus with its cell receptor, AAVR. *Elife*. 2019;8. Epub 2019/05/23. doi: 10.7554/eLife.44707. PubMed PMID: 31115336; PubMed Central PMCID: PMC6561701.

- 219.** Zhang R, Cao L, Cui M, Sun Z, Hu M, Zhang R, et al. Adeno-associated virus 2 bound to its cellular receptor AAVR. *Nat Microbiol.* 2019;4(4):675-82. Epub 2019/02/12. doi: 10.1038/s41564-018-0356-7. PubMed PMID: 30742069.
- 220.** Nonnenmacher M, Weber T. Intracellular transport of recombinant adeno-associated virus vectors. *Gene therapy.* 2012;19(6):649-58. Epub 2012/02/24. doi: 10.1038/gt.2012.6. PubMed PMID: 22357511; PubMed Central PMCID: PMC4465241.
- 221.** Ding W, Zhang L, Yan Z, Engelhardt JF. Intracellular trafficking of adeno-associated viral vectors. *Gene therapy.* 2005;12(11):873-80. Epub 2005/04/15. doi: 10.1038/sj.gt.3302527. PubMed PMID: 15829993.
- 222.** Vihinen-Ranta M, Kalela A, Makinen P, Kakkola L, Marjomaki V, Vuento M. Intracellular route of canine parvovirus entry. *Journal of virology.* 1998;72(1):802-6. Epub 1998/01/07. doi: 10.1128/JVI.72.1.802-806.1998. PubMed PMID: 9420290; PubMed Central PMCID: PMC109439.
- 223.** Nicolson SC, Samulski RJ. Recombinant adeno-associated virus utilizes host cell nuclear import machinery to enter the nucleus. *Journal of virology.* 2014;88(8):4132-44. Epub 2014/01/31. doi: 10.1128/JVI.02660-13. PubMed PMID: 24478436; PubMed Central PMCID: PMC3993727.
- 224.** Grieger JC, Snowdy S, Samulski RJ. Separate basic region motifs within the adeno-associated virus capsid proteins are essential for infectivity and assembly. *Journal of virology.* 2006;80(11):5199-210. Epub 2006/05/16. doi: 10.1128/JVI.02723-05. PubMed PMID: 16699000; PubMed Central PMCID: PMC1472161.
- 225.** Hoque M, Ishizu K, Matsumoto A, Han SI, Arisaka F, Takayama M, et al. Nuclear transport of the major capsid protein is essential for adeno-associated virus capsid formation. *Journal of virology.* 1999;73(9):7912-5. Epub 1999/08/10. PubMed PMID: 10438891; PubMed Central PMCID: PMC104328.
- 226.** Qiu J, Brown KE. A 110-kDa nuclear shuttle protein, nucleolin, specifically binds to adeno-associated virus type 2 (AAV-2) capsid. *Virology.* 1999;257(2):373-82. Epub 1999/05/18. doi: 10.1006/viro.1999.9664. PubMed PMID: 10329548.
- 227.** Bevington JM, Needham PG, Verrill KC, Collaco RF, Basrur V, Trempe JP. Adeno-associated virus interactions with B23/Nucleophosmin: identification of sub-nucleolar virion regions. *Virology.* 2007;357(1):102-13. Epub 2006/09/09. doi: 10.1016/j.virol.2006.07.050. PubMed PMID: 16959286; PubMed Central PMCID: PMC1829415.
- 228.** Berry GE, Asokan A. Cellular transduction mechanisms of adeno-associated viral vectors. *Curr Opin Virol.* 2016;21:54-60. Epub 2016/08/22. doi:

- 10.1016/j.coviro.2016.08.001. PubMed PMID: 27544821; PubMed Central PMCID: PMC5138113.
- 229.** Koczot FJ, Carter BJ, Garon CF, Rose JA. Self-complementarity of terminal sequences within plus or minus strands of adenovirus-associated virus DNA. *Proceedings of the National Academy of Sciences of the United States of America*. 1973;70(1):215-9. Epub 1973/01/01. doi: 10.1073/pnas.70.1.215. PubMed PMID: 4509654; PubMed Central PMCID: PMC433218.
- 230.** Fife KH, Berns KI, Murray K. Structure and nucleotide sequence of the terminal regions of adeno-associated virus DNA. *Virology*. 1977;78(2):475-7. Epub 1977/05/15. doi: 10.1016/0042-6822(77)90124-6. PubMed PMID: 194395.
- 231.** Tattersall P, Ward DC. Rolling hairpin model for replication of parvovirus and linear chromosomal DNA. *Nature*. 1976;263(5573):106-9. Epub 1976/09/09. doi: 10.1038/263106a0. PubMed PMID: 967244.
- 232.** Nash K, Chen W, Muzyczka N. Complete in vitro reconstitution of adeno-associated virus DNA replication requires the minichromosome maintenance complex proteins. *Journal of virology*. 2008;82(3):1458-64. Epub 2007/12/07. doi: 10.1128/JVI.01968-07. PubMed PMID: 18057257; PubMed Central PMCID: PMC2224442.
- 233.** Nash K, Chen W, McDonald WF, Zhou X, Muzyczka N. Purification of host cell enzymes involved in adeno-associated virus DNA replication. *Journal of virology*. 2007;81(11):5777-87. Epub 2007/03/16. doi: 10.1128/JVI.02651-06. PubMed PMID: 17360744; PubMed Central PMCID: PMC1900299.
- 234.** Ni TH, McDonald WF, Zolotukhin I, Melendy T, Waga S, Stillman B, et al. Cellular proteins required for adeno-associated virus DNA replication in the absence of adenovirus coinfection. *Journal of virology*. 1998;72(4):2777-87. Epub 1998/04/03. PubMed PMID: 9525597; PubMed Central PMCID: PMC109722.
- 235.** Stracker TH, Cassell GD, Ward P, Loo YM, van Breukelen B, Carrington-Lawrence SD, et al. The Rep protein of adeno-associated virus type 2 interacts with single-stranded DNA-binding proteins that enhance viral replication. *Journal of virology*. 2004;78(1):441-53. Epub 2003/12/13. doi: 10.1128/jvi.78.1.441-453.2004. PubMed PMID: 14671124; PubMed Central PMCID: PMC303412.
- 236.** Prindle MJ, Loeb LA. DNA polymerase delta in DNA replication and genome maintenance. *Environ Mol Mutagen*. 2012;53(9):666-82. Epub 2012/10/16. doi: 10.1002/em.21745. PubMed PMID: 23065663; PubMed Central PMCID: PMC3694620.

- 237.** Cruet-Hennequart S, Gallagher K, Sokol AM, Villalan S, Prendergast AM, Carty MP. DNA polymerase eta, a key protein in translesion synthesis in human cells. *Subcell Biochem.* 2010;50:189-209. Epub 2009/12/17. doi: 10.1007/978-90-481-3471-7_10. PubMed PMID: 20012583.
- 238.** Berns KI. Parvovirus replication. *Microbiological reviews.* 1990;54(3):316-29. Epub 1990/09/01. PubMed PMID: 2215424; PubMed Central PMCID: PMC372780.
- 239.** Zhou X, Zolotukhin I, Im DS, Muzyczka N. Biochemical characterization of adeno-associated virus rep68 DNA helicase and ATPase activities. *Journal of virology.* 1999;73(2):1580-90. Epub 1999/01/09. PubMed PMID: 9882364; PubMed Central PMCID: PMC103983.
- 240.** King JA, Dubielzig R, Grimm D, Kleinschmidt JA. DNA helicase-mediated packaging of adeno-associated virus type 2 genomes into preformed capsids. *EMBO J.* 2001;20(12):3282-91. Epub 2001/06/19. doi: 10.1093/emboj/20.12.3282. PubMed PMID: 11406604; PubMed Central PMCID: PMC150213.
- 241.** Yakobson B, Koch T, Winocour E. Replication of adeno-associated virus in synchronized cells without the addition of a helper virus. *Journal of virology.* 1987;61(4):972-81. Epub 1987/04/01. PubMed PMID: 3029431; PubMed Central PMCID: PMC254052.
- 242.** Yakobson B, Hrynko TA, Peak MJ, Winocour E. Replication of adeno-associated virus in cells irradiated with UV light at 254 nm. *Journal of virology.* 1989;63(3):1023-30. Epub 1989/03/01. PubMed PMID: 2536816; PubMed Central PMCID: PMC247794.
- 243.** Nicolas A, Jolinon N, Alazard-Dany N, Barateau V, Epstein AL, Greco A, et al. Factors influencing helper-independent adeno-associated virus replication. *Virology.* 2012;432(1):1-9. Epub 2012/06/26. doi: 10.1016/j.virol.2012.05.027. PubMed PMID: 22727829.
- 244.** Philpott NJ, Giraud-Wali C, Dupuis C, Gomos J, Hamilton H, Berns KI, et al. Efficient integration of recombinant adeno-associated virus DNA vectors requires a p5-rep sequence in cis. *Journal of virology.* 2002;76(11):5411-21. Epub 2002/05/07. doi: 10.1128/jvi.76.11.5411-5421.2002. PubMed PMID: 11991970; PubMed Central PMCID: PMC137060.
- 245.** Vogel R, Seyffert M, Pereira Bde A, Fraefel C. Viral and Cellular Components of AAV2 Replication Compartments. *Open Virol J.* 2013;7:98-120. Epub 2013/11/14. doi: 10.2174/1874357901307010098. PubMed PMID: 24222808; PubMed Central PMCID: PMC3822785.

- 246.** Tratschin JD, West MH, Sandbank T, Carter BJ. A human parvovirus, adeno-associated virus, as a eucaryotic vector: transient expression and encapsidation of the procaryotic gene for chloramphenicol acetyltransferase. *Mol Cell Biol.* 1984;4(10):2072-81. Epub 1984/10/01. doi: 10.1128/mcb.4.10.2072. PubMed PMID: 6095038; PubMed Central PMCID: PMC369024.
- 247.** Pereira DJ, McCarty DM, Muzyczka N. The adeno-associated virus (AAV) Rep protein acts as both a repressor and an activator to regulate AAV transcription during a productive infection. *Journal of virology.* 1997;71(2):1079-88. Epub 1997/02/01. PubMed PMID: 8995628; PubMed Central PMCID: PMC191159.
- 248.** Lackner DF, Muzyczka N. Studies of the mechanism of transactivation of the adeno-associated virus p19 promoter by Rep protein. *Journal of virology.* 2002;76(16):8225-35. Epub 2002/07/23. doi: 10.1128/jvi.76.16.8225-8235.2002. PubMed PMID: 12134028; PubMed Central PMCID: PMC155137.
- 249.** Lee JS, Galvin KM, See RH, Eckner R, Livingston D, Moran E, et al. Relief of YY1 transcriptional repression by adenovirus E1A is mediated by E1A-associated protein p300. *Genes Dev.* 1995;9(10):1188-98. Epub 1995/05/15. doi: 10.1101/gad.9.10.1188. PubMed PMID: 7758944.
- 250.** West MH, Trempe JP, Tratschin JD, Carter BJ. Gene expression in adeno-associated virus vectors: the effects of chimeric mRNA structure, helper virus, and adenovirus VA1 RNA. *Virology.* 1987;160(1):38-47. Epub 1987/09/01. doi: 10.1016/0042-6822(87)90041-9. PubMed PMID: 2820138.
- 251.** Weindler FW, Heilbronn R. A subset of herpes simplex virus replication genes provides helper functions for productive adeno-associated virus replication. *Journal of virology.* 1991;65(5):2476-83. Epub 1991/05/01. PubMed PMID: 1850024; PubMed Central PMCID: PMC240602.
- 252.** Slanina H, Weger S, Stow ND, Kuhrs A, Heilbronn R. Role of the herpes simplex virus helicase-primase complex during adeno-associated virus DNA replication. *Journal of virology.* 2006;80(11):5241-50. Epub 2006/05/16. doi: 10.1128/JVI.02718-05. PubMed PMID: 16699004; PubMed Central PMCID: PMC1472166.
- 253.** Stutika C, Huser D, Weger S, Rutz N, Hessler M, Heilbronn R. Definition of herpes simplex virus helper functions for the replication of adeno-associated virus type 5. *J Gen Virol.* 2015;96(Pt 4):840-50. Epub 2014/12/24. doi: 10.1099/vir.0.000034. PubMed PMID: 25535322.
- 254.** Calcedo R, Vandenberghe LH, Gao G, Lin J, Wilson JM. Worldwide epidemiology of neutralizing antibodies to adeno-associated viruses. *The*

- Journal of infectious diseases. 2009;199(3):381-90. Epub 2009/01/13. doi: 10.1086/595830. PubMed PMID: 19133809.
- 255.** Stilwell JL, Samulski RJ. Adeno-associated virus vectors for therapeutic gene transfer. *Biotechniques*. 2003;34(1):148-50, 52, 54 passim. Epub 2003/01/28. doi: 10.2144/03341dd01. PubMed PMID: 12545552.
- 256.** Wu Z, Asokan A, Samulski RJ. Adeno-associated virus serotypes: vector toolkit for human gene therapy. *Molecular therapy : the journal of the American Society of Gene Therapy*. 2006;14(3):316-27. Epub 2006/07/11. doi: 10.1016/j.ymthe.2006.05.009. PubMed PMID: 16824801.
- 257.** Srivastava A, Carter BJ. AAV Infection: Protection from Cancer. *Human gene therapy*. 2017;28(4):323-7. Epub 2016/11/12. doi: 10.1089/hum.2016.147. PubMed PMID: 27832705; PubMed Central PMCID: PMC5399746.
- 258.** Chen CL, Jensen RL, Schnepf BC, Connell MJ, Shell R, Sferra TJ, et al. Molecular characterization of adeno-associated viruses infecting children. *Journal of virology*. 2005;79(23):14781-92. Epub 2005/11/12. doi: 10.1128/JVI.79.23.14781-14792.2005. PubMed PMID: 16282478; PubMed Central PMCID: PMC1287571.
- 259.** Han L, Parmley TH, Keith S, Kozlowski KJ, Smith LJ, Hermonat PL. High prevalence of adeno-associated virus (AAV) type 2 rep DNA in cervical materials: AAV may be sexually transmitted. *Virus Genes*. 1996;12(1):47-52. Epub 1996/01/01. doi: 10.1007/BF00370000. PubMed PMID: 8879120.
- 260.** Erles K, Rohde V, Thaele M, Roth S, Edler L, Schlehofer JR. DNA of adeno-associated virus (AAV) in testicular tissue and in abnormal semen samples. *Hum Reprod*. 2001;16(11):2333-7. Epub 2001/10/27. doi: 10.1093/humrep/16.11.2333. PubMed PMID: 11679515.
- 261.** Sayyadi-Dehno Z, Seyed Khorrami SM, Ghavami N, Ghotbi-Zadeh F, Khushideh M, Hosseini M, et al. Molecular Detection of Adeno-Associated Virus DNA in Cases of Spontaneous and Therapeutic Abortion. *Fetal Pediatr Pathol*. 2019;38(3):206-14. Epub 2019/03/02. doi: 10.1080/15513815.2019.1576817. PubMed PMID: 30821558.
- 262.** Schlehofer JR, Boeke C, Reuland M, Eggert-Kruse W. Presence of DNA of adeno-associated virus in subfertile couples, but no association with fertility factors. *Hum Reprod*. 2012;27(3):770-8. Epub 2012/01/05. doi: 10.1093/humrep/der427. PubMed PMID: 22215624.
- 263.** Schlehofer JR. The tumor suppressive properties of adeno-associated viruses. *Mutat Res*. 1994;305(2):303-13. Epub 1994/03/01. doi: 10.1016/0027-5107(94)90250-x. PubMed PMID: 7510040.

- 264.** Alam S, Bowser BS, Conway MJ, Israr M, Tandon A, Meyers C. Adeno-associated virus type 2 infection activates caspase dependent and independent apoptosis in multiple breast cancer lines but not in normal mammary epithelial cells. *Mol Cancer*. 2011;10:97. Epub 2011/08/11. doi: 10.1186/1476-4598-10-97. PubMed PMID: 21827643; PubMed Central PMCID: PMC3199901.
- 265.** Fan Y, Sanyal S, Bruzzone R. Breaking Bad: How Viruses Subvert the Cell Cycle. *Front Cell Infect Microbiol*. 2018;8:396. Epub 2018/12/05. doi: 10.3389/fcimb.2018.00396. PubMed PMID: 30510918; PubMed Central PMCID: PMC6252338.
- 266.** Zhan D, Santin AD, Liu Y, Parham GP, Li C, Meyers C, et al. Binding of the human papillomavirus type 16 p97 promoter by the adeno-associated virus Rep78 major regulatory protein correlates with inhibition. *J Biol Chem*. 1999;274(44):31619-24. Epub 1999/10/26. doi: 10.1074/jbc.274.44.31619. PubMed PMID: 10531369.
- 267.** Hermonat PL. The adeno-associated virus Rep78 gene inhibits cellular transformation induced by bovine papillomavirus. *Virology*. 1989;172(1):253-61. Epub 1989/09/01. doi: 10.1016/0042-6822(89)90127-x. PubMed PMID: 2549714.
- 268.** Kokorina NA, Santin AD, Li C, Hermonat PL. Involvement of protein-DNA interaction in adeno-associated virus Rep78-mediated inhibition of HIV-1. *J Hum Virol*. 1998;1(7):441-50. Epub 1999/04/09. PubMed PMID: 10195265.
- 269.** Liu T, Cong M, Wang P, Jia J, Liu Y, Hermonat PL, et al. Adeno-associated virus Rep78 protein inhibits Hepatitis B virus replication through regulation of the HBV core promoter. *Biochemical and biophysical research communications*. 2009;385(1):106-11. Epub 2009/05/05. doi: 10.1016/j.bbrc.2009.04.132. PubMed PMID: 19410559.
- 270.** Raj K, Ogston P, Beard P. Virus-mediated killing of cells that lack p53 activity. *Nature*. 2001;412(6850):914-7. Epub 2001/08/31. doi: 10.1038/35091082. PubMed PMID: 11528480.
- 271.** Nault JC, Datta S, Imbeaud S, Franconi A, Mallet M, Couchy G, et al. Recurrent AAV2-related insertional mutagenesis in human hepatocellular carcinomas. *Nature genetics*. 2015;47(10):1187-93. Epub 2015/08/25. doi: 10.1038/ng.3389. PubMed PMID: 26301494.
- 272.** Donsante A, Miller DG, Li Y, Vogler C, Brunt EM, Russell DW, et al. AAV vector integration sites in mouse hepatocellular carcinoma. *Science*. 2007;317(5837):477. Epub 2007/07/28. doi: 10.1126/science.1142658. PubMed PMID: 17656716.

- 273.** Russell DW, Grompe M. Adeno-associated virus finds its disease. *Nature genetics*. 2015;47(10):1104-5. Epub 2015/09/30. doi: 10.1038/ng.3407. PubMed PMID: 26417859; PubMed Central PMCID: PMC4762592.
- 274.** Berns KI, Byrne BJ, Flotte TR, Gao G, Hauswirth WW, Herzog RW, et al. Adeno-Associated Virus Type 2 and Hepatocellular Carcinoma? *Human gene therapy*. 2015;26(12):779-81. Epub 2015/12/23. doi: 10.1089/hum.2015.29014.kib. PubMed PMID: 26690810; PubMed Central PMCID: PMC4809064.
- 275.** Li C, Narkbunnam N, Samulski RJ, Asokan A, Hu G, Jacobson LJ, et al. Neutralizing antibodies against adeno-associated virus examined prospectively in pediatric patients with hemophilia. *Gene therapy*. 2012;19(3):288-94. Epub 2011/06/24. doi: 10.1038/gt.2011.90. PubMed PMID: 21697954.
- 276.** Boutin S, Monteilhet V, Veron P, Leborgne C, Benveniste O, Montus MF, et al. Prevalence of serum IgG and neutralizing factors against adeno-associated virus (AAV) types 1, 2, 5, 6, 8, and 9 in the healthy population: implications for gene therapy using AAV vectors. *Human gene therapy*. 2010;21(6):704-12. Epub 2010/01/26. doi: 10.1089/hum.2009.182. PubMed PMID: 20095819.
- 277.** Huser D, Khalid D, Lutter T, Hammer EM, Weger S, Hessler M, et al. High Prevalence of Infectious Adeno-associated Virus (AAV) in Human Peripheral Blood Mononuclear Cells Indicative of T Lymphocytes as Sites of AAV Persistence. *Journal of virology*. 2017;91(4). Epub 2016/12/09. doi: 10.1128/JVI.02137-16. PubMed PMID: 27928011; PubMed Central PMCID: PMC5286889.
- 278.** Ronzitti G, Gross DA, Mingozzi F. Human Immune Responses to Adeno-Associated Virus (AAV) Vectors. *Front Immunol*. 2020;11:670. Epub 2020/05/05. doi: 10.3389/fimmu.2020.00670. PubMed PMID: 32362898; PubMed Central PMCID: PMC7181373.
- 279.** Fitzpatrick Z, Leborgne C, Barbon E, Masat E, Ronzitti G, van Wittenberghe L, et al. Influence of Pre-existing Anti-capsid Neutralizing and Binding Antibodies on AAV Vector Transduction. *Mol Ther Methods Clin Dev*. 2018;9:119-29. Epub 2018/05/17. doi: 10.1016/j.omtm.2018.02.003. PubMed PMID: 29766022; PubMed Central PMCID: PMC5948224.
- 280.** Li H, Lasaro MO, Jia B, Lin SW, Haut LH, High KA, et al. Capsid-specific T-cell responses to natural infections with adeno-associated viruses in humans differ from those of nonhuman primates. *Molecular therapy : the journal of the American Society of Gene Therapy*. 2011;19(11):2021-30. Epub 2011/05/19. doi: 10.1038/mt.2011.81. PubMed PMID: 21587208; PubMed Central PMCID: PMC3222540.

- 281.** Kovesdi I, Hedley SJ. Adenoviral producer cells. *Viruses*. 2010;2(8):1681-703. Epub 2010/08/01. doi: 10.3390/v2081681. PubMed PMID: 21994701; PubMed Central PMCID: PMC3185730.
- 282.** Danthinne X, Imperiale MJ. Production of first generation adenovirus vectors: a review. *Gene therapy*. 2000;7(20):1707-14. Epub 2000/11/18. doi: 10.1038/sj.gt.3301301. PubMed PMID: 11083491.
- 283.** Graham FL, Smiley J, Russell WC, Nairn R. Characteristics of a human cell line transformed by DNA from human adenovirus type 5. *J Gen Virol*. 1977;36(1):59-74. Epub 1977/07/01. doi: 10.1099/0022-1317-36-1-59. PubMed PMID: 886304.
- 284.** Louis N, Eveleigh C, Graham FL. Cloning and sequencing of the cellular-viral junctions from the human adenovirus type 5 transformed 293 cell line. *Virology*. 1997;233(2):423-9. Epub 1997/07/07. doi: 10.1006/viro.1997.8597. PubMed PMID: 9217065.
- 285.** Lusky M, Christ M, Rittner K, Dieterle A, Dreyer D, Mourot B, et al. In vitro and in vivo biology of recombinant adenovirus vectors with E1, E1/E2A, or E1/E4 deleted. *Journal of virology*. 1998;72(3):2022-32. Epub 1998/03/14. PubMed PMID: 9499056; PubMed Central PMCID: PMC109495.
- 286.** Hokanson CA, Dora E, Donahue BA, Rivkin M, Finer M, Mendez MJ. Hybrid yeast-bacteria cloning system used to capture and modify adenoviral and nonviral genomes. *Human gene therapy*. 2003;14(4):329-39. Epub 2003/03/28. doi: 10.1089/104303403321208934. PubMed PMID: 12659674.
- 287.** He TC, Zhou S, da Costa LT, Yu J, Kinzler KW, Vogelstein B. A simplified system for generating recombinant adenoviruses. *Proceedings of the National Academy of Sciences of the United States of America*. 1998;95(5):2509-14. Epub 1998/04/16. doi: 10.1073/pnas.95.5.2509. PubMed PMID: 9482916; PubMed Central PMCID: PMC19394.
- 288.** Hardy S, Kitamura M, Harris-Stansil T, Dai Y, Phipps ML. Construction of adenovirus vectors through Cre-lox recombination. *Journal of virology*. 1997;71(3):1842-9. Epub 1997/03/01. doi: 10.1128/JVI.71.3.1842-1849.1997. PubMed PMID: 9032314; PubMed Central PMCID: PMC191254.
- 289.** Alba R, Bosch A, Chillon M. Gutless adenovirus: last-generation adenovirus for gene therapy. *Gene therapy*. 2005;12 Suppl 1:S18-27. Epub 2005/10/19. doi: 10.1038/sj.gt.3302612. PubMed PMID: 16231052.
- 290.** Parks RJ, Chen L, Anton M, Sankar U, Rudnicki MA, Graham FL. A helper-dependent adenovirus vector system: removal of helper virus by Cre-mediated excision of the viral packaging signal. *Proceedings of the National Academy of Sciences of the United States of America*. 1996;93(24):13565-70. Epub

- 1996/11/26. doi: 10.1073/pnas.93.24.13565. PubMed PMID: 8942974; PubMed Central PMCID: PMC19345.
- 291.** Schiedner G, Morral N, Parks RJ, Wu Y, Koopmans SC, Langston C, et al. Genomic DNA transfer with a high-capacity adenovirus vector results in improved in vivo gene expression and decreased toxicity. *Nature genetics*. 1998;18(2):180-3. Epub 1998/02/14. doi: 10.1038/ng0298-180. PubMed PMID: 9462752.
- 292.** Morsy MA, Gu M, Motzel S, Zhao J, Lin J, Su Q, et al. An adenoviral vector deleted for all viral coding sequences results in enhanced safety and extended expression of a leptin transgene. *Proceedings of the National Academy of Sciences of the United States of America*. 1998;95(14):7866-71. Epub 1998/07/08. doi: 10.1073/pnas.95.14.7866. PubMed PMID: 9653106; PubMed Central PMCID: PMC20895.
- 293.** Morral N, Parks RJ, Zhou H, Langston C, Schiedner G, Quinones J, et al. High doses of a helper-dependent adenoviral vector yield supraphysiological levels of alpha1-antitrypsin with negligible toxicity. *Human gene therapy*. 1998;9(18):2709-16. Epub 1999/01/05. doi: 10.1089/hum.1998.9.18-2709. PubMed PMID: 9874269.
- 294.** Saha B, Wong CM, Parks RJ. The adenovirus genome contributes to the structural stability of the virion. *Viruses*. 2014;6(9):3563-83. Epub 2014/09/26. doi: 10.3390/v6093563. PubMed PMID: 25254384; PubMed Central PMCID: PMC4189039.
- 295.** Parks RJ, Graham FL. A helper-dependent system for adenovirus vector production helps define a lower limit for efficient DNA packaging. *Journal of virology*. 1997;71(4):3293-8. Epub 1997/04/01. PubMed PMID: 9060698; PubMed Central PMCID: PMC191467.
- 296.** Bett AJ, Prevec L, Graham FL. Packaging capacity and stability of human adenovirus type 5 vectors. *Journal of virology*. 1993;67(10):5911-21. Epub 1993/10/01. PubMed PMID: 8371349; PubMed Central PMCID: PMC238011.
- 297.** Sandig V, Youil R, Bett AJ, Franlin LL, Oshima M, Maione D, et al. Optimization of the helper-dependent adenovirus system for production and potency in vivo. *Proceedings of the National Academy of Sciences of the United States of America*. 2000;97(3):1002-7. Epub 2000/02/03. doi: 10.1073/pnas.97.3.1002. PubMed PMID: 10655474; PubMed Central PMCID: PMC15501.
- 298.** Parks RJ, Bramson JL, Wan Y, Addison CL, Graham FL. Effects of stuffer DNA on transgene expression from helper-dependent adenovirus vectors. *Journal of virology*. 1999;73(10):8027-34. Epub 1999/09/11. PubMed PMID: 10482551; PubMed Central PMCID: PMC112818.

- 299.** Ng P, Beauchamp C, Eveleigh C, Parks R, Graham FL. Development of a FLP/frt system for generating helper-dependent adenoviral vectors. *Molecular therapy : the journal of the American Society of Gene Therapy*. 2001;3(5 Pt 1):809-15. Epub 2001/05/18. doi: 10.1006/mthe.2001.0323. PubMed PMID: 11356086.
- 300.** Worgall S, Wolff G, Falck-Pedersen E, Crystal RG. Innate immune mechanisms dominate elimination of adenoviral vectors following in vivo administration. *Human gene therapy*. 1997;8(1):37-44. Epub 1997/01/01. doi: 10.1089/hum.1997.8.1-37. PubMed PMID: 8989993.
- 301.** Muruve DA, Barnes MJ, Stillman IE, Libermann TA. Adenoviral gene therapy leads to rapid induction of multiple chemokines and acute neutrophil-dependent hepatic injury in vivo. *Human gene therapy*. 1999;10(6):965-76. Epub 1999/05/01. doi: 10.1089/10430349950018364. PubMed PMID: 10223730.
- 302.** Liu Q, Muruve DA. Molecular basis of the inflammatory response to adenovirus vectors. *Gene therapy*. 2003;10(11):935-40. Epub 2003/05/21. doi: 10.1038/sj.gt.3302036. PubMed PMID: 12756413.
- 303.** Molinier-Frenkel V, Lengagne R, Gaden F, Hong SS, Choppin J, Gahery-Segard H, et al. Adenovirus hexon protein is a potent adjuvant for activation of a cellular immune response. *Journal of virology*. 2002;76(1):127-35. Epub 2001/12/12. doi: 10.1128/jvi.76.1.127-135.2002. PubMed PMID: 11739678; PubMed Central PMCID: PMC135719.
- 304.** Singh R, Al-Jamal KT, Lacerda L, Kostarelos K. Nanoengineering artificial lipid envelopes around adenovirus by self-assembly. *ACS Nano*. 2008;2(5):1040-50. Epub 2009/02/12. doi: 10.1021/nn8000565. PubMed PMID: 19206502.
- 305.** Wang CH, Chan LW, Johnson RN, Chu DS, Shi J, Schellinger JG, et al. The transduction of Coxsackie and Adenovirus Receptor-negative cells and protection against neutralizing antibodies by HPMA-co-oligolysine copolymer-coated adenovirus. *Biomaterials*. 2011;32(35):9536-45. Epub 2011/10/01. doi: 10.1016/j.biomaterials.2011.08.069. PubMed PMID: 21959008; PubMed Central PMCID: PMC3190026.
- 306.** Eto Y, Yoshioka Y, Ishida T, Yao X, Morishige T, Narimatsu S, et al. Optimized PEGylated adenovirus vector reduces the anti-vector humoral immune response against adenovirus and induces a therapeutic effect against metastatic lung cancer. *Biol Pharm Bull*. 2010;33(9):1540-4. Epub 2010/09/09. doi: 10.1248/bpb.33.1540. PubMed PMID: 20823571.
- 307.** Kreppel F, Kochanek S. Modification of adenovirus gene transfer vectors with synthetic polymers: a scientific review and technical guide. *Molecular therapy :*

- the journal of the American Society of Gene Therapy. 2008;16(1):16-29. Epub 2007/10/04. doi: 10.1038/sj.mt.6300321. PubMed PMID: 17912234.
- 308.** Leggiere E, Astone D, Cerullo V, Lombardo B, Mazzaccara C, Labruna G, et al. PEGylated helper-dependent adenoviral vector expressing human Apo A-I for gene therapy in LDLR-deficient mice. *Gene therapy*. 2013;20(12):1124-30. Epub 2013/07/26. doi: 10.1038/gt.2013.38. PubMed PMID: 23883962.
- 309.** Capasso C, Garofalo M, Hirvonen M, Cerullo V. The evolution of adenoviral vectors through genetic and chemical surface modifications. *Viruses*. 2014;6(2):832-55. Epub 2014/02/20. doi: 10.3390/v6020832. PubMed PMID: 24549268; PubMed Central PMCID: PMC3939484.
- 310.** Green NK, Herbert CW, Hale SJ, Hale AB, Mautner V, Harkins R, et al. Extended plasma circulation time and decreased toxicity of polymer-coated adenovirus. *Gene therapy*. 2004;11(16):1256-63. Epub 2004/06/25. doi: 10.1038/sj.gt.3302295. PubMed PMID: 15215884.
- 311.** Yilmazer A, Al-Jamal WT, Van den Bossche J, Kostarelos K. The effect of artificial lipid envelopment of Adenovirus 5 (Ad5) on liver de-targeting and hepatotoxicity. *Biomaterials*. 2013;34(4):1354-63. Epub 2012/11/14. doi: 10.1016/j.biomaterials.2012.10.053. PubMed PMID: 23146432.
- 312.** Hofherr SE, Shashkova EV, Weaver EA, Khare R, Barry MA. Modification of adenoviral vectors with polyethylene glycol modulates in vivo tissue tropism and gene expression. *Molecular therapy : the journal of the American Society of Gene Therapy*. 2008;16(7):1276-82. Epub 2008/05/08. doi: 10.1038/mt.2008.86. PubMed PMID: 18461056.
- 313.** Alba R, Bradshaw AC, Parker AL, Bhella D, Waddington SN, Nicklin SA, et al. Identification of coagulation factor (F)X binding sites on the adenovirus serotype 5 hexon: effect of mutagenesis on FX interactions and gene transfer. *Blood*. 2009;114(5):965-71. Epub 2009/05/12. doi: 10.1182/blood-2009-03-208835. PubMed PMID: 19429866; PubMed Central PMCID: PMC2721791.
- 314.** Alba R, Bradshaw AC, Coughlan L, Denby L, McDonald RA, Waddington SN, et al. Biodistribution and retargeting of FX-binding ablated adenovirus serotype 5 vectors. *Blood*. 2010;116(15):2656-64. Epub 2010/07/09. doi: 10.1182/blood-2009-12-260026. PubMed PMID: 20610817; PubMed Central PMCID: PMC2974579.
- 315.** Zhao Y, Li Y, Wang Q, Wang L, Yang H, Li M. Increased antitumor capability of fiber-modified adenoviral vector armed with TRAIL against bladder cancers. *Mol Cell Biochem*. 2011;353(1-2):93-9. Epub 2011/03/26. doi: 10.1007/s11010-011-0778-5. PubMed PMID: 21437625.

- 316.** Stratford-Perricaudet LD, Levrero M, Chasse JF, Perricaudet M, Briand P. Evaluation of the transfer and expression in mice of an enzyme-encoding gene using a human adenovirus vector. *Human gene therapy*. 1990;1(3):241-56. Epub 1990/01/01. doi: 10.1089/hum.1990.1.3-241. PubMed PMID: 2081192.
- 317.** Rosenfeld MA, Siegfried W, Yoshimura K, Yoneyama K, Fukayama M, Stier LE, et al. Adenovirus-mediated transfer of a recombinant alpha 1-antitrypsin gene to the lung epithelium in vivo. *Science*. 1991;252(5004):431-4. Epub 1991/04/19. doi: 10.1126/science.2017680. PubMed PMID: 2017680.
- 318.** Jaffe HA, Danel C, Longenecker G, Metzger M, Setoguchi Y, Rosenfeld MA, et al. Adenovirus-mediated in vivo gene transfer and expression in normal rat liver. *Nature genetics*. 1992;1(5):372-8. Epub 1992/08/01. doi: 10.1038/ng0892-372. PubMed PMID: 1302034.
- 319.** Crystal RG, McElvaney NG, Rosenfeld MA, Chu CS, Mastrangeli A, Hay JG, et al. Administration of an adenovirus containing the human CFTR cDNA to the respiratory tract of individuals with cystic fibrosis. *Nature genetics*. 1994;8(1):42-51. Epub 1994/09/01. doi: 10.1038/ng0994-42. PubMed PMID: 7527271.
- 320.** Crystal RG. Adenovirus: the first effective in vivo gene delivery vector. *Human gene therapy*. 2014;25(1):3-11. Epub 2014/01/22. doi: 10.1089/hum.2013.2527. PubMed PMID: 24444179; PubMed Central PMCID: PMC3900005.
- 321.** Zuckerman JB, Robinson CB, McCoy KS, Shell R, Sferra TJ, Chirmule N, et al. A phase I study of adenovirus-mediated transfer of the human cystic fibrosis transmembrane conductance regulator gene to a lung segment of individuals with cystic fibrosis. *Human gene therapy*. 1999;10(18):2973-85. Epub 1999/12/28. doi: 10.1089/10430349950016384. PubMed PMID: 10609658.
- 322.** Zabner J, Couture LA, Gregory RJ, Graham SM, Smith AE, Welsh MJ. Adenovirus-mediated gene transfer transiently corrects the chloride transport defect in nasal epithelia of patients with cystic fibrosis. *Cell*. 1993;75(2):207-16. Epub 1993/10/22. doi: 10.1016/0092-8674(93)80063-k. PubMed PMID: 7691415.
- 323.** Brunetti-Pierrri N, Ng P. Helper-dependent adenoviral vectors for liver-directed gene therapy. *Human molecular genetics*. 2011;20(R1):R7-13. Epub 2011/04/08. doi: 10.1093/hmg/ddr143. PubMed PMID: 21470977; PubMed Central PMCID: PMC3095052.
- 324.** Raper SE, Chirmule N, Lee FS, Wivel NA, Bagg A, Gao GP, et al. Fatal systemic inflammatory response syndrome in a ornithine transcarbamylase deficient patient following adenoviral gene transfer. *Mol Genet Metab*.

- 2003;80(1-2):148-58. Epub 2003/10/22. doi: 10.1016/j.ymgme.2003.08.016. PubMed PMID: 14567964.
- 325.** Sibbald B. Death but one unintended consequence of gene-therapy trial. *CMAJ*. 2001;164(11):1612. Epub 2001/06/14. PubMed PMID: 11402803; PubMed Central PMCID: PMC81135.
- 326.** Rinde M. The Death of Jesse Gelsinger, 20 Years Later <https://www.sciencehistory.org/distillations/the-death-of-jesse-gelsinger-20-years-later>: Science History Institute; 2019.
- 327.** Gelsinger P, Shamo AE. Eight years after Jesse 's death, are human research subjects any safer? *Hastings Cent Rep*. 2008;38(2):25-7. Epub 2008/05/07. doi: 10.1353/hcr.2008.0022. PubMed PMID: 18457225.
- 328.** Steinbrook R. The Gelsinger Case - The Oxford textbook of clinical research ethics. Emanuel EJ, editor. Oxford ; New York: Oxford University Press; 2008. xx, 827 p. p.
- 329.** Alemany R. Oncolytic Adenoviruses in Cancer Treatment. *Biomedicines*. 2014;2(1):36-49. Epub 2014/02/21. doi: 10.3390/biomedicines2010036. PubMed PMID: 28548059; PubMed Central PMCID: PMC5423481.
- 330.** Rein DT, Breidenbach M, Curiel DT. Current developments in adenovirus-based cancer gene therapy. *Future Oncol*. 2006;2(1):137-43. Epub 2006/03/25. doi: 10.2217/14796694.2.1.137. PubMed PMID: 16556080; PubMed Central PMCID: PMC1781528.
- 331.** Thorsteinsson L, O'Dowd GM, Harrington PM, Johnson PM. The complement regulatory proteins CD46 and CD59, but not CD55, are highly expressed by glandular epithelium of human breast and colorectal tumour tissues. *APMIS*. 1998;106(9):869-78. Epub 1998/11/10. doi: 10.1111/j.1699-0463.1998.tb00233.x. PubMed PMID: 9808413.
- 332.** Wang H, Li ZY, Liu Y, Persson J, Beyer I, Moller T, et al. Desmoglein 2 is a receptor for adenovirus serotypes 3, 7, 11 and 14. *Nature medicine*. 2011;17(1):96-104. Epub 2010/12/15. doi: 10.1038/nm.2270. PubMed PMID: 21151137; PubMed Central PMCID: PMC3074512.
- 333.** Bauerschmitz GJ, Lam JT, Kanerva A, Suzuki K, Nettelbeck DM, Dmitriev I, et al. Treatment of ovarian cancer with a tropism modified oncolytic adenovirus. *Cancer research*. 2002;62(5):1266-70. Epub 2002/03/13. PubMed PMID: 11888888.
- 334.** Dmitriev I, Krasnykh V, Miller CR, Wang M, Kashentseva E, Mikheeva G, et al. An adenovirus vector with genetically modified fibers demonstrates expanded tropism via utilization of a coxsackievirus and adenovirus receptor-independent cell entry mechanism. *Journal of virology*. 1998;72(12):9706-13.

- Epub 1998/11/13. PubMed PMID: 9811704; PubMed Central PMCID: PMC110480.
- 335.** Shashkova EV, May SM, Doronin K, Barry MA. Expanded anticancer therapeutic window of hexon-modified oncolytic adenovirus. *Molecular therapy : the journal of the American Society of Gene Therapy*. 2009;17(12):2121-30. Epub 2009/09/17. doi: 10.1038/mt.2009.217. PubMed PMID: 19755961; PubMed Central PMCID: PMC2814381.
- 336.** Lucas T, Benihoud K, Vigant F, Schmidt CQ, Wortmann A, Bachem MG, et al. Hexon modification to improve the activity of oncolytic adenovirus vectors against neoplastic and stromal cells in pancreatic cancer. *PLoS one*. 2015;10(2):e0117254. Epub 2015/02/19. doi: 10.1371/journal.pone.0117254. PubMed PMID: 25692292; PubMed Central PMCID: PMC4332860.
- 337.** Xu RH, Yuan ZY, Guan ZZ, Cao Y, Wang HQ, Hu XH, et al. [Phase II clinical study of intratumoral H101, an E1B deleted adenovirus, in combination with chemotherapy in patients with cancer]. *Ai Zheng*. 2003;22(12):1307-10. Epub 2003/12/25. PubMed PMID: 14693057.
- 338.** Heise C, Sampson-Johannes A, Williams A, McCormick F, Von Hoff DD, Kirn DH. ONYX-015, an E1B gene-attenuated adenovirus, causes tumor-specific cytolysis and antitumoral efficacy that can be augmented by standard chemotherapeutic agents. *Nature medicine*. 1997;3(6):639-45. Epub 1997/06/01. doi: 10.1038/nm0697-639. PubMed PMID: 9176490.
- 339.** Gomez-Manzano C, Yung WK, Alemany R, Fueyo J. Genetically modified adenoviruses against gliomas: from bench to bedside. *Neurology*. 2004;63(3):418-26. Epub 2004/08/12. doi: 10.1212/01.wnl.0000133302.15022.7f. PubMed PMID: 15304571.
- 340.** Fueyo J, Gomez-Manzano C, Alemany R, Lee PS, McDonnell TJ, Mitlianga P, et al. A mutant oncolytic adenovirus targeting the Rb pathway produces anti-glioma effect in vivo. *Oncogene*. 2000;19(1):2-12. Epub 2000/01/25. doi: 10.1038/sj.onc.1203251. PubMed PMID: 10644974.
- 341.** Bortolanza S, Bunuales M, Alzuguren P, Lamas O, Aldabe R, Prieto J, et al. Deletion of the E3-6.7K/gp19K region reduces the persistence of wild-type adenovirus in a permissive tumor model in Syrian hamsters. *Cancer gene therapy*. 2009;16(9):703-12. Epub 2009/02/21. doi: 10.1038/cgt.2009.12. PubMed PMID: 19229289.
- 342.** Man YKS, Davies JA, Coughlan L, Pantelidou C, Blazquez-Moreno A, Marshall JF, et al. The Novel Oncolytic Adenoviral Mutant Ad5-3Delta-A20T Retargeted to alphavbeta6 Integrins Efficiently Eliminates Pancreatic Cancer Cells. *Mol Cancer Ther*. 2018;17(2):575-87. Epub 2018/01/26. doi: 10.1158/1535-7163.MCT-17-0671. PubMed PMID: 29367266.

- 343.** McSharry BP, Burgert HG, Owen DP, Stanton RJ, Prod'homme V, Sester M, et al. Adenovirus E3/19K promotes evasion of NK cell recognition by intracellular sequestration of the NKG2D ligands major histocompatibility complex class I chain-related proteins A and B. *Journal of virology*. 2008;82(9):4585-94. Epub 2008/02/22. doi: 10.1128/JVI.02251-07. PubMed PMID: 18287244; PubMed Central PMCID: PMC2293069.
- 344.** Alemany R, Balague C, Curiel DT. Replicative adenoviruses for cancer therapy. *Nature biotechnology*. 2000;18(7):723-7. Epub 2000/07/11. doi: 10.1038/77283. PubMed PMID: 10888838.
- 345.** Bressy C, Benihoud K. Association of oncolytic adenoviruses with chemotherapies: an overview and future directions. *Biochem Pharmacol*. 2014;90(2):97-106. Epub 2014/05/17. doi: 10.1016/j.bcp.2014.05.003. PubMed PMID: 24832861.
- 346.** Koski A, Kangasniemi L, Escutenaire S, Pesonen S, Cerullo V, Diaconu I, et al. Treatment of cancer patients with a serotype 5/3 chimeric oncolytic adenovirus expressing GM-CSF. *Molecular therapy : the journal of the American Society of Gene Therapy*. 2010;18(10):1874-84. Epub 2010/07/29. doi: 10.1038/mt.2010.161. PubMed PMID: 20664527; PubMed Central PMCID: PMC2951567.
- 347.** Kuryk L, Vassilev L, Ranki T, Hemminki A, Karioja-Kallio A, Levalampi O, et al. Toxicological and bio-distribution profile of a GM-CSF-expressing, double-targeted, chimeric oncolytic adenovirus ONCOS-102 - Support for clinical studies on advanced cancer treatment. *PloS one*. 2017;12(8):e0182715. Epub 2017/08/11. doi: 10.1371/journal.pone.0182715. PubMed PMID: 28796812; PubMed Central PMCID: PMC5552138.
- 348.** Chang J, Zhao X, Wu X, Guo Y, Guo H, Cao J, et al. A Phase I study of KH901, a conditionally replicating granulocyte-macrophage colony-stimulating factor: armed oncolytic adenovirus for the treatment of head and neck cancers. *Cancer Biol Ther*. 2009;8(8):676-82. Epub 2009/02/27. doi: 10.4161/cbt.8.8.7913. PubMed PMID: 19242097.
- 349.** Bernt KM, Ni S, Tieu AT, Lieber A. Assessment of a combined, adenovirus-mediated oncolytic and immunostimulatory tumor therapy. *Cancer research*. 2005;65(10):4343-52. Epub 2005/05/19. doi: 10.1158/0008-5472.CAN-04-3527. PubMed PMID: 15899826.
- 350.** Baker AT, Aguirre-Hernandez C, Hallden G, Parker AL. Designer Oncolytic Adenovirus: Coming of Age. *Cancers (Basel)*. 2018;10(6). Epub 2018/06/16. doi: 10.3390/cancers10060201. PubMed PMID: 29904022; PubMed Central PMCID: PMC6025169.

- 351.** Cerullo V, Diaconu I, Romano V, Hirvinen M, Ugolini M, Escutenaire S, et al. An oncolytic adenovirus enhanced for toll-like receptor 9 stimulation increases antitumor immune responses and tumor clearance. *Molecular therapy : the journal of the American Society of Gene Therapy*. 2012;20(11):2076-86. Epub 2012/07/26. doi: 10.1038/mt.2012.137. PubMed PMID: 22828500; PubMed Central PMCID: PMC3498796.
- 352.** Diaconu I, Cerullo V, Hirvinen ML, Escutenaire S, Ugolini M, Pesonen SK, et al. Immune response is an important aspect of the antitumor effect produced by a CD40L-encoding oncolytic adenovirus. *Cancer research*. 2012;72(9):2327-38. Epub 2012/03/08. doi: 10.1158/0008-5472.CAN-11-2975. PubMed PMID: 22396493.
- 353.** Pesonen S, Diaconu I, Kangasniemi L, Ranki T, Kanerva A, Pesonen SK, et al. Oncolytic immunotherapy of advanced solid tumors with a CD40L-expressing replicating adenovirus: assessment of safety and immunologic responses in patients. *Cancer research*. 2012;72(7):1621-31. Epub 2012/02/11. doi: 10.1158/0008-5472.CAN-11-3001. PubMed PMID: 22323527.
- 354.** Tatsis N, Fitzgerald JC, Reyes-Sandoval A, Harris-McCoy KC, Hensley SE, Zhou D, et al. Adenoviral vectors persist in vivo and maintain activated CD8+ T cells: implications for their use as vaccines. *Blood*. 2007;110(6):1916-23. Epub 2007/05/19. doi: 10.1182/blood-2007-02-062117. PubMed PMID: 17510320; PubMed Central PMCID: PMC1976365.
- 355.** Quinn KM, Zak DE, Costa A, Yamamoto A, Kastenmuller K, Hill BJ, et al. Antigen expression determines adenoviral vaccine potency independent of IFN and STING signaling. *J Clin Invest*. 2015;125(3):1129-46. Epub 2015/02/03. doi: 10.1172/JCI78280. PubMed PMID: 25642773; PubMed Central PMCID: PMC4362254.
- 356.** Ewer KJ, Lambe T, Rollier CS, Spencer AJ, Hill AV, Dorrell L. Viral vectors as vaccine platforms: from immunogenicity to impact. *Curr Opin Immunol*. 2016;41:47-54. Epub 2016/06/11. doi: 10.1016/j.coi.2016.05.014. PubMed PMID: 27286566.
- 357.** Morelli AE, Larregina AT, Ganster RW, Zahorchak AF, Plowey JM, Takayama T, et al. Recombinant adenovirus induces maturation of dendritic cells via an NF-kappaB-dependent pathway. *Journal of virology*. 2000;74(20):9617-28. Epub 2000/09/23. doi: 10.1128/jvi.74.20.9617-9628.2000. PubMed PMID: 11000234; PubMed Central PMCID: PMC112394.
- 358.** Rea D, Schagen FH, Hoeben RC, Mehtali M, Havenga MJ, Toes RE, et al. Adenoviruses activate human dendritic cells without polarization toward a T-helper type 1-inducing subset. *Journal of virology*. 1999;73(12):10245-53.

- Epub 1999/11/13. doi: 10.1128/JVI.73.12.10245-10253.1999. PubMed PMID: 10559341; PubMed Central PMCID: PMC113078.
- 359.** Butterfield LH, Vujanovic L. New approaches to the development of adenoviral dendritic cell vaccines in melanoma. *Curr Opin Investig Drugs*. 2010;11(12):1399-408. Epub 2010/12/15. PubMed PMID: 21154122; PubMed Central PMCID: PMC3758558.
- 360.** Tiburcio R, Nunes S, Nunes I, Rosa Ampuero M, Silva IB, Lima R, et al. Molecular Aspects of Dendritic Cell Activation in Leishmaniasis: An Immunobiological View. *Front Immunol*. 2019;10:227. Epub 2019/03/16. doi: 10.3389/fimmu.2019.00227. PubMed PMID: 30873156; PubMed Central PMCID: PMC6401646.
- 361.** Tangye SG, Ferguson A, Avery DT, Ma CS, Hodgkin PD. Isotype switching by human B cells is division-associated and regulated by cytokines. *Journal of immunology*. 2002;169(8):4298-306. Epub 2002/10/09. doi: 10.4049/jimmunol.169.8.4298. PubMed PMID: 12370361.
- 362.** Saito I, Oya Y, Yamamoto K, Yuasa T, Shimojo H. Construction of nondefective adenovirus type 5 bearing a 2.8-kilobase hepatitis B virus DNA near the right end of its genome. *Journal of virology*. 1985;54(3):711-9. Epub 1985/06/01. PubMed PMID: 3999192; PubMed Central PMCID: PMC254856.
- 363.** Morin JE, Lubeck MD, Barton JE, Conley AJ, Davis AR, Hung PP. Recombinant adenovirus induces antibody response to hepatitis B virus surface antigen in hamsters. *Proceedings of the National Academy of Sciences of the United States of America*. 1987;84(13):4626-30. Epub 1987/07/01. doi: 10.1073/pnas.84.13.4626. PubMed PMID: 2955413; PubMed Central PMCID: PMC305143.
- 364.** Teigler JE, Iampietro MJ, Barouch DH. Vaccination with adenovirus serotypes 35, 26, and 48 elicits higher levels of innate cytokine responses than adenovirus serotype 5 in rhesus monkeys. *Journal of virology*. 2012;86(18):9590-8. Epub 2012/07/13. doi: 10.1128/JVI.00740-12. PubMed PMID: 22787208; PubMed Central PMCID: PMC3446581.
- 365.** Cheng C, Wang L, Ko SY, Kong WP, Schmidt SD, Gall JGD, et al. Combination recombinant simian or chimpanzee adenoviral vectors for vaccine development. *Vaccine*. 2015;33(51):7344-51. Epub 2015/10/31. doi: 10.1016/j.vaccine.2015.10.023. PubMed PMID: 26514419.
- 366.** Bangari DS, Mittal SK. Development of nonhuman adenoviruses as vaccine vectors. *Vaccine*. 2006;24(7):849-62. Epub 2005/11/22. doi: 10.1016/j.vaccine.2005.08.101. PubMed PMID: 16297508; PubMed Central PMCID: PMC1462960.

- 367.** Bouet-Cararo C, Contreras V, Fournier A, Jallet C, Guibert JM, Dubois E, et al. Canine adenoviruses elicit both humoral and cell-mediated immune responses against rabies following immunisation of sheep. *Vaccine*. 2011;29(6):1304-10. Epub 2010/12/08. doi: 10.1016/j.vaccine.2010.11.068. PubMed PMID: 21134446.
- 368.** Zhang C, Zhou D. Adenoviral vector-based strategies against infectious disease and cancer. *Hum Vaccin Immunother*. 2016;12(8):2064-74. Epub 2016/04/23. doi: 10.1080/21645515.2016.1165908. PubMed PMID: 27105067; PubMed Central PMCID: PMC4994731.
- 369.** Lopez-Gordo E, Podgorski, II, Downes N, Alemany R. Circumventing antivector immunity: potential use of nonhuman adenoviral vectors. *Human gene therapy*. 2014;25(4):285-300. Epub 2014/02/07. doi: 10.1089/hum.2013.228. PubMed PMID: 24499174; PubMed Central PMCID: PMC3997092.
- 370.** Priddy FH, Brown D, Kublin J, Monahan K, Wright DP, Lalezari J, et al. Safety and immunogenicity of a replication-incompetent adenovirus type 5 HIV-1 clade B gag/pol/nef vaccine in healthy adults. *Clinical infectious diseases : an official publication of the Infectious Diseases Society of America*. 2008;46(11):1769-81. Epub 2008/04/25. doi: 10.1086/587993. PubMed PMID: 18433307.
- 371.** Gray GE, Allen M, Moodie Z, Churchyard G, Bekker LG, Nchabeleng M, et al. Safety and efficacy of the HVTN 503/Phambili study of a clade-B-based HIV-1 vaccine in South Africa: a double-blind, randomised, placebo-controlled test-of-concept phase 2b study. *Lancet Infect Dis*. 2011;11(7):507-15. Epub 2011/05/17. doi: 10.1016/S1473-3099(11)70098-6. PubMed PMID: 21570355; PubMed Central PMCID: PMC3417349.
- 372.** Buchbinder SP, Mehrotra DV, Duerr A, Fitzgerald DW, Mogg R, Li D, et al. Efficacy assessment of a cell-mediated immunity HIV-1 vaccine (the Step Study): a double-blind, randomised, placebo-controlled, test-of-concept trial. *Lancet*. 2008;372(9653):1881-93. Epub 2008/11/18. doi: 10.1016/S0140-6736(08)61591-3. PubMed PMID: 19012954; PubMed Central PMCID: PMC2721012.
- 373.** Corey L, McElrath MJ, Kublin JG. Post-step modifications for research on HIV vaccines. *AIDS*. 2009;23(1):3-8. Epub 2008/12/04. doi: 10.1097/QAD.0b013e32830e6d6d. PubMed PMID: 19050380; PubMed Central PMCID: PMC2720076.
- 374.** Hammer SM, Sobieszczyk ME, Janes H, Karuna ST, Mulligan MJ, Grove D, et al. Efficacy trial of a DNA/rAd5 HIV-1 preventive vaccine. *The New England journal of medicine*. 2013;369(22):2083-92. Epub 2013/10/09. doi:

- 10.1056/NEJMoa1310566. PubMed PMID: 24099601; PubMed Central PMCID: PMC4030634.
- 375.** Koup RA, Roederer M, Lamoreaux L, Fischer J, Novik L, Nason MC, et al. Priming immunization with DNA augments immunogenicity of recombinant adenoviral vectors for both HIV-1 specific antibody and T-cell responses. *PLoS one*. 2010;5(2):e9015. Epub 2010/02/04. doi: 10.1371/journal.pone.0009015. PubMed PMID: 20126394; PubMed Central PMCID: PMC2814848.
- 376.** Churchyard GJ, Morgan C, Adams E, Hural J, Graham BS, Moodie Z, et al. A phase IIA randomized clinical trial of a multiclade HIV-1 DNA prime followed by a multiclade rAd5 HIV-1 vaccine boost in healthy adults (HVTN204). *PLoS one*. 2011;6(8):e21225. Epub 2011/08/23. doi: 10.1371/journal.pone.0021225. PubMed PMID: 21857901; PubMed Central PMCID: PMC3152265.
- 377.** Baden LR, Liu J, Li H, Johnson JA, Walsh SR, Kleinjan JA, et al. Induction of HIV-1-specific mucosal immune responses following intramuscular recombinant adenovirus serotype 26 HIV-1 vaccination of humans. *The Journal of infectious diseases*. 2015;211(4):518-28. Epub 2014/08/29. doi: 10.1093/infdis/jiu485. PubMed PMID: 25165165; PubMed Central PMCID: PMC4318919.
- 378.** Fuchs JD, Bart PA, Frahm N, Morgan C, Gilbert PB, Kochar N, et al. Safety and Immunogenicity of a Recombinant Adenovirus Serotype 35-Vectored HIV-1 Vaccine in Adenovirus Serotype 5 Seronegative and Seropositive Individuals. *J AIDS Clin Res*. 2015;6(5). Epub 2015/11/21. doi: 10.4172/2155-6113.1000461. PubMed PMID: 26587311; PubMed Central PMCID: PMC4648371.
- 379.** Tatsis N, Ertl HC. Adenoviruses as vaccine vectors. *Molecular therapy : the journal of the American Society of Gene Therapy*. 2004;10(4):616-29. Epub 2004/09/29. doi: 10.1016/j.yymthe.2004.07.013. PubMed PMID: 15451446; PubMed Central PMCID: PMC7106330.
- 380.** Wang C, Dulal P, Zhou X, Xiang Z, Goharriz H, Banyard A, et al. A simian-adenovirus-vectored rabies vaccine suitable for thermostabilisation and clinical development for low-cost single-dose pre-exposure prophylaxis. *PLoS Negl Trop Dis*. 2018;12(10):e0006870. Epub 2018/10/30. doi: 10.1371/journal.pntd.0006870. PubMed PMID: 30372438; PubMed Central PMCID: PMC6224154 development of the ChAdOx2 vector. AVSH and SJD are named inventors on a patent relating to the use of the intron-containing promoter used in ChAdOx2 RabG. The University of Oxford and the Wistar Institute have entered into a partnership to share any future revenue from development of the ChAdOx2 RabG vaccine.
- 381.** McCoy K, Tatsis N, Koriath-Schmitz B, Lasaro MO, Hensley SE, Lin SW, et al. Effect of preexisting immunity to adenovirus human serotype 5 antigens on

- the immune responses of nonhuman primates to vaccine regimens based on human- or chimpanzee-derived adenovirus vectors. *Journal of virology*. 2007;81(12):6594-604. Epub 2007/04/13. doi: 10.1128/JVI.02497-06. PubMed PMID: 17428852; PubMed Central PMCID: PMC1900096.
- 382.** Choi J, Yang DK, Kim HH, Jo HY, Choi SS, Kim JT, et al. Application of recombinant adenoviruses expressing glycoprotein or nucleoprotein of rabies virus to Korean raccoon dogs. *Clin Exp Vaccine Res*. 2015;4(2):189-94. Epub 2015/08/15. doi: 10.7774/cevr.2015.4.2.189. PubMed PMID: 26273578; PubMed Central PMCID: PMC4524904.
- 383.** Hampson K, Coudeville L, Lembo T, Sambo M, Kieffer A, Atflan M, et al. Estimating the global burden of endemic canine rabies. *PLoS Negl Trop Dis*. 2015;9(4):e0003709. Epub 2015/04/17. doi: 10.1371/journal.pntd.0003709. PubMed PMID: 25881058; PubMed Central PMCID: PMC4400070.
- 384.** Ignatyev GM, Agafonov AP, Streltsova MA, Kashentseva EA. Inactivated Marburg virus elicits a nonprotective immune response in Rhesus monkeys. *J Biotechnol*. 1996;44(1-3):111-8. Epub 1996/01/26. doi: 10.1016/0168-1656(95)00104-2. PubMed PMID: 8717394.
- 385.** Hevey M, Negley D, VanderZanden L, Tammariello RF, Geisbert J, Schmaljohn C, et al. Marburg virus vaccines: comparing classical and new approaches. *Vaccine*. 2001;20(3-4):586-93. Epub 2001/10/24. doi: 10.1016/s0264-410x(01)00353-x. PubMed PMID: 11672925.
- 386.** Sullivan NJ, Sanchez A, Rollin PE, Yang ZY, Nabel GJ. Development of a preventive vaccine for Ebola virus infection in primates. *Nature*. 2000;408(6812):605-9. Epub 2000/12/16. doi: 10.1038/35046108. PubMed PMID: 11117750.
- 387.** Santra S, Seaman MS, Xu L, Barouch DH, Lord CI, Lifton MA, et al. Replication-defective adenovirus serotype 5 vectors elicit durable cellular and humoral immune responses in nonhuman primates. *Journal of virology*. 2005;79(10):6516-22. Epub 2005/04/29. doi: 10.1128/JVI.79.10.6516-6522.2005. PubMed PMID: 15858035; PubMed Central PMCID: PMC1091731.
- 388.** Sullivan NJ, Geisbert TW, Geisbert JB, Xu L, Yang ZY, Roederer M, et al. Accelerated vaccination for Ebola virus haemorrhagic fever in non-human primates. *Nature*. 2003;424(6949):681-4. Epub 2003/08/09. doi: 10.1038/nature01876. PubMed PMID: 12904795; PubMed Central PMCID: PMC7095492.
- 389.** Wang D, Raja NU, Trubey CM, Juompan LY, Luo M, Woraratanadharm J, et al. Development of a cAdVax-based bivalent ebola virus vaccine that induces immune responses against both the Sudan and Zaire species of Ebola virus.

- Journal of virology. 2006;80(6):2738-46. Epub 2006/02/28. doi: 10.1128/JVI.80.6.2738-2746.2006. PubMed PMID: 16501083; PubMed Central PMCID: PMC1395467.
- 390.** Swenson DL, Wang D, Luo M, Warfield KL, Woraratanadharm J, Holman DH, et al. Vaccine to confer to nonhuman primates complete protection against multistrain Ebola and Marburg virus infections. *Clin Vaccine Immunol.* 2008;15(3):460-7. Epub 2008/01/25. doi: 10.1128/CVI.00431-07. PubMed PMID: 18216185; PubMed Central PMCID: PMC2268273.
- 391.** Ledgerwood JE, DeZure AD, Stanley DA, Coates EE, Novik L, Enama ME, et al. Chimpanzee Adenovirus Vector Ebola Vaccine. *The New England journal of medicine.* 2017;376(10):928-38. Epub 2014/11/27. doi: 10.1056/NEJMoa1410863. PubMed PMID: 25426834.
- 392.** Dolzhikova IV, Tokarskaya EA, Dzharullaeva AS, Tukhvatulin AI, Shcheblyakov DV, Voronina OL, et al. Virus-Vectored Ebola Vaccines. *Acta Naturae.* 2017;9(3):4-11. Epub 2017/11/07. PubMed PMID: 29104771; PubMed Central PMCID: PMC5662269.
- 393.** Musso D, Ko AI, Baud D. Zika Virus Infection - After the Pandemic. *The New England journal of medicine.* 2019;381(15):1444-57. Epub 2019/10/10. doi: 10.1056/NEJMra1808246. PubMed PMID: 31597021.
- 394.** Lopez-Camacho C, Abbink P, Larocca RA, Dejnirattisai W, Boyd M, Badamchi-Zadeh A, et al. Rational Zika vaccine design via the modulation of antigen membrane anchors in chimpanzee adenoviral vectors. *Nature communications.* 2018;9(1):2441. Epub 2018/06/24. doi: 10.1038/s41467-018-04859-5. PubMed PMID: 29934593; PubMed Central PMCID: PMC6015009.
- 395.** Hassan AO, Dmitriev IP, Kashentseva EA, Zhao H, Brough DE, Fremont DH, et al. A Gorilla Adenovirus-Based Vaccine against Zika Virus Induces Durable Immunity and Confers Protection in Pregnancy. *Cell Rep.* 2019;28(10):2634-46 e4. Epub 2019/09/05. doi: 10.1016/j.celrep.2019.08.005. PubMed PMID: 31484074; PubMed Central PMCID: PMC6750284.
- 396.** Larocca RA, Mendes EA, Abbink P, Peterson RL, Martinot AJ, Iampietro MJ, et al. Adenovirus Vector-Based Vaccines Confer Maternal-Fetal Protection against Zika Virus Challenge in Pregnant IFN- α R(-/-) Mice. *Cell Host Microbe.* 2019;26(5):591-600 e4. Epub 2019/11/02. doi: 10.1016/j.chom.2019.10.001. PubMed PMID: 31668877; PubMed Central PMCID: PMC6863051.
- 397.** Holman DH, Wang D, Raviprakash K, Raja NU, Luo M, Zhang J, et al. Two complex, adenovirus-based vaccines that together induce immune responses to all four dengue virus serotypes. *Clin Vaccine Immunol.* 2007;14(2):182-9.

- Epub 2006/12/29. doi: 10.1128/CVI.00330-06. PubMed PMID: 17192403; PubMed Central PMCID: PMC1797786.
- 398.** Raviprakash K, Wang D, Ewing D, Holman DH, Block K, Woraratanadharm J, et al. A tetravalent dengue vaccine based on a complex adenovirus vector provides significant protection in rhesus monkeys against all four serotypes of dengue virus. *Journal of virology*. 2008;82(14):6927-34. Epub 2008/05/16. doi: 10.1128/JVI.02724-07. PubMed PMID: 18480438; PubMed Central PMCID: PMC2446963.
- 399.** Dora EG, Rossi SL, Weaver SC, Tucker SN, Mateo R. An adjuvanted adenovirus 5-based vaccine elicits neutralizing antibodies and protects mice against chikungunya virus-induced footpad swelling. *Vaccine*. 2019;37(24):3146-50. Epub 2019/05/03. doi: 10.1016/j.vaccine.2019.04.069. PubMed PMID: 31047675.
- 400.** Campos RK, Preciado-Llanes L, Azar SR, Lopez-Camacho C, Reyes-Sandoval A, Rossi SL. A Single and Un-Adjuvanted Dose of a Chimpanzee Adenovirus-Vectored Vaccine against Chikungunya Virus Fully Protects Mice from Lethal Disease. *Pathogens*. 2019;8(4). Epub 2019/11/14. doi: 10.3390/pathogens8040231. PubMed PMID: 31718104; PubMed Central PMCID: PMC6963200.
- 401.** Wang D, Suhrbier A, Penn-Nicholson A, Woraratanadharm J, Gardner J, Luo M, et al. A complex adenovirus vaccine against chikungunya virus provides complete protection against viraemia and arthritis. *Vaccine*. 2011;29(15):2803-9. Epub 2011/02/16. doi: 10.1016/j.vaccine.2011.01.108. PubMed PMID: 21320541; PubMed Central PMCID: PMC3061842.
- 402.** Williams AJ, O'Brien LM, Phillipotts RJ, Perkins SD. Improved efficacy of a gene optimised adenovirus-based vaccine for venezuelan equine encephalitis virus. *Virology journal*. 2009;6:118. Epub 2009/08/04. doi: 10.1186/1743-422X-6-118. PubMed PMID: 19646224; PubMed Central PMCID: PMC2732613.
- 403.** Shiratsuchi T, Rai U, Kaneko I, Zhang M, Iwanaga S, Yuda M, et al. A potent malaria vaccine based on adenovirus with dual modifications at Hexon and pVII. *Vaccine*. 2017;35(50):6990-7000. Epub 2017/11/02. doi: 10.1016/j.vaccine.2017.10.066. PubMed PMID: 29089194; PubMed Central PMCID: PMC5709203.
- 404.** Fonseca JA, Cabrera-Mora M, Kashentseva EA, Villegas JP, Fernandez A, Van Pelt A, et al. A Plasmodium Promiscuous T Cell Epitope Delivered within the Ad5 Hexon Protein Enhances the Protective Efficacy of a Protein Based Malaria Vaccine. *PloS one*. 2016;11(4):e0154819. Epub 2016/04/30. doi: 10.1371/journal.pone.0154819. PubMed PMID: 27128437; PubMed Central PMCID: PMC4851317.

- 405.** Organization GWH. WHO coronavirus disease (COVID-19) dashboard <https://covid19.who.int/2020>. Available from: <https://covid19.who.int/>.
- 406.** Pormohammad A, Ghorbani S, Khatami A, Farzi R, Baradaran B, Turner DL, et al. Comparison of confirmed COVID-19 with SARS and MERS cases - Clinical characteristics, laboratory findings, radiographic signs and outcomes: A systematic review and meta-analysis. *Rev Med Virol.* 2020:e2112. Epub 2020/06/06. doi: 10.1002/rmv.2112. PubMed PMID: 32502331; PubMed Central PMCID: PMC7300470.
- 407.** Gao W, Tamin A, Soloff A, D'Aiuto L, Nwanegbo E, Robbins PD, et al. Effects of a SARS-associated coronavirus vaccine in monkeys. *Lancet.* 2003;362(9399):1895-6. Epub 2003/12/12. doi: 10.1016/S0140-6736(03)14962-8. PubMed PMID: 14667748; PubMed Central PMCID: PMC7112457.
- 408.** See RH, Zakhartchouk AN, Petric M, Lawrence DJ, Mok CP, Hogan RJ, et al. Comparative evaluation of two severe acute respiratory syndrome (SARS) vaccine candidates in mice challenged with SARS coronavirus. *J Gen Virol.* 2006;87(Pt 3):641-50. Epub 2006/02/16. doi: 10.1099/vir.0.81579-0. PubMed PMID: 16476986.
- 409.** Kobinger GP, Figueredo JM, Rowe T, Zhi Y, Gao G, Sanmiguel JC, et al. Adenovirus-based vaccine prevents pneumonia in ferrets challenged with the SARS coronavirus and stimulates robust immune responses in macaques. *Vaccine.* 2007;25(28):5220-31. Epub 2007/06/15. doi: 10.1016/j.vaccine.2007.04.065. PubMed PMID: 17559989; PubMed Central PMCID: PMC7115643.
- 410.** Liu RY, Wu LZ, Huang BJ, Huang JL, Zhang YL, Ke ML, et al. Adenoviral expression of a truncated S1 subunit of SARS-CoV spike protein results in specific humoral immune responses against SARS-CoV in rats. *Virus research.* 2005;112(1-2):24-31. Epub 2005/07/19. doi: 10.1016/j.virusres.2005.02.009. PubMed PMID: 16022898; PubMed Central PMCID: PMC7114075.
- 411.** van Doremalen N, Haddock E, Feldmann F, Meade-White K, Bushmaker T, Fischer RJ, et al. A single dose of ChAdOx1 MERS provides protective immunity in rhesus macaques. *Sci Adv.* 2020;6(24):eaba8399. Epub 2020/06/25. doi: 10.1126/sciadv.aba8399. PubMed PMID: 32577525; PubMed Central PMCID: PMC7286676.
- 412.** Folegatti PM, Bittaye M, Flaxman A, Lopez FR, Bellamy D, Kupke A, et al. Safety and immunogenicity of a candidate Middle East respiratory syndrome coronavirus viral-vectored vaccine: a dose-escalation, open-label, non-randomised, uncontrolled, phase 1 trial. *Lancet Infect Dis.* 2020;20(7):816-26. Epub 2020/04/24. doi: 10.1016/S1473-3099(20)30160-2. PubMed PMID: 32325038; PubMed Central PMCID: PMC7172901.

- 413.** Munster VJ, Wells D, Lambe T, Wright D, Fischer RJ, Bushmaker T, et al. Protective efficacy of a novel simian adenovirus vaccine against lethal MERS-CoV challenge in a transgenic human DPP4 mouse model. *NPJ Vaccines*. 2017;2:28. Epub 2017/12/22. doi: 10.1038/s41541-017-0029-1. PubMed PMID: 29263883; PubMed Central PMCID: PMC5643297 is developing a vectored MERS vaccine. Remaining authors declares that they have no competing financial interests.
- 414.** Zhu FC, Li YH, Guan XH, Hou LH, Wang WJ, Li JX, et al. Safety, tolerability, and immunogenicity of a recombinant adenovirus type-5 vectored COVID-19 vaccine: a dose-escalation, open-label, non-randomised, first-in-human trial. *Lancet*. 2020;395(10240):1845-54. Epub 2020/05/26. doi: 10.1016/S0140-6736(20)31208-3. PubMed PMID: 32450106; PubMed Central PMCID: PMC7255193.
- 415.** van Doremalen N, Lambe T, Spencer A, Belij-Rammerstorfer S, Purushotham JN, Port JR, et al. ChAdOx1 nCoV-19 vaccination prevents SARS-CoV-2 pneumonia in rhesus macaques. *bioRxiv*. 2020. Epub 2020/06/09. doi: 10.1101/2020.05.13.093195. PubMed PMID: 32511340; PubMed Central PMCID: PMC7241103 on a patent covering use of ChAdOx1-vectored vaccines and a patent application covering a SARS-CoV-2 (nCoV-19) vaccine. Teresa Lambe is named as an inventor on a patent application covering a SARS-CoV-2 (nCoV-19) vaccine. The remaining authors declare no competing interests.
- 416.** McClements ME, MacLaren RE. Adeno-associated Virus (AAV) Dual Vector Strategies for Gene Therapy Encoding Large Transgenes. *Yale J Biol Med*. 2017;90(4):611-23. Epub 2017/12/21. PubMed PMID: 29259525; PubMed Central PMCID: PMC5733846.
- 417.** Tiffany M, Kay MA. 253. Expanded Packaging Capacity of AAV by Luminal Charge Alteration. *Molecular Therapy*. 2016;24:S99-S100. doi: [https://doi.org/10.1016/S1525-0016\(16\)33062-3](https://doi.org/10.1016/S1525-0016(16)33062-3).
- 418.** M AK, Schaffer DV. Engineered AAV vectors for improved central nervous system gene delivery. *Neurogenesis (Austin)*. 2015;2(1):e1122700. Epub 2015/01/01. doi: 10.1080/23262133.2015.1122700. PubMed PMID: 27606332; PubMed Central PMCID: PMC4973602.
- 419.** Li C, Samulski RJ. Engineering adeno-associated virus vectors for gene therapy. *Nature reviews Genetics*. 2020;21(4):255-72. Epub 2020/02/12. doi: 10.1038/s41576-019-0205-4. PubMed PMID: 32042148.
- 420.** Grimm D, Lee JS, Wang L, Desai T, Akache B, Storm TA, et al. In vitro and in vivo gene therapy vector evolution via multispecies interbreeding and retargeting of adeno-associated viruses. *Journal of virology*. 2008;82(12):5887-

911. Epub 2008/04/11. doi: 10.1128/JVI.00254-08. PubMed PMID: 18400866; PubMed Central PMCID: PMC2395137.
- 421.** McLaughlin SK, Collis P, Hermonat PL, Muzyczka N. Adeno-associated virus general transduction vectors: analysis of proviral structures. *Journal of virology*. 1988;62(6):1963-73. Epub 1988/06/01. PubMed PMID: 2835501; PubMed Central PMCID: PMC253280.
- 422.** Samulski RJ, Chang LS, Shenk T. Helper-free stocks of recombinant adeno-associated viruses: normal integration does not require viral gene expression. *Journal of virology*. 1989;63(9):3822-8. Epub 1989/09/01. doi: 10.1128/JVI.63.9.3822-3828.1989. PubMed PMID: 2547998; PubMed Central PMCID: PMC250975.
- 423.** Zhang X, Li CY. Generation of recombinant adeno-associated virus vectors by a complete adenovirus-mediated approach. *Molecular therapy : the journal of the American Society of Gene Therapy*. 2001;3(5 Pt 1):787-92. Epub 2001/05/18. doi: 10.1006/mthe.2001.0306. PubMed PMID: 11356083.
- 424.** Grimm D, Kay MA, Kleinschmidt JA. Helper virus-free, optically controllable, and two-plasmid-based production of adeno-associated virus vectors of serotypes 1 to 6. *Molecular therapy : the journal of the American Society of Gene Therapy*. 2003;7(6):839-50. Epub 2003/06/06. doi: 10.1016/s1525-0016(03)00095-9. PubMed PMID: 12788658.
- 425.** Matsushita T, Elliger S, Elliger C, Podsakoff G, Villarreal L, Kurtzman GJ, et al. Adeno-associated virus vectors can be efficiently produced without helper virus. *Gene therapy*. 1998;5(7):938-45. Epub 1998/11/14. doi: 10.1038/sj.gt.3300680. PubMed PMID: 9813665.
- 426.** Gao GP, Lu F, Sanmiguel JC, Tran PT, Abbas Z, Lynd KS, et al. Rep/Cap gene amplification and high-yield production of AAV in an A549 cell line expressing Rep/Cap. *Molecular therapy : the journal of the American Society of Gene Therapy*. 2002;5(5 Pt 1):644-9. Epub 2002/05/07. doi: 10.1006/mthe.2001.0591. PubMed PMID: 11991756.
- 427.** Qiao C, Wang B, Zhu X, Li J, Xiao X. A novel gene expression control system and its use in stable, high-titer 293 cell-based adeno-associated virus packaging cell lines. *Journal of virology*. 2002;76(24):13015-27. Epub 2002/11/20. doi: 10.1128/jvi.76.24.13015-13027.2002. PubMed PMID: 12438627; PubMed Central PMCID: PMC136669.
- 428.** Chadeuf G, Favre D, Tessier J, Provost N, Nony P, Kleinschmidt J, et al. Efficient recombinant adeno-associated virus production by a stable rep-cap HeLa cell line correlates with adenovirus-induced amplification of the integrated rep-cap genome. *The journal of gene medicine*. 2000;2(4):260-8. Epub

- 2000/08/23. doi: 10.1002/1521-2254(200007/08)2:4<260::AID-JGM111>3.0.CO;2-8. PubMed PMID: 10953917.
- 429.** Aponte-Ubillus JJ, Barajas D, Peltier J, Bardliving C, Shamlou P, Gold D. Molecular design for recombinant adeno-associated virus (rAAV) vector production. *Applied microbiology and biotechnology*. 2018;102(3):1045-54. Epub 2017/12/06. doi: 10.1007/s00253-017-8670-1. PubMed PMID: 29204900; PubMed Central PMCID: PMC5778157.
- 430.** Wang D, Tai PWL, Gao G. Adeno-associated virus vector as a platform for gene therapy delivery. *Nat Rev Drug Discov*. 2019;18(5):358-78. Epub 2019/02/03. doi: 10.1038/s41573-019-0012-9. PubMed PMID: 30710128; PubMed Central PMCID: PMC6927556.
- 431.** Maheshri N, Koerber JT, Kaspar BK, Schaffer DV. Directed evolution of adeno-associated virus yields enhanced gene delivery vectors. *Nature biotechnology*. 2006;24(2):198-204. Epub 2006/01/24. doi: 10.1038/nbt1182. PubMed PMID: 16429148.
- 432.** Pulicherla N, Shen S, Yadav S, Debbink K, Govindasamy L, Agbandje-McKenna M, et al. Engineering liver-detargeted AAV9 vectors for cardiac and musculoskeletal gene transfer. *Molecular therapy : the journal of the American Society of Gene Therapy*. 2011;19(6):1070-8. Epub 2011/03/03. doi: 10.1038/mt.2011.22. PubMed PMID: 21364538; PubMed Central PMCID: PMC3129791.
- 433.** Koerber JT, Jang JH, Schaffer DV. DNA shuffling of adeno-associated virus yields functionally diverse viral progeny. *Molecular therapy : the journal of the American Society of Gene Therapy*. 2008;16(10):1703-9. Epub 2008/08/30. doi: 10.1038/mt.2008.167. PubMed PMID: 18728640; PubMed Central PMCID: PMC2683895.
- 434.** Gray SJ, Blake BL, Criswell HE, Nicolson SC, Samulski RJ, McCown TJ, et al. Directed evolution of a novel adeno-associated virus (AAV) vector that crosses the seizure-compromised blood-brain barrier (BBB). *Molecular therapy : the journal of the American Society of Gene Therapy*. 2010;18(3):570-8. Epub 2009/12/31. doi: 10.1038/mt.2009.292. PubMed PMID: 20040913; PubMed Central PMCID: PMC2831133.
- 435.** Li W, Asokan A, Wu Z, Van Dyke T, DiPrimio N, Johnson JS, et al. Engineering and selection of shuffled AAV genomes: a new strategy for producing targeted biological nanoparticles. *Molecular therapy : the journal of the American Society of Gene Therapy*. 2008;16(7):1252-60. Epub 2008/05/27. doi: 10.1038/mt.2008.100. PubMed PMID: 18500254; PubMed Central PMCID: PMC2632803.

- 436.** Herrmann AK, Grosse S, Borner K, Kramer C, Wiedtke E, Gunkel M, et al. Impact of the Assembly-Activating Protein on Molecular Evolution of Synthetic Adeno-Associated Virus Capsids. *Human gene therapy*. 2019;30(1):21-35. Epub 2018/07/07. doi: 10.1089/hum.2018.085. PubMed PMID: 29978729.
- 437.** Gao GP, Alvira MR, Wang L, Calcedo R, Johnston J, Wilson JM. Novel adeno-associated viruses from rhesus monkeys as vectors for human gene therapy. *Proceedings of the National Academy of Sciences of the United States of America*. 2002;99(18):11854-9. Epub 2002/08/23. doi: 10.1073/pnas.182412299. PubMed PMID: 12192090; PubMed Central PMCID: PMC129358.
- 438.** Li Y, Ge X, Zhang H, Zhou P, Zhu Y, Zhang Y, et al. Host range, prevalence, and genetic diversity of adenoviruses in bats. *Journal of virology*. 2010;84(8):3889-97. Epub 2010/01/22. doi: 10.1128/JVI.02497-09. PubMed PMID: 20089640; PubMed Central PMCID: PMC2849498.
- 439.** Bello A, Tran K, Chand A, Doria M, Allocca M, Hildinger M, et al. Isolation and evaluation of novel adeno-associated virus sequences from porcine tissues. *Gene therapy*. 2009;16(11):1320-8. Epub 2009/07/25. doi: 10.1038/gt.2009.82. PubMed PMID: 19626054.
- 440.** Yates VJ, el-Mishad AM, McCormick KJ, Trentin JJ. Isolation and characterization of an Avian adenovirus-associated virus. *Infect Immun*. 1973;7(6):973-80. Epub 1973/06/01. doi: 10.1128/IAI.7.6.973-980.1973. PubMed PMID: 4351971; PubMed Central PMCID: PMC422790.
- 441.** Shen S, Horowitz ED, Troupes AN, Brown SM, Pulicherla N, Samulski RJ, et al. Engraftment of a galactose receptor footprint onto adeno-associated viral capsids improves transduction efficiency. *J Biol Chem*. 2013;288(40):28814-23. Epub 2013/08/14. doi: 10.1074/jbc.M113.482380. PubMed PMID: 23940044; PubMed Central PMCID: PMC3789977.
- 442.** Murlidharan G, Sakamoto K, Rao L, Corriher T, Wang D, Gao G, et al. CNS-restricted Transduction and CRISPR/Cas9-mediated Gene Deletion with an Engineered AAV Vector. *Mol Ther Nucleic Acids*. 2016;5(7):e338. Epub 2016/07/21. doi: 10.1038/mtna.2016.49. PubMed PMID: 27434683; PubMed Central PMCID: PMC5330941.
- 443.** Bowles DE, McPhee SW, Li C, Gray SJ, Samulski JJ, Camp AS, et al. Phase 1 gene therapy for Duchenne muscular dystrophy using a translational optimized AAV vector. *Molecular therapy : the journal of the American Society of Gene Therapy*. 2012;20(2):443-55. Epub 2011/11/10. doi: 10.1038/mt.2011.237. PubMed PMID: 22068425; PubMed Central PMCID: PMC3277234.

- 444.** Asokan A, Conway JC, Phillips JL, Li C, Hegge J, Sinnott R, et al. Reengineering a receptor footprint of adeno-associated virus enables selective and systemic gene transfer to muscle. *Nature biotechnology*. 2010;28(1):79-82. Epub 2009/12/29. doi: 10.1038/nbt.1599. PubMed PMID: 20037580; PubMed Central PMCID: PMC2912150.
- 445.** Borner K, Kienle E, Huang LY, Weinmann J, Sacher A, Bayer P, et al. Pre-arrayed Pan-AAV Peptide Display Libraries for Rapid Single-Round Screening. *Molecular therapy : the journal of the American Society of Gene Therapy*. 2020;28(4):1016-32. Epub 2020/02/28. doi: 10.1016/j.ymthe.2020.02.009. PubMed PMID: 32105604; PubMed Central PMCID: PMC7132618.
- 446.** Muller OJ, Kaul F, Weitzman MD, Pasqualini R, Arap W, Kleinschmidt JA, et al. Random peptide libraries displayed on adeno-associated virus to select for targeted gene therapy vectors. *Nature biotechnology*. 2003;21(9):1040-6. Epub 2003/08/05. doi: 10.1038/nbt856. PubMed PMID: 12897791.
- 447.** Adachi K, Nakai H. A New Recombinant Adeno-Associated Virus (Aav)-Based Random Peptide Display Library System: Infection-Defective Aav1.9-3 as a Novel Detargeted Platform for Vector Evolution. *Gene Ther Regul*. 2010;5(1):31-55. Epub 2011/05/24. doi: 10.1142/S1568558610000197. PubMed PMID: 21603583; PubMed Central PMCID: PMC3095953.
- 448.** Dalkara D, Byrne LC, Klimczak RR, Visel M, Yin L, Merigan WH, et al. In vivo-directed evolution of a new adeno-associated virus for therapeutic outer retinal gene delivery from the vitreous. *Science translational medicine*. 2013;5(189):189ra76. Epub 2013/06/14. doi: 10.1126/scitranslmed.3005708. PubMed PMID: 23761039.
- 449.** Deverman BE, Pravdo PL, Simpson BP, Kumar SR, Chan KY, Banerjee A, et al. Cre-dependent selection yields AAV variants for widespread gene transfer to the adult brain. *Nature biotechnology*. 2016;34(2):204-9. Epub 2016/02/02. doi: 10.1038/nbt.3440. PubMed PMID: 26829320; PubMed Central PMCID: PMC5088052.
- 450.** Matsuzaki Y, Konno A, Mochizuki R, Shinohara Y, Nitta K, Okada Y, et al. Intravenous administration of the adeno-associated virus-PHP.B capsid fails to upregulate transduction efficiency in the marmoset brain. *Neurosci Lett*. 2018;665:182-8. Epub 2017/11/28. doi: 10.1016/j.neulet.2017.11.049. PubMed PMID: 29175632.
- 451.** Liguore WA, Domire JS, Button D, Wang Y, Dufour BD, Srinivasan S, et al. AAV-PHP.B Administration Results in a Differential Pattern of CNS Biodistribution in Non-human Primates Compared with Mice. *Molecular therapy : the journal of the American Society of Gene Therapy*. 2019;27(11):2018-37. Epub 2019/08/20. doi: 10.1016/j.ymthe.2019.07.017. PubMed PMID: 31420242; PubMed Central PMCID: PMC6838922.

- 452.** Hordeaux J, Wang Q, Katz N, Buza EL, Bell P, Wilson JM. The Neurotropic Properties of AAV-PHP.B Are Limited to C57BL/6J Mice. *Molecular therapy : the journal of the American Society of Gene Therapy*. 2018;26(3):664-8. Epub 2018/02/13. doi: 10.1016/j.ymthe.2018.01.018. PubMed PMID: 29428298; PubMed Central PMCID: PMC5911151.
- 453.** Carvalho LS, Xiao R, Wassmer SJ, Langsdorf A, Zinn E, Pacouret S, et al. Synthetic Adeno-Associated Viral Vector Efficiently Targets Mouse and Nonhuman Primate Retina In Vivo. *Human gene therapy*. 2018;29(7):771-84. Epub 2018/01/13. doi: 10.1089/hum.2017.154. PubMed PMID: 29325457; PubMed Central PMCID: PMC6066192.
- 454.** Zinn E, Pacouret S, Khaychuk V, Turunen HT, Carvalho LS, Andres-Mateos E, et al. In Silico Reconstruction of the Viral Evolutionary Lineage Yields a Potent Gene Therapy Vector. *Cell Rep*. 2015;12(6):1056-68. Epub 2015/08/04. doi: 10.1016/j.celrep.2015.07.019. PubMed PMID: 26235624; PubMed Central PMCID: PMC4536165.
- 455.** Santiago-Ortiz J, Ojala DS, Westesson O, Weinstein JR, Wong SY, Steinsapir A, et al. AAV ancestral reconstruction library enables selection of broadly infectious viral variants. *Gene therapy*. 2015;22(12):934-46. Epub 2015/07/18. doi: 10.1038/gt.2015.74. PubMed PMID: 26186661; PubMed Central PMCID: PMC4509550.
- 456.** Hirsch ML, Agbandje-McKenna M, Samulski RJ. Little vector, big gene transduction: fragmented genome reassembly of adeno-associated virus. *Molecular therapy : the journal of the American Society of Gene Therapy*. 2010;18(1):6-8. Epub 2010/01/06. doi: 10.1038/mt.2009.280. PubMed PMID: 20048740; PubMed Central PMCID: PMC2839225.
- 457.** Duan D, Yue Y, Engelhardt JF. Expanding AAV packaging capacity with trans-splicing or overlapping vectors: a quantitative comparison. *Molecular therapy : the journal of the American Society of Gene Therapy*. 2001;4(4):383-91. Epub 2001/10/11. doi: 10.1006/mthe.2001.0456. PubMed PMID: 11592843.
- 458.** Choi VW, McCarty DM, Samulski RJ. Host cell DNA repair pathways in adeno-associated viral genome processing. *Journal of virology*. 2006;80(21):10346-56. Epub 2006/10/17. doi: 10.1128/JVI.00841-06. PubMed PMID: 17041215; PubMed Central PMCID: PMC1641795.
- 459.** Halbert CL, Allen JM, Miller AD. Efficient mouse airway transduction following recombination between AAV vectors carrying parts of a larger gene. *Nature biotechnology*. 2002;20(7):697-701. Epub 2002/06/29. doi: 10.1038/nbt0702-697. PubMed PMID: 12089554.

- 460.** Allocca M, Doria M, Petrillo M, Colella P, Garcia-Hoyos M, Gibbs D, et al. Serotype-dependent packaging of large genes in adeno-associated viral vectors results in effective gene delivery in mice. *The Journal of clinical investigation*. 2008;118(5):1955-64. Epub 2008/04/17. doi: 10.1172/JCI34316. PubMed PMID: 18414684; PubMed Central PMCID: PMC2298836.
- 461.** Wu Z, Yang H, Colosi P. Effect of genome size on AAV vector packaging. *Molecular therapy : the journal of the American Society of Gene Therapy*. 2010;18(1):80-6. Epub 2009/11/12. doi: 10.1038/mt.2009.255. PubMed PMID: 19904234; PubMed Central PMCID: PMC2839202.
- 462.** Dong B, Nakai H, Xiao W. Characterization of genome integrity for oversized recombinant AAV vector. *Molecular therapy : the journal of the American Society of Gene Therapy*. 2010;18(1):87-92. Epub 2009/11/12. doi: 10.1038/mt.2009.258. PubMed PMID: 19904236; PubMed Central PMCID: PMC2803017.
- 463.** Lai Y, Yue Y, Duan D. Evidence for the failure of adeno-associated virus serotype 5 to package a viral genome \geq 8.2 kb. *Molecular therapy : the journal of the American Society of Gene Therapy*. 2010;18(1):75-9. Epub 2009/11/12. doi: 10.1038/mt.2009.256. PubMed PMID: 19904238; PubMed Central PMCID: PMC2839223.
- 464.** Dyka FM, Boye SL, Chiodo VA, Hauswirth WW, Boye SE. Dual adeno-associated virus vectors result in efficient in vitro and in vivo expression of an oversized gene, MYO7A. *Human gene therapy methods*. 2014;25(2):166-77. Epub 2014/02/27. doi: 10.1089/hgtb.2013.212. PubMed PMID: 24568220; PubMed Central PMCID: PMC3991978.
- 465.** Trapani I, Toriello E, de Simone S, Colella P, Iodice C, Polishchuk EV, et al. Improved dual AAV vectors with reduced expression of truncated proteins are safe and effective in the retina of a mouse model of Stargardt disease. *Human molecular genetics*. 2015;24(23):6811-25. Epub 2015/10/01. doi: 10.1093/hmg/ddv386. PubMed PMID: 26420842; PubMed Central PMCID: PMC4634381.
- 466.** Ferrari FK, Samulski T, Shenk T, Samulski RJ. Second-strand synthesis is a rate-limiting step for efficient transduction by recombinant adeno-associated virus vectors. *Journal of virology*. 1996;70(5):3227-34. Epub 1996/05/01. PubMed PMID: 8627803; PubMed Central PMCID: PMC190186.
- 467.** Alexander IE, Russell DW, Miller AD. DNA-damaging agents greatly increase the transduction of nondividing cells by adeno-associated virus vectors. *Journal of virology*. 1994;68(12):8282-7. Epub 1994/12/01. PubMed PMID: 7966621; PubMed Central PMCID: PMC237296.

- 468.** Weitzman MD, Fisher KJ, Wilson JM. Recruitment of wild-type and recombinant adeno-associated virus into adenovirus replication centers. *Journal of virology*. 1996;70(3):1845-54. Epub 1996/03/01. PubMed PMID: 8627709; PubMed Central PMCID: PMC190012.
- 469.** Fisher KJ, Gao GP, Weitzman MD, DeMatteo R, Burda JF, Wilson JM. Transduction with recombinant adeno-associated virus for gene therapy is limited by leading-strand synthesis. *Journal of virology*. 1996;70(1):520-32. Epub 1996/01/01. PubMed PMID: 8523565; PubMed Central PMCID: PMC189840.
- 470.** Nakai H, Storm TA, Kay MA. Recruitment of single-stranded recombinant adeno-associated virus vector genomes and intermolecular recombination are responsible for stable transduction of liver in vivo. *Journal of virology*. 2000;74(20):9451-63. Epub 2000/09/23. doi: 10.1128/jvi.74.20.9451-9463.2000. PubMed PMID: 11000214; PubMed Central PMCID: PMC112374.
- 471.** Fu H, Muenzer J, Samulski RJ, Breese G, Sifford J, Zeng X, et al. Self-complementary adeno-associated virus serotype 2 vector: global distribution and broad dispersion of AAV-mediated transgene expression in mouse brain. *Molecular therapy : the journal of the American Society of Gene Therapy*. 2003;8(6):911-7. Epub 2003/12/11. doi: 10.1016/j.ymthe.2003.08.021. PubMed PMID: 14664793.
- 472.** Wu Z, Sun J, Zhang T, Yin C, Yin F, Van Dyke T, et al. Optimization of self-complementary AAV vectors for liver-directed expression results in sustained correction of hemophilia B at low vector dose. *Molecular therapy : the journal of the American Society of Gene Therapy*. 2008;16(2):280-9. Epub 2007/12/07. doi: 10.1038/sj.mt.6300355. PubMed PMID: 18059373.
- 473.** Raj D, Davidoff AM, Nathwani AC. Self-complementary adeno-associated viral vectors for gene therapy of hemophilia B: progress and challenges. *Expert Rev Hematol*. 2011;4(5):539-49. Epub 2011/09/24. doi: 10.1586/ehm.11.48. PubMed PMID: 21939421; PubMed Central PMCID: PMC3200187.
- 474.** McCarty DM. Self-complementary AAV vectors; advances and applications. *Molecular therapy : the journal of the American Society of Gene Therapy*. 2008;16(10):1648-56. Epub 2008/08/07. doi: 10.1038/mt.2008.171. PubMed PMID: 18682697.
- 475.** McCarty DM, Fu H, Monahan PE, Toulson CE, Naik P, Samulski RJ. Adeno-associated virus terminal repeat (TR) mutant generates self-complementary vectors to overcome the rate-limiting step to transduction in vivo. *Gene therapy*. 2003;10(26):2112-8. Epub 2003/11/20. doi: 10.1038/sj.gt.3302134. PubMed PMID: 14625565.

- 476.** Chamorro C, Mencia A, Almarza D, Duarte B, Buning H, Sallach J, et al. Gene Editing for the Efficient Correction of a Recurrent COL7A1 Mutation in Recessive Dystrophic Epidermolysis Bullosa Keratinocytes. *Mol Ther Nucleic Acids*. 2016;5:e307. Epub 2016/04/06. doi: 10.1038/mtna.2016.19. PubMed PMID: 27045209; PubMed Central PMCID: PMC5014520.
- 477.** Wang J, Exline CM, DeClercq JJ, Llewellyn GN, Hayward SB, Li PW, et al. Homology-driven genome editing in hematopoietic stem and progenitor cells using ZFN mRNA and AAV6 donors. *Nature biotechnology*. 2015;33(12):1256-63. Epub 2015/11/10. doi: 10.1038/nbt.3408. PubMed PMID: 26551060; PubMed Central PMCID: PMC4842001.
- 478.** Epstein BE, Schaffer DV. Combining Engineered Nucleases with Adeno-associated Viral Vectors for Therapeutic Gene Editing. *Advances in experimental medicine and biology*. 2017;1016:29-42. Epub 2017/11/14. doi: 10.1007/978-3-319-63904-8_2. PubMed PMID: 29130152; PubMed Central PMCID: PMC5702533.
- 479.** Guggino WB, Cebotaru L. Adeno-Associated Virus (AAV) gene therapy for cystic fibrosis: current barriers and recent developments. *Expert opinion on biological therapy*. 2017;17(10):1265-73. Epub 2017/06/29. doi: 10.1080/14712598.2017.1347630. PubMed PMID: 28657358; PubMed Central PMCID: PMC5858933.
- 480.** Batty P, Lillicrap D. Advances and challenges for hemophilia gene therapy. *Human molecular genetics*. 2019;28(R1):R95-R101. Epub 2019/07/25. doi: 10.1093/hmg/ddz157. PubMed PMID: 31332444.
- 481.** Pierce EA, Bennett J. The Status of RPE65 Gene Therapy Trials: Safety and Efficacy. *Cold Spring Harb Perspect Med*. 2015;5(9):a017285. Epub 2015/01/31. doi: 10.1101/cshperspect.a017285. PubMed PMID: 25635059; PubMed Central PMCID: PMC4561397.
- 482.** Crudele JM, Chamberlain JS. AAV-based gene therapies for the muscular dystrophies. *Human molecular genetics*. 2019;28(R1):R102-R7. Epub 2019/06/27. doi: 10.1093/hmg/ddz128. PubMed PMID: 31238336; PubMed Central PMCID: PMC6796995.
- 483.** Kirik D, Cederfjall E, Halliday G, Petersen A. Gene therapy for Parkinson's disease: Disease modification by GDNF family of ligands. *Neurobiol Dis*. 2017;97(Pt B):179-88. Epub 2016/09/13. doi: 10.1016/j.nbd.2016.09.008. PubMed PMID: 27616425.
- 484.** Naso MF, Tomkowicz B, Perry WL, 3rd, Strohl WR. Adeno-Associated Virus (AAV) as a Vector for Gene Therapy. *BioDrugs*. 2017;31(4):317-34. Epub 2017/07/03. doi: 10.1007/s40259-017-0234-5. PubMed PMID: 28669112; PubMed Central PMCID: PMC5548848.

- 485.** Penny WF, Hammond HK. Randomized Clinical Trials of Gene Transfer for Heart Failure with Reduced Ejection Fraction. *Human gene therapy*. 2017;28(5):378-84. Epub 2017/03/23. doi: 10.1089/hum.2016.166. PubMed PMID: 28322590; PubMed Central PMCID: PMC5444414.
- 486.** Shahryari A, Saghaeian Jazi M, Mohammadi S, Razavi Nikoo H, Nazari Z, Hosseini ES, et al. Development and Clinical Translation of Approved Gene Therapy Products for Genetic Disorders. *Front Genet*. 2019;10:868. Epub 2019/10/15. doi: 10.3389/fgene.2019.00868. PubMed PMID: 31608113; PubMed Central PMCID: PMC6773888.
- 487.** Chen R, Mukhopadhyay S, Merits A, Bolling B, Nasar F, Coffey LL, et al. ICTV Virus Taxonomy Profile: Togaviridae. *J Gen Virol*. 2018;99(6):761-2. Epub 2018/05/11. doi: 10.1099/jgv.0.001072. PubMed PMID: 29745869.
- 488.** La Linn M, Gardner J, Warrilow D, Darnell GA, McMahon CR, Field I, et al. Arbovirus of marine mammals: a new alphavirus isolated from the elephant seal louse, *Lepidophthirus macrorhini*. *Journal of virology*. 2001;75(9):4103-9. Epub 2001/04/05. doi: 10.1128/JVI.75.9.4103-4109.2001. PubMed PMID: 11287559; PubMed Central PMCID: PMC114155.
- 489.** Weston J, Villoing S, Bremont M, Castric J, Pfeffer M, Jewhurst V, et al. Comparison of two aquatic alphaviruses, salmon pancreas disease virus and sleeping disease virus, by using genome sequence analysis, monoclonal reactivity, and cross-infection. *Journal of virology*. 2002;76(12):6155-63. Epub 2002/05/22. doi: 10.1128/jvi.76.12.6155-6163.2002. PubMed PMID: 12021349; PubMed Central PMCID: PMC136221.
- 490.** Leung JY, Ng MM, Chu JJ. Replication of alphaviruses: a review on the entry process of alphaviruses into cells. *Adv Virol*. 2011;2011:249640. Epub 2012/02/09. doi: 10.1155/2011/249640. PubMed PMID: 22312336; PubMed Central PMCID: PMC3265296.
- 491.** Kim DY, Reynaud JM, Rasaloukaya A, Akhrymuk I, Mobley JA, Frolov I, et al. New World and Old World Alphaviruses Have Evolved to Exploit Different Components of Stress Granules, FXR and G3BP Proteins, for Assembly of Viral Replication Complexes. *PLoS pathogens*. 2016;12(8):e1005810. Epub 2016/08/11. doi: 10.1371/journal.ppat.1005810. PubMed PMID: 27509095; PubMed Central PMCID: PMC4980055.
- 492.** Borgherini G, Poubeau P, Jossaume A, Gouix A, Cotte L, Michault A, et al. Persistent arthralgia associated with chikungunya virus: a study of 88 adult patients on reunion island. *Clinical infectious diseases : an official publication of the Infectious Diseases Society of America*. 2008;47(4):469-75. Epub 2008/07/10. doi: 10.1086/590003. PubMed PMID: 18611153.

- 493.** Salimi H, Cain MD, Klein RS. Encephalitic Arboviruses: Emergence, Clinical Presentation, and Neuropathogenesis. *Neurotherapeutics*. 2016;13(3):514-34. Epub 2016/05/26. doi: 10.1007/s13311-016-0443-5. PubMed PMID: 27220616; PubMed Central PMCID: PMC4965410.
- 494.** Young NA, Johnson KM. Antigenic variants of Venezuelan equine encephalitis virus: their geographic distribution and epidemiologic significance. *Am J Epidemiol*. 1969;89(3):286-307. Epub 1969/03/01. doi: 10.1093/oxfordjournals.aje.a120942. PubMed PMID: 5773424.
- 495.** Levinson RS, Strauss JH, Strauss EG. Complete sequence of the genomic RNA of O'nyong-nyong virus and its use in the construction of alphavirus phylogenetic trees. *Virology*. 1990;175(1):110-23. Epub 1990/03/01. doi: 10.1016/0042-6822(90)90191-s. PubMed PMID: 2155505.
- 496.** Forrester NL, Palacios G, Tesh RB, Savji N, Guzman H, Sherman M, et al. Genome-scale phylogeny of the alphavirus genus suggests a marine origin. *Journal of virology*. 2012;86(5):2729-38. Epub 2011/12/23. doi: 10.1128/JVI.05591-11. PubMed PMID: 22190718; PubMed Central PMCID: PMC3302268.
- 497.** Powers AM, Brault AC, Shirako Y, Strauss EG, Kang W, Strauss JH, et al. Evolutionary relationships and systematics of the alphaviruses. *Journal of virology*. 2001;75(21):10118-31. Epub 2001/10/03. doi: 10.1128/JVI.75.21.10118-10131.2001. PubMed PMID: 11581380; PubMed Central PMCID: PMC114586.
- 498.** Weaver SC, Winegar R, Manger ID, Forrester NL. Alphaviruses: population genetics and determinants of emergence. *Antiviral Res*. 2012;94(3):242-57. Epub 2012/04/24. doi: 10.1016/j.antiviral.2012.04.002. PubMed PMID: 22522323; PubMed Central PMCID: PMC3737490.
- 499.** Weaver SC, Kang W, Shirako Y, Rumenapf T, Strauss EG, Strauss JH. Recombinational history and molecular evolution of western equine encephalomyelitis complex alphaviruses. *Journal of virology*. 1997;71(1):613-23. Epub 1997/01/01. PubMed PMID: 8985391; PubMed Central PMCID: PMC191092.
- 500.** Carey BD, Bakovic A, Callahan V, Narayanan A, Kehn-Hall K. New World alphavirus protein interactomes from a therapeutic perspective. *Antiviral Res*. 2019;163:125-39. Epub 2019/01/30. doi: 10.1016/j.antiviral.2019.01.015. PubMed PMID: 30695702.
- 501.** Rupp JC, Sokoloski KJ, Gebhart NN, Hardy RW. Alphavirus RNA synthesis and non-structural protein functions. *J Gen Virol*. 2015;96(9):2483-500. Epub 2015/07/30. doi: 10.1099/jgv.0.000249. PubMed PMID: 26219641; PubMed Central PMCID: PMC4635493.

- 502.** Hefti E, Bishop DH, Dubin DT, Stollar V. 5' nucleotide sequence of sindbis viral RNA. *Journal of virology*. 1975;17(1):149-59. Epub 1975/01/01. PubMed PMID: 173879; PubMed Central PMCID: PMC515398.
- 503.** Hyde JL, Chen R, Trobaugh DW, Diamond MS, Weaver SC, Klimstra WB, et al. The 5' and 3' ends of alphavirus RNAs--Non-coding is not non-functional. *Virus research*. 2015;206:99-107. Epub 2015/01/30. doi: 10.1016/j.virusres.2015.01.016. PubMed PMID: 25630058; PubMed Central PMCID: PMC4654126.
- 504.** Wielgosz MM, Huang HV. A novel viral RNA species in Sindbis virus-infected cells. *Journal of virology*. 1997;71(12):9108-17. Epub 1997/11/26. PubMed PMID: 9371567; PubMed Central PMCID: PMC230211.
- 505.** Levis R, Schlesinger S, Huang HV. Promoter for Sindbis virus RNA-dependent subgenomic RNA transcription. *Journal of virology*. 1990;64(4):1726-33. Epub 1990/04/01. PubMed PMID: 2319651; PubMed Central PMCID: PMC249310.
- 506.** Jose J, Snyder JE, Kuhn RJ. A structural and functional perspective of alphavirus replication and assembly. *Future Microbiol*. 2009;4(7):837-56. Epub 2009/09/03. doi: 10.2217/fmb.09.59. PubMed PMID: 19722838; PubMed Central PMCID: PMC2762864.
- 507.** Frolov I, Hardy R, Rice CM. Cis-acting RNA elements at the 5' end of Sindbis virus genome RNA regulate minus- and plus-strand RNA synthesis. *RNA*. 2001;7(11):1638-51. Epub 2001/11/27. doi: 10.1017/s135583820101010x. PubMed PMID: 11720292; PubMed Central PMCID: PMC1370205.
- 508.** Hardy RW. The role of the 3' terminus of the Sindbis virus genome in minus-strand initiation site selection. *Virology*. 2006;345(2):520-31. Epub 2005/11/22. doi: 10.1016/j.virol.2005.10.018. PubMed PMID: 16297426.
- 509.** Frolova E, Frolov I, Schlesinger S. Packaging signals in alphaviruses. *Journal of virology*. 1997;71(1):248-58. Epub 1997/01/01. PubMed PMID: 8985344; PubMed Central PMCID: PMC191045.
- 510.** Kim DY, Firth AE, Atasheva S, Frolova EI, Frolov I. Conservation of a packaging signal and the viral genome RNA packaging mechanism in alphavirus evolution. *Journal of virology*. 2011;85(16):8022-36. Epub 2011/06/18. doi: 10.1128/JVI.00644-11. PubMed PMID: 21680508; PubMed Central PMCID: PMC3147971.
- 511.** Ahola T, Karlin DG. Sequence analysis reveals a conserved extension in the capping enzyme of the alphavirus supergroup, and a homologous domain in nodaviruses. *Biol Direct*. 2015;10:16. Epub 2015/04/19. doi: 10.1186/s13062-

- 015-0050-0. PubMed PMID: 25886938; PubMed Central PMCID: PMC4392871.
- 512.** Rozanov MN, Koonin EV, Gorbalenya AE. Conservation of the putative methyltransferase domain: a hallmark of the 'Sindbis-like' supergroup of positive-strand RNA viruses. *J Gen Virol.* 1992;73 (Pt 8):2129-34. Epub 1992/08/01. doi: 10.1099/0022-1317-73-8-2129. PubMed PMID: 1645151.
- 513.** Ahola T, Kaariainen L. Reaction in alphavirus mRNA capping: formation of a covalent complex of nonstructural protein nsP1 with 7-methyl-GMP. *Proceedings of the National Academy of Sciences of the United States of America.* 1995;92(2):507-11. Epub 1995/01/17. doi: 10.1073/pnas.92.2.507. PubMed PMID: 7831320; PubMed Central PMCID: PMC42770.
- 514.** Lampio A, Kilpelainen I, Pesonen S, Karhi K, Auvinen P, Somerharju P, et al. Membrane binding mechanism of an RNA virus-capping enzyme. *J Biol Chem.* 2000;275(48):37853-9. Epub 2000/09/14. doi: 10.1074/jbc.M004865200. PubMed PMID: 10984480.
- 515.** Spuul P, Salonen A, Merits A, Jokitalo E, Kaariainen L, Ahola T. Role of the amphipathic peptide of Semliki forest virus replicase protein nsP1 in membrane association and virus replication. *Journal of virology.* 2007;81(2):872-83. Epub 2006/11/10. doi: 10.1128/JVI.01785-06. PubMed PMID: 17093195; PubMed Central PMCID: PMC1797454.
- 516.** Suopanki J, Sawicki DL, Sawicki SG, Kaariainen L. Regulation of alphavirus 26S mRNA transcription by replicase component nsP2. *J Gen Virol.* 1998;79 (Pt 2):309-19. Epub 1998/02/24. doi: 10.1099/0022-1317-79-2-309. PubMed PMID: 9472615.
- 517.** Rikonen M, Peranen J, Kaariainen L. ATPase and GTPase activities associated with Semliki Forest virus nonstructural protein nsP2. *Journal of virology.* 1994;68(9):5804-10. Epub 1994/09/01. PubMed PMID: 8057461; PubMed Central PMCID: PMC236984.
- 518.** Gomez de Cedron M, Ehsani N, Mikkola ML, Garcia JA, Kaariainen L. RNA helicase activity of Semliki Forest virus replicase protein NSP2. *FEBS Lett.* 1999;448(1):19-22. Epub 1999/04/27. doi: 10.1016/s0014-5793(99)00321-x. PubMed PMID: 10217401.
- 519.** Vasiljeva L, Merits A, Auvinen P, Kaariainen L. Identification of a novel function of the alphavirus capping apparatus. RNA 5'-triphosphatase activity of Nsp2. *J Biol Chem.* 2000;275(23):17281-7. Epub 2000/04/05. doi: 10.1074/jbc.M910340199. PubMed PMID: 10748213.
- 520.** Akhrymuk I, Kulemzin SV, Frolova EI. Evasion of the innate immune response: the Old World alphavirus nsP2 protein induces rapid degradation of

- Rpb1, a catalytic subunit of RNA polymerase II. *Journal of virology*. 2012;86(13):7180-91. Epub 2012/04/20. doi: 10.1128/JVI.00541-12. PubMed PMID: 22514352; PubMed Central PMCID: PMC3416352.
- 521.** Tamm K, Merits A, Sarand I. Mutations in the nuclear localization signal of nsP2 influencing RNA synthesis, protein expression and cytotoxicity of Semliki Forest virus. *J Gen Virol*. 2008;89(Pt 3):676-86. Epub 2008/02/15. doi: 10.1099/vir.0.83320-0. PubMed PMID: 18272758; PubMed Central PMCID: PMC2275301.
- 522.** Gotte B, Liu L, McInerney GM. The Enigmatic Alphavirus Non-Structural Protein 3 (nsP3) Revealing Its Secrets at Last. *Viruses*. 2018;10(3). Epub 2018/03/03. doi: 10.3390/v10030105. PubMed PMID: 29495654; PubMed Central PMCID: PMC5869498.
- 523.** Park E, Griffin DE. The nsP3 macro domain is important for Sindbis virus replication in neurons and neurovirulence in mice. *Virology*. 2009;388(2):305-14. Epub 2009/04/28. doi: 10.1016/j.virol.2009.03.031. PubMed PMID: 19395054; PubMed Central PMCID: PMC2683903.
- 524.** Lulla A, Lulla V, Merits A. Macromolecular assembly-driven processing of the 2/3 cleavage site in the alphavirus replicase polyprotein. *Journal of virology*. 2012;86(1):553-65. Epub 2011/10/28. doi: 10.1128/JVI.05195-11. PubMed PMID: 22031949; PubMed Central PMCID: PMC3255916.
- 525.** De I, Fata-Hartley C, Sawicki SG, Sawicki DL. Functional analysis of nsP3 phosphoprotein mutants of Sindbis virus. *Journal of virology*. 2003;77(24):13106-16. Epub 2003/12/03. doi: 10.1128/jvi.77.24.13106-13116.2003. PubMed PMID: 14645567; PubMed Central PMCID: PMC296081.
- 526.** Lastarza MW, Grakoui A, Rice CM. Deletion and duplication mutations in the C-terminal nonconserved region of Sindbis virus nsP3: effects on phosphorylation and on virus replication in vertebrate and invertebrate cells. *Virology*. 1994;202(1):224-32. Epub 1994/07/01. doi: 10.1006/viro.1994.1338. PubMed PMID: 7912020.
- 527.** Tuittila M, Hinkkanen AE. Amino acid mutations in the replicase protein nsP3 of Semliki Forest virus cumulatively affect neurovirulence. *J Gen Virol*. 2003;84(Pt 6):1525-33. Epub 2003/05/29. doi: 10.1099/vir.0.18936-0. PubMed PMID: 12771422.
- 528.** Varjak M, Zusinaite E, Merits A. Novel functions of the alphavirus nonstructural protein nsP3 C-terminal region. *Journal of virology*. 2010;84(5):2352-64. Epub 2009/12/18. doi: 10.1128/JVI.01540-09. PubMed PMID: 20015978; PubMed Central PMCID: PMC2820926.

- 529.** Rupp JC, Jundt N, Hardy RW. Requirement for the amino-terminal domain of sindbis virus nsP4 during virus infection. *Journal of virology*. 2011;85(7):3449-60. Epub 2011/01/21. doi: 10.1128/JVI.02058-10. PubMed PMID: 21248049; PubMed Central PMCID: PMC3067876.
- 530.** Shirako Y, Strauss JH. Requirement for an aromatic amino acid or histidine at the N terminus of Sindbis virus RNA polymerase. *Journal of virology*. 1998;72(3):2310-5. Epub 1998/03/14. PubMed PMID: 9499091; PubMed Central PMCID: PMC109530.
- 531.** Melancon P, Garoff H. Processing of the Semliki Forest virus structural polyprotein: role of the capsid protease. *Journal of virology*. 1987;61(5):1301-9. Epub 1987/05/01. PubMed PMID: 3553612; PubMed Central PMCID: PMC254103.
- 532.** Owen KE, Kuhn RJ. Identification of a region in the Sindbis virus nucleocapsid protein that is involved in specificity of RNA encapsidation. *Journal of virology*. 1996;70(5):2757-63. Epub 1996/05/01. PubMed PMID: 8627749; PubMed Central PMCID: PMC190132.
- 533.** Hong EM, Perera R, Kuhn RJ. Alphavirus capsid protein helix I controls a checkpoint in nucleocapsid core assembly. *Journal of virology*. 2006;80(18):8848-55. Epub 2006/08/31. doi: 10.1128/JVI.00619-06. PubMed PMID: 16940497; PubMed Central PMCID: PMC1563918.
- 534.** Bonatti S, Migliaccio G, Blobel G, Walter P. Role of signal recognition particle in the membrane assembly of Sindbis viral glycoproteins. *Eur J Biochem*. 1984;140(3):499-502. Epub 1984/05/02. doi: 10.1111/j.1432-1033.1984.tb08130.x. PubMed PMID: 6723645.
- 535.** Snyder JE, Kulcsar KA, Schultz KL, Riley CP, Neary JT, Marr S, et al. Functional characterization of the alphavirus TF protein. *Journal of virology*. 2013;87(15):8511-23. Epub 2013/05/31. doi: 10.1128/JVI.00449-13. PubMed PMID: 23720714; PubMed Central PMCID: PMC3719798.
- 536.** Parrott MM, Sitarski SA, Arnold RJ, Picton LK, Hill RB, Mukhopadhyay S. Role of conserved cysteines in the alphavirus E3 protein. *Journal of virology*. 2009;83(6):2584-91. Epub 2008/12/26. doi: 10.1128/JVI.02158-08. PubMed PMID: 19109378; PubMed Central PMCID: PMC2648270.
- 537.** Voss JE, Vaney MC, Duquerroy S, Vonnrhein C, Girard-Blanc C, Crublet E, et al. Glycoprotein organization of Chikungunya virus particles revealed by X-ray crystallography. *Nature*. 2010;468(7324):709-12. Epub 2010/12/03. doi: 10.1038/nature09555. PubMed PMID: 21124458.
- 538.** Firth AE, Chung BY, Fleeton MN, Atkins JF. Discovery of frameshifting in Alphavirus 6K resolves a 20-year enigma. *Virology journal*. 2008;5:108. Epub

- 2008/09/30. doi: 10.1186/1743-422X-5-108. PubMed PMID: 18822126; PubMed Central PMCID: PMC2569925.
- 539.** Yao JS, Strauss EG, Strauss JH. Interactions between PE2, E1, and 6K required for assembly of alphaviruses studied with chimeric viruses. *Journal of virology*. 1996;70(11):7910-20. Epub 1996/11/01. PubMed PMID: 8892914; PubMed Central PMCID: PMC190863.
- 540.** McInerney GM, Smit JM, Liljestrom P, Wilschut J. Semliki Forest virus produced in the absence of the 6K protein has an altered spike structure as revealed by decreased membrane fusion capacity. *Virology*. 2004;325(2):200-6. Epub 2004/07/13. doi: 10.1016/j.virol.2004.04.043. PubMed PMID: 15246260.
- 541.** Wang KS, Kuhn RJ, Strauss EG, Ou S, Strauss JH. High-affinity laminin receptor is a receptor for Sindbis virus in mammalian cells. *Journal of virology*. 1992;66(8):4992-5001. Epub 1992/08/01. PubMed PMID: 1385835; PubMed Central PMCID: PMC241351.
- 542.** Klimstra WB, Nangle EM, Smith MS, Yurochko AD, Ryman KD. DC-SIGN and L-SIGN can act as attachment receptors for alphaviruses and distinguish between mosquito cell- and mammalian cell-derived viruses. *Journal of virology*. 2003;77(22):12022-32. Epub 2003/10/29. doi: 10.1128/jvi.77.22.12022-12032.2003. PubMed PMID: 14581539; PubMed Central PMCID: PMC254289.
- 543.** Kononchik JP, Jr., Hernandez R, Brown DT. An alternative pathway for alphavirus entry. *Virology journal*. 2011;8:304. Epub 2011/06/17. doi: 10.1186/1743-422X-8-304. PubMed PMID: 21676248; PubMed Central PMCID: PMC3315796.
- 544.** Kielian M, Chanel-Vos C, Liao M. Alphavirus Entry and Membrane Fusion. *Viruses*. 2010;2(4):796-825. Epub 2010/03/26. doi: 10.3390/v2040796. PubMed PMID: 21546978; PubMed Central PMCID: PMC3086016.
- 545.** Wintachai P, Wikan N, Kuadkitkan A, Jaimipuk T, Ubol S, Pulmanausahakul R, et al. Identification of prohibitin as a Chikungunya virus receptor protein. *J Med Virol*. 2012;84(11):1757-70. Epub 2012/09/22. doi: 10.1002/jmv.23403. PubMed PMID: 22997079.
- 546.** Zhang R, Kim AS, Fox JM, Nair S, Basore K, Klimstra WB, et al. Mxra8 is a receptor for multiple arthritogenic alphaviruses. *Nature*. 2018;557(7706):570-4. Epub 2018/05/18. doi: 10.1038/s41586-018-0121-3. PubMed PMID: 29769725; PubMed Central PMCID: PMC5970976.
- 547.** Bernard E, Solignat M, Gay B, Chazal N, Higgs S, Devaux C, et al. Endocytosis of chikungunya virus into mammalian cells: role of clathrin and

- early endosomal compartments. *PloS one*. 2010;5(7):e11479. Epub 2010/07/16. doi: 10.1371/journal.pone.0011479. PubMed PMID: 20628602; PubMed Central PMCID: PMC2900206.
- 548.** Marsh M, Helenius A. Adsorptive endocytosis of Semliki Forest virus. *Journal of molecular biology*. 1980;142(3):439-54. Epub 1980/09/25. doi: 10.1016/0022-2836(80)90281-8. PubMed PMID: 7463480.
- 549.** Carvalho CAM, Silva JL, Oliveira AC, Gomes AMO. On the entry of an emerging arbovirus into host cells: Mayaro virus takes the highway to the cytoplasm through fusion with early endosomes and caveolae-derived vesicles. *PeerJ*. 2017;5:e3245. Epub 2017/05/04. doi: 10.7717/peerj.3245. PubMed PMID: 28462045; PubMed Central PMCID: PMC5410162.
- 550.** Wahlberg JM, Boere WA, Garoff H. The heterodimeric association between the membrane proteins of Semliki Forest virus changes its sensitivity to low pH during virus maturation. *Journal of virology*. 1989;63(12):4991-7. Epub 1989/12/01. PubMed PMID: 2479769; PubMed Central PMCID: PMC251158.
- 551.** Kolokoltsov AA, Fleming EH, Davey RA. Venezuelan equine encephalitis virus entry mechanism requires late endosome formation and resists cell membrane cholesterol depletion. *Virology*. 2006;347(2):333-42. Epub 2006/01/24. doi: 10.1016/j.virol.2005.11.051. PubMed PMID: 16427678.
- 552.** Freitas M, Da Poian AT, Barth OM, Rebello MA, Silva JL, Gaspar LP. The fusogenic state of Mayaro virus induced by low pH and by hydrostatic pressure. *Cell Biochem Biophys*. 2006;44(3):325-35. Epub 2006/05/09. doi: 10.1385/cbb:44:3:325. PubMed PMID: 16679519.
- 553.** van Duijl-Richter MK, Hoornweg TE, Rodenhuis-Zybert IA, Smit JM. Early Events in Chikungunya Virus Infection-From Virus Cell Binding to Membrane Fusion. *Viruses*. 2015;7(7):3647-74. Epub 2015/07/23. doi: 10.3390/v7072792. PubMed PMID: 26198242; PubMed Central PMCID: PMC4517121.
- 554.** Kielian MC, Marsh M, Helenius A. Kinetics of endosome acidification detected by mutant and wild-type Semliki Forest virus. *EMBO J*. 1986;5(12):3103-9. Epub 1986/12/01. PubMed PMID: 3816755; PubMed Central PMCID: PMC1167299.
- 555.** Vashishtha M, Phalen T, Marquardt MT, Ryu JS, Ng AC, Kielian M. A single point mutation controls the cholesterol dependence of Semliki Forest virus entry and exit. *J Cell Biol*. 1998;140(1):91-9. Epub 1998/02/14. doi: 10.1083/jcb.140.1.91. PubMed PMID: 9425157; PubMed Central PMCID: PMC2132589.
- 556.** Wengler G, Wengler G. Identification of a transfer of viral core protein to cellular ribosomes during the early stages of alphavirus infection. *Virology*.

- 1984;134(2):435-42. Epub 1984/04/30. doi: 10.1016/0042-6822(84)90310-6. PubMed PMID: 6545074.
- 557.** Wengler G, Wurfner D, Wengler G. Identification of a sequence element in the alphavirus core protein which mediates interaction of cores with ribosomes and the disassembly of cores. *Virology*. 1992;191(2):880-8. Epub 1992/12/01. doi: 10.1016/0042-6822(92)90263-o. PubMed PMID: 1333127.
- 558.** Lundberg L, Carey B, Kehn-Hall K. Venezuelan Equine Encephalitis Virus Capsid-The Clever Caper. *Viruses*. 2017;9(10). Epub 2017/09/30. doi: 10.3390/v9100279. PubMed PMID: 28961161; PubMed Central PMCID: PMC5691631.
- 559.** Takkinen K. Complete nucleotide sequence of the nonstructural protein genes of Semliki Forest virus. *Nucleic acids research*. 1986;14(14):5667-82. Epub 1986/07/25. doi: 10.1093/nar/14.14.5667. PubMed PMID: 3488539; PubMed Central PMCID: PMC311584.
- 560.** Li G, Rice CM. The signal for translational readthrough of a UGA codon in Sindbis virus RNA involves a single cytidine residue immediately downstream of the termination codon. *Journal of virology*. 1993;67(8):5062-7. Epub 1993/08/01. PubMed PMID: 8331741; PubMed Central PMCID: PMC237898.
- 561.** de Groot RJ, Hardy WR, Shirako Y, Strauss JH. Cleavage-site preferences of Sindbis virus polyproteins containing the non-structural proteinase. Evidence for temporal regulation of polyprotein processing in vivo. *EMBO J*. 1990;9(8):2631-8. Epub 1990/08/01. PubMed PMID: 2142454; PubMed Central PMCID: PMC552296.
- 562.** Shirako Y, Strauss JH. Cleavage between nsP1 and nsP2 initiates the processing pathway of Sindbis virus nonstructural polyprotein P123. *Virology*. 1990;177(1):54-64. Epub 1990/07/01. doi: 10.1016/0042-6822(90)90459-5. PubMed PMID: 2141206.
- 563.** Shin G, Yost SA, Miller MT, Elrod EJ, Grakoui A, Marcotrigiano J. Structural and functional insights into alphavirus polyprotein processing and pathogenesis. *Proceedings of the National Academy of Sciences of the United States of America*. 2012;109(41):16534-9. Epub 2012/09/27. doi: 10.1073/pnas.1210418109. PubMed PMID: 23010928; PubMed Central PMCID: PMC3478664.
- 564.** Kim KH, Rumenapf T, Strauss EG, Strauss JH. Regulation of Semliki Forest virus RNA replication: a model for the control of alphavirus pathogenesis in invertebrate hosts. *Virology*. 2004;323(1):153-63. Epub 2004/05/29. doi: 10.1016/j.virol.2004.03.009. PubMed PMID: 15165827.

- 565.** Hellstrom K, Kallio K, Utt A, Quirin T, Jokitalo E, Merits A, et al. Partially Uncleaved Alphavirus Replicase Forms Spherule Structures in the Presence and Absence of RNA Template. *Journal of virology*. 2017;91(18). Epub 2017/07/14. doi: 10.1128/JVI.00787-17. PubMed PMID: 28701392; PubMed Central PMCID: PMC5571266.
- 566.** Frolova EI, Gorchakov R, Pereboeva L, Atasheva S, Frolov I. Functional Sindbis virus replicative complexes are formed at the plasma membrane. *Journal of virology*. 2010;84(22):11679-95. Epub 2010/09/10. doi: 10.1128/JVI.01441-10. PubMed PMID: 20826696; PubMed Central PMCID: PMC2977861.
- 567.** Sjoberg M, Lindqvist B, Garoff H. Activation of the alphavirus spike protein is suppressed by bound E3. *Journal of virology*. 2011;85(11):5644-50. Epub 2011/03/25. doi: 10.1128/JVI.00130-11. PubMed PMID: 21430054; PubMed Central PMCID: PMC3094962.
- 568.** Lee CY, Kam YW, Fric J, Malleret B, Koh EG, Prakash C, et al. Chikungunya virus neutralization antigens and direct cell-to-cell transmission are revealed by human antibody-escape mutants. *PLoS pathogens*. 2011;7(12):e1002390. Epub 2011/12/07. doi: 10.1371/journal.ppat.1002390. PubMed PMID: 22144891; PubMed Central PMCID: PMC3228792.
- 569.** Martinez MG, Kielian M. Intercellular Extensions Are Induced by the Alphavirus Structural Proteins and Mediate Virus Transmission. *PLoS pathogens*. 2016;12(12):e1006061. Epub 2016/12/16. doi: 10.1371/journal.ppat.1006061. PubMed PMID: 27977778; PubMed Central PMCID: PMC5158078.
- 570.** Richards SL, Anderson SL, Smartt CT. Vector competence of Florida mosquitoes for chikungunya virus. *J Vector Ecol*. 2010;35(2):439-43. Epub 2010/12/24. doi: 10.1111/j.1948-7134.2010.00105.x. PubMed PMID: 21175954; PubMed Central PMCID: PMC3076135.
- 571.** Lim EXY, Lee WS, Madzokere ET, Herrero LJ. Mosquitoes as Suitable Vectors for Alphaviruses. *Viruses*. 2018;10(2). Epub 2018/02/15. doi: 10.3390/v10020084. PubMed PMID: 29443908; PubMed Central PMCID: PMC5850391.
- 572.** Russell RC. Ross River virus: ecology and distribution. *Annu Rev Entomol*. 2002;47:1-31. Epub 2001/12/01. doi: 10.1146/annurev.ento.47.091201.145100. PubMed PMID: 11729067.
- 573.** Franz AW, Kantor AM, Passarelli AL, Clem RJ. Tissue Barriers to Arbovirus Infection in Mosquitoes. *Viruses*. 2015;7(7):3741-67. Epub 2015/07/18. doi: 10.3390/v7072795. PubMed PMID: 26184281; PubMed Central PMCID: PMC4517124.

- 574.** Romoser WS, Wasieloski LP, Jr., Pushko P, Kondig JP, Lerdthusnee K, Neira M, et al. Evidence for arbovirus dissemination conduits from the mosquito (Diptera: Culicidae) midgut. *J Med Entomol.* 2004;41(3):467-75. Epub 2004/06/10. doi: 10.1603/0022-2585-41.3.467. PubMed PMID: 15185952.
- 575.** Dong S, Kantor AM, Lin J, Passarelli AL, Clem RJ, Franz AW. Infection pattern and transmission potential of chikungunya virus in two New World laboratory-adapted *Aedes aegypti* strains. *Sci Rep.* 2016;6:24729. Epub 2016/04/23. doi: 10.1038/srep24729. PubMed PMID: 27102548; PubMed Central PMCID: PMC4840389.
- 576.** Turell MJ. Effect of environmental temperature on the vector competence of *Aedes taeniorhynchus* for Rift Valley fever and Venezuelan equine encephalitis viruses. *Am J Trop Med Hyg.* 1993;49(6):672-6. Epub 1993/12/01. doi: 10.4269/ajtmh.1993.49.672. PubMed PMID: 8279634.
- 577.** Westbrook CJ, Reiskind MH, Pesko KN, Greene KE, Lounibos LP. Larval environmental temperature and the susceptibility of *Aedes albopictus* Skuse (Diptera: Culicidae) to Chikungunya virus. *Vector Borne Zoonotic Dis.* 2010;10(3):241-7. Epub 2009/09/04. doi: 10.1089/vbz.2009.0035. PubMed PMID: 19725768; PubMed Central PMCID: PMC2883477.
- 578.** Go YY, Balasuriya UB, Lee CK. Zoonotic encephalitides caused by arboviruses: transmission and epidemiology of alphaviruses and flaviviruses. *Clin Exp Vaccine Res.* 2014;3(1):58-77. Epub 2014/01/16. doi: 10.7774/cevr.2014.3.1.58. PubMed PMID: 24427764; PubMed Central PMCID: PMC3890452.
- 579.** Yu W, Dale P, Turner L, Tong S. Projecting the impact of climate change on the transmission of Ross River virus: methodological challenges and research needs. *Epidemiol Infect.* 2014;142(10):2013-23. Epub 2014/03/13. doi: 10.1017/S0950268814000399. PubMed PMID: 24612684.
- 580.** Poirier EZ, Mounce BC, Rozen-Gagnon K, Hooikaas PJ, Stapleford KA, Moratorio G, et al. Low-Fidelity Polymerases of Alphaviruses Recombine at Higher Rates To Overproduce Defective Interfering Particles. *Journal of virology.* 2015;90(5):2446-54. Epub 2015/12/18. doi: 10.1128/JVI.02921-15. PubMed PMID: 26676773; PubMed Central PMCID: PMC4810721.
- 581.** Webster JL, Stapleford KA. Arbovirus Adaptation: Roles in Transmission and Emergence. *Current Clinical Microbiology Reports.* 2017;4(3):159-66. doi: 10.1007/s40588-017-0068-4.
- 582.** Schuffenecker I, Iteaman I, Michault A, Murri S, Frangeul L, Vaney MC, et al. Genome microevolution of chikungunya viruses causing the Indian Ocean outbreak. *PLoS medicine.* 2006;3(7):e263. Epub 2006/05/17. doi:

- 10.1371/journal.pmed.0030263. PubMed PMID: 16700631; PubMed Central PMCID: PMC1463904.
- 583.** Vazeille M, Moutailler S, Coudrier D, Rousseaux C, Khun H, Huerre M, et al. Two Chikungunya isolates from the outbreak of La Reunion (Indian Ocean) exhibit different patterns of infection in the mosquito, *Aedes albopictus*. *PLoS one*. 2007;2(11):e1168. Epub 2007/11/15. doi: 10.1371/journal.pone.0001168. PubMed PMID: 18000540; PubMed Central PMCID: PMC2064959.
- 584.** Arias-Goeta C, Mousson L, Rougeon F, Failloux AB. Dissemination and transmission of the E1-226V variant of chikungunya virus in *Aedes albopictus* are controlled at the midgut barrier level. *PLoS one*. 2013;8(2):e57548. Epub 2013/02/26. doi: 10.1371/journal.pone.0057548. PubMed PMID: 23437397; PubMed Central PMCID: PMC3578806.
- 585.** Izurieta RO, Macaluso M, Watts DM, Tesh RB, Guerra B, Cruz LM, et al. Hunting in the Rainforest and Mayaro Virus Infection: An emerging Alphavirus in Ecuador. *J Glob Infect Dis*. 2011;3(4):317-23. Epub 2012/01/10. doi: 10.4103/0974-777X.91049. PubMed PMID: 22223990; PubMed Central PMCID: PMC3249982.
- 586.** Sun J, Wu. Mayaro virus, a regional or global threat? *Travel Med Infect Dis*. 2019:101462. Epub 2019/07/29. doi: 10.1016/j.tmaid.2019.07.018. PubMed PMID: 31352004.
- 587.** Theilacker C, Held J, Allering L, Emmerich P, Schmidt-Chanasit J, Kern WV, et al. Prolonged polyarthralgia in a German traveller with Mayaro virus infection without inflammatory correlates. *BMC infectious diseases*. 2013;13:369. Epub 2013/08/10. doi: 10.1186/1471-2334-13-369. PubMed PMID: 23927600; PubMed Central PMCID: PMC3750572.
- 588.** Kurkela S, Ratti O, Huhtamo E, Uzcategui NY, Nuorti JP, Laakkonen J, et al. Sindbis virus infection in resident birds, migratory birds, and humans, Finland. *Emerg Infect Dis*. 2008;14(1):41-7. Epub 2008/02/09. doi: 10.3201/eid1401.070510. PubMed PMID: 18258075; PubMed Central PMCID: PMC2600146.
- 589.** Monaghan AJ, Eisen RJ, Eisen L, McAllister J, Savage HM, Mutebi JP, et al. Consensus and uncertainty in the geographic range of *Aedes aegypti* and *Aedes albopictus* in the contiguous United States: Multi-model assessment and synthesis. *PLoS computational biology*. 2019;15(10):e1007369. Epub 2019/10/11. doi: 10.1371/journal.pcbi.1007369. PubMed PMID: 31600194; PubMed Central PMCID: PMC6786520.
- 590.** Ryan SJ, Carlson CJ, Mordecai EA, Johnson LR. Global expansion and redistribution of *Aedes*-borne virus transmission risk with climate change. *PLoS Negl Trop Dis*. 2019;13(3):e0007213. Epub 2019/03/29. doi:

- 10.1371/journal.pntd.0007213. PubMed PMID: 30921321; PubMed Central PMCID: PMC6438455.
- 591.** Li M, Yang T, Kandul NP, Bui M, Gamez S, Raban R, et al. Development of a confinable gene drive system in the human disease vector *Aedes aegypti*. *Elife*. 2020;9. Epub 2020/01/22. doi: 10.7554/eLife.51701. PubMed PMID: 31960794; PubMed Central PMCID: PMC6974361.
- 592.** Bhatt S, Gething PW, Brady OJ, Messina JP, Farlow AW, Moyes CL, et al. The global distribution and burden of dengue. *Nature*. 2013;496(7446):504-7. Epub 2013/04/09. doi: 10.1038/nature12060. PubMed PMID: 23563266; PubMed Central PMCID: PMC3651993.
- 593.** Niang EHA, Bassene H, Fenollar F, Mediannikov O. Biological Control of Mosquito-Borne Diseases: The Potential of Wolbachia-Based Interventions in an IVM Framework. *J Trop Med*. 2018;2018:1470459. Epub 2018/12/26. doi: 10.1155/2018/1470459. PubMed PMID: 30581476; PubMed Central PMCID: PMC6276417.
- 594.** Djouaka RF, Bakare AA, Bankole HS, Doannio JM, Kossou H, Akogbeto MC. Quantification of the efficiency of treatment of *Anopheles gambiae* breeding sites with petroleum products by local communities in areas of insecticide resistance in the Republic of Benin. *Malar J*. 2007;6:56. Epub 2007/05/10. doi: 10.1186/1475-2875-6-56. PubMed PMID: 17488523; PubMed Central PMCID: PMC1885267.
- 595.** Stage HH. Use of Petroleum Oils in Mosquito Control. *AGRICULTURAL APPLICATIONS OF PETROLEUM PRODUCTS*. *Advances in Chemistry*. 7: AMERICAN CHEMICAL SOCIETY; 1952. p. 43-51.
- 596.** Demok S, Endersby-Harshman N, Vinit R, Timinao L, Robinson LJ, Susapu M, et al. Insecticide resistance status of *Aedes aegypti* and *Aedes albopictus* mosquitoes in Papua New Guinea. *Parasit Vectors*. 2019;12(1):333. Epub 2019/07/05. doi: 10.1186/s13071-019-3585-6. PubMed PMID: 31269965; PubMed Central PMCID: PMC6609403.
- 597.** Kawada H, Futami K, Higa Y, Rai G, Suzuki T, Rai SK. Distribution and pyrethroid resistance status of *Aedes aegypti* and *Aedes albopictus* populations and possible phylogenetic reasons for the recent invasion of *Aedes aegypti* in Nepal. *Parasit Vectors*. 2020;13(1):213. Epub 2020/04/24. doi: 10.1186/s13071-020-04090-6. PubMed PMID: 32321546; PubMed Central PMCID: PMC7178601.
- 598.** Barrera R, Amador M, Acevedo V, Hemme RR, Felix G. Sustained, area-wide control of *Aedes aegypti* using CDC autocidal gravid ovitraps. *Am J Trop Med Hyg*. 2014;91(6):1269-76. Epub 2014/09/17. doi: 10.4269/ajtmh.14-0426. PubMed PMID: 25223937; PubMed Central PMCID: PMC4257658.

- 599.** Paz-Soldan VA, Yukich J, Soonthornhdada A, Giron M, Apperson CS, Ponnusamy L, et al. Design and Testing of Novel Lethal Ovitrap to Reduce Populations of Aedes Mosquitoes: Community-Based Participatory Research between Industry, Academia and Communities in Peru and Thailand. *PloS one*. 2016;11(8):e0160386. Epub 2016/08/18. doi: 10.1371/journal.pone.0160386. PubMed PMID: 27532497; PubMed Central PMCID: PMC4988764.
- 600.** El-Sabaawi RW, Frauendorf TC, Marques PS, Mackenzie RA, Manna LR, Mazzoni R, et al. Biodiversity and ecosystem risks arising from using guppies to control mosquitoes. *Biol Lett*. 2016;12(10). Epub 2017/01/26. doi: 10.1098/rsbl.2016.0590. PubMed PMID: 28120806; PubMed Central PMCID: PMC5095194.
- 601.** Achee NL, Grieco JP, Vatandoost H, Seixas G, Pinto J, Ching-Ng L, et al. Alternative strategies for mosquito-borne arbovirus control. *PLoS Negl Trop Dis*. 2019;13(1):e0006822. Epub 2019/01/04. doi: 10.1371/journal.pntd.0006822. PubMed PMID: 30605475; PubMed Central PMCID: PMC6317787.
- 602.** Caragata EP, Dutra HLC, Moreira LA. Exploiting Intimate Relationships: Controlling Mosquito-Transmitted Disease with Wolbachia. *Trends Parasitol*. 2016;32(3):207-18. Epub 2016/01/19. doi: 10.1016/j.pt.2015.10.011. PubMed PMID: 26776329.
- 603.** Martinez J, Ok S, Smith S, Snoeck K, Day JP, Jiggins FM. Should Symbionts Be Nice or Selfish? Antiviral Effects of Wolbachia Are Costly but Reproductive Parasitism Is Not. *PLoS pathogens*. 2015;11(7):e1005021. Epub 2015/07/02. doi: 10.1371/journal.ppat.1005021. PubMed PMID: 26132467; PubMed Central PMCID: PMC4488530.
- 604.** Evans BR, Kotsakiozi P, Costa-da-Silva AL, Ioshino RS, Garziera L, Pedrosa MC, et al. Transgenic Aedes aegypti Mosquitoes Transfer Genes into a Natural Population. *Sci Rep*. 2019;9(1):13047. Epub 2019/09/12. doi: 10.1038/s41598-019-49660-6. PubMed PMID: 31506595; PubMed Central PMCID: PMC6736937.
- 605.** Carvalho DO, McKemey AR, Garziera L, Lacroix R, Donnelly CA, Alphey L, et al. Suppression of a Field Population of Aedes aegypti in Brazil by Sustained Release of Transgenic Male Mosquitoes. *PLoS Negl Trop Dis*. 2015;9(7):e0003864. Epub 2015/07/03. doi: 10.1371/journal.pntd.0003864. PubMed PMID: 26135160; PubMed Central PMCID: PMC4489809.
- 606.** Gorman K, Young J, Pineda L, Marquez R, Sosa N, Bernal D, et al. Short-term suppression of Aedes aegypti using genetic control does not facilitate Aedes albopictus. *Pest Manag Sci*. 2016;72(3):618-28. Epub 2015/09/17. doi: 10.1002/ps.4151. PubMed PMID: 26374668; PubMed Central PMCID: PMC5057309.

- 607.** Kyrou K, Hammond AM, Galizi R, Kranjc N, Burt A, Beaghton AK, et al. A CRISPR-Cas9 gene drive targeting doublesex causes complete population suppression in caged *Anopheles gambiae* mosquitoes. *Nature biotechnology*. 2018;36(11):1062-6. Epub 2018/09/25. doi: 10.1038/nbt.4245. PubMed PMID: 30247490; PubMed Central PMCID: PMC6871539.
- 608.** Schmidt H, Collier TC, Hanemaaijer MJ, Houston PD, Lee Y, Lanzaro GC. Abundance of conserved CRISPR-Cas9 target sites within the highly polymorphic genomes of *Anopheles* and *Aedes* mosquitoes. *Nature communications*. 2020;11(1):1425. Epub 2020/03/20. doi: 10.1038/s41467-020-15204-0. PubMed PMID: 32188851; PubMed Central PMCID: PMC7080748.
- 609.** Pingen M, Bryden SR, Pondeville E, Schnettler E, Kohl A, Merits A, et al. Host Inflammatory Response to Mosquito Bites Enhances the Severity of Arbovirus Infection. *Immunity*. 2016;44(6):1455-69. Epub 2016/06/23. doi: 10.1016/j.immuni.2016.06.002. PubMed PMID: 27332734; PubMed Central PMCID: PMC4920956.
- 610.** McCarthy MK, Davenport BJ, Reynoso GV, Lucas ED, May NA, Elmore SA, et al. Chikungunya virus impairs draining lymph node function by inhibiting HEV-mediated lymphocyte recruitment. *JCI Insight*. 2018;3(13). Epub 2018/07/13. doi: 10.1172/jci.insight.121100. PubMed PMID: 29997290; PubMed Central PMCID: PMC6124534.
- 611.** MacDonald GH, Johnston RE. Role of dendritic cell targeting in Venezuelan equine encephalitis virus pathogenesis. *Journal of virology*. 2000;74(2):914-22. Epub 2000/01/07. doi: 10.1128/jvi.74.2.914-922.2000. PubMed PMID: 10623754; PubMed Central PMCID: PMC111612.
- 612.** Labadie K, Larcher T, Joubert C, Mannioui A, Delache B, Brochard P, et al. Chikungunya disease in nonhuman primates involves long-term viral persistence in macrophages. *The Journal of clinical investigation*. 2010;120(3):894-906. Epub 2010/02/25. doi: 10.1172/JCI40104. PubMed PMID: 20179353; PubMed Central PMCID: PMC2827953.
- 613.** Steele KE, Twenhafel NA. REVIEW PAPER: pathology of animal models of alphavirus encephalitis. *Veterinary pathology*. 2010;47(5):790-805. Epub 2010/06/17. doi: 10.1177/0300985810372508. PubMed PMID: 20551475.
- 614.** Assuncao-Miranda I, Cruz-Oliveira C, Da Poian AT. Molecular mechanisms involved in the pathogenesis of alphavirus-induced arthritis. *Biomed Res Int*. 2013;2013:973516. Epub 2013/09/27. doi: 10.1155/2013/973516. PubMed PMID: 24069610; PubMed Central PMCID: PMC3771267.
- 615.** Carpentier KS, Morrison TE. Innate immune control of alphavirus infection. *Curr Opin Virol*. 2018;28:53-60. Epub 2017/11/28. doi:

- 10.1016/j.coviro.2017.11.006. PubMed PMID: 29175515; PubMed Central PMCID: PMC5835171.
- 616.** Gall B, Pryke K, Abraham J, Mizuno N, Botto S, Sali TM, et al. Emerging Alphaviruses Are Sensitive to Cellular States Induced by a Novel Small-Molecule Agonist of the STING Pathway. *Journal of virology*. 2018;92(6). Epub 2017/12/22. doi: 10.1128/JVI.01913-17. PubMed PMID: 29263267; PubMed Central PMCID: PMC5827377.
- 617.** Akhrymuk I, Frolov I, Frolova EI. Both RIG-I and MDA5 detect alphavirus replication in concentration-dependent mode. *Virology*. 2016;487:230-41. Epub 2015/11/10. doi: 10.1016/j.virol.2015.09.023. PubMed PMID: 26550947; PubMed Central PMCID: PMC4721224.
- 618.** Chen H, Jiang Z. The essential adaptors of innate immune signaling. *Protein Cell*. 2013;4(1):27-39. Epub 2012/09/22. doi: 10.1007/s13238-012-2063-0. PubMed PMID: 22996173; PubMed Central PMCID: PMC4875439.
- 619.** Her Z, Teng TS, Tan JJ, Teo TH, Kam YW, Lum FM, et al. Loss of TLR3 aggravates CHIKV replication and pathology due to an altered virus-specific neutralizing antibody response. *EMBO Mol Med*. 2015;7(1):24-41. Epub 2014/12/03. doi: 10.15252/emmm.201404459. PubMed PMID: 25452586; PubMed Central PMCID: PMC4309666.
- 620.** Mostafavi H, Abeyratne E, Zaid A, Taylor A. Arthritogenic Alphavirus-Induced Immunopathology and Targeting Host Inflammation as A Therapeutic Strategy for Alphaviral Disease. *Viruses*. 2019;11(3). Epub 2019/03/27. doi: 10.3390/v11030290. PubMed PMID: 30909385; PubMed Central PMCID: PMC6466158.
- 621.** Ni G, Ma Z, Damania B. cGAS and STING: At the intersection of DNA and RNA virus-sensing networks. *PLoS pathogens*. 2018;14(8):e1007148. Epub 2018/08/17. doi: 10.1371/journal.ppat.1007148. PubMed PMID: 30114241; PubMed Central PMCID: PMC6095619.
- 622.** Schulz O, Pichlmair A, Rehwinkel J, Rogers NC, Scheuner D, Kato H, et al. Protein kinase R contributes to immunity against specific viruses by regulating interferon mRNA integrity. *Cell Host Microbe*. 2010;7(5):354-61. Epub 2010/05/19. doi: 10.1016/j.chom.2010.04.007. PubMed PMID: 20478537; PubMed Central PMCID: PMC2919169.
- 623.** Ivashkiv LB, Donlin LT. Regulation of type I interferon responses. *Nat Rev Immunol*. 2014;14(1):36-49. Epub 2013/12/24. doi: 10.1038/nri3581. PubMed PMID: 24362405; PubMed Central PMCID: PMC4084561.
- 624.** White LK, Sali T, Alvarado D, Gatti E, Pierre P, Streblow D, et al. Chikungunya virus induces IPS-1-dependent innate immune activation and

- protein kinase R-independent translational shutoff. *Journal of virology*. 2011;85(1):606-20. Epub 2010/10/22. doi: 10.1128/JVI.00767-10. PubMed PMID: 20962078; PubMed Central PMCID: PMC3014158.
- 625.** Couderc T, Chretien F, Schilte C, Disson O, Brigitte M, Guivel-Benhassine F, et al. A mouse model for Chikungunya: young age and inefficient type-I interferon signaling are risk factors for severe disease. *PLoS pathogens*. 2008;4(2):e29. Epub 2008/02/20. doi: 10.1371/journal.ppat.0040029. PubMed PMID: 18282093; PubMed Central PMCID: PMC2242832.
- 626.** Schilte C, Couderc T, Chretien F, Sourisseau M, Gangneux N, Guivel-Benhassine F, et al. Type I IFN controls chikungunya virus via its action on nonhematopoietic cells. *J Exp Med*. 2010;207(2):429-42. Epub 2010/02/04. doi: 10.1084/jem.20090851. PubMed PMID: 20123960; PubMed Central PMCID: PMC2822618.
- 627.** Rudd PA, Wilson J, Gardner J, Larcher T, Babarit C, Le TT, et al. Interferon response factors 3 and 7 protect against Chikungunya virus hemorrhagic fever and shock. *Journal of virology*. 2012;86(18):9888-98. Epub 2012/07/05. doi: 10.1128/JVI.00956-12. PubMed PMID: 22761364; PubMed Central PMCID: PMC3446587.
- 628.** Cook LE, Locke MC, Young AR, Monte K, Hedberg ML, Shimak RM, et al. Distinct Roles of Interferon Alpha and Beta in Controlling Chikungunya Virus Replication and Modulating Neutrophil-Mediated Inflammation. *Journal of virology*. 2019;94(1). Epub 2019/10/18. doi: 10.1128/JVI.00841-19. PubMed PMID: 31619554; PubMed Central PMCID: PMC6912113.
- 629.** Chow A, Her Z, Ong EK, Chen JM, Dimatatac F, Kwek DJ, et al. Persistent arthralgia induced by Chikungunya virus infection is associated with interleukin-6 and granulocyte macrophage colony-stimulating factor. *The Journal of infectious diseases*. 2011;203(2):149-57. Epub 2011/02/04. doi: 10.1093/infdis/jiq042. PubMed PMID: 21288813; PubMed Central PMCID: PMC3071069.
- 630.** Kelvin AA, Banner D, Silvi G, Moro ML, Spataro N, Gaibani P, et al. Inflammatory cytokine expression is associated with chikungunya virus resolution and symptom severity. *PLoS Negl Trop Dis*. 2011;5(8):e1279. Epub 2011/08/23. doi: 10.1371/journal.pntd.0001279. PubMed PMID: 21858242; PubMed Central PMCID: PMC3156690.
- 631.** Ng LF, Chow A, Sun YJ, Kwek DJ, Lim PL, Dimatatac F, et al. IL-1beta, IL-6, and RANTES as biomarkers of Chikungunya severity. *PloS one*. 2009;4(1):e4261. Epub 2009/01/22. doi: 10.1371/journal.pone.0004261. PubMed PMID: 19156204; PubMed Central PMCID: PMC2625438.

- 632.** Fox JM, Diamond MS. Immune-Mediated Protection and Pathogenesis of Chikungunya Virus. *Journal of immunology*. 2016;197(11):4210-8. Epub 2016/11/20. doi: 10.4049/jimmunol.1601426. PubMed PMID: 27864552; PubMed Central PMCID: PMC5120763.
- 633.** Teo TH, Her Z, Tan JJ, Lum FM, Lee WW, Chan YH, et al. Caribbean and La Reunion Chikungunya Virus Isolates Differ in Their Capacity To Induce Proinflammatory Th1 and NK Cell Responses and Acute Joint Pathology. *Journal of virology*. 2015;89(15):7955-69. Epub 2015/05/23. doi: 10.1128/JVI.00909-15. PubMed PMID: 25995257; PubMed Central PMCID: PMC4505608.
- 634.** Fox JM, Long F, Edeling MA, Lin H, van Duijl-Richter MKS, Fong RH, et al. Broadly Neutralizing Alphavirus Antibodies Bind an Epitope on E2 and Inhibit Entry and Egress. *Cell*. 2015;163(5):1095-107. Epub 2015/11/11. doi: 10.1016/j.cell.2015.10.050. PubMed PMID: 26553503; PubMed Central PMCID: PMC4659373.
- 635.** Binn LN, Harrison VR, Randall R. Patterns of viremia and antibody observed in rhesus monkeys inoculated with chikungunya and other serologically related group A arboviruses. *Am J Trop Med Hyg*. 1967;16(6):782-5. Epub 1967/11/01. PubMed PMID: 4965218.
- 636.** Martins KA, Gregory MK, Valdez SM, Sprague TR, Encinales L, Pacheco N, et al. Neutralizing Antibodies from Convalescent Chikungunya Virus Patients Can Cross-Neutralize Mayaro and Una Viruses. *Am J Trop Med Hyg*. 2019;100(6):1541-4. Epub 2019/04/25. doi: 10.4269/ajtmh.18-0756. PubMed PMID: 31017081; PubMed Central PMCID: PMC6553899.
- 637.** Silva LA, Dermody TS. Chikungunya virus: epidemiology, replication, disease mechanisms, and prospective intervention strategies. *The Journal of clinical investigation*. 2017;127(3):737-49. Epub 2017/03/02. doi: 10.1172/JCI84417. PubMed PMID: 28248203; PubMed Central PMCID: PMC5330729.
- 638.** Laine M, Luukkainen R, Toivanen A. Sindbis viruses and other alphaviruses as cause of human arthritic disease. *J Intern Med*. 2004;256(6):457-71. Epub 2004/11/24. doi: 10.1111/j.1365-2796.2004.01413.x. PubMed PMID: 15554947.
- 639.** Nair S, Poddar S, Shimak RM, Diamond MS. Interferon Regulatory Factor 1 Protects against Chikungunya Virus-Induced Immunopathology by Restricting Infection in Muscle Cells. *Journal of virology*. 2017;91(22). Epub 2017/08/25. doi: 10.1128/JVI.01419-17. PubMed PMID: 28835505; PubMed Central PMCID: PMC5660487.

- 640.** Ozden S, Huerre M, Riviere JP, Coffey LL, Afonso PV, Mouly V, et al. Human muscle satellite cells as targets of Chikungunya virus infection. *PloS one*. 2007;2(6):e527. Epub 2007/06/15. doi: 10.1371/journal.pone.0000527. PubMed PMID: 17565380; PubMed Central PMCID: PMC1885285.
- 641.** Mehta R, Gerardin P, de Brito CAA, Soares CN, Ferreira MLB, Solomon T. The neurological complications of chikungunya virus: A systematic review. *Rev Med Virol*. 2018;28(3):e1978. Epub 2018/04/20. doi: 10.1002/rmv.1978. PubMed PMID: 29671914; PubMed Central PMCID: PMC5969245.
- 642.** Matusali G, Colavita F, Bordi L, Lalle E, Ippolito G, Capobianchi MR, et al. Tropism of the Chikungunya Virus. *Viruses*. 2019;11(2). Epub 2019/02/23. doi: 10.3390/v11020175. PubMed PMID: 30791607; PubMed Central PMCID: PMC6410217.
- 643.** Kurkela S, Helve T, Vaheri A, Vapalahti O. Arthritis and arthralgia three years after Sindbis virus infection: clinical follow-up of a cohort of 49 patients. *Scand J Infect Dis*. 2008;40(2):167-73. Epub 2007/09/14. doi: 10.1080/00365540701586996. PubMed PMID: 17852949.
- 644.** Gerardin P, Fianu A, Malvy D, Mussard C, Boussaid K, Rollot O, et al. Perceived morbidity and community burden after a Chikungunya outbreak: the TELECHIK survey, a population-based cohort study. *BMC Med*. 2011;9:5. Epub 2011/01/18. doi: 10.1186/1741-7015-9-5. PubMed PMID: 21235760; PubMed Central PMCID: PMC3029216.
- 645.** Frolova EI, Fayzulin RZ, Cook SH, Griffin DE, Rice CM, Frolov I. Roles of nonstructural protein nsP2 and Alpha/Beta interferons in determining the outcome of Sindbis virus infection. *Journal of virology*. 2002;76(22):11254-64. Epub 2002/10/22. doi: 10.1128/jvi.76.22.11254-11264.2002. PubMed PMID: 12388685; PubMed Central PMCID: PMC136776.
- 646.** Fros JJ, Liu WJ, Prow NA, Geertsema C, Ligtenberg M, Vanlandingham DL, et al. Chikungunya virus nonstructural protein 2 inhibits type I/II interferon-stimulated JAK-STAT signaling. *Journal of virology*. 2010;84(20):10877-87. Epub 2010/08/06. doi: 10.1128/JVI.00949-10. PubMed PMID: 20686047; PubMed Central PMCID: PMC2950581.
- 647.** Carrasco L, Sanz MA, Gonzalez-Almela E. The Regulation of Translation in Alphavirus-Infected Cells. *Viruses*. 2018;10(2). Epub 2018/02/09. doi: 10.3390/v10020070. PubMed PMID: 29419763; PubMed Central PMCID: PMC5850377.
- 648.** Koromilas AE. Roles of the translation initiation factor eIF2alpha serine 51 phosphorylation in cancer formation and treatment. *Biochimica et biophysica acta*. 2015;1849(7):871-80. Epub 2014/12/17. doi: 10.1016/j.bbagr.2014.12.007. PubMed PMID: 25497381.

- 649.** Rathore AP, Ng ML, Vasudevan SG. Differential unfolded protein response during Chikungunya and Sindbis virus infection: CHIKV nsP4 suppresses eIF2alpha phosphorylation. *Virology journal*. 2013;10:36. Epub 2013/01/30. doi: 10.1186/1743-422X-10-36. PubMed PMID: 23356742; PubMed Central PMCID: PMC3605262.
- 650.** Fros JJ, Pijlman GP. Alphavirus Infection: Host Cell Shut-Off and Inhibition of Antiviral Responses. *Viruses*. 2016;8(6). Epub 2016/06/15. doi: 10.3390/v8060166. PubMed PMID: 27294951; PubMed Central PMCID: PMC4926186.
- 651.** Gorchakov R, Frolova E, Williams BR, Rice CM, Frolov I. PKR-dependent and -independent mechanisms are involved in translational shutoff during Sindbis virus infection. *Journal of virology*. 2004;78(16):8455-67. Epub 2004/07/29. doi: 10.1128/JVI.78.16.8455-8467.2004. PubMed PMID: 15280454; PubMed Central PMCID: PMC479073.
- 652.** Akhrymuk I, Frolov I, Frolova EI. Sindbis Virus Infection Causes Cell Death by nsP2-Induced Transcriptional Shutoff or by nsP3-Dependent Translational Shutoff. *Journal of virology*. 2018;92(23). Epub 2018/09/21. doi: 10.1128/JVI.01388-18. PubMed PMID: 30232189; PubMed Central PMCID: PMC6232463.
- 653.** Ventoso I, Sanz MA, Molina S, Berlanga JJ, Carrasco L, Esteban M. Translational resistance of late alphavirus mRNA to eIF2alpha phosphorylation: a strategy to overcome the antiviral effect of protein kinase PKR. *Genes Dev*. 2006;20(1):87-100. Epub 2006/01/05. doi: 10.1101/gad.357006. PubMed PMID: 16391235; PubMed Central PMCID: PMC1356103.
- 654.** Ventoso I. Adaptive changes in alphavirus mRNA translation allowed colonization of vertebrate hosts. *Journal of virology*. 2012;86(17):9484-94. Epub 2012/07/05. doi: 10.1128/JVI.01114-12. PubMed PMID: 22761388; PubMed Central PMCID: PMC3416173.
- 655.** Toribio R, Diaz-Lopez I, Boskovic J, Ventoso I. An RNA trapping mechanism in Alphavirus mRNA promotes ribosome stalling and translation initiation. *Nucleic acids research*. 2016;44(9):4368-80. Epub 2016/03/18. doi: 10.1093/nar/gkw172. PubMed PMID: 26984530; PubMed Central PMCID: PMC4872096.
- 656.** Phelps AL, O'Brien LM, Eastaugh LS, Davies C, Lever MS, Ennis J, et al. Susceptibility and Lethality of Western Equine Encephalitis Virus in Balb/c Mice When Infected by the Aerosol Route. *Viruses*. 2017;9(7). Epub 2017/06/28. doi: 10.3390/v9070163. PubMed PMID: 28654007; PubMed Central PMCID: PMC5537655.

- 657.** Zacks MA, Paessler S. Encephalitic alphaviruses. *Vet Microbiol.* 2010;140(3-4):281-6. Epub 2009/09/25. doi: 10.1016/j.vetmic.2009.08.023. PubMed PMID: 19775836; PubMed Central PMCID: PMC2814892.
- 658.** Gould EA, Coutard B, Malet H, Morin B, Jamal S, Weaver S, et al. Understanding the alphaviruses: recent research on important emerging pathogens and progress towards their control. *Antiviral Res.* 2010;87(2):111-24. Epub 2009/07/21. doi: 10.1016/j.antiviral.2009.07.007. PubMed PMID: 19616028; PubMed Central PMCID: PMC7114216.
- 659.** Charles PC, Walters E, Margolis F, Johnston RE. Mechanism of neuroinvasion of Venezuelan equine encephalitis virus in the mouse. *Virology.* 1995;208(2):662-71. Epub 1995/04/20. doi: 10.1006/viro.1995.1197. PubMed PMID: 7747437.
- 660.** Charles PC, Trgovcich J, Davis NL, Johnston RE. Immunopathogenesis and immune modulation of Venezuelan equine encephalitis virus-induced disease in the mouse. *Virology.* 2001;284(2):190-202. Epub 2001/06/01. doi: 10.1006/viro.2001.0878. PubMed PMID: 11384219.
- 661.** Schoneboom BA, Fultz MJ, Miller TH, McKinney LC, Grieder FB. Astrocytes as targets for Venezuelan equine encephalitis virus infection. *J Neurovirol.* 1999;5(4):342-54. Epub 1999/08/27. doi: 10.3109/13550289909029475. PubMed PMID: 10463856.
- 662.** Grieder FB, Davis NL, Aronson JF, Charles PC, Sellon DC, Suzuki K, et al. Specific restrictions in the progression of Venezuelan equine encephalitis virus-induced disease resulting from single amino acid changes in the glycoproteins. *Virology.* 1995;206(2):994-1006. Epub 1995/02/01. doi: 10.1006/viro.1995.1022. PubMed PMID: 7856110.
- 663.** Jackson AC, SenGupta SK, Smith JF. Pathogenesis of Venezuelan equine encephalitis virus infection in mice and hamsters. *Veterinary pathology.* 1991;28(5):410-8. Epub 1991/09/01. doi: 10.1177/030098589102800509. PubMed PMID: 1750167.
- 664.** Esen N, Blakely PK, Rainey-Barger EK, Irani DN. Complexity of the microglial activation pathways that drive innate host responses during lethal alphavirus encephalitis in mice. *ASN Neuro.* 2012;4(4):207-21. Epub 2012/04/05. doi: 10.1042/AN20120016. PubMed PMID: 22471445; PubMed Central PMCID: PMC3342594.
- 665.** Metcalf TU, Griffin DE. Alphavirus-induced encephalomyelitis: antibody-secreting cells and viral clearance from the nervous system. *Journal of virology.* 2011;85(21):11490-501. Epub 2011/08/26. doi: 10.1128/JVI.05379-11. PubMed PMID: 21865385; PubMed Central PMCID: PMC3194963.

- 666.** Tyor WR, Wesselingh S, Levine B, Griffin DE. Long term intraparenchymal Ig secretion after acute viral encephalitis in mice. *Journal of immunology.* 1992;149(12):4016-20. Epub 1992/12/15. PubMed PMID: 1334109.
- 667.** Atasheva S, Garmashova N, Frolov I, Frolova E. Venezuelan equine encephalitis virus capsid protein inhibits nuclear import in Mammalian but not in mosquito cells. *Journal of virology.* 2008;82(8):4028-41. Epub 2008/02/08. doi: 10.1128/JVI.02330-07. PubMed PMID: 18256144; PubMed Central PMCID: PMC2293000.
- 668.** Atasheva S, Fish A, Fornerod M, Frolova EI. Venezuelan equine Encephalitis virus capsid protein forms a tetrameric complex with CRM1 and importin alpha/beta that obstructs nuclear pore complex function. *Journal of virology.* 2010;84(9):4158-71. Epub 2010/02/12. doi: 10.1128/JVI.02554-09. PubMed PMID: 20147401; PubMed Central PMCID: PMC2863722.
- 669.** Garmashova N, Atasheva S, Kang W, Weaver SC, Frolova E, Frolov I. Analysis of Venezuelan equine encephalitis virus capsid protein function in the inhibition of cellular transcription. *Journal of virology.* 2007;81(24):13552-65. Epub 2007/10/05. doi: 10.1128/JVI.01576-07. PubMed PMID: 17913819; PubMed Central PMCID: PMC2168819.
- 670.** Aguilar PV, Weaver SC, Basler CF. Capsid protein of eastern equine encephalitis virus inhibits host cell gene expression. *Journal of virology.* 2007;81(8):3866-76. Epub 2007/02/03. doi: 10.1128/JVI.02075-06. PubMed PMID: 17267491; PubMed Central PMCID: PMC1866141.
- 671.** Acosta-Ampudia Y, Monsalve DM, Rodriguez Y, Pacheco Y, Anaya JM, Ramirez-Santana C. Mayaro: an emerging viral threat? *Emerg Microbes Infect.* 2018;7(1):163. Epub 2018/09/27. doi: 10.1038/s41426-018-0163-5. PubMed PMID: 30254258; PubMed Central PMCID: PMC6156602.
- 672.** Powers AM, Aguilar PV, Chandler LJ, Brault AC, Meakins TA, Watts D, et al. Genetic relationships among Mayaro and Una viruses suggest distinct patterns of transmission. *Am J Trop Med Hyg.* 2006;75(3):461-9. Epub 2006/09/14. PubMed PMID: 16968922.
- 673.** Auguste AJ, Liria J, Forrester NL, Giambalvo D, Moncada M, Long KC, et al. Evolutionary and Ecological Characterization of Mayaro Virus Strains Isolated during an Outbreak, Venezuela, 2010. *Emerg Infect Dis.* 2015;21(10):1742-50. Epub 2015/09/25. doi: 10.3201/eid2110.141660. PubMed PMID: 26401714; PubMed Central PMCID: PMC4593426.
- 674.** Mackay IM, Arden KE. Mayaro virus: a forest virus primed for a trip to the city? *Microbes Infect.* 2016;18(12):724-34. Epub 2016/12/19. doi: 10.1016/j.micinf.2016.10.007. PubMed PMID: 27989728.

- 675.** de Thoisy B, Gardon J, Salas RA, Morvan J, Kazanji M. Mayaro virus in wild mammals, French Guiana. *Emerg Infect Dis.* 2003;9(10):1326-9. Epub 2003/11/12. doi: 10.3201/eid0910.030161. PubMed PMID: 14609474; PubMed Central PMCID: PMC3033094.
- 676.** Blohm G, Elbadry MA, Mavian C, Stephenson C, Loeb J, White S, et al. Mayaro as a Caribbean traveler: Evidence for multiple introductions and transmission of the virus into Haiti. *Int J Infect Dis.* 2019;87:151-3. Epub 2019/08/06. doi: 10.1016/j.ijid.2019.07.031. PubMed PMID: 31382049.
- 677.** Paniz-Mondolfi AE, Rodriguez-Morales AJ, Blohm G, Marquez M, Villamil-Gomez WE. ChikDenMaZika Syndrome: the challenge of diagnosing arboviral infections in the midst of concurrent epidemics. *Ann Clin Microbiol Antimicrob.* 2016;15(1):42. Epub 2016/07/28. doi: 10.1186/s12941-016-0157-x. PubMed PMID: 27449770; PubMed Central PMCID: PMC4957883.
- 678.** Ganjian N, Riviere-Cinnamond A. Mayaro virus in Latin America and the Caribbean. *Rev Panam Salud Publica.* 2020;44:e14. Epub 2020/02/14. doi: 10.26633/RPSP.2020.14. PubMed PMID: 32051685; PubMed Central PMCID: PMC7008609.
- 679.** Taylor A, Herrero LJ, Rudd PA, Mahalingam S. Mouse models of alphavirus-induced inflammatory disease. *J Gen Virol.* 2015;96(Pt 2):221-38. Epub 2014/10/30. doi: 10.1099/vir.0.071282-0. PubMed PMID: 25351726.
- 680.** Mota MTO, Costa VV, Sugimoto MA, Guimaraes GF, Queiroz-Junior CM, Moreira TP, et al. In-depth characterization of a novel live-attenuated Mayaro virus vaccine candidate using an immunocompetent mouse model of Mayaro disease. *Sci Rep.* 2020;10(1):5306. Epub 2020/03/27. doi: 10.1038/s41598-020-62084-x. PubMed PMID: 32210270; PubMed Central PMCID: PMC7093544.
- 681.** Santos FM, Dias RS, de Oliveira MD, Costa I, Fernandes LS, Pessoa CR, et al. Animal model of arthritis and myositis induced by the Mayaro virus. *PLoS Negl Trop Dis.* 2019;13(5):e0007375. Epub 2019/05/06. doi: 10.1371/journal.pntd.0007375. PubMed PMID: 31050676; PubMed Central PMCID: PMC6519846.
- 682.** Figueiredo CM, Neris R, Gavino-Leopoldino D, da Silva MOL, Almeida JS, Dos-Santos JS, et al. Mayaro Virus Replication Restriction and Induction of Muscular Inflammation in Mice Are Dependent on Age, Type-I Interferon Response, and Adaptive Immunity. *Front Microbiol.* 2019;10:2246. Epub 2019/10/22. doi: 10.3389/fmicb.2019.02246. PubMed PMID: 31632368; PubMed Central PMCID: PMC6779782.
- 683.** Haese NN, Broeckel RM, Hawman DW, Heise MT, Morrison TE, Streblow DN. Animal Models of Chikungunya Virus Infection and Disease. *The Journal*

- of infectious diseases. 2016;214(suppl 5):S482-S7. Epub 2016/12/07. doi: 10.1093/infdis/jiw284. PubMed PMID: 27920178; PubMed Central PMCID: PMC5137241.
- 684.** Nguyen W, Nakayama E, Yan K, Tang B, Le TT, Liu L, et al. Arthritogenic Alphavirus Vaccines: Serogrouping Versus Cross-Protection in Mouse Models. *Vaccines (Basel)*. 2020;8(2). Epub 2020/05/10. doi: 10.3390/vaccines8020209. PubMed PMID: 32380760; PubMed Central PMCID: PMC7349283.
- 685.** Hallengard D, Lum FM, Kummerer BM, Lulla A, Lulla V, Garcia-Arriaza J, et al. Prime-boost immunization strategies against Chikungunya virus. *Journal of virology*. 2014;88(22):13333-43. Epub 2014/09/12. doi: 10.1128/JVI.01926-14. PubMed PMID: 25210177; PubMed Central PMCID: PMC4249109.
- 686.** Broeckel RM, Haese N, Ando T, Dmitriev I, Kreklywich CN, Powers J, et al. Vaccine-Induced Skewing of T Cell Responses Protects Against Chikungunya Virus Disease. *Front Immunol*. 2019;10:2563. Epub 2019/11/19. doi: 10.3389/fimmu.2019.02563. PubMed PMID: 31736977; PubMed Central PMCID: PMC6834551.
- 687.** Levitt NH, Ramsburg HH, Hasty SE, Repik PM, Cole FE, Jr., Lupton HW. Development of an attenuated strain of chikungunya virus for use in vaccine production. *Vaccine*. 1986;4(3):157-62. Epub 1986/09/01. doi: 10.1016/0264-410x(86)90003-4. PubMed PMID: 3020820.
- 688.** Gorchakov R, Wang E, Leal G, Forrester NL, Plante K, Rossi SL, et al. Attenuation of Chikungunya virus vaccine strain 181/clone 25 is determined by two amino acid substitutions in the E2 envelope glycoprotein. *Journal of virology*. 2012;86(11):6084-96. Epub 2012/03/30. doi: 10.1128/JVI.06449-11. PubMed PMID: 22457519; PubMed Central PMCID: PMC3372191.
- 689.** Edelman R, Tacket CO, Wasserman SS, Bodison SA, Perry JG, Mangiafico JA. Phase II safety and immunogenicity study of live chikungunya virus vaccine TSI-GSD-218. *Am J Trop Med Hyg*. 2000;62(6):681-5. Epub 2001/04/17. doi: 10.4269/ajtmh.2000.62.681. PubMed PMID: 11304054.
- 690.** BERGE TO, BANKS IS, TIGERTT WD. ATTENUATION OF VENEZUELAN EQUINE ENCEPHALOMYELITIS VIRUS BY IN VITRO CULTIVATION IN GUINEA-PIG HEART CELLS 1. *American Journal of Epidemiology*. 1961;73(2):209-18. doi: 10.1093/oxfordjournals.aje.a120178.
- 691.** Kinney RM, Chang GJ, Tsuchiya KR, Sneider JM, Roehrig JT, Woodward TM, et al. Attenuation of Venezuelan equine encephalitis virus strain TC-83 is encoded by the 5'-noncoding region and the E2 envelope glycoprotein. *Journal of virology*. 1993;67(3):1269-77. Epub 1993/03/01. doi: 10.1128/JVI.67.3.1269-1277.1993. PubMed PMID: 7679745; PubMed Central PMCID: PMC237493.

- 692.** Alevizatos AC, McKinney RW, Feigin RD. Live, attenuated Venezuelan equine encephalomyelitis virus vaccine. I. Clinical effects in man. *Am J Trop Med Hyg.* 1967;16(6):762-8. Epub 1967/11/01. PubMed PMID: 6066224.
- 693.** Pittman PR, Makuch RS, Mangiafico JA, Cannon TL, Gibbs PH, Peters CJ. Long-term duration of detectable neutralizing antibodies after administration of live-attenuated VEE vaccine and following booster vaccination with inactivated VEE vaccine. *Vaccine.* 1996;14(4):337-43. Epub 1996/03/01. doi: 10.1016/0264-410x(95)00168-z. PubMed PMID: 8744562.
- 694.** Davis NL, Brown KW, Greenwald GF, Zajac AJ, Zacny VL, Smith JF, et al. Attenuated mutants of Venezuelan equine encephalitis virus containing lethal mutations in the PE2 cleavage signal combined with a second-site suppressor mutation in E1. *Virology.* 1995;212(1):102-10. Epub 1995/09/10. doi: 10.1006/viro.1995.1458. PubMed PMID: 7676619.
- 695.** Hart MK, Lind C, Bakken R, Robertson M, Tammariello R, Ludwig GV. Onset and duration of protective immunity to IA/IB and IE strains of Venezuelan equine encephalitis virus in vaccinated mice. *Vaccine.* 2001;20(3-4):616-22. Epub 2001/10/24. doi: 10.1016/s0264-410x(01)00337-1. PubMed PMID: 11672929.
- 696.** Hart MK, Caswell-Stephan K, Bakken R, Tammariello R, Pratt W, Davis N, et al. Improved mucosal protection against Venezuelan equine encephalitis virus is induced by the molecularly defined, live-attenuated V3526 vaccine candidate. *Vaccine.* 2000;18(26):3067-75. Epub 2000/05/29. doi: 10.1016/s0264-410x(00)00042-6. PubMed PMID: 10825611.
- 697.** Fine DL, Roberts BA, Terpening SJ, Mott J, Vasconcelos D, House RV. Neurovirulence evaluation of Venezuelan equine encephalitis (VEE) vaccine candidate V3526 in nonhuman primates. *Vaccine.* 2008;26(27-28):3497-506. Epub 2008/05/30. doi: 10.1016/j.vaccine.2008.04.044. PubMed PMID: 18508163.
- 698.** Martin SS, Bakken RR, Lind CM, Reed DS, Price JL, Koeller CA, et al. Telemetric analysis to detect febrile responses in mice following vaccination with a live-attenuated virus vaccine. *Vaccine.* 2009;27(49):6814-23. Epub 2009/09/19. doi: 10.1016/j.vaccine.2009.09.013. PubMed PMID: 19761841; PubMed Central PMCID: PMC2783281.
- 699.** Davis NL, Fuller FJ, Dougherty WG, Olmsted RA, Johnston RE. A single nucleotide change in the E2 glycoprotein gene of Sindbis virus affects penetration rate in cell culture and virulence in neonatal mice. *Proceedings of the National Academy of Sciences of the United States of America.* 1986;83(18):6771-5. Epub 1986/09/01. doi: 10.1073/pnas.83.18.6771. PubMed PMID: 3462725; PubMed Central PMCID: PMC386591.

- 700.** Heidner HW, Johnston RE. The amino-terminal residue of Sindbis virus glycoprotein E2 influences virus maturation, specific infectivity for BHK cells, and virulence in mice. *Journal of virology*. 1994;68(12):8064-70. Epub 1994/12/01. doi: 10.1128/JVI.68.12.8064-8070.1994. PubMed PMID: 7966596; PubMed Central PMCID: PMC237270.
- 701.** Wang E, Petrakova O, Adams AP, Aguilar PV, Kang W, Paessler S, et al. Chimeric Sindbis/eastern equine encephalitis vaccine candidates are highly attenuated and immunogenic in mice. *Vaccine*. 2007;25(43):7573-81. Epub 2007/10/02. doi: 10.1016/j.vaccine.2007.07.061. PubMed PMID: 17904699; PubMed Central PMCID: PMC2094013.
- 702.** Paessler S, Fayzulin RZ, Anishchenko M, Greene IP, Weaver SC, Frolov I. Recombinant sindbis/Venezuelan equine encephalitis virus is highly attenuated and immunogenic. *Journal of virology*. 2003;77(17):9278-86. Epub 2003/08/14. doi: 10.1128/jvi.77.17.9278-9286.2003. PubMed PMID: 12915543; PubMed Central PMCID: PMC187387.
- 703.** Wang E, Volkova E, Adams AP, Forrester N, Xiao SY, Frolov I, et al. Chimeric alphavirus vaccine candidates for chikungunya. *Vaccine*. 2008;26(39):5030-9. Epub 2008/08/12. doi: 10.1016/j.vaccine.2008.07.054. PubMed PMID: 18692107; PubMed Central PMCID: PMC2571998.
- 704.** Plante K, Wang E, Partidos CD, Weger J, Gorchakov R, Tsetsarkin K, et al. Novel chikungunya vaccine candidate with an IRES-based attenuation and host range alteration mechanism. *PLoS pathogens*. 2011;7(7):e1002142. Epub 2011/08/11. doi: 10.1371/journal.ppat.1002142. PubMed PMID: 21829348; PubMed Central PMCID: PMC3145802.
- 705.** Weise WJ, Hermance ME, Forrester N, Adams AP, Langsjoen R, Gorchakov R, et al. A novel live-attenuated vaccine candidate for mayaro Fever. *PLoS Negl Trop Dis*. 2014;8(8):e2969. Epub 2014/08/08. doi: 10.1371/journal.pntd.0002969. PubMed PMID: 25101995; PubMed Central PMCID: PMC4125120.
- 706.** Rossi SL, Guerbois M, Gorchakov R, Plante KS, Forrester NL, Weaver SC. IRES-based Venezuelan equine encephalitis vaccine candidate elicits protective immunity in mice. *Virology*. 2013;437(2):81-8. Epub 2013/01/29. doi: 10.1016/j.virol.2012.11.013. PubMed PMID: 23351391; PubMed Central PMCID: PMC3767167.
- 707.** Jin J, Sherman MB, Chafets D, Dinglasan N, Lu K, Lee TH, et al. An attenuated replication-competent chikungunya virus with a fluorescently tagged envelope. *PLoS Negl Trop Dis*. 2018;12(7):e0006693. Epub 2018/08/01. doi: 10.1371/journal.pntd.0006693. PubMed PMID: 30063703; PubMed Central PMCID: PMC6086482.

- 708.** Pratt WD, Gibbs P, Pitt ML, Schmaljohn AL. Use of telemetry to assess vaccine-induced protection against parenteral and aerosol infections of Venezuelan equine encephalitis virus in non-human primates. *Vaccine*. 1998;16(9-10):1056-64. Epub 1998/07/31. doi: 10.1016/s0264-410x(97)00192-8. PubMed PMID: 9682359.
- 709.** Jahrling PB, Stephenson EH. Protective efficacies of live attenuated and formaldehyde-inactivated Venezuelan equine encephalitis virus vaccines against aerosol challenge in hamsters. *J Clin Microbiol*. 1984;19(3):429-31. Epub 1984/03/01. doi: 10.1128/JCM.19.3.429-431.1984. PubMed PMID: 6715512; PubMed Central PMCID: PMC271080.
- 710.** Gardner J, Anraku I, Le TT, Larcher T, Major L, Roques P, et al. Chikungunya virus arthritis in adult wild-type mice. *Journal of virology*. 2010;84(16):8021-32. Epub 2010/06/04. doi: 10.1128/JVI.02603-09. PubMed PMID: 20519386; PubMed Central PMCID: PMC2916516.
- 711.** Nakao E, Hotta S. Immunogenicity of purified, inactivated chikungunya virus in monkeys. *Bull World Health Organ*. 1973;48(5):559-62. Epub 1973/05/01. PubMed PMID: 4204490; PubMed Central PMCID: PMC2482923.
- 712.** Partidos CD, Paykel J, Weger J, Borland EM, Powers AM, Seymour R, et al. Cross-protective immunity against o'nyong-nyong virus afforded by a novel recombinant chikungunya vaccine. *Vaccine*. 2012;30(31):4638-43. Epub 2012/05/16. doi: 10.1016/j.vaccine.2012.04.099. PubMed PMID: 22583812; PubMed Central PMCID: PMC3372665.
- 713.** Langsjoen RM, Haller SL, Roy CJ, Vinet-Oliphant H, Bergren NA, Erasmus JH, et al. Chikungunya Virus Strains Show Lineage-Specific Variations in Virulence and Cross-Protective Ability in Murine and Nonhuman Primate Models. *mBio*. 2018;9(2). Epub 2018/03/08. doi: 10.1128/mBio.02449-17. PubMed PMID: 29511072; PubMed Central PMCID: PMC5844994.
- 714.** Robinson DM, Cole FE, Jr., McManus AT, Pedersen CE, Jr. Inactivated Mayaro vaccine produced in human diploid cell cultures. *Mil Med*. 1976;141(3):163-6. Epub 1976/03/01. PubMed PMID: 815839.
- 715.** Mussgay M, Weiland E. Preparation of inactivated vaccines against alphaviruses using Semliki Forest virus-white mouse as a model. I. Inactivation experiments and evaluation of double inactivated subunit vaccines. *Intervirology*. 1973;1(4):259-68. Epub 1973/01/01. doi: 10.1159/000148854. PubMed PMID: 4775474.
- 716.** Reed SG, Orr MT, Fox CB. Key roles of adjuvants in modern vaccines. *Nature medicine*. 2013;19(12):1597-608. Epub 2013/12/07. doi: 10.1038/nm.3409. PubMed PMID: 24309663.

- 717.** Metz SW, Gardner J, Geertsema C, Le TT, Goh L, Vlak JM, et al. Effective chikungunya virus-like particle vaccine produced in insect cells. *PLoS Negl Trop Dis.* 2013;7(3):e2124. Epub 2013/03/22. doi: 10.1371/journal.pntd.0002124. PubMed PMID: 23516657; PubMed Central PMCID: PMC3597470.
- 718.** Chang LJ, Dowd KA, Mendoza FH, Saunders JG, Sitar S, Plummer SH, et al. Safety and tolerability of chikungunya virus-like particle vaccine in healthy adults: a phase 1 dose-escalation trial. *Lancet.* 2014;384(9959):2046-52. Epub 2014/08/19. doi: 10.1016/S0140-6736(14)61185-5. PubMed PMID: 25132507.
- 719.** Akahata W, Yang ZY, Andersen H, Sun S, Holdaway HA, Kong WP, et al. A virus-like particle vaccine for epidemic Chikungunya virus protects nonhuman primates against infection. *Nature medicine.* 2010;16(3):334-8. Epub 2010/01/30. doi: 10.1038/nm.2105. PubMed PMID: 20111039; PubMed Central PMCID: PMC2834826.
- 720.** Ko SY, Akahata W, Yang ES, Kong WP, Burke CW, Honnold SP, et al. A virus-like particle vaccine prevents equine encephalitis virus infection in nonhuman primates. *Science translational medicine.* 2019;11(492). Epub 2019/05/17. doi: 10.1126/scitranslmed.aav3113. PubMed PMID: 31092692.
- 721.** Kumar M, Sudeep AB, Arankalle VA. Evaluation of recombinant E2 protein-based and whole-virus inactivated candidate vaccines against chikungunya virus. *Vaccine.* 2012;30(43):6142-9. Epub 2012/08/14. doi: 10.1016/j.vaccine.2012.07.072. PubMed PMID: 22884660.
- 722.** Khan M, Dhanwani R, Rao PV, Parida M. Subunit vaccine formulations based on recombinant envelope proteins of Chikungunya virus elicit balanced Th1/Th2 response and virus-neutralizing antibodies in mice. *Virus research.* 2012;167(2):236-46. Epub 2012/05/23. doi: 10.1016/j.virusres.2012.05.004. PubMed PMID: 22610133.
- 723.** Khan S, Khan A, Rehman AU, Ahmad I, Ullah S, Khan AA, et al. Immunoinformatics and structural vaccinology driven prediction of multi-epitope vaccine against Mayaro virus and validation through in-silico expression. *Infect Genet Evol.* 2019;73:390-400. Epub 2019/06/08. doi: 10.1016/j.meegid.2019.06.006. PubMed PMID: 31173935.
- 724.** Suschak JJ, Williams JA, Schmaljohn CS. Advancements in DNA vaccine vectors, non-mechanical delivery methods, and molecular adjuvants to increase immunogenicity. *Hum Vaccin Immunother.* 2017;13(12):2837-48. Epub 2017/06/13. doi: 10.1080/21645515.2017.1330236. PubMed PMID: 28604157; PubMed Central PMCID: PMC5718814.
- 725.** Choi H, Kudchodkar SB, Reuschel EL, Asija K, Borole P, Ho M, et al. Protective immunity by an engineered DNA vaccine for Mayaro virus. *PLoS*

- Negl Trop Dis. 2019;13(2):e0007042. Epub 2019/02/08. doi: 10.1371/journal.pntd.0007042. PubMed PMID: 30730897; PubMed Central PMCID: PMC6366747.
- 726.** Muthumani K, Lankaraman KM, Laddy DJ, Sundaram SG, Chung CW, Sako E, et al. Immunogenicity of novel consensus-based DNA vaccines against Chikungunya virus. *Vaccine*. 2008;26(40):5128-34. Epub 2008/05/13. doi: 10.1016/j.vaccine.2008.03.060. PubMed PMID: 18471943; PubMed Central PMCID: PMC2582145.
- 727.** Mallilankaraman K, Shedlock DJ, Bao H, Kawalekar OU, Fagone P, Ramanathan AA, et al. A DNA vaccine against chikungunya virus is protective in mice and induces neutralizing antibodies in mice and nonhuman primates. *PLoS Negl Trop Dis*. 2011;5(1):e928. Epub 2011/01/26. doi: 10.1371/journal.pntd.0000928. PubMed PMID: 21264351; PubMed Central PMCID: PMC3019110.
- 728.** Dupuy LC, Richards MJ, Ellefsen B, Chau L, Luxembourg A, Hannaman D, et al. A DNA vaccine for venezuelan equine encephalitis virus delivered by intramuscular electroporation elicits high levels of neutralizing antibodies in multiple animal models and provides protective immunity to mice and nonhuman primates. *Clin Vaccine Immunol*. 2011;18(5):707-16. Epub 2011/04/01. doi: 10.1128/CVI.00030-11. PubMed PMID: 21450977; PubMed Central PMCID: PMC3122536.
- 729.** Pastorino B, Baronti C, Gould EA, Charrel RN, de Lamballerie X. Effect of chemical stabilizers on the thermostability and infectivity of a representative panel of freeze dried viruses. *PLoS one*. 2015;10(4):e0118963. Epub 2015/04/30. doi: 10.1371/journal.pone.0118963. PubMed PMID: 25923434; PubMed Central PMCID: PMC4414529.
- 730.** Evans RK, Nawrocki DK, Isopi LA, Williams DM, Casimiro DR, Chin S, et al. Development of stable liquid formulations for adenovirus-based vaccines. *J Pharm Sci*. 2004;93(10):2458-75. Epub 2004/09/07. doi: 10.1002/jps.20157. PubMed PMID: 15349956.
- 731.** Dicks MD, Spencer AJ, Edwards NJ, Wadell G, Bojang K, Gilbert SC, et al. A novel chimpanzee adenovirus vector with low human seroprevalence: improved systems for vector derivation and comparative immunogenicity. *PLoS one*. 2012;7(7):e40385. Epub 2012/07/19. doi: 10.1371/journal.pone.0040385. PubMed PMID: 22808149; PubMed Central PMCID: PMC3396660.
- 732.** Kroon Campos R, Preciado-Llanes L, Azar SR, Kim YC, Brandon O, López-Camacho C, et al. Adenoviral-Vectored Mayaro and Chikungunya Virus Vaccine Candidates Afford Partial Cross-Protection From Lethal Challenge in A129 Mouse Model. *Frontiers in Immunology*. 2020;11. doi: 10.3389/fimmu.2020.591885.

- 733.** Lopez-Camacho C, Kim YC, Blight J, Lazaro Moreli M, Montoya-Diaz E, Huiskonen JT, et al. Assessment of Immunogenicity and Neutralisation Efficacy of Viral-Vectored Vaccines Against Chikungunya Virus. *Viruses*. 2019;11(4). Epub 2019/04/17. doi: 10.3390/v11040322. PubMed PMID: 30987160; PubMed Central PMCID: PMC6521086.
- 734.** Phillpotts RJ, O'Brien L, Appleton RE, Carr S, Bennett A. Intranasal immunisation with defective adenovirus serotype 5 expressing the Venezuelan equine encephalitis virus E2 glycoprotein protects against airborne challenge with virulent virus. *Vaccine*. 2005;23(13):1615-23. Epub 2005/02/08. doi: 10.1016/j.vaccine.2004.06.056. PubMed PMID: 15694514.
- 735.** Chattopadhyay A, Wang E, Seymour R, Weaver SC, Rose JK. A chimeric vesiculo/alphavirus is an effective alphavirus vaccine. *Journal of virology*. 2013;87(1):395-402. Epub 2012/10/19. doi: 10.1128/JVI.01860-12. PubMed PMID: 23077320; PubMed Central PMCID: PMC3536361.
- 736.** Brandler S, Ruffie C, Combredet C, Brault JB, Najburg V, Prevost MC, et al. A recombinant measles vaccine expressing chikungunya virus-like particles is strongly immunogenic and protects mice from lethal challenge with chikungunya virus. *Vaccine*. 2013;31(36):3718-25. Epub 2013/06/08. doi: 10.1016/j.vaccine.2013.05.086. PubMed PMID: 23742993.
- 737.** Ramsauer K, Schwameis M, Firbas C, Mullner M, Putnak RJ, Thomas SJ, et al. Immunogenicity, safety, and tolerability of a recombinant measles-virus-based chikungunya vaccine: a randomised, double-blind, placebo-controlled, active-comparator, first-in-man trial. *Lancet Infect Dis*. 2015;15(5):519-27. Epub 2015/03/06. doi: 10.1016/S1473-3099(15)70043-5. PubMed PMID: 25739878.
- 738.** Webb EM, Azar SR, Haller SL, Langsjoen RM, Cuthbert CE, Ramjag AT, et al. Effects of Chikungunya virus immunity on Mayaro virus disease and epidemic potential. *Sci Rep*. 2019;9(1):20399. Epub 2020/01/02. doi: 10.1038/s41598-019-56551-3. PubMed PMID: 31892710; PubMed Central PMCID: PMC6938517.
- 739.** Tiwari M, Parida M, Santhosh SR, Khan M, Dash PK, Rao PV. Assessment of immunogenic potential of Vero adapted formalin inactivated vaccine derived from novel ECSA genotype of Chikungunya virus. *Vaccine*. 2009;27(18):2513-22. Epub 2009/04/17. doi: 10.1016/j.vaccine.2009.02.062. PubMed PMID: 19368794.
- 740.** Bancos S, Bernard MP, Topham DJ, Phipps RP. Ibuprofen and other widely used non-steroidal anti-inflammatory drugs inhibit antibody production in human cells. *Cell Immunol*. 2009;258(1):18-28. Epub 2009/04/07. doi: 10.1016/j.cellimm.2009.03.007. PubMed PMID: 19345936; PubMed Central PMCID: PMC2693360.

- 741.** Gigante A, Gomez-SanJuan A, Delang L, Li C, Bueno O, Gamo AM, et al. Antiviral activity of [1,2,3]triazolo[4,5-d]pyrimidin-7(6H)-ones against chikungunya virus targeting the viral capping nsP1. *Antiviral Res.* 2017;144:216-22. Epub 2017/06/18. doi: 10.1016/j.antiviral.2017.06.003. PubMed PMID: 28619679.
- 742.** Haese N, Powers J, Streblow DN. Small Molecule Inhibitors Targeting Chikungunya Virus. *Current topics in microbiology and immunology.* 2020. Epub 2020/01/25. doi: 10.1007/82_2020_195. PubMed PMID: 31974761.
- 743.** Das PK, Puusepp L, Varghese FS, Utt A, Ahola T, Kananovich DG, et al. Design and Validation of Novel Chikungunya Virus Protease Inhibitors. *Antimicrob Agents Chemother.* 2016;60(12):7382-95. Epub 2016/11/01. doi: 10.1128/AAC.01421-16. PubMed PMID: 27736770; PubMed Central PMCID: PMC5119020.
- 744.** Chung DH, Jonsson CB, Tower NA, Chu YK, Sahin E, Golden JE, et al. Discovery of a novel compound with anti-venezuelan equine encephalitis virus activity that targets the nonstructural protein 2. *PLoS pathogens.* 2014;10(6):e1004213. Epub 2014/06/27. doi: 10.1371/journal.ppat.1004213. PubMed PMID: 24967809; PubMed Central PMCID: PMC4072787.
- 745.** Seyedi SS, Shukri M, Hassandarvish P, Oo A, Shankar EM, Abubakar S, et al. Computational Approach Towards Exploring Potential Anti-Chikungunya Activity of Selected Flavonoids. *Sci Rep.* 2016;6:24027. Epub 2016/04/14. doi: 10.1038/srep24027. PubMed PMID: 27071308; PubMed Central PMCID: PMC4829834.
- 746.** Amaya M, Voss K, Sampey G, Senina S, de la Fuente C, Mueller C, et al. The role of IKKbeta in Venezuelan equine encephalitis virus infection. *PLoS one.* 2014;9(2):e86745. Epub 2014/03/04. doi: 10.1371/journal.pone.0086745. PubMed PMID: 24586253; PubMed Central PMCID: PMC3929299.
- 747.** Furuta Y, Komeno T, Nakamura T. Favipiravir (T-705), a broad spectrum inhibitor of viral RNA polymerase. *Proc Jpn Acad Ser B Phys Biol Sci.* 2017;93(7):449-63. Epub 2017/08/05. doi: 10.2183/pjab.93.027. PubMed PMID: 28769016; PubMed Central PMCID: PMC5713175.
- 748.** Ferreira AC, Reis PA, de Freitas CS, Sacramento CQ, Villas Boas Hoelz L, Bastos MM, et al. Beyond Members of the Flaviviridae Family, Sofosbuvir Also Inhibits Chikungunya Virus Replication. *Antimicrob Agents Chemother.* 2019;63(2). Epub 2018/11/21. doi: 10.1128/AAC.01389-18. PubMed PMID: 30455237; PubMed Central PMCID: PMC6355571.
- 749.** Urakova N, Kuznetsova V, Crossman DK, Sokratian A, Guthrie DB, Kolykhalov AA, et al. beta-d-N (4)-Hydroxycytidine Is a Potent Anti-alphavirus Compound That Induces a High Level of Mutations in the Viral Genome.

- Journal of virology. 2018;92(3). Epub 2017/11/24. doi: 10.1128/JVI.01965-17. PubMed PMID: 29167335; PubMed Central PMCID: PMC5774879.
- 750.** Wust CJ, Nicholas JA, Fredin D, Dodd DC, Brideau RJ, Lively ME, et al. Monoclonal antibodies that cross-react with the E1 glycoprotein of different alphavirus serogroups: characterization including passive protection in vivo. *Virus research*. 1989;13(2):101-12. Epub 1989/06/01. doi: 10.1016/0168-1702(89)90009-9. PubMed PMID: 2773592.
- 751.** Mathews JH, Roehrig JT, Trent DW. Role of complement and the Fc portion of immunoglobulin G in immunity to Venezuelan equine encephalomyelitis virus infection with glycoprotein-specific monoclonal antibodies. *Journal of virology*. 1985;55(3):594-600. Epub 1985/09/01. doi: 10.1128/JVI.55.3.594-600.1985. PubMed PMID: 2410632; PubMed Central PMCID: PMC255017.
- 752.** Boere WA, Benaissa-Trouw BJ, Harmsen M, Kraaijeveld CA, Snippe H. Neutralizing and non-neutralizing monoclonal antibodies to the E2 glycoprotein of Semliki Forest virus can protect mice from lethal encephalitis. *J Gen Virol*. 1983;64 (Pt 6):1405-8. Epub 1983/06/01. doi: 10.1099/0022-1317-64-6-1405. PubMed PMID: 6854274.
- 753.** Rabinowitz SG, Adler WH. Host defenses during primary Venezuelan equine encephalomyelitis virus infection in mice. I. Passive transfer of protection with immune serum and immune cells. *Journal of immunology*. 1973;110(5):1345-53. Epub 1973/05/01. PubMed PMID: 4348975.
- 754.** Smith SA, Silva LA, Fox JM, Flyak AI, Kose N, Sapparapu G, et al. Isolation and Characterization of Broad and Ultrapotent Human Monoclonal Antibodies with Therapeutic Activity against Chikungunya Virus. *Cell Host Microbe*. 2015;18(1):86-95. Epub 2015/07/15. doi: 10.1016/j.chom.2015.06.009. PubMed PMID: 26159721; PubMed Central PMCID: PMC4501771.
- 755.** Pal P, Dowd KA, Brien JD, Edeling MA, Gorlatov S, Johnson S, et al. Development of a highly protective combination monoclonal antibody therapy against Chikungunya virus. *PLoS pathogens*. 2013;9(4):e1003312. Epub 2013/05/03. doi: 10.1371/journal.ppat.1003312. PubMed PMID: 23637602; PubMed Central PMCID: PMC3630103.
- 756.** Broeckel R, Fox JM, Haese N, Kreklywich CN, Sukulpovi-Petty S, Legasse A, et al. Therapeutic administration of a recombinant human monoclonal antibody reduces the severity of chikungunya virus disease in rhesus macaques. *PLoS Negl Trop Dis*. 2017;11(6):e0005637. Epub 2017/06/20. doi: 10.1371/journal.pntd.0005637. PubMed PMID: 28628616; PubMed Central PMCID: PMC5491320.
- 757.** Smith JL, Pugh CL, Cisney ED, Keasey SL, Guevara C, Ampuero JS, et al. Human Antibody Responses to Emerging Mayaro Virus and Cocirculating

- Alphavirus Infections Examined by Using Structural Proteins from Nine New and Old World Lineages. *mSphere*. 2018;3(2). Epub 2018/03/27. doi: 10.1128/mSphere.00003-18. PubMed PMID: 29577083; PubMed Central PMCID: PMC5863033.
- 758.** Brown RS, Wan JJ, Kielian M. The Alphavirus Exit Pathway: What We Know and What We Wish We Knew. *Viruses*. 2018;10(2). Epub 2018/02/23. doi: 10.3390/v10020089. PubMed PMID: 29470397; PubMed Central PMCID: PMC5850396.
- 759.** Weber JM, Ruzindana-Umunyana A, Imbeault L, Sircar S. Inhibition of adenovirus infection and adenain by green tea catechins. *Antiviral Res*. 2003;58(2):167-73. Epub 2003/05/14. PubMed PMID: 12742577.
- 760.** Dagley A, Ennis J, Turner JD, Rood KA, Van Wettere AJ, Gowen BB, et al. Protection against Chikungunya virus induced arthralgia following prophylactic treatment with adenovirus vectored interferon (mDEF201). *Antiviral Res*. 2014;108:1-9. Epub 2014/05/17. doi: 10.1016/j.antiviral.2014.05.004. PubMed PMID: 24833276; PubMed Central PMCID: PMC4101997.
- 761.** Brustolin M, Pujhari S, Henderson CA, Rasgon JL. Anopheles mosquitoes may drive invasion and transmission of Mayaro virus across geographically diverse regions. *PLoS Negl Trop Dis*. 2018;12(11):e0006895. Epub 2018/11/08. doi: 10.1371/journal.pntd.0006895. PubMed PMID: 30403665; PubMed Central PMCID: PMC6242690.
- 762.** Arvas A. Vaccination in patients with immunosuppression. *Turk Pediatri Ars*. 2014;49(3):181-5. Epub 2015/06/17. doi: 10.5152/tpa.2014.2206. PubMed PMID: 26078660; PubMed Central PMCID: PMC4462293.
- 763.** Medical Advisory Committee of the Immune Deficiency F, Shearer WT, Fleisher TA, Buckley RH, Ballas Z, Ballow M, et al. Recommendations for live viral and bacterial vaccines in immunodeficient patients and their close contacts. *The Journal of allergy and clinical immunology*. 2014;133(4):961-6. Epub 2014/03/04. doi: 10.1016/j.jaci.2013.11.043. PubMed PMID: 24582311; PubMed Central PMCID: PMC4009347.
- 764.** Erasmus JH, Rossi SL, Weaver SC. Development of Vaccines for Chikungunya Fever. *The Journal of infectious diseases*. 2016;214(suppl 5):S488-S96. Epub 2016/12/07. doi: 10.1093/infdis/jiw271. PubMed PMID: 27920179; PubMed Central PMCID: PMC5137239.
- 765.** Chira S, Jackson CS, Oprea I, Ozturk F, Pepper MS, Diaconu I, et al. Progresses towards safe and efficient gene therapy vectors. *Oncotarget*. 2015;6(31):30675-703. Epub 2015/09/13. doi: 10.18632/oncotarget.5169. PubMed PMID: 26362400; PubMed Central PMCID: PMC4741561.

- 766.** Figueiredo ML, Figueiredo LT. Emerging alphaviruses in the Americas: Chikungunya and Mayaro. *Rev Soc Bras Med Trop.* 2014;47(6):677-83. Epub 2015/01/30. doi: 10.1590/0037-8682-0246-2014. PubMed PMID: 25626645.
- 767.** Lwande OW, Obanda V, Bucht G, Mosomtai G, Otieno V, Ahlm C, et al. Global emergence of Alphaviruses that cause arthritis in humans. *Infect Ecol Epidemiol.* 2015;5:29853. Epub 2015/12/23. doi: 10.3402/iee.v5.29853. PubMed PMID: 26689654; PubMed Central PMCID: PMC4685977.
- 768.** Navarro J-C, Carrera J-P, Liria J, Auguste AJ, Weaver SC. Alphaviruses in Latin America and the Introduction of Chikungunya Virus. In: Ludert JE, Pujol FH, Arbiza J, editors. *Human Virology in Latin America: From Biology to Control.* Cham: Springer International Publishing; 2017. p. 169-92.
- 769.** Taylor A, Liu X, Zaid A, Goh LY, Hobson-Peters J, Hall RA, et al. Mutation of the N-Terminal Region of Chikungunya Virus Capsid Protein: Implications for Vaccine Design. *mBio.* 2017;8(1). Epub 2017/02/23. doi: 10.1128/mBio.01970-16. PubMed PMID: 28223458; PubMed Central PMCID: PMC5358915.
- 770.** Taylor A, Melton JV, Herrero LJ, Thaa B, Karo-Astover L, Gage PW, et al. Effects of an In-Frame Deletion of the 6k Gene Locus from the Genome of Ross River Virus. *Journal of virology.* 2016;90(8):4150-9. Epub 2016/02/13. doi: 10.1128/JVI.03192-15. PubMed PMID: 26865723; PubMed Central PMCID: PMC4810561.
- 771.** Mezenzio JM, Rebello MA. Mayaro virus proteins. *Mem Inst Oswaldo Cruz.* 1993;88(2):299-304. Epub 1993/04/01. doi: 10.1590/s0074-02761993000200020. PubMed PMID: 8107591.
- 772.** Yap ML, Klose T, Urakami A, Hasan SS, Akahata W, Rossmann MG. Structural studies of Chikungunya virus maturation. *Proceedings of the National Academy of Sciences of the United States of America.* 2017;114(52):13703-7. Epub 2017/12/06. doi: 10.1073/pnas.1713166114. PubMed PMID: 29203665; PubMed Central PMCID: PMC5748190.
- 773.** Vita R, Mahajan S, Overton JA, Dhanda SK, Martini S, Cantrell JR, et al. The Immune Epitope Database (IEDB): 2018 update. *Nucleic acids research.* 2019;47(D1):D339-D43. Epub 2018/10/26. doi: 10.1093/nar/gky1006. PubMed PMID: 30357391; PubMed Central PMCID: PMC6324067.
- 774.** Marin-Lopez A, Calvo-Pinilla E, Moreno S, Utrilla-Trigo S, Nogales A, Brun A, et al. Modeling Arboviral Infection in Mice Lacking the Interferon Alpha/Beta Receptor. *Viruses.* 2019;11(1). Epub 2019/01/11. doi: 10.3390/v11010035. PubMed PMID: 30625992; PubMed Central PMCID: PMC6356211.
- 775.** Hassing RJ, Leparc-Goffart I, Blank SN, Thevarayan S, Tolou H, van Doornum G, et al. Imported Mayaro virus infection in the Netherlands. *J Infect.*

- 2010;61(4):343-5. Epub 2010/07/06. doi: 10.1016/j.jinf.2010.06.009. PubMed PMID: 20600300.
- 776.** Llagonne-Barets M, Icard V, Leparç-Goffart I, Prat C, Perpoint T, Andre P, et al. A case of Mayaro virus infection imported from French Guiana. *J Clin Virol.* 2016;77:66-8. Epub 2016/02/28. doi: 10.1016/j.jcv.2016.02.013. PubMed PMID: 26921736.
- 777.** Pezzi L, Rodriguez-Morales AJ, Reusken CB, Ribeiro GS, LaBeaud AD, Lourenco-de-Oliveira R, et al. GloPID-R report on chikungunya, o'nyong-nyong and Mayaro virus, part 3: Epidemiological distribution of Mayaro virus. *Antiviral Res.* 2019;172:104610. Epub 2019/09/24. doi: 10.1016/j.antiviral.2019.104610. PubMed PMID: 31545981.
- 778.** Chattopadhyay A, Aguilar PV, Bopp NE, Yarovinsky TO, Weaver SC, Rose JK. A recombinant virus vaccine that protects against both Chikungunya and Zika virus infections. *Vaccine.* 2018;36(27):3894-900. Epub 2018/05/29. doi: 10.1016/j.vaccine.2018.05.095. PubMed PMID: 29807712.
- 779.** Gavin AL, Barnes N, Dijkstra HM, Hogarth PM. Identification of the mouse IgG3 receptor: implications for antibody effector function at the interface between innate and adaptive immunity. *Journal of immunology.* 1998;160(1):20-3. Epub 1998/04/29. PubMed PMID: 9551950.
- 780.** Collins AM. IgG subclass co-expression brings harmony to the quartet model of murine IgG function. *Immunol Cell Biol.* 2016;94(10):949-54. Epub 2016/08/10. doi: 10.1038/icb.2016.65. PubMed PMID: 27502143.
- 781.** Harmer NJ, Chahwan R. Isotype switching: Mouse IgG3 constant region drives increased affinity for polysaccharide antigens. *Virulence.* 2016;7(6):623-6. Epub 2016/05/26. doi: 10.1080/21505594.2016.1193278. PubMed PMID: 27224549; PubMed Central PMCID: PMC4991320.
- 782.** Arevalo MT, Huang Y, Jones CA, Ross TM. Vaccination with a chikungunya virus-like particle vaccine exacerbates disease in aged mice. *PLoS Negl Trop Dis.* 2019;13(4):e0007316. Epub 2019/04/27. doi: 10.1371/journal.pntd.0007316. PubMed PMID: 31026260; PubMed Central PMCID: PMC6485612.
- 783.** Hensley SE, Cun AS, Giles-Davis W, Li Y, Xiang Z, Lasaro MO, et al. Type I interferon inhibits antibody responses induced by a chimpanzee adenovirus vector. *Molecular therapy : the journal of the American Society of Gene Therapy.* 2007;15(2):393-403. Epub 2007/01/20. doi: 10.1038/sj.mt.6300024. PubMed PMID: 17235319.
- 784.** Mateo L, La Linn M, McColl SR, Cross S, Gardner J, Suhrbier A. An arthrogenic alphavirus induces monocyte chemoattractant protein-1 and

- interleukin-8. *Intervirology*. 2000;43(1):55-60. Epub 2000/04/25. doi: 10.1159/000025023. PubMed PMID: 10773738.
- 785.** Lasaro MO, Ertl HC. New insights on adenovirus as vaccine vectors. *Molecular therapy : the journal of the American Society of Gene Therapy*. 2009;17(8):1333-9. Epub 2009/06/11. doi: 10.1038/mt.2009.130. PubMed PMID: 19513019; PubMed Central PMCID: PMC2835230.
- 786.** Zhu FC, Guan XH, Li YH, Huang JY, Jiang T, Hou LH, et al. Immunogenicity and safety of a recombinant adenovirus type-5-vectored COVID-19 vaccine in healthy adults aged 18 years or older: a randomised, double-blind, placebo-controlled, phase 2 trial. *Lancet*. 2020;396(10249):479-88. Epub 2020/07/24. doi: 10.1016/S0140-6736(20)31605-6. PubMed PMID: 32702299.
- 787.** Folegatti PM, Ewer KJ, Aley PK, Angus B, Becker S, Belij-Rammerstorfer S, et al. Safety and immunogenicity of the ChAdOx1 nCoV-19 vaccine against SARS-CoV-2: a preliminary report of a phase 1/2, single-blind, randomised controlled trial. *Lancet*. 2020;396(10249):467-78. Epub 2020/07/24. doi: 10.1016/S0140-6736(20)31604-4. PubMed PMID: 32702298; PubMed Central PMCID: PMC7445431.
- 788.** Matthews DA, Cummings D, Eveleigh C, Graham FL, Prevec L. Development and use of a 293 cell line expressing lac repressor for the rescue of recombinant adenoviruses expressing high levels of rabies virus glycoprotein. *J Gen Virol*. 1999;80 (Pt 2):345-53. PubMed PMID: 10073694.
- 789.** Safronetz D, Hegde NR, Ebihara H, Denton M, Kobinger GP, St Jeor S, et al. Adenovirus vectors expressing hantavirus proteins protect hamsters against lethal challenge with andes virus. *J Virol*. 2009;83(14):7285-95. Epub 2009/04/29. doi: 10.1128/jvi.00373-09. PubMed PMID: 19403663; PubMed Central PMCID: PMC2704762.
- 790.** Lynch A, Meyers AE, Williamson AL, Rybicki EP. Stability studies of HIV-1 Pr55gag virus-like particles made in insect cells after storage in various formulation media. *Virology journal*. 2012;9:210. Epub 2012/09/20. doi: 10.1186/1743-422X-9-210. PubMed PMID: 22988963; PubMed Central PMCID: PMC3502365.
- 791.** Lingappa VR, Hurt CR, Garvey E. Capsid assembly as a point of intervention for novel anti-viral therapeutics. *Curr Pharm Biotechnol*. 2013;14(5):513-23. Epub 2012/03/21. doi: 10.2174/13892010113149990201. PubMed PMID: 22429134.
- 792.** Mateu MG. Introduction: the structural basis of virus function. *Subcell Biochem*. 2013;68:3-51. Epub 2013/06/06. doi: 10.1007/978-94-007-6552-8_1. PubMed PMID: 23737047; PubMed Central PMCID: PMC7120296.

- 793.** Mingozzi F, High KA. Therapeutic in vivo gene transfer for genetic disease using AAV: progress and challenges. *Nature reviews Genetics*. 2011;12(5):341-55. Epub 2011/04/19. doi: 10.1038/nrg2988. PubMed PMID: 21499295.
- 794.** Carpentier AC, Frisch F, Labbe SM, Gagnon R, de Wal J, Greentree S, et al. Effect of alipogene tiparvovec (AAV1-LPL(S447X)) on postprandial chylomicron metabolism in lipoprotein lipase-deficient patients. *J Clin Endocrinol Metab*. 2012;97(5):1635-44. Epub 2012/03/23. doi: 10.1210/jc.2011-3002. PubMed PMID: 22438229.
- 795.** Jacobson SG, Cideciyan AV, Ratnakaram R, Heon E, Schwartz SB, Roman AJ, et al. Gene therapy for leber congenital amaurosis caused by RPE65 mutations: safety and efficacy in 15 children and adults followed up to 3 years. *Archives of ophthalmology*. 2012;130(1):9-24. Epub 2011/09/14. doi: 10.1001/archophthalmol.2011.298. PubMed PMID: 21911650; PubMed Central PMCID: PMC3600816.
- 796.** Nathwani AC, Reiss UM, Tuddenham EG, Rosales C, Chowdary P, McIntosh J, et al. Long-term safety and efficacy of factor IX gene therapy in hemophilia B. *The New England journal of medicine*. 2014;371(21):1994-2004. Epub 2014/11/20. doi: 10.1056/NEJMoa1407309. PubMed PMID: 25409372; PubMed Central PMCID: PMC4278802.
- 797.** Becerra SP, Koczot F, Fabisch P, Rose JA. Synthesis of adeno-associated virus structural proteins requires both alternative mRNA splicing and alternative initiations from a single transcript. *Journal of virology*. 1988;62(8):2745-54. Epub 1988/08/01. doi: 10.1128/JVI.62.8.2745-2754.1988. PubMed PMID: 2839699; PubMed Central PMCID: PMC253708.
- 798.** Wistuba A, Kern A, Weger S, Grimm D, Kleinschmidt JA. Subcellular compartmentalization of adeno-associated virus type 2 assembly. *Journal of virology*. 1997;71(2):1341-52. Epub 1997/02/01. doi: 10.1128/JVI.71.2.1341-1352.1997. PubMed PMID: 8995658; PubMed Central PMCID: PMC191189.
- 799.** Huang MT, Gorman CM. Intervening sequences increase efficiency of RNA 3' processing and accumulation of cytoplasmic RNA. *Nucleic acids research*. 1990;18(4):937-47. Epub 1990/02/25. doi: 10.1093/nar/18.4.937. PubMed PMID: 1690394; PubMed Central PMCID: PMC330348.
- 800.** Kuck D, Kern A, Kleinschmidt JA. Development of AAV serotype-specific ELISAs using novel monoclonal antibodies. *J Virol Methods*. 2007;140(1-2):17-24. Epub 2006/11/28. doi: 10.1016/j.jviromet.2006.10.005. PubMed PMID: 17126418.
- 801.** Girod A, Wobus CE, Zadori Z, Ried M, Leike K, Tijssen P, et al. The VP1 capsid protein of adeno-associated virus type 2 is carrying a phospholipase A2

- domain required for virus infectivity. *J Gen Virol.* 2002;83(Pt 5):973-8. Epub 2002/04/19. doi: 10.1099/0022-1317-83-5-973. PubMed PMID: 11961250.
- 802.** Stahnke S, Lux K, Uhrig S, Kreppel F, Hosel M, Coutelle O, et al. Intrinsic phospholipase A2 activity of adeno-associated virus is involved in endosomal escape of incoming particles. *Virology.* 2011;409(1):77-83. Epub 2010/10/27. doi: 10.1016/j.virol.2010.09.025. PubMed PMID: 20974479.
- 803.** Adachi K, Enoki T, Kawano Y, Veraz M, Nakai H. Drawing a high-resolution functional map of adeno-associated virus capsid by massively parallel sequencing. *Nature communications.* 2014;5:3075. Epub 2014/01/18. doi: 10.1038/ncomms4075. PubMed PMID: 24435020; PubMed Central PMCID: PMC3941020.
- 804.** Asokan A, Schaffer DV, Samulski RJ. The AAV vector toolkit: poised at the clinical crossroads. *Molecular therapy : the journal of the American Society of Gene Therapy.* 2012;20(4):699-708. Epub 2012/01/26. doi: 10.1038/mt.2011.287. PubMed PMID: 22273577; PubMed Central PMCID: PMC3321598.
- 805.** Salvetti A, Greco A. Viruses and the nucleolus: the fatal attraction. *Biochimica et biophysica acta.* 2014;1842(6):840-7. Epub 2014/01/01. doi: 10.1016/j.bbadis.2013.12.010. PubMed PMID: 24378568; PubMed Central PMCID: PMC7135015.
- 806.** Pederson T. The nucleolus. *Cold Spring Harb Perspect Biol.* 2011;3(3). Epub 2010/11/26. doi: 10.1101/cshperspect.a000638. PubMed PMID: 21106648; PubMed Central PMCID: PMC3039934.
- 807.** Matthews D, Emmott E, Hiscox J. Viruses and the Nucleolus. In: Olson MOJ, editor. *The Nucleolus.* New York, NY: Springer New York; 2011. p. 321-45.
- 808.** Johnson JS, Samulski RJ. Enhancement of adeno-associated virus infection by mobilizing capsids into and out of the nucleolus. *Journal of virology.* 2009;83(6):2632-44. Epub 2008/12/26. doi: 10.1128/JVI.02309-08. PubMed PMID: 19109385; PubMed Central PMCID: PMC2648275.
- 809.** Grimm D, Zhou S, Nakai H, Thomas CE, Storm TA, Fuess S, et al. Preclinical in vivo evaluation of pseudotyped adeno-associated virus vectors for liver gene therapy. *Blood.* 2003;102(7):2412-9. Epub 2003/06/07. doi: 10.1182/blood-2003-02-0495. PubMed PMID: 12791653.
- 810.** Kawano Y, Neeley S, Adachi K, Nakai H. An experimental and computational evolution-based method to study a mode of co-evolution of overlapping open reading frames in the AAV2 viral genome. *PLoS one.* 2013;8(6):e66211. Epub 2013/07/05. doi: 10.1371/journal.pone.0066211. PubMed PMID: 23826091; PubMed Central PMCID: PMC3691236.

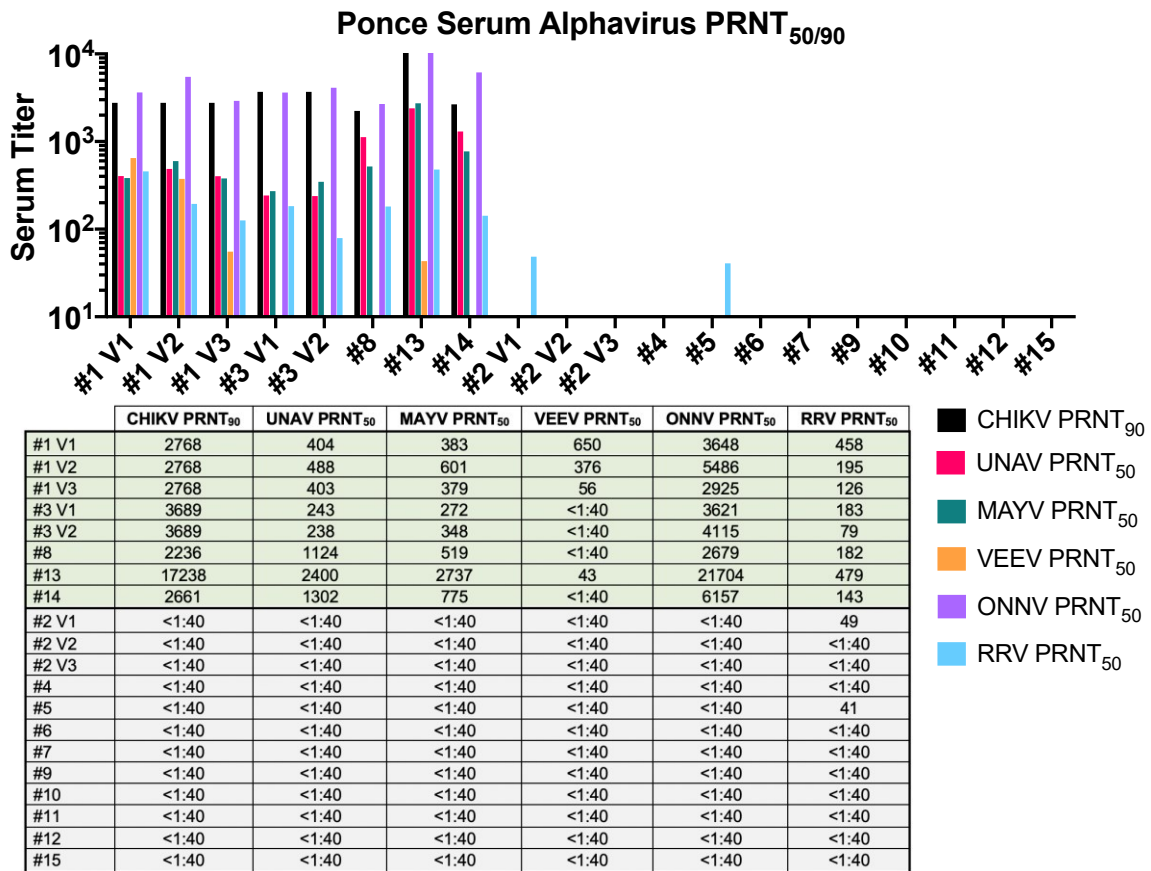
- 811.** Aurnhammer C, Haase M, Muether N, Hausl M, Rauschhuber C, Huber I, et al. Universal real-time PCR for the detection and quantification of adeno-associated virus serotype 2-derived inverted terminal repeat sequences. *Human gene therapy methods*. 2012;23(1):18-28. Epub 2012/03/21. doi: 10.1089/hgtb.2011.034. PubMed PMID: 22428977.
- 812.** Clark KR, Liu X, McGrath JP, Johnson PR. Highly purified recombinant adeno-associated virus vectors are biologically active and free of detectable helper and wild-type viruses. *Human gene therapy*. 1999;10(6):1031-9. Epub 1999/05/01. doi: 10.1089/10430349950018427. PubMed PMID: 10223736.
- 813.** Grimm D, Kern A, Pawlita M, Ferrari F, Samulski R, Kleinschmidt J. Titration of AAV-2 particles via a novel capsid ELISA: packaging of genomes can limit production of recombinant AAV-2. *Gene therapy*. 1999;6(7):1322-30. Epub 1999/08/24. doi: 10.1038/sj.gt.3300946. PubMed PMID: 10455443.
- 814.** Sommer JM, Smith PH, Parthasarathy S, Isaacs J, Vijay S, Kieran J, et al. Quantification of adeno-associated virus particles and empty capsids by optical density measurement. *Molecular therapy : the journal of the American Society of Gene Therapy*. 2003;7(1):122-8. Epub 2003/02/08. doi: 10.1016/s1525-0016(02)00019-9. PubMed PMID: 12573625.
- 815.** Wobus CE, Hugle-Dorr B, Girod A, Petersen G, Hallek M, Kleinschmidt JA. Monoclonal antibodies against the adeno-associated virus type 2 (AAV-2) capsid: epitope mapping and identification of capsid domains involved in AAV-2-cell interaction and neutralization of AAV-2 infection. *Journal of virology*. 2000;74(19):9281-93. Epub 2000/09/12. doi: 10.1128/jvi.74.19.9281-9293.2000. PubMed PMID: 10982375; PubMed Central PMCID: PMC102127.
- 816.** Fagone P, Wright JF, Nathwani AC, Nienhuis AW, Davidoff AM, Gray JT. Systemic errors in quantitative polymerase chain reaction titration of self-complementary adeno-associated viral vectors and improved alternative methods. *Human gene therapy methods*. 2012;23(1):1-7. Epub 2012/03/21. doi: 10.1089/hgtb.2011.104. PubMed PMID: 22428975; PubMed Central PMCID: PMC3640491.
- 817.** Farkas SL, Zadori Z, Benko M, Essbauer S, Harrach B, Tijssen P. A parvovirus isolated from royal python (*Python regius*) is a member of the genus Dependovirus. *J Gen Virol*. 2004;85(Pt 3):555-61. Epub 2004/03/03. doi: 10.1099/vir.0.19616-0. PubMed PMID: 14993638.
- 818.** NEB. 2017-2018 Catalog & Technical Reference. 2017-2018 Catalog & Technical Reference: New England Biolabs; 2017. p. pages 302-68.
- 819.** Sambrook J, Fritsch EF, Maniatis T. *Molecular cloning: a laboratory manual*. Cold Spring Harbor, NY: Cold Spring Harbor Laboratory Press; 1989. xxxviii + 1546 pp. p.

- 820.** Addgene. Bacterial Transformation www.addgene.com2017. Available from: <http://www.addgene.org/protocols/bacterial-transformation/>.
- 821.** Addgene. Sequence Analysis of your Addgene Plasmid www.addgene.org: Addgene; 2017. Available from: <https://www.addgene.org/recipient-instructions/sequence-analysis/>.
- 822.** Bio-Rad. Bio-Dot® microfiltration apparatus instruction manual [PDF]. Available from: <http://www.bio-rad.com/webroot/web/pdf/lsr/literature/M1706545.pdf>.
- 823.** Burton M, Nakai H, Colosi P, Cunningham J, Mitchell R, Couto L. Coexpression of factor VIII heavy and light chain adeno-associated viral vectors produces biologically active protein. *Proceedings of the National Academy of Sciences of the United States of America*. 1999;96(22):12725-30. Epub 1999/10/27. doi: 10.1073/pnas.96.22.12725. PubMed PMID: 10535990; PubMed Central PMCID: PMC23069.
- 824.** Grimm D, Pandey K, Kay MA. Adeno-associated virus vectors for short hairpin RNA expression. *Methods in enzymology*. 2005;392:381-405. Epub 2005/01/13. doi: 10.1016/S0076-6879(04)92023-X. PubMed PMID: 15644194.
- 825.** Leonard JN, Ferstl P, Delgado A, Schaffer DV. Enhanced preparation of adeno-associated viral vectors by using high hydrostatic pressure to selectively inactivate helper adenovirus. *Biotechnol Bioeng*. 2007;97(5):1170-9. Epub 2007/01/26. doi: 10.1002/bit.21355. PubMed PMID: 17252611.
- 826.** Lock M, Alvira MR, Chen SJ, Wilson JM. Absolute determination of single-stranded and self-complementary adeno-associated viral vector genome titers by droplet digital PCR. *Human gene therapy methods*. 2014;25(2):115-25. Epub 2013/12/18. doi: 10.1089/hgtb.2013.131. PubMed PMID: 24328707; PubMed Central PMCID: PMC3991984.
- 827.** Werling NJ, Satkunanathan S, Thorpe R, Zhao Y. Systematic Comparison and Validation of Quantitative Real-Time PCR Methods for the Quantitation of Adeno-Associated Viral Products. *Human gene therapy methods*. 2015;26(3):82-92. Epub 2015/05/09. doi: 10.1089/hgtb.2015.013. PubMed PMID: 25953194; PubMed Central PMCID: PMC4492554.
- 828.** Kafatos FC, Jones CW, Efstratiadis A. Determination of nucleic acid sequence homologies and relative concentrations by a dot hybridization procedure. *Nucleic acids research*. 1979;7(6):1541-52. Epub 1979/11/24. doi: 10.1093/nar/7.6.1541. PubMed PMID: 503860; PubMed Central PMCID: PMC342326.

- 829.** Clementi M, Menzo S, Bagnarelli P, Manzin A, Valenza A, Varaldo PE. Quantitative PCR and RT-PCR in virology. *PCR Methods Appl.* 1993;2(3):191-6. Epub 1993/02/01. doi: 10.1101/gr.2.3.191. PubMed PMID: 7680263.
- 830.** Reue K. mRNA quantitation techniques: considerations for experimental design and application. *J Nutr.* 1998;128(11):2038-44. Epub 1998/11/10. doi: 10.1093/jn/128.11.2038. PubMed PMID: 9808663.
- 831.** Mezzina M, Merten OW. Adeno-associated viruses. *Methods in molecular biology.* 2011;737:211-34. Epub 2011/05/19. doi: 10.1007/978-1-61779-095-9_9. PubMed PMID: 21590399.
- 832.** Chen WJ, Liao TH. Structure and function of bovine pancreatic deoxyribonuclease I. *Protein Pept Lett.* 2006;13(5):447-53. Epub 2006/06/28. doi: 10.2174/092986606776819475. PubMed PMID: 16800797.

Appendix.

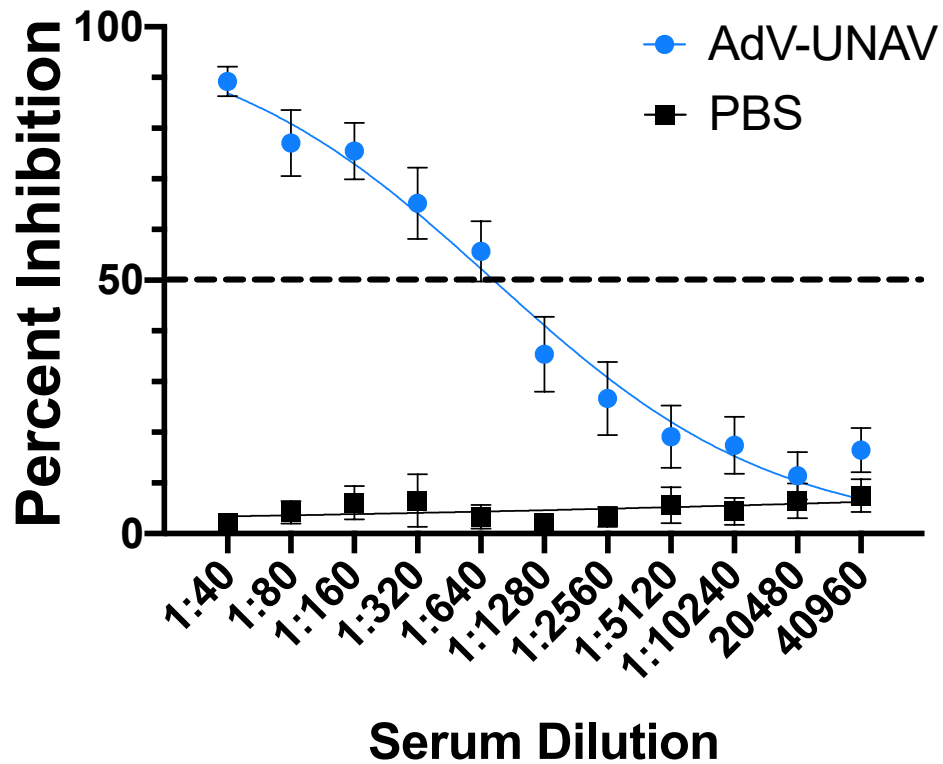
Supplemental Figures



Supplemental Figure 1 Convalescent Plasma Samples from Chikungunya Patients Display Detectable Levels of Cross-Protective Antibodies

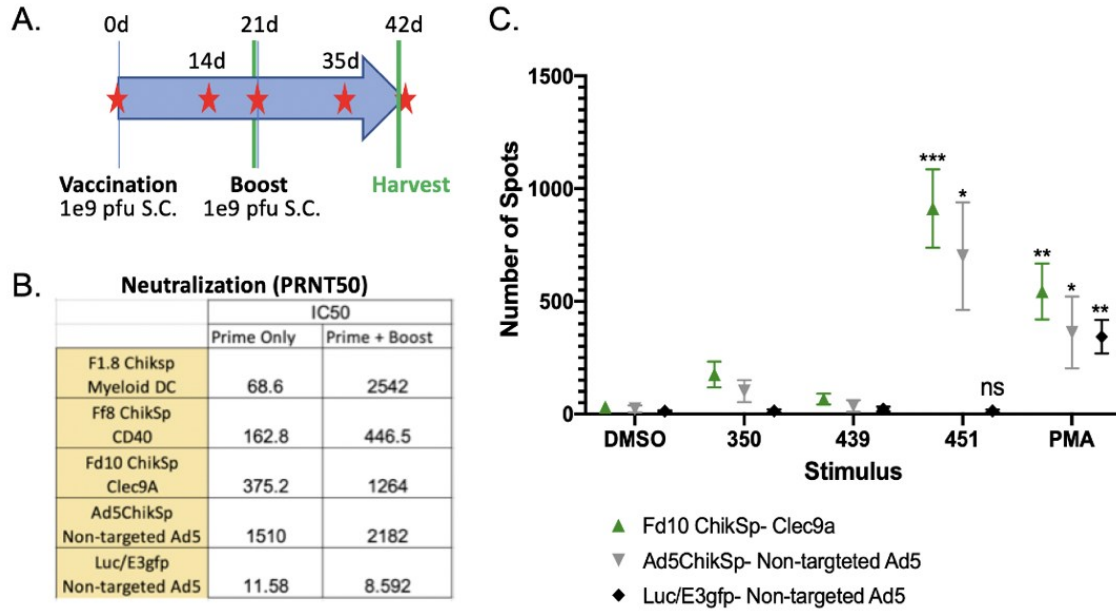
Serum samples from fifteen patients were evaluated for neutralizing and binding antibodies against a panel of alphaviruses. Plaque neutralization assays were conducted against Chikungunya (CHIKV), Una virus (UNAV), Mayaro virus (MAYV), Venezuelan Equine Encephalitis Virus (VEEV) O'nyong'nyong virus (ONNV), and Ross River virus (RRV). Values are reported as PRNT₉₀ for CHIKV, and PRNT₅₀ for Una, MAYV, VEEV, ONNV, and RRV.

AdV-UNAV 82 dpv PRNT₅₀



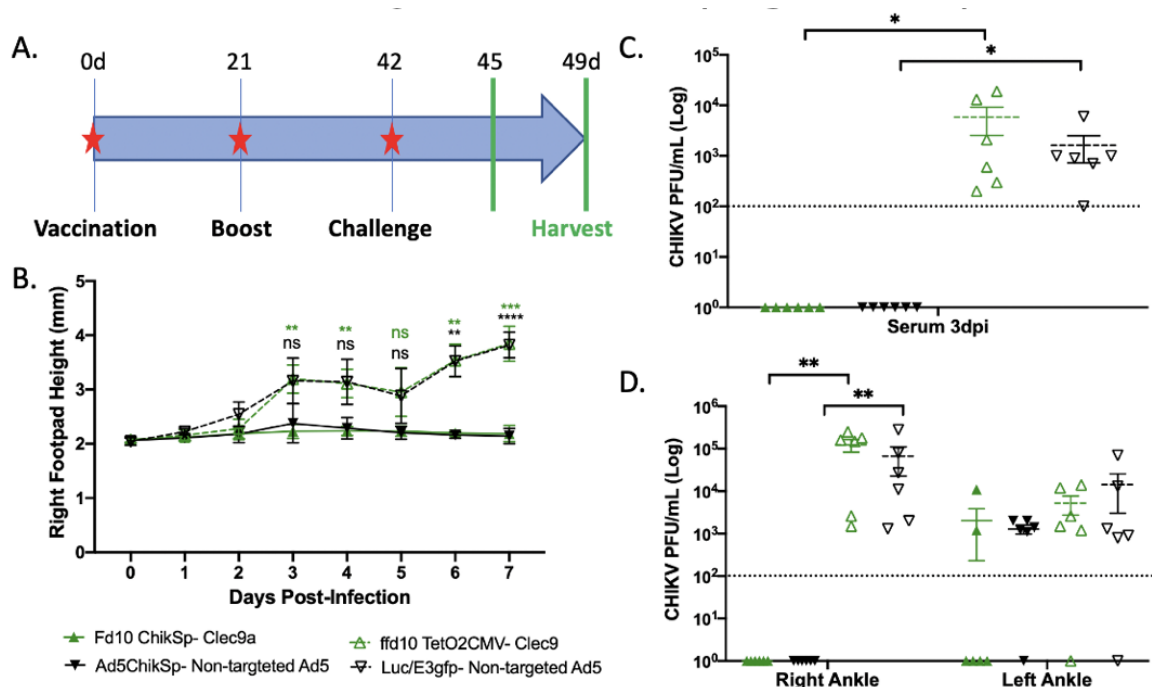
Supplemental Figure 2 AdV-UNAV Induces Long Lasting Neutralizing Antibody Responses

A group of C57BL/6 mice (n=10) were vaccinated with 10⁸ PFU AdV-UNAV with a boost vaccination at 14 dpv. At 82 dpv blood was collected and serum analyzed for neutralizing antibodies. Neutralization assays identified a PRNT₅₀ of 735 by variable slope non-linear regression, consistent with the strong antibody responses observed following vaccination of mice with AdV-MAYV. Error bars represent SEM.



Supplemental Figure 3 AdV-CHIKV Vectors Stimulate Strong Immune Responses

C57BL/6 mice were vaccinated in groups of 5 with Ad5 vectors expressing the CHIKV structural protein (ChikSp) or a control vector expressing luciferase and green fluorescent protein (Luc/EGFP). Vectors F1.8 ChikSp, Ff8 ChikSp, and Fd10 ChikSp were designed with a modified fiber gene to replace the knob coding regions with the trimerization domain derived from phage T4 fibritin and fused with single domain antibodies against dendritic cell markers. F1.8 ChikSp targeted immature myeloid dendritic cells, Ff8 ChikSp targeted the CD40 receptor, and Fd10 ChikSp targeted the Clec9a receptor. **(A)** Time course of experiment. Mice were vaccinated with 10^9 PFU on day 0 and 21. **(B)** Serum was collected at 21 and 42 dpv and neutralizing antibody responses were evaluated by PRNT₅₀ assays. Vectors expressing the CHIKV structural proteins are displayed increased immune responses following boost vaccination. **(C)** At 42 dpv mice were sacrificed and splenocytes were processed for ELIspot analysis. Vectors targeting the Clec9a receptor displayed higher T cell specific responses to CHIKV peptides compared to wild-type AdV. PRNT₅₀ values were calculated by variable-slope non-linear regression analysis.



Supplemental Figure 4 AdV-CHIKV Vaccination Protects WT Mice from CHIKV Challenge

AdV-CHIKV vaccine vectors were evaluated for ability to control infection following CHIKV challenge. **(A)** Mice were vaccinated and boosted at 21 dpv, and challenged at 42 dpv with 10^4 PFU of CHIKV. Serum was collected at 3 dpi and mice were sacrificed at 7 dpi. **(B)** Footpad swelling was monitored and was significantly reduced in mice vaccinated with targeting and non-targeting vectors expressing ChikSp when compared to control vectors. **(C)** Serum viremia was measured at 3 dpi by plaque assay. Mice vaccinated with ChikSp expressing vectors had no observable viremia and was significantly reduced compared to control vectors. **(D)** Mice vaccinated with ChikSp expressing vectors had significantly reduced viral load in their right ankle, and a trend towards reduced levels in their left ankle.

Supplemental Chapter 1.

A Quantitative Dot Blot Assay for AAV Titration and Its Use for Functional Assessment of the Adeno-associated Virus Assembly-activating Proteins

John M. Powers¹, Xiao Lan Chang¹, Zhen Song¹, and Hiroyuki Nakai^{1,2}

Departments of Molecular and Medical Genetics¹ and Molecular Microbiology and Immunology², Oregon Health & Science University, Portland, Oregon 97239, United States of America

John Powers conducted all of the experiments, with assistance from Zhen Song and Xiao Lan Chang. Experimental design was conducted by John Powers and Hiroyuki Nakai. Zheng Song and Xiao Lan Chang participated in filming of the protocol. John Powers and Hiroyuki Nakai wrote the manuscript.

S.1 Abstract

While adeno-associated virus (AAV) is widely accepted as an attractive vector for gene therapy, it also serves as a model virus for understanding virus biology. In the latter respect, the recent discovery of a non-structural AAV protein, termed assembly-activating protein (AAP), has shed new light on the processes involved in assembly of the viral capsid VP proteins into a capsid. Although many AAV serotypes require AAP for assembly, we have recently reported that AAV4, 5, and 11 are exceptions to this rule. Furthermore, we demonstrated that AAPs and assembled capsids of different serotypes localize to different subcellular compartments. This unexpected heterogeneity in the biological properties and

functional roles of AAPs among different AAV serotypes underscores the importance of studies on AAPs derived from diverse serotypes. This manuscript details a straightforward dot blot assay for AAV quantitation and its application to assess AAP dependency and serotype specificity in capsid assembly. To demonstrate the utility of this dot blot assay, we set out to characterize capsid assembly and AAP dependency of Snake AAV, a previously uncharacterized reptile AAV, as well as AAV5 and AAV9, which have previously been shown to be AAP-independent and AAP-dependent serotypes, respectively. The assay revealed that Snake AAV capsid assembly requires Snake AAP and cannot be promoted by AAPs from AAV5 and AAV9. The assay also showed that, unlike many of the common serotype AAPs that promote heterologous capsid assembly by cross-complementation, Snake AAP does not promote assembly of AAV9 capsids. In addition, we show that the choice of nuclease significantly affects the readout of the dot blot assay, and thus, choosing an optimal enzyme is critical for successful assessment of AAV titers.

S.2 Introduction

Adeno-associated virus (AAV) is a small, non-enveloped, single-stranded DNA virus with a genome of approximately 4.7 kilobases (kb). The AAV genome contains open-reading frames (ORFs) for the *rep* and *cap* genes. In 2010, a previously unidentified nonstructural protein encoded by a +1 frame-shifted ORF within the AAV2 *cap* gene was discovered by Sonntag *et al.* and found to play a critical role in the assembly of AAV2 capsid VP monomer proteins into a viral

capsid [197]. This novel protein has been named assembly-activating protein (AAP) after the role it plays in promoting capsid assembly [197].

The ORFs for AAP have been identified bioinformatically in the genomes of all parvoviruses within the genus *Dependoparvovirus*, but not within the genomes of viruses of different genera of the parvovirus family [197, 201]. Functional studies of this novel protein were initially focused on the AAP from the prototype AAV2 (AAP2), which has established the essential role of AAP2 in targeting unassembled VP proteins to the nucleolus for their accumulation and formation into fully assembled capsids [197, 200, 202]. The inability of the AAV2 capsids to assemble in the absence of AAP expression has been independently confirmed by multiple groups, including ours [197, 200-202, 810]. Subsequent studies on AAV serotypes 1, 8, and 9 corroborated the critical role of AAPs in capsid assembly, as VP3 monomer proteins of AAV1, 8, and 9 were unable to form a fully assembled capsid in the absence of co-expression of AAP [201].

Recently, through approaches that include the use of quantitative dot blot assays, we investigated the ability of AAV1 to 12 VP3 monomers to assemble into capsids in the absence of AAP expression and the ability of AAP1 to 12 to promote assembly of VP3 monomers from heterologous serotypes. This study has revealed that AAV4, 5, and 11 VP3 monomers can assemble without AAP. Additionally, it was found that eight out of the twelve AAP serotypes we examined (*i.e.*, all but AAP4, 5, 11, and 12) displayed a broad ability to support capsid assembly of heterologous AAV serotype capsids, while AAP4, 5, 11 and 12 displayed a

substantially limited ability in this regard [198]. These four serotypes are phylogenetically distant from the other AAP serotypes [200, 201]. Moreover, the study has uncovered significant heterogeneity in subcellular localizations of different AAPs [198]. Furthermore, the study has suggested that the tight association of AAP with assembled capsids and the nucleolus, the hallmark of AAV2 capsid assembly, cannot necessarily be extended to other serotypes including AAV5, 8, and 9, which display nucleolar exclusion of assembled capsids [198]. Thus, the information gained from the study of any particular serotype AAP is not broadly applicable to all AAP biology. Such puzzling nature of AAP biology underscores the need to investigate the role and function of each AAP from both canonical and non-canonical AAV serotypes.

The biological role of AAP in capsid assembly can be assessed by determining the fully-packaged AAV viral particle titers produced in human embryonic kidney (HEK) 293 cells, the most commonly used cell line for AAV vector production, with or without AAP protein expression. The standard methods for AAV quantitation are quantitative PCR (qPCR)-based assays and quantitative dot blot-based assays [422, 811, 812]. Other methods for AAV viral particle quantitation such as enzyme-linked immunosorbent assay or optical density measurement are not ideal for samples derived from many different AAV serotypes or samples contaminated with impurities (crude lysates or culture media), which are often the samples used for AAV research [813-815]. Currently, qPCR is most widely used for AAV quantitation; however, it is necessary to acknowledge potential caveats of the

qPCR-based assay, as the assay can result in systemic errors and significant titer variations [816, 817]. PCR-based assays are affected by a number of potentially confounding factors, such as the presence of covalently closed terminal hairpins in PCR templates that inhibit amplification [816]. Even an experienced individual can introduce potential confounding factors into a qPCR-based assay unknowingly [816]. In contrast, quantitative dot blot assays are a classical molecular biology technique that does not involve genome amplification and uses a much simpler principle with a minimal risk of errors as compared to qPCR-based assays. The method is less technically challenging; therefore, the assay results are reasonably reproducible even by inexperienced individuals.

In this report, we describe the methodological details of a quantitative dot blot assay we routinely use for AAV vector quantitation and provide an example of how to apply the assay to study the assembly-promoting role of AAPs in common serotypes (AAV5 and AAV9) and a previously uncharacterized AAP from Snake AAV [817]. In nature, AAV VP proteins and AAP proteins are expressed in cis from a single gene (*i.e.*, VP-AAP cis-complementation), while in the assay described here, VP and AAP proteins are supplied in trans from two separate plasmids (*i.e.*, VP-AAP trans-complementation). Since each VP or AAP protein from different serotypes can be expressed from each independent plasmid, it becomes possible to test heterologous VP-AAP combinations for capsid assembly (*i.e.*, VP-AAP cross-complementation). Briefly, AAV VP3 from various serotypes is expressed in HEK 293 cells by plasmid DNA transfection to package an AAV vector genome in

the presence or absence of the cognate serotype AAP, or in the presence of a heterologous serotype AAP. Following production, culture media and cell lysates are subjected to a dot blot assay to quantify the viral genome within the capsid shell. The first step of the dot blot assay is to treat samples with a nuclease to remove contaminating plasmid DNAs and unpackaged AAV genomes in samples. Failure to do so would increase the background signals in particular when unpurified samples are assayed. This is then followed by a protease treatment to break viral capsids and release nuclease-resistant viral genomes into sample solutions. Next, viral genomes are denatured, blotted on a membrane, and hybridized with a viral genome-specific DNA probe for quantitation. In the example assay reported here, we demonstrate that Snake AAV VP3 requires Snake AAP for capsid assembly and that Snake AAP does not promote the assembly of AAV9 capsids unlike many of the AAPs derived from AAP-dependent serotypes that can also promote assembly of heterologous serotype capsids. Lastly, we report an important caveat to qPCR or dot blot-based AAV quantitation assays that the choice of nuclease significantly affects the assay results.

S.3 Methods/Protocol

NOTE: Recipes for the solutions and buffers needed for this protocol are provided in **Table 4.1**. The protocol described below is for the VP-AAP cross-complementation dot blot assay to study the roles of the AAP proteins in capsid assembly. The method for the more generic quantitative dot blot assay for purified AAV vector titration is explained in the **Results** section.

Construction of VP3, AAP, and AAV2 Rep Expressing Plasmids

1 Construction of pCMV-AAVx-VP3 (x = serotypes)

1.1 PCR-amplify the entire VP3 ORF (1.6 kb) using a high-fidelity DNA polymerase and the following primer pair: VP3 forward, CTAA-RE1-CACC-N25 (the first 25 nucleotides of the VP3 ORF); VP3 reverse, TCTT-RE2-N25 (the last 25 nucleotides of the VP3 ORF). NOTE: RE1 and RE2 are sites for restriction enzymes (REs) for cloning. CTAA and TCTT are the terminal 5' and 3' tetranucleotides added to facilitate restriction enzyme digestion near the end of double-stranded DNA. CACC is a Kozak consensus sequence.

1.2 Clone the RE-digested PCR products between the corresponding RE sites of a mammalian expression vector that uses the human cytomegalovirus immediately-early (CMV-IE) enhancer-promoter for high-level expression. NOTE: For molecular cloning, digest 5 µg of the backbone plasmid DNA with a restriction enzyme(s) at a concentration of 4 U/µg DNA for 1 h at an optimal temperature. For PCR fragments, increase the units of enzymes used (e.g., 10 U/µg of the 1.6 kb VP3 ORF PCR product) and a longer incubation time (e.g., 4 h) due to an increase of the number of restriction enzyme recognition sites per unit length. Helpful information in molecular biology enzymes and cloning procedures including bacterial transformation can be found elsewhere [818-820].

2 Construction of pCMV-FLAG-AAPx (x = serotypes)

- 2.1 PCR-amplify the entire AAP ORF (0.6 kb) except for the first amino acid using a high-fidelity DNA polymerase and the following primer pair: AAP forward, CTAA-RE1-CACCATGGACTACAAGGACGACGATGACAAA-N25 (the 25 nucleotides from the 4th nucleotide in the AAP ORF); AAP reverse, TCTT-RE2-N25 (the last 25 nucleotides of the AAP ORF). NOTE: GACTACAAGGACGACGATGACAAA codes a FLAG tag, which has been shown to have no detrimental effects but can be omitted if unnecessary [202, 810].
- 2.2 Clone the RE-digested PCR products between the corresponding sites of a mammalian expression vector with the CMV-IE enhancer-promoter [818-820].

3 Construction of pHLP-Rep

- 3.1 Digest 5 µg of the pAAV-RC2 plasmid (7.3 kb) with 20 units each of Xho I and Xcm I, and purify the DNA using a commercial DNA purification kit or by phenol-chloroform extraction. NOTE: Removal of the 1.8 kb Xho I-Xcm I fragment from the 7.3 kb pAAV-RC2 plasmid results in a loss of capsid VP protein expression while preserving the Rep protein expression.
- 3.2 Blunt the DNA ends with 6 units of T4 DNA Polymerase, agarose gel-purify the 5.5 kb DNA fragment, and self-ligate the purified fragment using 50 to

100 ng of DNA and 400 units of T4 DNA ligase according to the manufacturer's recommendation [818].

3.3 Follow the standard bacterial transformation procedure referenced in step 1.1.2 Note.

- 4 Verify the plasmid constructs by restriction enzyme digestion and sequencing [818, 821].
- 5 Perform plasmid minipreps or maxipreps using commercially available kits to obtain a sufficient amount of plasmid DNA for the downstream AAV production experiments.

Production of AAV in HEK 293 Cells by Plasmid DNA Transfection (Cross-complementation Assay)

- 1 Culture HEK 293 cells in Dulbecco's Modified Eagle Medium (DMEM)-high glucose (4.5 g/L) supplemented with 10% fetal bovine serum (FBS), 1% Penicillin & Streptomycin Mix, and 1 mM L-glutamine, in a 37 °C incubator with 5% carbon dioxide (CO₂). NOTE: AAV titers significantly vary depending on the source of HEK 293 cells. Caution: Although AAV can be handled at biosafety level 1 (BSL1) containment, BSL2 containment is recommended for HEK 293 cell work.
- 2 On Day -1 (24 h prior to transfection), plate 6–7 x 10⁵ HEK 293 cells/well in 2 mL of the complete medium described in step 2.1 in a 6-well plate(s). This generally achieves ~90% confluency the next day.

3 Day 0: Transfection

3.1 Preparation for DNA transfection

3.1.1 Make sure that cells have reached ~90% confluency.

3.1.2 Warm up DMEM supplemented with 1% Penicillin & Streptomycin Mix and 1 mM L-glutamine but without 10% FBS (i.e., serum-free medium) in a 37 °C water bath.

3.1.3 Allow the polyethylenimine (PEI) solution to reach room temperature.

3.2 Preparation of plasmid DNA mixture

3.2.1 Mix the plasmids in 96 μL of phosphate buffered saline (PBS) without CaCl_2 or MgCl_2 in sterile 1.5 mL microcentrifuge tubes as indicated in **Table 4.2**. The total amount of DNA is 2 μg /well. NOTE: The volumes for plasmid DNA solution can be disregarded if they are nominal. Volume adjustment is recommended if the total volume of the plasmid DNA solutions is ≥ 10 μL .

3.3 PEI transfection

3.3.1 Add 4 μL of PEI solution (1 mg/mL) to the PBS-plasmid DNA mix (prepared as above). The final volume is approximately 100 μL (5% volume of the culture medium). Vortex the tubes briefly and incubate the DNA:PEI mixture for 15 min at room temperature.

- 3.3.2 While waiting for the 15 min incubation to complete, replace the culture medium with prewarmed serum-free medium described in step 2.3.1.2.
- 3.3.3 Once the 15-min incubation of the DNA: PEI mixture is complete, briefly spin the tubes with a microcentrifuge to collect the liquid to the bottom of the tubes, and add the DNA:PEI mixture dropwise to the culture medium in each well of the HEK 293 culture plate. Gently agitate the plates and return them to a 37 °C incubator with 5% CO₂.
- 3.3.4 Maintain the cells in this transfection medium until the harvest at Day 5 (no medium change is required).
- 4 On Day 1 and Day 2, observe cells transfected with pCMV-GFP plasmid under an inverted fluorescence microscope to assess transfection efficiency. NOTE: For fluorescence microscopy, here a 10X/0.25 numerical aperture objective in combination with a 10× eyepiece was used, and 450–490 nm excitation bandpass filter and 515–565 nm bandpass emission filter were employed. The above condition normally yields more than 70% transfection efficiency. Cells may exhibit some morphologic changes (e.g. cells have become slim) due to the serum-free condition.
- 5 On Days 3–5, continue to culture the transfected cells in a 37 °C incubator with 5% CO₂.

- 6 On Day 5, collect both cells and virus-containing medium into 15 mL polypropylene conical tubes by pipetting up and down or by scraping with a cell scraper.
- 7 Store the samples at -80 °C until use.

Dot Blot Assay for AAV Quantitation

1 Recovery of viral particles

- 1.1 Quickly thaw the frozen tubes in a 37 °C water bath. Vortex the tubes vigorously for 1 min to maximize the recovery of AAV from cells.
- 1.2 Pellet the cell debris by centrifuging at 3,700 x g at 4 °C for 10 min. Take 200 µL of the supernatant from each tube and transfer it into a labeled microcentrifuge tube with a screw cap for the dot blot assay. NOTE: Aliquot the remaining supernatant into microcentrifuge tubes and store them frozen at -80 °C for future use. Here, polypropylene microcentrifuge tubes attached with screw caps and an O-ring were used. Tight sealing is required to prevent spills of AAV and phenol-chloroform.

2 Treatment with *Serratia marcescens* endonuclease

- 2.1 Prepare Mix A and Mix B reagents (Table 4.3). Add 10 µL of Mix A and 10 µL of Mix B into each tube. Vortex the tubes for 5 s, briefly spin the tubes to collect the liquid to the bottom of the tubes and incubate the tubes at 37 °C at least for 1 h. NOTE: Mix A contains NaOH and optimizes pH for treatment with *S. marcescens* endonuclease. Mix B supplements

magnesium. Concentration of *S. marcescens* endonuclease in commercially available enzyme stocks may vary. The volume of *S. marcescens* endonuclease needs to be adjusted accordingly to make 200 U/mL after adding Mix A and Mix B into tubes in step 3.2.1. NOTE: A longer incubation time, up to 4 h, can decrease background signals.

2.2 At the end of the incubation, briefly spin the tubes with a benchtop centrifuge to collect condensation and solution from the top and sides of the tubes. NOTE: The protocol can be paused here. The samples can be stored frozen at -20 °C or -80 °C.

3 Proteinase K treatment

3.1 Prepare the Mix C reagent (Table 4.3). Add 180 µL of Mix C into each tube. Vortex the tubes for 5 s, briefly spin the tubes and incubate the tubes at 55 °C for 1 h. NOTE: The EDTA in the Mix C reagent chelates free magnesium ions and inactivates *S. marcescens* endonuclease.

3.2 At the end of the incubation, allow samples to reach room temperature, and briefly spin the tubes with a benchtop centrifuge to collect condensation and solution from the top and sides of the tubes. NOTE: The protocol can be paused here. The samples can be stored frozen at -20 °C or -80 °C. To resume the protocol, incubate the tubes at 55 °C for 5 to 10 min to dissolve SDS crystals contained in the buffer completely.

4 Phenol-chloroform extraction and ethanol precipitation

- 4.1 Add 200 μL of phenol-chloroform to the samples and vortex them for 1 min. Spin the samples in a microcentrifuge at $\geq 16,100 \times g$ for ≥ 5 min at room temperature. CAUTION: Phenol-chloroform should be handled in a chemical fume hood with appropriate personal protective equipment (PPE; i.e., nitrile gloves, goggles or face shield, and lab coat with long sleeves).
- 4.2 Transfer 320 μL of the aqueous layer (160 μL twice with a P200 pipette) to a new standard microcentrifuge tube (80% of aqueous fluid volume). NOTE: It is vitally important to take the same volume of aqueous solution between samples, otherwise the assay loses quantitative accuracy.
- 4.3 Prepare the Mix D reagent (Table 4.3). Add 833 μL of Mix D into each tube. Vortex the tubes for 5 s, and incubate the tubes at -80°C for ≥ 20 min. NOTE: Mix D is a mixture of ethanol, sodium acetate, and glycogen for convenient ethanol precipitation of DNA. Samples can be stored at -80°C at this step and the protocol can be resumed later.
- 4.4 Centrifuge samples with a microcentrifuge at $\geq 16,100 \times g$ at 4°C for ≥ 15 min. Pour off supernatant and blot once on a clean paper towel. Put approximately 500 μL of 70% ethanol into each tube, vortex the tubes for 5 s, and centrifuge the tubes with a benchtop microcentrifuge at $\geq 16,100 \times g$ at 4°C for ≥ 5 min.

4.5 Pour off the supernatant and blot once on a clean paper towel. Dry pellets at 65 °C; pellets can be dried completely. NOTE: Do not use a pipette to remove excess ethanol that remains after blotting the tubes. Pellets can also be dried at room temperature overnight. The protocol can be paused here and dried DNA pellets can be stored at room temperature for several days with the tube lid closed.

5 Resuspension of viral DNA in TE buffer

5.1 Dissolve the DNA pellets in 120 µL each of TE buffer by shaking each tube for 30 min to 1 h at room temperature.

6 Dot blot

6.1 Preparation of plasmid DNA standards

6.1.1 Dilute AAV vector genome plasmid DNA to 10 ng/µL in water or Tris-HCl buffer (10 mM, pH 8.0). Take 25 µL of this dilution and digest with an appropriate restriction enzyme for 1 h to linearize the plasmid DNA, in a reaction volume of 50 µL. NOTE: We make a duplicated set of digestion (see step 3.6.4.1). The appropriate enzyme should be one that cuts the plasmid DNA outside the dot blot probe-binding region. For convenience, the diluted plasmid DNA can be aliquoted (25 µL/tube) and stored frozen at -20 °C for future use. Digest the plasmid DNA while the tubes are shaking in step 3.5.1. Do not over-digest the plasmid DNA standard.

6.1.2 Add 450 μL of water or TE to the tube containing the digested plasmid DNA standard and mix thoroughly. Transfer 70 μL of this mixture to a new 1.5 mL microcentrifuge tube with 1,330 μL of water or TE to make a diluted plasmid standard (25 $\text{pg}/\mu\text{L}$).

6.1.3 Follow Table 4.4 to create a set of two-fold serial dilutions (600 $\mu\text{L}/\text{tube}$). Mix the dilutions thoroughly by vortexing for 5 s.

6.2 Denaturing of standards and viral DNA samples

6.2.1 Add 600 μL of 2x Alkaline Solution to each standard dilution. Mix well by vortexing for 5 to 10 s. Incubate at room temperature for 10 min.

6.2.2 Add 120 μL of 2x Alkaline Solution to each viral DNA sample. Mix well by vortexing for 5 to 10 s. Incubate at room temperature for 10 min.

6.3 Setting up the dot blot apparatus

6.3.1 Using scissors, cut a blotting (e.g., zeta-probe) membrane to an appropriate size for the number of samples and standards. Soak the membrane with water for 10 min before placing it on a dot blot apparatus. Cover unused wells on the membrane apparatus. NOTE: Handle the membrane with clean tweezers. To cover empty wells, the light blue protection sheet that comes with the membrane can be used. Do not allow the membrane to dry prior to binding samples and standards. For more details on the assembly and use of the apparatus, please refer to the user manual [822].

6.3.2 Add water to the wells to which samples will be loaded. Apply vacuum and pull water through the wells to check for errors and retest when fixed. Re-tighten the screws while applying vacuum to ensure tight sealing. NOTE: Incomplete sealing may cause sample leakage between the wells.

6.3.3 Once water is completely pulled through, release the vacuum completely (i.e., the vacuum manifold should be open to air pressure).

6.4 Loading standards and samples to the dot blot apparatus

6.4.1 Apply 400 μL of each diluted plasmid DNA standard to each well and run four lanes of standard dilutions. Use two separate aliquots of the standard digest and load each in duplicate. Apply 200 μL /well of each viral DNA sample. NOTE: Using the remaining ~ 40 μL of denatured samples, diluted samples can be prepared (e.g., 10-fold diluted samples using 20 μL of sample plus 180 μL of 1x Alkaline Solution) and blotted if necessary.

6.4.2 Apply gentle vacuum to pull the DNA solutions through the well. NOTE: Vacuum pressure needs to be adjusted by partially opening a three-way valve so that the vacuum pressure is applied to the dot blot apparatus as well as the atmosphere (i.e., with the stopcock arms positioned at an approximately 45° angle where it makes a louder suction noise).

- 6.4.3 Once all the wells have emptied, release the vacuum by adjusting the three-way valve. Add 400 μ L of 1x Alkaline Solution to each well that contained standards and samples. Wait for 5 min before re-applying vacuum to empty the wells.
- 6.4.4 Re-apply the vacuum in the same way (see step 3.6.4.2).
- 6.4.5 Disassemble the dot blot apparatus under vacuum, remove the membrane, and rinse it with 2x SSC. Place the membrane on a clean paper towel with the DNA-bound side facing up to remove excess 2x SSC.
- 6.4.6 UV-crosslink the blotted DNA to the membrane with an appropriate UV crosslinker; the membrane is now ready for hybridization. NOTE: Wet membranes can be used for UV crosslinking. The dried, UV-crosslinked membranes can be stored at room temperature. Further information can be found in the Table of Materials.

7 Hybridization and washing

- 7.1 Warm up the Hybridization Buffer in a 65 °C water bath.
- 7.2 Enzymatically label a DNA probe with radioactive α -³²P dCTP and purify it using commercially available kits according to the manufacturer's recommendation. NOTE: We use a probe of 0.5–2.0 kb in length from an enhancer-promoter region or a protein-coding sequence in the viral genome. Although this protocol utilizes ³²P-labeled radioactive probes for

signal detection, non-radioactive chemiluminescent or fluorescent probes can also be used (please refer to the Discussion section).

- 7.3 Place the membrane in a hybridization bottle with the DNA-bound side up, rinse the membrane with 5 mL prewarmed Hybridization Buffer, and discard the buffer. Then add 10 mL of prewarmed Hybridization Buffer and place the bottle in a rotating hybridization oven set at 65 °C. Rotate for ≥5 min.
- 7.4 Heat-denature 20 µL of 10 mg/mL sheared herring or salmon sperm DNA solution and the ³²P-labeled probe (≥10⁷ cpm) for 5 min by placing the tubes on a heat block set at 100 °C. Then snap-chill them on ice for ≥2 min, spin briefly, and keep on ice until use. Caution: For radioactive DNA probes, 1.5 mL tubes with screw cap and O-ring must be used.
- 7.5 Quickly add the denatured sperm DNA and radioactive probe to the Hybridization Buffer in the hybridization bottle and shake the bottle for 10 s to mix. Return the bottle to the 65 °C oven and incubate the bottle with rotation at 65 °C for ≥4 h.
- 7.6 Once hybridization is complete, stop the rotation, remove the hybridization bottle, and then pour the radioactive probe solution into a 50 mL conical tube with a leak-proof plug seal cap. Store the probe in an appropriate container placed in a refrigerator designated for radioactive materials.
NOTE: Used Hybridization Buffer with a probe that is stored at 4 °C can be re-used at least 5 times by placing the 50 mL conical tube with a leak-proof

plug seal cap that contains Hybridization Buffer in a 100 °C water bath for 5 min.

7.7 Wash the membrane with Wash Buffer heated to 65 °C. Add 20 to 30 mL of Wash Buffer to the hybridization bottle and rotate for 5 min. Repeat this wash 2 more times. NOTE: Measure radioactivity of wash solutions and record it if required by the local institute.

7.8 While washing the membrane, place a phosphor imaging screen on an image eraser for 5 min.

7.9 After the third wash, remove the membrane from the hybridization bottle, remove excess buffer on the membrane with paper towels, and place the membrane in a clear plastic paper holder. Check radioactive signals on the membrane using a Geiger counter. Expose the erased phosphor imaging screen to the membrane for 10 min to overnight depending on the signal intensity.

7.10 Scan the screen using a phosphor image scanning system and obtain the data on signal intensity of each dot.

8 Data analysis

8.1 Draw a standard curve using spreadsheet and data analysis software (e.g., Excel). NOTE: Log-log linear regression was used to draw a standard curve.

8.2 Determine nanogram-equivalent (ng-eq) for each of the viral DNA samples by interpolation. The ng-eq is the amount of the plasmid DNA used to draw a standard curve that is equivalent to the number of viral DNA molecules. When the length of the plasmid DNA is 8,000 bp, 1 ng-eq of single-stranded AAV viral DNA corresponds to 2.275×10^8 particles. NOTE: The ng-eq can be converted to the number of viral particles by the following equations:

Equation 1

$$\text{Number of single-stranded AAV particles} = \frac{1.82 \times \text{ng-eq}}{\text{length of plasmid (bp)}} \times 10^{12}$$

Equation 2

$$\text{Number of double-stranded AAV particles} = \frac{0.91 \times \text{ng-eq}}{\text{length of plasmid (bp)}} \times 10^{12}$$

The number of AAV particles are conventionally expressed as "vg" (vector genomes) or "DRP" (DNase I-resistant particles).

8.3 Calculate the AAV concentrations of the starting materials. Because the blotted viral DNA represents 66.7% of the viral DNA in the starting materials, 1 ng-eq corresponds to 1.7×10^9 particles/mL. NOTE: This correction is not needed if all the viral DNA contained in the starting material is blotted on a membrane without loss (Figure 4.1).

S.4 Results

A representative result of quantitative dot blots for quantitation of purified AAV vector stocks produced on a large scale is shown in **Figure S.1**. With this dot blot

assay, the titer of a double-stranded AAV2G9-CMV-GFP vector stock was determined. The vector was purified by two rounds of cesium chloride (CsCl) density-gradient ultracentrifugation followed by dialysis as previously described [823]. In general, for purified AAV vector stocks, three different volumes of each AAV vector stock (e.g., 0.3 μ L, 0.1 μ L, and 0.03 μ L) are subjected to the dot blot procedure described above in duplicate with a modification. DNase I Enzyme A is used in place of *S. marcescens* endonuclease in step 3.2, and a commercially available kit to extract and purify viral DNA is used in step 3.4 (see **Table of Materials**). In the example shown in **Figure S.1**, signal intensity values (arbitrary unit) obtained from each plasmid DNA standard (**Figure S.1A**) were plotted against the known DNA quantities to draw a standard curve (**Figure S.1B**), showing a correlation coefficient of 0.998. Using this standard curve, it was determined by interpolation that 0.3, 0.1 and 0.03 μ L aliquots of the AAV2G9 vector showed 1.487 and 1.522 ng-eq (0.3 μ L), 0.487 and 0.507 ng-eq (0.1 μ L), and 0.158 and 0.171 ng-eq (0.03 μ L). This gave the following six values: 4.957, 5.073, 4.870, 5.070, 5.267, and 5.700 ng-eq/ μ L for this particular AAV2G9 vector stock, leading to an average of 5.16 ± 0.27 ng-eq/ μ L (mean \pm SD). Since the length of the plasmid used as the standard (pEMBL-CMV-GFP) is 5,848 bp, the titer of this AAV2G9 vector was determined to be 8.0×10^{11} vg/mL according to **Equation 2** in step 3.8.2. This assay is repeated at least twice to determine the final titers of AAV vector stocks.

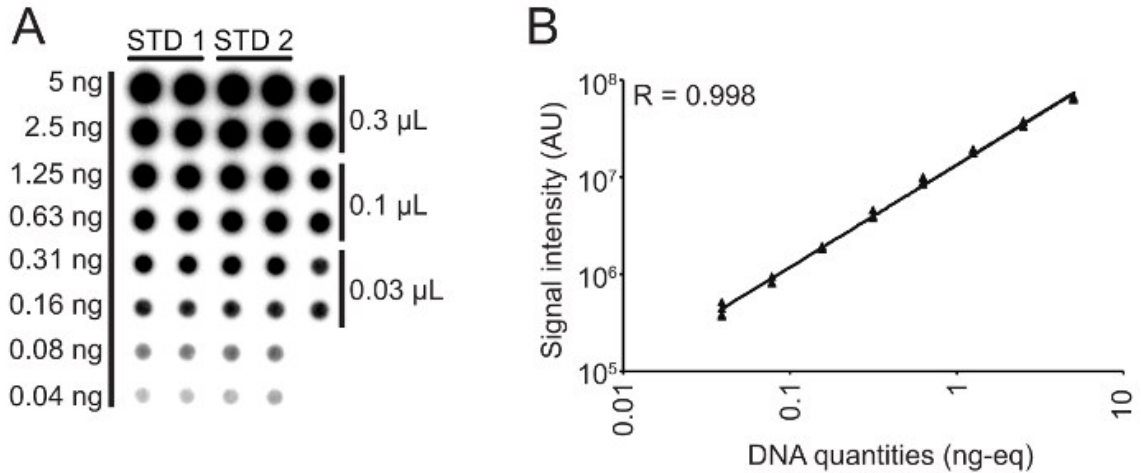


Figure S.1 A Representative Dot Blot Analysis to Determine the Titer of a CsCl-Purified AAV Vector.

(A) Double-stranded AAV2G9-CMV-GFP vector was produced in HEK 293 cells by a standard adenovirus-free three plasmid transfection method on a large scale, and purified by two rounds of CsCl gradient ultracentrifugation, followed by dialysis. 0.3, 0.1 and 0.03 μL of the purified AAV vector stock (blotted on the rightmost column) were subjected to the quantitative dot blot assay in duplicate with two sets of duplicated plasmid DNA standards (STDs). The blot was hybridized with a ³²P-labeled GFP probe (0.77 kb), and the image was obtained using a phosphor image scanning system. (B) A standard curve showing the relationship between known plasmid DNA quantities (ng-eq, X-axis) and dot intensities (arbitrary unit (AU), Y-axis). The numbers on the Y-axis were obtained with the phosphor image scanning system. R indicates Pearson's correlation coefficient.

A representative result of cross-complementation assays to assess the AAP dependency in VP3 capsid assembly and the ability for AAPs to assemble VP3 proteins of heterologous origins is displayed in **Figure S.2**. *In vitro* studies of AAV often do not require virus purification to make conclusions, and experiments using unpurified virus preparations such as crude cell lysates and virus-containing culture media are sufficient to yield meaningful results. In this experiment, AAV viral particle production was assessed from all possible AAV VP3-AAP combinations among AAV5, AAV9, and Snake AAV including VP3-no AAP combinations by a quantitative dot blot assay. The samples obtained in a

duplicated set of an experiment were blotted at 1x and 10x dilutions (Set A and Set B in **Figure S.2A**, respectively). The graph shown in **Figure S.2B** summarizes the quantitative analysis of the dots. The results show that: (1) AAV5VP3 assembles regardless of whether AAP was provided in trans, (2) AAP5 and AAP9 can promote AAV9VP3 capsid assembly although AAP5 functions less effectively than AAP9, (3) neither AAP5 nor AAP9 exhibits an assembly promoting activity on Snake AAV VP3, and (4) Snake AAP only promotes assembly of Snake AAV VP3. (1) and (2) are in line with previous observations [198], but the uniquely specific AAV VP3-AAP interaction in Snake AAV is a novel discovery in this experiment. One weakness of the cross-complementation assay based on quantitative dot blot is that the negative control always shows appreciable levels of background signals that cannot be totally eliminated. Therefore, the dot blot assay by itself cannot exclude the possibility that capsid assembles to a level below the sensitivity of the assay. In this regard, it should be noted that, to generate the negative controls, a condition is used under which AAV viral genomes exponentially replicate in the absence of the capsid VP3 protein. Such negative controls can be generated by transfecting HEK 293 cells with pAAV-Reporter, pHLP-Rep, and pHelper (**Table 4.2**), and are used to reduce false positives.

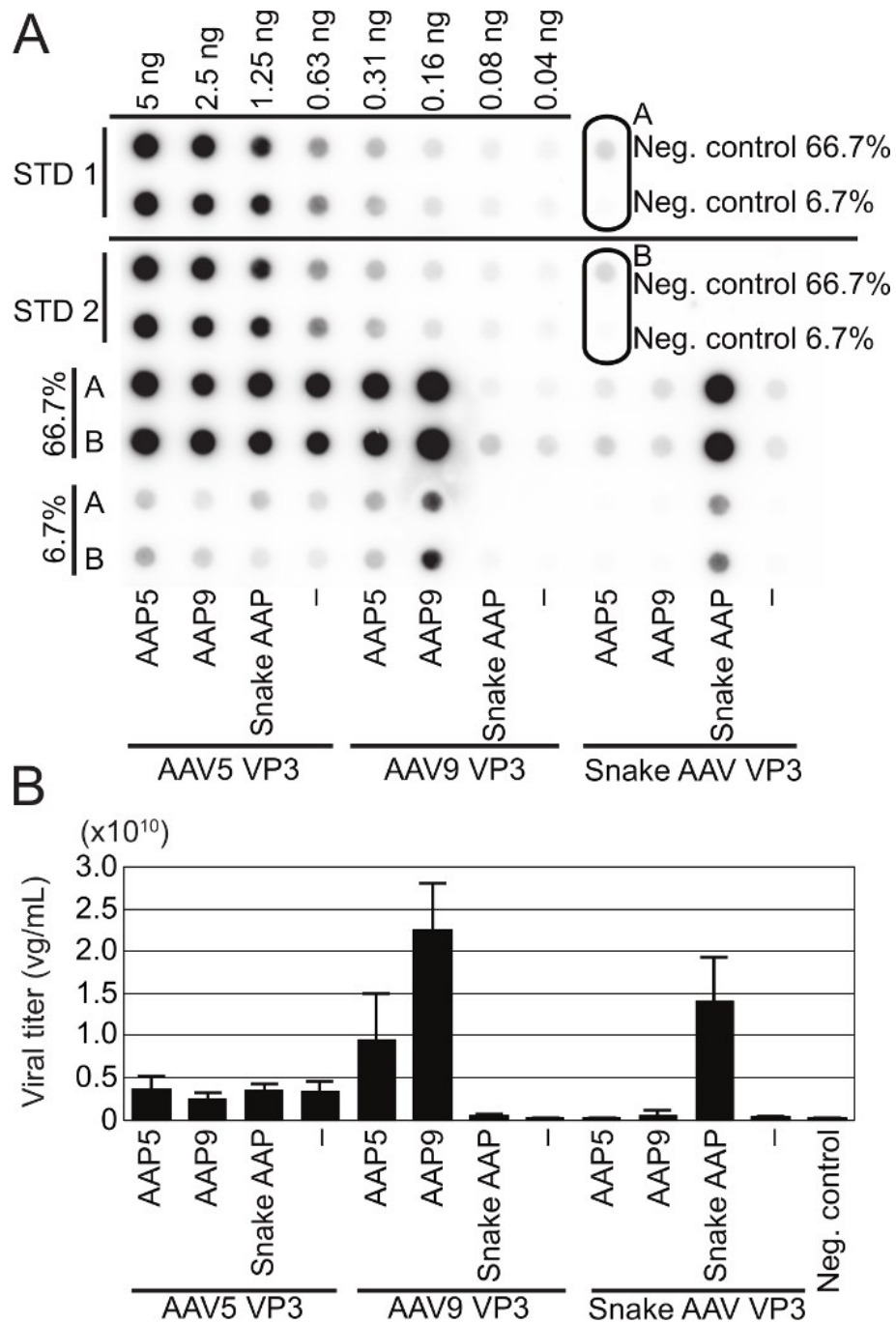


Figure S.2 AAV VP3-AAP Cross-Complementation Dot Blot Assay

Double-stranded AAV-CMV-GFP vector particle production was tested for the VP3 proteins from AAV5, AAV9, and Snake AAV in the presence or absence of their cognate AAPs or in the presence of AAPs of heterologous origins. (A) The assay was performed in a biologically duplicated set of experiments (Set A and Set B) with 4 h incubation time with *S. marcescens* endonuclease, and the AAV vector titer obtained from each combination was determined by a quantitative dot blot method described in the Protocol section. Each dot represents two-thirds (the 5th and 6th rows, 66.7%) or

two-thirtieths (the 7th and 8th rows, 6.7%) of DNA recovered from each 200 μ L of medium collected from the samples or the negative control. The top four rows (1st to 4th rows) represent two sets of plasmid DNA standards (STD 1 and STD 2) blotted in duplicate (*i.e.*, linearized pEMBL-CMV-GFP plasmid, which is the plasmid used for double-stranded AAV-CMV-GFP vector production). The dot blot membrane was probed with a 32 P-labeled GFP probe. The pair of dots indicated with rounded rectangles are negative controls. The top two rows (STD 1) are from the bottom of the original blot but have been cut and moved to the top without altering image intensity to display both plasmid standards (STD 1 and STD 2) side by side. This manipulation is indicated with a black line in the figure. **(B)** Viral titer was determined for the combinations of VP3 and AAP proteins by the dot blot assay. The graph represents a biologically quadruplicated set of data, two from Panel A and two from another dot blot that is not shown. Error bars indicates mean \pm SD ($n = 4$).

DNase I has been widely used as a nuclease in dot blot and qPCR-based assays for AAV quantitation to remove residual plasmid DNAs and unpackaged viral genomes that have contaminated AAV preparations. These contaminants would otherwise lead to an overestimation of titers; therefore, the nuclease digestion is a very important step for accurately quantifying viral genome titers. DNase I enzymes are available from various manufacturers and commercial vendors; however, the importance of the selection of DNase I in AAV quantitation appears to have been underappreciated. To investigate how the choice of nuclease might affect the outcomes of the dot blot assay, the following three nucleases were compared for their ability to remove background signals from the AAV vector-containing culture media prepared as described above in steps 2 and 3: DNase I Enzyme A, DNase I Enzyme B, and *S. marcescens* endonuclease (**Table of Materials**). Published studies have used the former two DNase I enzymes and we have been using *S. marcescens* endonuclease in previous and current studies [816, 824-827]. To our surprise, it was identified that DNase I Enzyme A is not at all an appropriate choice for the dot blot assay using the virus-containing media in

the various conditions tested, resulting in high background signals from the negative control, while DNase I Enzyme B and *S. marcescens* endonuclease effectively reduced the background signals with DNase I Enzyme B being ~2-fold more effective than *S. marcescens* endonuclease (**Figure S.3A, B**). DNase I Enzyme C was also found to be very effective to reduce the background signals (data not shown). These data demonstrate that there are significant differences in enzyme activities among commercially available nucleases when the enzyme reactions are performed in unpurified AAV preparations although nuclease digestion should be effective when a small quantity of purified viral preps is treated under an optimized condition. Thus, these data highlight the importance of the correct selection of nuclease in the assay when unpurified AAV preparations undergo a quantitative dot blot or qPCR assay.

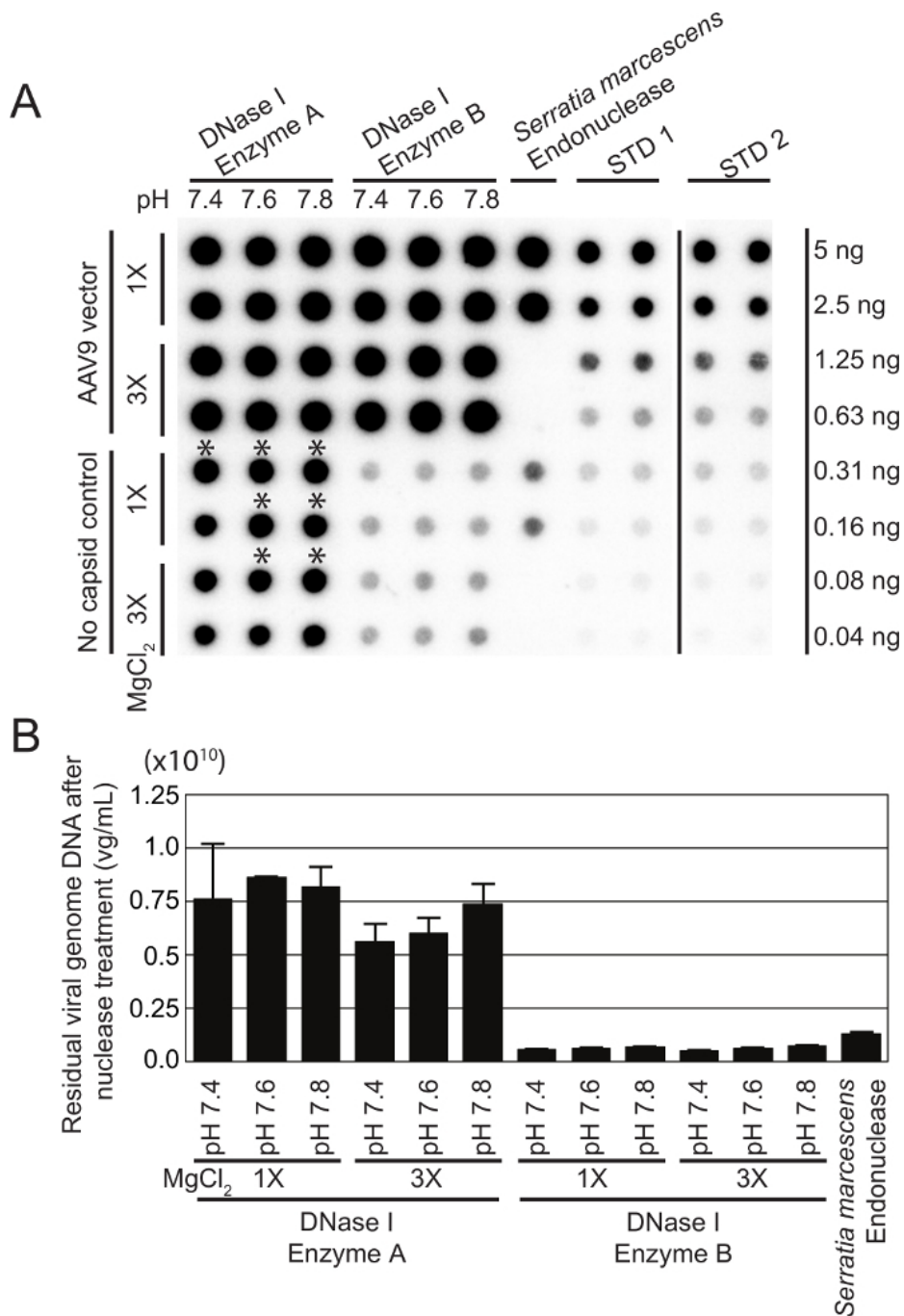


Figure S.3 A Comparison of Enzymatic Activities of Different Nucleases in Unpurified AAV Vector Preparations

(A) A quantitative dot blot showing the efficacy of each nuclease treatment in eliminating background signals. A double-stranded AAV9-CMV-GFP vector-containing preparation ("AAV9 vector") and a "no-capsid control" were produced by HEK 293 cell transfection with plasmid DNAs and subjected to the assay. The no-capsid control did not contain viral particles but contained

exponentially amplified unpackaged CMV-GFP vector genomes. $MgCl_2$ was supplemented at one or three-times the recommended amounts (6 mM and 18 mM for DNase I Enzyme A; and 2.5 mM and 7.5 mM for DNase I Enzyme B) without taking into account the 0.8 mM $MgSO_4$ present in the medium. For the treatment with *S. marcescens* endonuclease, only one condition described in the Protocol section was tested. All the samples were treated with each nuclease for 1 h. The dot blot membrane was probed with a ^{32}P -labeled GFP probe. The right two columns (STD 2) are from the left of the original blot but have been cut and moved to the right without altering image intensity to display both plasmid standards (STD 1 and STD 2) side by side. This manipulation is indicated with a thin black line in the figure. **(B)** Dots in the no-capsid control samples in Panel A are quantified and displayed as mean \pm [each value — mean value]. Seven out of the 12 samples treated with DNase I Enzyme A (indicated with an asterisk) show values only slightly higher than the highest standard; therefore, they are included in this graph for comparison. Error bars represent SD.

S.5 Discussion

In this report, the utility of quantitative dot blot assays to study AAV AAPs and their role in capsid assembly is described. Knowledge gained from these studies can provide detailed insights into the innate differences in the process of AAV capsid assembly and the functional role of AAPs between different serotypes. In this respect, the AAV VP3-AAP cross-complementation dot blot assay revealed that Snake AAV VP3 displayed a strict dependency on the co-expression of its cognate AAP for capsid assembly and that Snake AAP does not promote capsid assembly of heterologous serotypes. This observation is intriguing because the AAP-dependent AAV serotypes that were previously investigated (AAV1, 2, 3, 6, 7, 8, 9, and 12) are all able to process assembly at least to some degree by utilizing a heterologous AAP [198].

Quantitative dot or slot blot hybridization is a traditional method for quantitation of nucleic acids contained in multiple samples at the same time in a convenient manner [828]. The method had been widely used for DNA and RNA quantitation until qPCR became prevalent in the 1990s [829, 830]. Although qPCR has

advantages over quantitative dot blot and other hybridization-based assays in that qPCR exhibits a higher sensitivity and a wider dynamic range, it also carries an inherent risk of exponentially augmenting errors unknowingly, which was the case for titers of AAV vector stocks determined by qPCR [816, 826]. Quantitative dot blot assays are easily set up with an inexpensive cost and easily carried out as long as researchers have access to a quantitative molecular imaging system that can acquire signals from dot blot membranes hybridized with either a radioactive probe or a non-radioactive chemiluminescent or fluorescent probe. Although this protocol utilizes ^{32}P -labeled radioactive probes for signal detection, others successfully use non-radioactive DNA probes directly labeled with a commercially available thermostable alkaline phosphatase [831]. Dot blot assays use a straightforward principle and the assay by itself does not pose a technical challenge to performers; therefore, the results are generally reproducible even by inexperienced individuals.

Besides the applications described here, we routinely use a simplified and expedited version of the dot blot procedure that can semi-quantify AAV particles quickly. Advantages of dot blot assays in this context include: (1) the assay does not require purification or enzymatic amplification of viral genomes which takes hours, (2) a combination of heat and alkaline denaturation is sufficient to break AAV particles in a sample solution and release denatured viral genomes into the solution that are ready to bind to a dot blot membrane, and (3) the presence of salt at high concentrations in samples does not significantly affect the assay results.

For example, it is possible to semi-quantify AAV particles in CsCl-rich solutions (e.g., fractions obtained by CsCl density-gradient ultracentrifugation) by putting a small aliquot (≤ 10 μL) of samples into 100 μL of 1x Alkaline Solution, heating at 100 °C for 10 min, and blotting onto a membrane with or without standards prepared in advance, followed by a 15 min hybridization, 3 x 3 min washes and exposure to a phosphor imaging screen for 15 min (or longer when using a probe with decreased radioactivity). The whole procedure can be completed in 1 h once the user becomes familiar with the procedure. We use this expedited method, which we customarily call "boiling dot blot method", to identify AAV particle-rich CsCl fractions during the vector purification process and roughly determine titers of purified AAV vector stocks before beginning the extensive processes for vector characterization. Thus, although dot blot assays might be viewed as an outmoded method to quantify nucleic acids and have already been replaced with various PCR-based methods in a wide range of scientific disciplines, there are still a number of advantages to this method that should make researchers consider employing it in their laboratories.

The most critical step in the protocol is the nuclease treatment of samples. If this step is not carried out in an optimal condition, it would cause high background signals. We use *S. marcescens* endonuclease while DNase I enzymes of different sources are widely used in other laboratories for viral DNA quantification. The DNase I of bovine pancreas origin has been most widely used by researchers. This is in part because the bovine pancreatic DNase I was first identified and most

extensively characterized biochemically [832]. The DNase I enzymes currently available from commercial vendors are produced from several different biological sources such as *Pichia pastoris* (DNase I Enzyme A), the native form purified from the bovine pancreas (e.g., DNase I Enzyme B), and recombinant enzymes produced in either a yeast species or *Escherichia coli* (DNase I Enzyme C). We have found that the DNase I enzymes from all three of these different sources have been used in published AAV vector quantitation studies; however, to our knowledge, none of the previous studies have investigated whether the enzymes from different sources are equally effective in digesting contaminating DNA molecules in AAV vector preparations. It should be noted that DNase I treatment for AAV vector assays is often carried out under non-optimized conditions due to the presence of impurities derived from culture medium and cells. The observation that DNase I Enzyme A is only partially active in the culture medium we used has significant implications in designing the assay for AAV vector quantitation by dot blot and qPCR, and alerts researchers to this previously unidentified issue. In this regard, *S. marcescens* endonuclease expressed in *E. coli*, is an ideal endonuclease not only for the purpose of manufacturing AAV vectors but also for AAV vector quantitation. This is because its enzymatic activity can be retained over a wide range of pH values and concentrations of magnesium ions and monovalent cations. For this reason, and because *S. marcescens* endonuclease is approximately 2 times less expensive than DNase I Enzyme B on a per-unit basis, we prefer to use *S. marcescens* endonuclease in routine quantitative dot blot analyses.

In summary, quantitative dot blot assays are a relatively straightforward procedure that can readily provide information on the ability to produce viral particles under varying conditions. Compared to alternative titering approaches, such as qPCR, this approach requires little, if any, optimization. It can also be readily applied to vectors of any serotype and can be used to titer both single- and double-stranded vectors without modifying the protocol. Following transfections and harvest of AAV vector-containing samples (culture medium and/or cells), the whole protocol can be completed in a day, thus rapidly answering questions about the ability to produce viral particles from diverse conditions, including various combinations of AAV VP3 and AAP proteins. Quantitative dot blots offer an expedient method to address various unanswered questions as to VP-AAP interactions and their roles in capsid assembly in a wide variety of different AAV serotypes and isolates.

S.6 Materials

Table S.1 Solution and Buffer Recipes for Dot Blot

<i>Serratia marcescens</i> Endonuclease Buffer
50 mM Tris-HCl
2 mM MgCl ₂
Adjust to pH 8.5 with 4 M NaOH.
10x Proteinase K Buffer
100 mM Tris-HCl pH 8.0
100 mM EDTA pH 8.0
5% SDS
2x Alkaline Solution

800 mM NaOH	
20 mM EDTA	
20x SSC (1L)	
175.3 g NaCl	
88.2 g Sodium citrate tribasic ($\text{Na}_3\text{C}_6\text{H}_5\text{O}_7$)	
Denhardt's Solution 100x (50 mL)	
1 g Bovine serum albumin (fraction V)	NOTE: Filtering is critical in order to remove small particles as they cause background hybridization signals.
1 g Polysucrose 400	
1 g Polyvinylpyrrolidone	
Dissolve in 20 mL of water in a 55 °C water bath.	
Adjust final volume to 50 mL.	
Filter-sterilize with a 0.22 µm filter.	
Hybridization Buffer	
1% SDS	NOTE: Store Hybridization Buffer at 4 °C and heat to 65 °C in a water bath prior to use.
6x SSC	
5x Denhardt's Solution	
10 mM Tris-HCl pH 8.0	
Wash Buffer	
0.1% SDS	
0.1x SSC	
Polyethylenimine (PEI) Solution (1 mg/mL, 500 mL)	
Add 500 mg PEI in 450 mL of water and stir.	NOTE: For longer storage, -80 °C is recommended.
Add concentrated HCl to bring pH down to <2.0 to dissolve PEI (approximately 800 µL of HCl will be required).	

Add 10 M NaOH to bring pH up to 7.0 (approximately 500 μ L of 10 M NaOH will be required).	
Adjust the volume to 500 mL of water.	
Filter-sterilize with a 0.22 μ m filter.	
Aliquot and store at -20 °C.	
Phenol-chloroform (1:1 mix) for quantitative dot blotting	
Add buffer-saturated phenol (pH 8.0) and chloroform at a 1:1 ratio in a 50 mL polypropylene conical tube.	NOTE: The buffer covering the organic layer, if left in the tube, can be carried over into sample tubes through pipetting and may make the assay inaccurate.
Vortex the tube vigorously to mix.	
Allow for phase separation by centrifugation and then remove the aqueous layer completely.	
Store at 4 °C.	

Recipes for solutions and buffers needed to complete the quantitative dot blot protocol.

Table S.2 Plasmid Combinations for AAV VP3-AAP Cross-Complementation Assay Performed in a 6-well Plate Format

Plasmid	AAP(+) (μ g)	AAP(-) (μ g)	Negative control (μ g)	Transfection control (μ g)
pCMV-AAVx-VP3	0.4	0.4		
pCMV-FLAG-AAPx	0.4			
pAAV-Reporter	0.4	0.4	0.4	
pHLP-Rep	0.4	0.4	0.4	
pHelper	0.4	0.4	0.4	
pCMV (Empty)		0.4	0.8	
pCMV-GFP				2.0
Total	2.0	2.0	2.0	2.0

Plasmid combinations for AAV VP3-AAP cross-complementation assay performed in a 6-well plate format. Combinations of the plasmid DNAs to be used for HEK 293 cell transfection in each experimental group are shown. pCMV-AAVx-VP3, a plasmid expressing AAV serotype x (x = 1, 2, 3, etc.) VP3 protein under the CMV-IE enhancer-promoter; pCMV-FLAG-AAPx, a plasmid expressing AAV serotype x (x = 1,2, 3, etc.) AAP protein under the CMV-IE enhancer-promoter; pAAV-Reporter, a plasmid that has two AAV2 inverted terminal repeats (ITRs) and is designed for recombinant AAV vector production; pHLP-Rep, a plasmid expressing AAV2 Rep protein; pHelper, an adenovirus helper plasmid; pCMV (Empty), an empty plasmid added to control the experimental conditions; pCMV-GFP, a plasmid expressing a fluorescence marker gene(e.g., GFP) to verify successful transfection. Transfections are conducted in 6-well plates and use a total of 2 µg of plasmid DNA.

Table S.3 List of Master Mix Reagents

Mix A	For 10 tubes (µL)
<i>Serratia marcescens</i> Endonuclease Buffer	91.2
0.1 M NaOH	8.8
Total	100
Mix B	For 10 tubes (µL)
<i>Serratia marcescens</i> Endonuclease Buffer	91.2
1 M MgCl ₂	7.04
<i>Serratia marcescens</i> Endonuclease (250 units/µL)	0.176
Total	100
Mix C	For 10 tubes (µL)
10x Proteinase K Buffer	400
Proteinase K (20 mg/mL)	100
H ₂ O	1,300
Total	1,800
Mix D	For 10 tubes (µL)
100% Ethanol	8,000

3 M Sodium acetate (pH 5.2)	320
Oyster glycogen (20 mg/mL)	10
Total	8,330

Mix A and Mix B are used for the *S. marcescens* endonuclease treatment in step 3.2. These two mixtures should be made separately to prevent precipitation of magnesium hydroxide. Mix C is used for Proteinase K treatment in step 3.3. Mix D is used for ethanol precipitation in step 3.4.3. The volumes indicated in the table are for master mix reagents for 10 tubes.

Acknowledgments

We thank Xiao Xiao at the University of North Carolina at Chapel Hill for providing us with the pEMBL-CMV-GFP plasmid. We thank Christopher Cheng and Samuel J. Huang for critical reading of the manuscript.